The link between copper homeostasis and Alzheimer's disease as a route to therapy

Eliona Tsefou

A Thesis Submitted for the Degree of Doctor of Philosophy

September 2016

Institute for Cell and Molecular Biosciences

Newcastle University

Abstract

Ageing is a natural process, which is characterised by progressive decline in physiological functions and increased susceptibility to disease and death. Brain is particularly susceptible to structural and functional changes, which is more evident in disorders associated with ageing such as Alzheimer disease (AD). Copper is necessary for the protection against oxidative stress, energy production and neurotransmitter processing in the brain. However, higher copper levels can increase oxidative stress, resulting in neuronal damage. In order to avoid copper induced cytotoxicity, cells have to regulate copper levels through distribution into three intracellular pathways. By identifying changes in the copper pathways in the healthy and AD brain and by estimating the effects of copper chelation or supplementation in model cell line a better understanding of copper function in the brain will be obtained. In order to accomplish that copper, activity and protein levels of cytochrome *c* oxidase (COX) and superoxide dismutase (SOD) were measured in the healthy, AD brain and in HEK293 cell treated with copper chelators or supplemented with copper. Copper concentration was significantly decrease by more than 40% in healthy ageing brain and in the AD brain. Copper loss did not seem to affect the activity or protein level of the COX and SOD, since their levels were significantly increased in the ageing and AD brain. On the other hand, cells treated with copper chelators for three days faced a more than 75% decrease in intracellular copper concentration, which led to a more than 85% inhibition of the COX and SOD activity. Copper levels should be regulated properly in order to meet body's metabolic demands and avoid cytotoxicity. Brain seems to have a mechanism where its energy demands have to be fulfilled even under low copper concentrations. Whereas, the prolonged and severe copper loss can dramatically affect the energy production and antioxidant defence systems which could be fatal to the cells.

Declaration

I declare that this thesis contains my own work, except where acknowledged, and that no part of this work has been submitted in support of an application for other qualifications at this or any other institution.

I would like to dedicate this thesis

To my mum

Acknowledgements

Undertaking the Ph.D. journey has been a unique and life changing experience, hence I take this opportunity to remember and acknowledge the cooperation, goodwill and support both moral and technical extent by several individuals out of which this project has evolved. I shall always cherish my association with them.

Foremost, I would like to thank my supervisory team Prof. Christopher Dennison, Dr. Christopher Morris and Dr. Kevin Waldron for their guidance, advices and patience throughout this venture. To proceed, I would like to thank Prof. Dennison for the opportunity given to undertake this Ph.D. project and for his valuable advices which I will always remember. I would also like to express my deepest gratitude towards Dr. Morris for being always there when I mostly needed advice or guidance when faced with various project challenges and for sharing his unlimited knowledge and mostly for preparing all the brain samples for my experiments.

I would like to extend my gratefulness beyond my supervision team to all those who helped in the background at the Institute for Cell and Molecular Biosciences and Medical Toxicology Centre: Dr. Nicolas Vita, Kerrie Brusby, Gianpiero Landolfi, Stephanie Mayer, Preeti Sing and Daniel Erskine for making these four years of my Ph.D. full of happy memories and being there when I needed someone to talk. Especially, I would like to thank Dr. Semeli Platsaki for her friendship and her advices of how to approach the procedure of writing and also for the quick lessons in copper chemistry. Furthermore, I would like to express my gratitude to Dr. Peter Hanson and Dave Henderson for their technical advices in various experimental approaches.

My verbal abilities limit my expression of my heart full feelings toward my parents, Olga and Panagiotis. Words cannot express how grateful I am to them for dedicating their life to make sure that myself and my sisters will accomplish our dreams and have a better future. I would also like to take this opportunity to express my gratefulness towards my mum which has been a rock for me which has kept me going and made lot of sacrifices in order to make my dreams come true. Furthermore, I would like to thank my sisters, Marieta and Eua, and my little niece Maria Zoe for making my life happier and fill me with joy along the way. Their faith in me always gave the strength I needed to carry on. A special gratitude must go to Sul for being part of my life, always pushing me to become better, listening to all my problems and especially for standing by me no matter how difficult things were.

Finally, special acknowledgement goes to National Institute for Health Research Newcastle Biomedical Research Centre based at Newcastle Hospitals NHS Foundation Trust and Newcastle University who awarded me the scholarship to undertake this project.

Table of Contents

List of Figures

List of Tables

Abbreviations

Ab	Albumin
AChEIs	Acetylcholinesterase inhibitors
AD	Alzheimer's disease
AICD	Cytoplasmic polypeptide APP intracellular domain
APH -1	Anterior pharynx defective
ApoE	Apolipoprotein E
APP	Amyloid precursor protein
Atox1	Human antioxidant protein 1
ATP	Adenosine triphosphate
ATP7a/b	Copper-transporting P-type ATPases
Aβ	β-amyloid peptide
BACE1	β-site APP-cleaving enzyme/β-secretase
BBB	Blood-brain barrier
BCB	Blood-cerebrospinal fluid barrier
BCS	Bathocuproinedisulfonic acid
BGHpolyA	Bovine growth hormone
bp	Base pair
BSA	Bovine serum albumin
CAT	Catalase
CCS	Copper Chaperone for Cu,Zn superoxide dismutase
CCT	Collision cell technology
CMV	Cytomegalovirus
CNS	Central Nervous System
COMMD1	Copper Metabolism (Murr1) Domain Containing 1
COX	Cytochrome *c* oxidase
COX1	Cytochrome *c* oxidase subunit I
COX2	Cytochrome *c* oxidase subunit II
Cp	Ceruloplasmin
CQ	5-Chloro-7-iodo-quinolin-8-ol, Clioquinol
CS	Citrate synthase
CSF	Cerebrospinal fluid
CTF	C-terminal fragment of APP
CTFα	C-terminal fragment C83 of APP

Ctr1	Copper transporter 1
Cu^{1+}	Cuprous
Cu^{2+}	Cupric
DMT1	Divalent Metal Transporter 1
DNA	Deoxyribonucleic acid
D-pen	D-penicillamine
ECAR	Extracellular acidification rate
EDTA	Ethylenediaminetetraacetic acid
EMA	Europe Medicines Agency
EOAD	Early onset Alzheimer disease
ETC	Electron transport chain
FACS	Fluorescence activated cell sorting
FADH	Flavin adenine dinucleotide
FALS	Familial Amyotrophic Lateral Sclerosis
FBS	Fetal bovine serum
FCCP	Carbonyl cyanide-4-(trifluoromethoxy)phenylhydrazone
FDA	Food and Drug Administration
FMNH	Reduced Flavin mononucleotide
g	gram
GAPDH	glyceraldehyde 3-phosphate dehydrogenase
GFAAS	Graphite furnace atomic absorption spectrometry
GFD	Growth factor domain
GPI-Cp	Glycosylphosphatidylinositol-anchored Cp
GPx	Glutathione peroxidase
GSH	Glutathione
H_2O_2	Hydrogen peroxide
HEK293	Human Embryonic Kidney 293
hGHpolyA	Human growth hormone polyA
HUVEC	Human Umbilical Vein Endothelial Cells
ICP-MS	Inductively coupled plasma mass spectrometry
IMS	Inter-membrane space
INAA	Instrumental neutron activation analysis
K_b	Copper binding affinity or association constant
kDa	Kilodalton

KPI	Kunitz-type protease inhibitor
LA-ICP-MS	Laser ablation inductively coupled plasma mass spectrometry
LOAD	Late onset Alzheimer disease
M	Molar
MEFs	Mouse Embryonic Fibroblasts
mg	milligram
min	minutes
MMPs	Metalloproteinase
MRI	magnetic resonance imaging
mRNA	Messenger ribonucleic acid
MTs	Metallothioneins
mV	millivolt
NADH	Nicotinamide adenine dinucleotide
NADPH	Nicotinamide adenine dinucleotide phosphate
NBTR	Newcastle Brain Tissue Resources
NDUFS1	NADH:ubiquinone oxidoreductase core subunit S1
NDUFV1	NADH:ubiquinone oxidoreductase core subunit V1
NFTs	Neurofibrillary tangle
ng	nanogram
NLS	Nuclear localization signal
NMDA	N-methyl-D-aspartase
NMR	Nuclear magnetic resonance
NPs	Neuritic plaques
NTF	N-terminal fragment of presenilins
O_2^-	Superoxide anions
OCR	Oxygen consumption rate
$OH^\bullet$	Hydroxyl radical
PAM	α-amidating monoxygenase
PBS	Phosphate buffer salina
PEI	Polyethylenimine
PHF	Paired helical filaments
pmoles	picomoles
PS	presenilins
ROS	Reactive oxygen species

sAPPα	soluble N-terminal ectodomain of APP
Sco	Cytochrome *c* oxidase assembly protein
sCp	secreted form of Cp
siRNA	Small interfering RNA
SOD	Superoxide Dismutase
TBS	Tris buffered saline
TEPA	Tetraethylenepentamine
TGN	trans-Golgi network
Trientine	Triethylene tetramine
TTM	Ammonium tetrathiomolybdate
VBM	Voxel based morphometry
VDAC1	Voltage-dependent anion-selective channel 1
WHO	World Health Organization
$\Delta\Psi_m$	Mitochondrial membrane potential
µg	microgram
µM	micromolar
µmol	micromoles

1 Introduction

1.1 Copper in mammalian cells

Copper is an essential trace element found in a variety of cells and tissues, with the highest concentrations being found in organs such as liver and brain[1]. Copper ions exist in both oxidized, cupric (Cu^{2+}), and reduced, cuprous (Cu^{1+}) states[2]. Copper's ability to accept and donate electrons has been utilized in various biological possesses such as mitochondrial respiration, tissue formation, pigmentation, iron oxidation, neurotransmitter processing and antioxidant defence[3, 4].

Mammals obtain copper mainly from sources such as oysters, liver, nuts, legumes, whole grains and beans[5]. Generally, copper absorption in the gut depends on dietary habits, food choices or supplementary vitamins and minerals which may promote or inhibit its absorption[6]. About 30-40% of the ingested copper, mostly Cu^{2+}, is absorbed in the small intestine and to lesser extent in the stomach[7]. The absorbed copper, from the small intestine, is transported through intestinal cells to the blood where it is found predominantly bound to albumin (Ab) and transcuprein, a protein that belongs to the macroglobulin family[8, 9]. Copper will be transported to the liver where it can be stored within hepatocytes, secreted into plasma by incorporation into Ceruloplasmin (Cp) or excreted into the bile[1]. The World Health Organization (WHO) has announced that the minimum requirements for copper are 0.6 mg/day for a woman and 0.7 mg/day for men. The body has established a homeostatic regulation mechanism via increased adsorption or excretion in order to fulfil the body requirements and avoid toxicity[1].

Copper levels have to be regulated properly since an imbalance on its levels can increase oxidative stress, lead to neuronal damage and initiate degradation of proteins, DNA and lipids. The effects of copper metabolism imbalance can be seen in two rare disorders, Wilson's and Menkes disease. Wilson's disease is an autosomal recessive metabolic disorder characterised by increased levels of copper in the liver and brain and by specific symptoms including hepatic, ophthalmological, neurological and/or psychiatric changes[10]. Menkes disease is an X-linked copper deficiency disorder where patients exhibit severe mental and developmental impairment[11]. The clinical symptoms of Menkes disease include progressive neurological degeneration, connective tissue abnormalities, muscular hypotonia and hypopigmentation of skin and hair[12]. Except of these two neurodegenerative disorders studies have shown that copper is also implicated with other neurological diseases such as Alzheimer's (AD)[13, 14] or Parkinson (PD)[15, 16]. Several studies have shown that copper and copper binding protein are facing significant changes in the AD brain but that will be further

discuss at section 1.5.2. As far as it concerns the implication of copper in PD a study from Popescu *et al.* where they used rapid-scanning x-ray fluorescence, has shown that copper levels were decreased in the PD brain but only in substantia nigra, one of the most affected brain regions in PD cases[16]. However, in that study they do not report if that change was statistical significant. The results from Popescu and college study are in good agreement with a study coming from Dexter *et al.* who used inductively coupled plasma spectrometry (ICP-MS) to measure copper in frozen brain tissue[16, 17]. In that study Dexter *et al.* showed a general non-significant copper loss in the PD brain with only substantia nigra presenting a statistical significant copper loss of more than 35%[17].

1.2 The mechanism of copper toxicity

The benefits of utilizing copper for cellular processes come at a price since copper can cause cellular toxicity. The main theory about copper induced cellular toxicity is based on the ability of copper ions to participate in the formation of reactive oxygen species (ROS). In the presence of superoxide (O_2^-) or reducing agents such as ascorbic acid or glutathione (GSH), Cu^{2+} can be reduced to Cu^{1+} (equation 1.1), which is capable of catalysing the formation of hydroxyl radicals ($OH^\bullet$) from hydrogen peroxide (H_2O_2) via the Haber-Weiss reaction (equation 1.2)[2].

$$O_2^- + Cu^{2+} \rightarrow O_2 + Cu^{1+} \qquad \textbf{(1. 1)}$$

$$Cu^{1+} + H_2O_2 \rightarrow Cu^{2+} + OH^- + OH^\bullet \qquad \textbf{(1. 2)}$$

The produced hydroxyl radicals are the most powerful oxidizing radical likely to arise in biological systems and can react with almost every biological molecule within the cell[18]. Hydroxyl radicals are able to abstract a hydrogen form unsaturated fatty acids leading to lipid radical formation which can eventually lead to the repetitive formation of short-chain alkanes and lipid acid aldehydes, resulting in the disruption of the lipid membrane[19]. Proteins are also another possible target where the oxidation can be initiated by the binding of reduced copper to enzymes where it will form a coordination complex which consequently will react with hydrogen peroxide to form hydroxyl radicals[20]. The produced hydroxyl radicals can abstract hydrogen from amino-bearing carbon, leading to the formation of a carbon-centred protein radical that undergoes a series of reactions, resulting in the hydrolysis of the amino group and the formation of an aldehyde or protein carbonyl[20]. The same reactions can be driven by iron, via Fenton chemistry, where the produced hydroxyl radical can act as oxidants of DNA and cause both mutagenesis and lethality to the cells[21].

The mechanisms of copper induced toxicity have been studied in both mammalian and bacterial cells. A recent study in *Escherichia coli* has shown that copper is capable of rapidly inactivating the catalytic iron-sulfur cluster of dehydratases[22]. This enzyme family has representatives in central catabolic and biosynthetic pathways and is vulnerable to chemical damage because their clusters are substantially exposed to solvent[23]. The iron-sulfur clusters are vulnerable to molecules such as O_2^- and H_2O_2 since they are small enough to invade the active site, where they coordinate and oxidise the iron-sulfur active site[24]. Macomber *et al.* showed that these clusters are the primary target of copper[22]. Copper will displace the iron atoms from the solvent exposed cluster which suggest that copper damages the dehydratases by liganding to the coordinating sulfur atoms[22]. The observation that copper can damage iron-sulfur clusters in *E.coli* revealed the possibility that the released iron atoms will potentially overload in the cells and proportionately will accelerate any iron-based Fenton chemistry which can cause DNA damage or stimulate excessive iron import into the cells[22].

Studies from copper overload disorders have shown that mitochondria are one of the targets for copper toxicity, since copper can oxidise the mitochondrial lipid membrane and damage the enzymes of the tricarboxylic acid cycle and oxidative phosphorylation[25]. Copper induced mitochondrial toxicity has been studied in hepatocytes and neuronal cell lines and in both cases increased copper concentrations stimulated the production of ROS which eventually led to decreased cell viability[26, 27]. Studies in rat hepatocytes has shown that copper can cause not only a rapid decline in the mitochondrial membrane potential ($\Delta\Psi_m$) and induce the increased formation of mitochondrial derived ROS but also induce the increased cellular lipid peroxidation and the depletion of reduced GSH[28]. Similar findings have also been observed in a neuronal cell line, where copper accumulated inside the mitochondria causing initially metabolic arrest which eventually led to cell death because of increased ROS production[26]. Mitochondrial proteins were also targets of copper induced toxicity since the proteins that form the Complex I (NDUFs) of the respiratory chain were significantly decreased by higher copper concentrations[26].

1.3 Copper homeostasis pathway in mammalian cells

Inside the human body, cells have to maintain copper levels within a range in order to meet both the cellular metabolic demands for copper but also to avoid cytotoxicity. Hence, specific mechanisms are needed to regulate the dynamic fluctuations of extracellular and intracellular copper levels[29]. Mammalian cells need to regulate copper concentration not only at the level of a single cell, but also at the whole organism, since certain organs have specific demands for

copper which reflect their normal function in the body[29]. After insertion in cells, copper can be distributed into three different pathways: secretory, mitochondrial and cytosolic.

1.3.1 Copper influx into cells

Copper uptake on the apical surface of intestinal epithelial cells is mediated primarily through the specific copper transporter, copper transporter 1 (Ctr1/SLC31A1)[30], and to lesser extent, the divalent metal transporter 1 (DMT1/ SLC11A2)[31]. Ctr1 is ubiquitously expressed in all tissues and is particularly abundant in the gut, choroid plexus of the brain, renal tubules and in connective tissues of the eye, ovary and testis[32].

1.3.1.1 Copper transporter 1 (Ctr1)

Ctr1 is an integral membrane protein that is structurally and functionally conserved from yeast to humans, composed of 190 amino acids in human with a molecular mass of 23 kDa[30]. Mammalian Ctr1 has an overall architecture consisting of an extracellular N-terminal domain, three transmembrane domains and an intracellular C-terminal domain containing a cysteine-histidine cluster (HCH) [33]. Ctr1 contains on its sequence certain elements that are essential for copper uptake which are the MX_3M motif on the second transmembrane domain and two methionine (M1 and M2) and two histidine (H1 and H2) rich motifs on the N-terminal. The last two elements are also significant in copper binding/sensing activity [33-35] with the methionines on M2 being particularly important for copper transport activity under copper limited conditions[34, 36].

In the cell membrane Ctr1 has to be oligomerized as a trimer in order to form a pore that allows copper to pass through the plasma membrane[37, 38]. Copper uptake by Ctr1 is not dependent on ATP hydrolysis or an ion gradient and the whole mechanism of copper transport though the pore is not fully elucidated[37, 38]. The suggested mechanism supports that copper ions are reduced extracellularly maybe by binding to the methionine and histidine rich domains in the N-terminal which is followed by shuttling of the reduced copper ion in through the pore[37, 38]. The last stop of copper is the HCH motif in the C-terminal which seems to act as an open/close switch of the internal pore. A recent study has determined the copper binding affinity or association constant (K_b) of the HCH motif as 4.3×10^{13} M^{-1}[39].

In cells, Ctr1 is found in two locations: the plasma membrane and intracellular vesicles and Ctr1 regulation of localization depends on extracellular copper levels (Figure 1.1)[40, 41]. Molloy *et al.* reported that at very low copper concentration (less than 1 μM) the majority of Ctr1 was detectable at the plasma membrane and a small amount (14%) in internal vesicles[41].

When extracellular copper levels were between a range of 2.5-100 μM this triggered the internalization rate of Ctr1, resulting in a greater proportion of Ctr1, more than 40%, locating in the intracellular compartment[41]. When copper was removed from the extracellular media, the internalization rate of Ctr1 returned back to the original value where Ctr1 mainly localized to the plasma membrane[42].

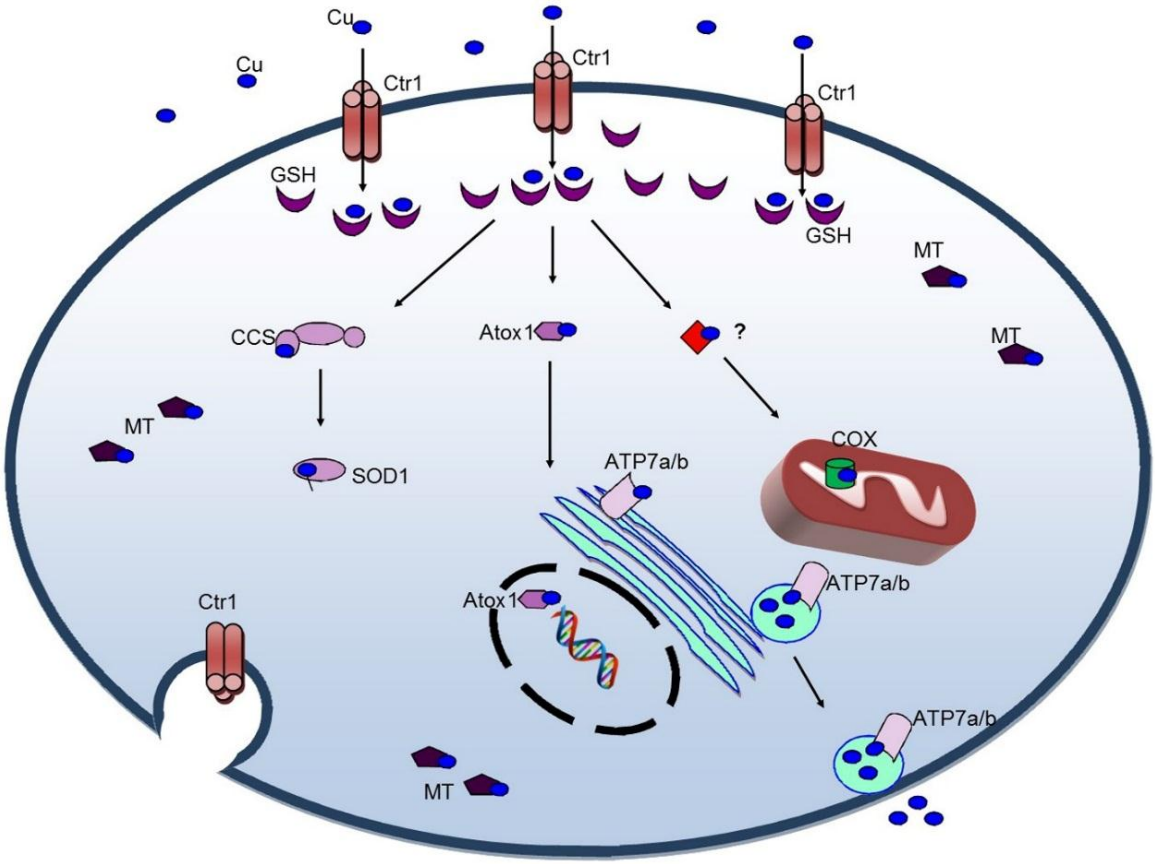

Figure 1.1 Representative Model of Copper Homeostasis Pathways in Mammalian Cells. In the cell membrane copper uptake is mediated through Ctr1. Inside the cells copper is initially bound to thiol metabolites such as glutathione (GSH) and then is distributed into three different pathways. In the cytosolic pathway, the copper chaperone for Cu,Zn superoxide dismutase (CCS) delivers copper to the Cu,Zn superoxide dismutase 1 (SOD1) in the cytosol. In the secretory pathway, the chaperone Atox1 (human antioxidant protein 1) will transport copper to the copper-transporting P-type ATPases, ATP7a/b, in the Golgi membranes for incorporation into newly synthesized proteins/enzymes or excretion from the cells. In the mitochondrial pathway, an unknown molecule transfers copper to the mitochondrial inner membrane where is required for the functionn of cytochrome *c* oxidase (COX). Excess of copper will be stored in metallothioneins (MTs). Figure was adapted from Cotruvo *et al.*[43].

After transportation of copper into the cytosol a ligand exchange will take place between copper which is bound to the CHC motif of Ctr1 and intracellular molecules such as copper chaperones or GSH[37]. A study from Maryon and colleagues has tried to identify which are the possible intracellular copper acceptors in cells that overexpress Ctr1 and found that GSH

is possibly the first molecule to accept copper from Ctr1[44]. They concluded this since overexpression of the copper chaperones did not affect cellular copper uptake, but depletion of GSH (by inhibiting its synthesis) caused significant inhibition of copper uptake[44]. The GSH copper affinity K_b is around 1×10^{11} M^{-1} which places it the lowest amongst the other copper binding chaperones[45]. Even if GSH has the lowest K_b its levels are considerably higher in the cytosol which further supports the idea that copper is first transported to GSH and then GSH delivers copper to the chaperons (Figure 1.1)[44].

The importance of Ctr1 function in the body has been studied in a mouse model which showed that Ctr1 is essential for the embryonic development. The deletion of Ctr1 gene was embryonic lethal, possibly because of the reduced supply of copper in the developing embryo[32, 46]. Heterozygous mice for Ctr1 (mouse Ctr1 is 90% identical to human[47]) showed that copper levels in the brain and spleen decreased by 50% but in other organs such as liver, kidneys and intestine copper levels remained unchanged[32, 46]. The above observations suggest that Ctr1 is more important for copper supplementation in the brain and spleen compared to other organs which might have a Ctr1-independent copper import system[46]. The existence of the Ctr1-indepedent copper transport system was further supported from studies with embryonic Ctr1-homozygous knockout cells which were able to transport 30% of the extracellular copper[35].

In the brain, the highest expression levels of Ctr1 were detected in the choroid plexus and capillary endothelial cells[48-50]. In the choroid plexus Ctr1 is mainly located in the apical membrane where it might extract copper from the cerebrospinal fluid (CSF), a function that is related to the proposed role of the choroid plexus in maintenance of copper homeostasis in brain extracellular fluid[49, 50]. In brain capillary endothelia cells, Ctr1 is located on the luminal side where it probably regulates copper uptake from the blood[50]. Ctr1 is also expressed in neurons in different brain regions such as visual cortex, anterior cingulate cortex, caudate and putamen, whilst in cerebellum Ctr1 is mainly expressed in Bergmann glia[48].

1.3.2 The secretory pathway of copper homeostasis

Once absorbed, copper needs to be transferred out of the intestinal enterocytes to the blood and also to sites of synthesis of copper-containing proteins within cells. In the human body there are a number of secreted and plasma membrane proteins that require copper for their function. Copper must therefore be transferred to the Golgi compartment where it will be incorporated into newly synthesized proteins, such as the multicopper ferroxidases Cp and Hephaestin, tyrosinase, lysyl oxidase and blood clotting factors. In the cytosol the dedicated

copper chaperone Atox1 (human antioxidant protein 1 or HAH1) delivers copper to the copper-transporting P-type ATPases, ATP7a and ATP7b, located in the trans-Golgi membrane, where copper can be incorporated into newly synthesized proteins or secreted from the cells (Figure 1.1).

1.3.2.1 The Atox1 copper chaperone

Atox1 was the first copper chaperone to be identified and it consists of 68 amino acids with a molecular mass of 7.5 kDa[51]. Atox1 contains the highly conserved copper binding domain, MXCXXC[51, 52], near its N-terminus where it binds copper with a K_b around 6×10^{17} M^{-1}[45, 53]. On its sequence Atox1 also contains a nuclear localization signal (NLS), KKTGK motif, near its C-terminus[51, 54]. In the human body the expression of Atox1 is abundant and is ubiquitously expressed in both peripheral tissues and in the central nervous system (CNS)[51]. In the brain, the highest protein levels of Atox1 were found in the choroid plexus and substantia nigra[45, 53].

Atox1, in addition to its function as a copper chaperone, has a suggested second role in mammalian cells that of a transcription factor. Studies from Itoh and colleagues have indicated that Atox1 functions as a copper dependent transcription factor which induces the expression of cyclin D1 and the extracellular Cu,Zn Superoxide Dismutase 3 (SOD3)[54, 55]. Cyclin D1, is an important regulator of G_1-S cell cycle progression and SOD3 is an extracellular enzyme that requires copper for its activity which acquires it through the secretory pathway[56]. Initially, Itoh *et al.* found that in mouse embryonic fibroblasts (MEFs) copper normally increases proliferation but in Atox1 deficient MEFs, their proliferation was decreases independent of copper concentration in their growth medium. It seems that in MEFs there is an Atox1 dependent increase in the mRNA and protein expression of cyclin D1[54]. The study from Itoh *et al.* established, for the first time, that copper can regulate the transcription factor function of Atox1 at multiple steps which include: nuclear transport, DNA binding to the promoter region of cyclin D1 and transcriptional activation[54]. In another study by Itoh and colleagues, it was demonstrated that Atox1 regulates not only the catalytic activity of SOD3 but also its transcription[55].

The importance of Atox1 in the body was also demonstrated by the effects of Atox1 gene disruption in mice[57]. Knockout mice face severe phenotypic alteration which includes failure to thrive, growth retardation, congenital eye defects, hypopigmentation and seizures[57]. The Atox1 knockout phenotype was similar to that observed in mice when they experienced a

copper deprived diet from early in life[58]. Also, the lack of Atox1 in cells resulted in accumulation and failure to excrete copper from the cells[57].

1.3.2.2 Copper-transporting P-type ATPases: ATP7a and ATP7b

Human cells contain two homologues of the copper ATPases: ATP7a and ATP7b[59, 60] which undergo ATP-dependent cycles of phosphorylation and dephosphorylation in order to catalyze the translocation of copper across cellular membranes[61]. ATP7a and ATP7b have a dual role in the cells: 1) a biosynthetic role, where they deliver copper to various secreted enzymes such as SOD3[62], tyrosinase[63] and peptidylglycine α-amidating monooxygenase (PAM)[64], and 2) a homeostatic role where they export excess copper from the cells[65]. Under normal conditions, ATP7a and ATP7b are localized to the trans-Golgi network (TGN) where they provide copper to cuproenzymes synthesised in the secretory pathway[60, 66].

ATP7a and ATP7b are 160-170 kDa membrane proteins with very similar structure and function sharing 60% amino acid identity[59]. Both ATP7a and ATP7b consist of eight transmembrane domains which form a pore through the cell membranes for copper translocation with a large cytosolic N-terminus domain which contains six copper binding domains with a conserved GMXCXXC motif[59]. ATP7a and ATP7b obtain copper through interaction with Atox1 copper binding domain which is similar to their own copper binding domains[67] and in order to translocate copper into the lumen of the Golgi ATP7a/b undergo cycles of phosphorylation dephosphorylation. Competition experiments were used to determine the K_b affinity of the six ATP7a and ATP7b copper binding domains and based on these experiments the six copper binding sites of ATP7b have a K_b varying from 2.2×10^{10} M^{-1} to 4.7×10^{10} M^{-1} [53]. Whereas ATP7a copper binding sites appear to have a higher K_b which is between the range of 9.6×10^{12} to 3.8×10^{14} M^{-1} [45, 53].

The mechanism that regulated the cellular copper levels, by the copper-ATPases transporters, is based on their cellular localization in response to changes in the intracellular copper concentration[68, 69]. When cellular copper levels are higher ATP7a and ATP7b will traffic from the TGN to the cell membrane in order to export the excess copper[70]. The mechanism of translocation of ATP7a/b has been observed in both polarized cells (Caco-2, HepG2, WIF-B)[70, 71] and non-polarized cells (CHO-K1, human fibroblasts, HeLa)[69, 72]. In non-polarized cells the transporters traffic to the plasma membrane and/or to distinct cytosolic vesicles close to the plasma membrane[69]. In polarized cells, ATP7a traffics from the TGN to a recycling vesicular pool which is located in the basolateral membrane[66, 70], whereas ATP7b traffics to

sub-apical vesicles[71]. When copper levels return back to normal/non-toxic for the cell type levels, ATP7a and ATP7b recycle back to the TGN[66, 68, 71].

ATP7a is ubiquitously expressed in all tissues except liver and according to some studies is important for the supply of copper both to and within the different brain regions[73]. ATP7a highest expression levels in the brain are detected in the cerebellum and on the basolateral surface of the polarized choroid plexus cells[48]. ATP7b expression has a more limited pattern, with liver being the highest expressing organ[74], where ATP7b is also the only copper-transporting P-type ATPase, with lowest levels observed in the kidneys, placenta, heart and brain[59]. ATP7b's function in the brain is not completely understood but ATP7b is expressed in many brain regions including the hippocampus, Purkinje cells in cerebellum, in cerebral capillaries and in the apical membrane of choroidal epithelial cells[48, 73].

The importance of ATP7a and ATP7b in the human body can be appreciated in cases where these genes are absent or inactivated as happens with the inherited disorders Menkes and Wilson's disease. Mutations in the ATP7a gene are responsible for Menkes disease which is mainly caused by impaired intestinal absorption that leads to systemic copper deficiency and eventually reduced activity of important copper binding enzymes[75]. ATP7b mutations lead to Wilson's disease where inactivation of ATP7b results in impaired copper excretion from the liver and consequently accumulation which results in hepatic copper overload, liver damage, apoptotic cell death and release of free copper into the plasma and CSF [74, 76]. In Wilson's disease copper deposition also occurs in the eye and the basal ganglia of the brain.

1.3.2.3 Secreted copper binding proteins

As already mentioned above quite a few secreted proteins require copper for their function or activity with the most abundant of them both being Cp which is a ferroxidase that contains copper and plays an essential role in iron homeostasis in mammalian cell[77]. Cp belong to a multicopper oxidase family of enzymes that utilizes the electron chemistry of bound copper ions to couple iron oxidation with the four-electron reduction of dioxygen[77]. In the human body Cp is synthesized in hepatocytes where it incorporates six copper atoms and is then secreted into the plasma where it carries 95% of the serum copper[78, 79]. Cp binds copper with K_b at the level of 10^5 M^{-1}[80]. Studies have shown that copper levels do not affect the rate of Cp synthesis or secretion, however failure to incorporate copper during its synthesis will result in unstable apo-protein that is devoid of oxidase activity and which starts degrading rapidly in the plasma[81]. In the brain, two different isoforms of Cp have been identified with one at approximately 135 kDa which may represent the glycosylphosphatidylinositol (GPI)-

anchored Cp (GPI-Cp) form of Cp that is bound to the cell membranes of astrocytes. The second isoform of Cp at 125 kDa may represent the secreted form of Cp (sCp)[82, 83].

1.3.3 The mitochondrial copper pathway

Mitochondria are dynamic organelles that localize within the cytosol and are essential for several cellular metabolic pathways[84, 85]. Mitochondria are responsible for the production of ATP through oxidative phosphorylation, serve as calcium stores and play an important role in programmed cell death[84, 85]. Mitochondria are also responsible for the production of the majority of the ROS in the cells since they are by-product of the oxidative phosphorylation[86]. The mitochondrion is surrounded by two phospholipid bilayer membranes, the inner and outer membrane, and together they create two different mitochondrial compartments: the internal matrix and the inter-membrane space (IMS)[84]. Mitochondria require copper for the function of cytochrome *c* oxidase (COX), the terminal enzyme of the respiratory electron transport chain (Figure 1.1). COX reduces molecular oxygen to water by using electrons from cytochrome *c*, and couples this to the pumping of protons from the matrix into the IMS [87].

Mammalian COX is a 205 kDa hetero-oligomeric complex that is localized in the inner mitochondrial membrane[88]. It consists of 13 subunits encoded by both mitochondrial and nuclear genes. The three mitochondria encoded subunits, COX1, COX2 and COX3, form the core of the enzyme which incorporates all necessary redox-active cofactors[88, 89]. The remaining 10 subunits are all nuclear encoded, synthesized in the cytoplasm and required for the stability/protection of the core enzyme and to regulate its activity[88, 89]. The enzyme was originally crystallized as a dimer with interaction between the subcomplexes taking place through COX6a and COX6b[88, 90]. The dimerization of COX probably plays a structural role which offers maximum stability to the complex[90, 91].

COX contains four redox-active centres which consists by two heme *a* moieties and three copper ions which are contained within the conserved domains of COX1 (*a*, a_3 and Cu_B) and COX2 (Cu_A). The mononuclear Cu_B sit in COX1 interacts with heme a_3 to form a heterobimetallic heme a_3-Cu_B centre[88, 92-94]. Whereas the Cu_A site contained within the COX2 exists as a cysteine-bridged, binuclear, mixed covalent centre (Cu^{2+}/Cu^{1+})[88, 92-94]. The oxygen reductions requires four electrons which are transferred from the reduced cytochrome *c* (Fe^{2+}-cytochrome *c*) to the Cu_A centre and subsequently to the low spin heme *a* which is located in COX1[88, 92-94]. From heme *a*, electrons are transferred intermolecularly to the heme a_3-Cu_B centre where the bound molecular oxygen which will be reduced to water (equation 1.3)[88, 92-94]. The K_b affinity has only been determined for the Cu^{1+} site of the COX2 and is

1.7 x 10^{16} M^{-1}[45, 95]. Copper is essential not only for the catalytic activity of COX but also for its biogenesis, assembly and stability. Studies have shown that when copper is absent from COX1 and particularly from COX2 that will initiate their degradation which will eventually lead to failure of the final complex assembly[96, 97].

$$4\ Fe^{2+}\text{-cytochrome } c + 8\ H^{+}_{in} + O_2 \rightarrow 4\ Fe^{3+}\text{-cytochrome } c + 2\ H_2O + 4\ H^{+}_{out} \qquad \textbf{(1. 3)}$$

Since the insertion of copper into COX takes place within the mitochondrial IMS, copper has to be transferred into mitochondria however how copper is trafficked to the mitochondria still remain an open question. Initially, several proteins (COX17, COX19 and COX23) have been considered for that role on the base of their dual localisation in both the cytosol and the mitochondrial IMS as well as on the base of the effects that they cause in COX activity on their deficiency[98-100]. Consequent studies have shown that none of this protein have any role in copper shuttling to the mitochondria but each protein has its own role within the IMS in copper trafficking[101, 102]. Recently, studies have shown that a labile pool of copper exist in the mitochondria of both yeast and human cells which was proposed to act as the source of copper for COX[101, 103]. The labile copper pool is formed by a low mass ligand complex that resides within the matrix and stably bind Cu^{1+} in an anionic complex (CuL)[101, 103].

By an unknown mechanism, copper from the mitochondria matrix pool will be used to metallate the COX17 in the IMS. COX17 is a small (7 kDa) cysteine rich protein that contains the CX_9C copper binding motif additional to that it has also two cysteines in close proximity to the CX_9C motif which will form a CC-Cu^{1+} binding site[104]. The K_b for COX17 has be determined as 5.7 x 10^{13} M^{-1}[45]. As already mentioned COX17 exist in both the cytosol and the IMS and initially was believed to be the chaperone that transports copper to the mitochondria. However, an elegant tethering experiment in yeast showed that COX17 does not need to leave the IMS in order to obtain copper and deliver to COX but it is possible to obtain copper within the IMS[101]. In the IMS COX17 can deliver copper to Sco1/2 and COX11 which eventually transfer copper to the Cu_A centre of COX2 and the Cu_B centre of COX1, respectively (Figure 1.2)[101, 105, 106]. The Sco proteins are integral inner membrane proteins components that are consisting by a globular copper binding domain which protrudes into the IMS[107]. A single Cu^{1+} binding site is formed by the cysteines residues of the CX_3C motif and the histidine residue found within the globular domain[108]. Both Sco proteins bind copper with similar K_b of 2.7 to 3.2 × 10^{15} M^{-1} [45]. Sco's are anchored in the inner membrane through a single N-terminal transmembrane helix which is more important for Sco1

function[109]. The conformer of Sco2 resembles that of Sco1 with the exception that Sco2 seems to exhibit greater conformational dynamics[110].

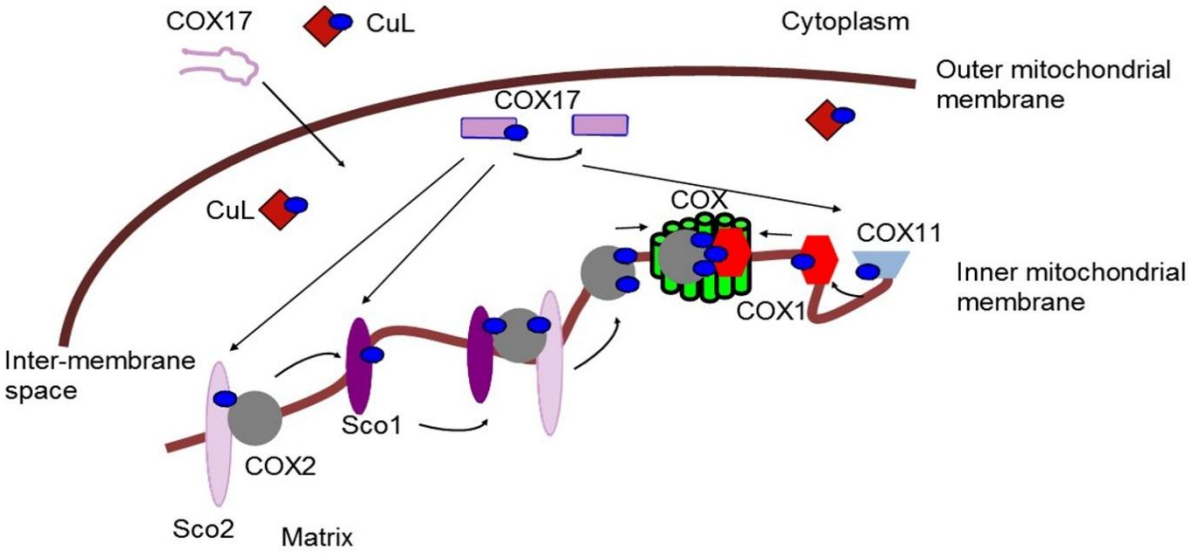

Figure 1.2 Copper Insertion into COX in the IMS.
Mitochondria obtain copper through an unknown copper ligand (CuL). In the IMS copper is bound to COX17 which delivers copper to either Sco1/2 or COX11. Sco1 with the collaboration of Sco2 transfers copper to COX2. COX11 transfers copper to COX1 which will then initiate the assembly of COX complex. Figure was adapted from Cotruvo *et al.*[43].

Studies in mammalian cells have shown that Sco1 and Sco2 have non-overlapping but cooperative functions in the maturation of the Cu_A centre of the COX2 subunit[111]. The specific mechanism of copper delivery to the Cu_A centre in COX2 by the Sco proteins has been studied mostly in human fibroblasts and the proposed mechanism suggests that Cu^{1+}Sco2 initially associates with the newly synthesized COX2 which then triggers the recruitment of Sco1 in the COX2-Sco2 complex. Then, Sco1 will obtain copper from COX17[111]. A temporally distinct complex consisting of Sco1-Sco2-COX2 is then formed (Figure 1.2)[111]. Copper is then transferred sequentially by each Sco protein to from the Cu_A centre which will result to the dissociation of the ternary complex and incorporation of the mature COX2 into the nascent complex that start to assemble[111]. After copper is transferred to COX2, Sco2 acts as a thiol-disulphide oxidoreductase in order to oxidize the cysteines of Sco1, a reaction that will prime the cysteines of both Sco1 and Sco2 ready to initiate a new round of COX2 synthesis and maturation[111]. The dissociation of COX2 from the temporal complex and insertion to the nascent complex is triggered by the full formation of the Cu_A centre and re-priming of the Sco cysteines[111]. What is not yet clear is whether Sco1 delivers both Cu^{1+} and Cu^{2+} ions in order to build the binuclear, mixed valence Cu_A centre in COX2, and if Sco1 does not undertake this role from where does COX2 obtain the Cu^{2+}[112]. Studies

in human fibroblasts have shown that COX2 requires copper insertion for maturation and stabilization and lack of the Cu_A centre will cause COX2 degradation[96, 113].

The Cu_B centre is located in the hydrophobic interior of COX1 formed by one copper ion coordinated with three histidine residues and is in close proximity with the heme a_3 group[88]. COX1 is the only universally expressed mitochondrial subunit of COX but how copper enters COX1 is not completely understood in mammalian cells although some studies from yeast propose a mechanism where the COX11 assembly factor is involved in the formation of Cu_B centre[106]. COX11 is anchored to the inner membrane by a single transmembrane helix whereas its C-terminal domain protrudes to the IMS where Cu^{1+} is also bound[114]. Cu^{1+} is bound to three conserved cysteine residues which seems to have an important role is COX function since mutations in these residues has as a result not only reduce Cu^{1+}-binding but also reduced COX activity[115]. Cu^{1+} transfer from COX11 to COX1 appears to occur in the nascent COX1 protein during its insertion and folding to the inner membrane[116]. Since the Cu_B site is heterobimetallic site consisting by Cu^{1+} and heme a_3, the insertion of copper to COX1 might happen parallel to the incorporation of heme a_3 in the protein[117].

The assembly process of COX has been identified by conducting two dimensional gel electrophoresis in human cell lysates and the results showed that the process takes place in three steps and is initiated around a seed formed by COX1[96, 118, 119]. The first step is the insertion of the metal co-factors (Cu_B and heme a/a_3) at COX1, which occurs after or during COX1 insertion into the inner membrane (subcomplex 1, S1)[96, 118, 119]. COX4 and COX5 are then added to the mature COX1 to form the S2 subcomplex[96, 118, 119]. Incorporation of the metallated COX2 and the remaining structural subunits (COX3, COX5b, COX6b, COX6c, COX7a or b, COX7c and COX8) will form the S3 subcomplex and the final complex (S4) will be formed with the insertion of the COX6a and COX7a or COX7b (Figure 1.3)[96, 118, 119].

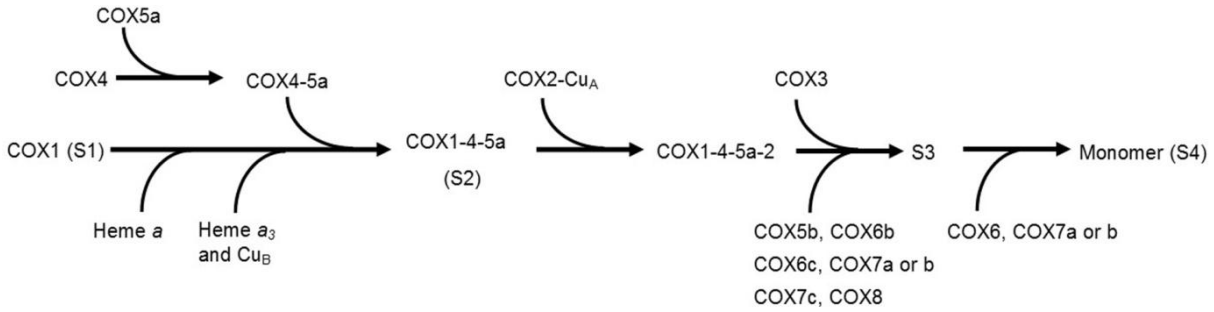

Figure 1.3 Proposed Model of COX Assembly in Human Cells.

The assembly of the COX initiated around a seed form by COX1. The different proteins and prosthetic groups are also indicated. Subcomplex, S1-S4, indicate the identified assembly intermediate. Dimerization of the 13 subunit holo-enzyme will form the final COX complex. (Adapted from Stiburerek *et al.*[88])

1.3.4 The copper pathway in the cytosol

In the cytosolic pathway, copper is delivered to Cu,Zn superoxide dismutase 1 (SOD1) by the copper chaperone for SOD1 (CCS) (Figure 1.1). SOD1 is a cytosolic enzyme that requires copper for its activity in the cellular antioxidant defence system. In mammals, CSS and SOD1 are ubiquitously expressed in all tissues and are mainly localized in the cytosol and to lesser extent in the mitochondrial IMS (<1%)[120-122]. Of the two cytosolic chaperones, CCS levels appears to be about ten times lower than that of Atox1 (3.2×10^5 copies of Atox1/cell compared to 1.5×10^4 copies of CCS/cell)[44]. CCS protein levels seems also to be less compared to SOD1 since studies in human cells have shown that its concentration is half relative to SOD1 (around 70-45 μM for SOD1 and 15-50 μM for CCS)[121, 123].

1.3.4.1 Copper chaperone for the Cu,Zn superoxide dismutase (CCS)

Almost 20 years ago CCS was identified by Culotta *et al.* as the copper chaperone that not only delivers copper into Sod1 in yeast cells but it is also responsible for its activation[124]. Culotta *et al.* used yeast cells mutated for the Ccs gene and transfection with a human CCS construct was able to restore yeast Sod1 activity[124]. The specific role of yeast Ccs was also indicated by the fact that in the mutant yeast cells for Ccs copper trafficking/activity in the other two pathways (secretory and mitochondrial) was not affected[124].

Human CCS is a homodimer of 30 kDa subunits and each monomer is composed of three different domains (D). An N-terminal (D1) which is structurally homologous to the yeast Atx1 (it has a ferredoxin fold) and contains the MXCXXC copper binding motif where Cu^{1+} is bound[125, 126]. It has been reported that the human D1 domain is essential for copper acquisition *in vivo*[127] whereas the yeast Ccs D1 is important for copper insertion into Sod1 under copper limited conditions *in vitro*[126]. D2 of CCS is structurally similar to SOD1 and mediates interaction with SOD1[128]. The human D2 is unable to bind copper however it binds zinc ions with the same ligands as SOD1, which are absent from the yeast D2 domain. Zinc binding to CCS seems to be important for CCS function since it contributes to CCS stabilization[129]. The C-terminal domain of CCS (D3) is a short 30-40 amino acid sequence that contains the CXC (Cys-246 and Cys-246) copper binding motif[126]. CCS D3 is highly conserved amongst organisms and is required for SOD1 activation[126]. The K_b has been determined for the different domains of CCS and the holo-protein which is on the range of 4.1×10^{14} to 5.5×10^{17} M^{-1}[45, 130]. The affinity for D1 was estimated at 5.5×10^{17} M^{-1} and for D3 of around 6.4×10^{16} M^{-1}[130]. D1 affinity for copper is 10 fold higher than that of D3 which further supports the opinion that D1 is important for copper acquisition[130].

CCS is ubiquitously expressed in the human body but highly expressed in the liver and kidneys[131]. CCS is also expressed in great abundance in the brain, where it is mainly detected in neurons, to a lesser extent in the astrocytes, and in the spinal cord where CCS is highly expressed in motor neurons[131]. The importance of CCS for SOD1 activity has been shown initially in studies with deficient Ccc yeast cells and was further established by studies with CCS knockout mice[124, 132]. The CCS knockout mice they were viable however the exhibit remarkable loss of SOD1 activity especially in the liver and kidneys, without the protein levels of SOD1 been effected[132]. Wong *et al.* were the first to report that in CCS deficient mice there was an alternative mechanism of copper acquisition for SOD1 since in some tissues SOD1 was active but at lower levels, a pathway that was later established by Carrol *et al.* in experiments with yeast systems (see section 1.3.4.2)[132, 133]. Another important finding from the Wong *et al.* study was that in the liver and kidneys copper incorporation to SOD1 was higher relative to fibroblasts or neuronal cells which probably implies that mammalian cells have different capacity for copper, where certain cells require higher intracellular copper concentration whereas other have lower requirements for copper[132].

Intracellular copper levels also seem to regulate the protein levels of CCS[127, 134, 135]. Initially, a study in rats on a copper deficient diet showed that CCS levels were 2 to 3 fold higher in tissues such as liver, heart, brain and kidneys but at the same time CCS mRNA levels remained unchanged which implied a post-transcriptional mechanism of CCS turnover[135]. Studies in different cell lines, (H4IIE, HepG2 hepatocytes and fibroblasts) investigated the effects of copper chelation on CCS protein expression[127, 134] and found that under low cellular copper levels, CCS shows increased protein stability but when copper levels return to concentration where they normally grow or to higher due to addition of extra copper, this promotes CCS degradation through the 26S proteasome[134]. A study in CCS knockout fibroblasts has shown that the CXC motif in D3 plays an important role in CCS copper-dependent regulation and turnover, since mutation of the two cysteines has the effect of making CCS unable to respond to higher or lower copper levels[127].

1.3.4.2 The Cu,Zn superoxide dismutase 1 (SOD1)

SOD1 is mainly found as a dimmer of 32 kDa which contains one copper and zinc ion per subunit and catalyses the disproportionation reaction of superoxide anion to oxygen and hydrogen peroxide at a bound copper ion (equation 1.4 and 1.5)[136]. This represents an important reaction for the cellular antioxidant defence system which prevents the oxidative damage of proteins, DNA and lipids[136]. SOD1 is a remarkable stable enzyme in the

homodimer form however the nascent monomer requires several post-translational modifications which includes incorporation of zinc and copper ion and the formation of intrasubunit disulphide bond between the Cys57 and Cys146 near the active site[137]. In a study conducted by Banci *et al.* they used cells that overexpressed SOD1 and grown without the addition of extra copper or zinc[121]. In that study they showed that SOD1 exists in two forms in a monomeric apo form (metal free) and a dimeric form where zinc is bound to each monomer of SOD1[121]. In these form of SOD1 the cysteines that are responsible for the formation of the intrasubunit disulphide bond were reduced[121].

$$O_2^- + Zn^{2+},Cu^{2+}\text{-SOD1} \rightarrow Zn^{2+},Cu^{1+}\text{-SOD1} + O_2 \qquad \textbf{(1. 4)}$$

$$Zn^{2+},Cu^{1+}\text{-SOD1} + O_2^- + 2H^+ \rightarrow Zn^{2+},Cu^{2+}\text{-SOD1} + H_2O_2 \qquad \textbf{(1. 5)}$$

A number of studies have tried to identify the mechanism of CCS-dependent SOD1 maturation and activation[121, 127, 138]. The current model of SOD1 activation by CCS was based on a study by Banci and colleagues in 2012 where they conducted experiments with electrospray ionization mass spectrometry and nuclear magnetic resonance (NMR)[138]. The proposed model for SOD1 activation involves at least six steps (Figure 1.4); initially, the nascent apo-SOD1 monomer acquires zinc from an unknown source creating the E,Zn^{2+}-SOD1 monomer a process which also provides structural integrity to the protein (Step 1)[138, 139]. The E,Zn^{2+} SOD1 will form a heterodimer with a Cu^{1+}-CCS (Step 2), D1 of CCS will transfer copper to SOD1 (Step 3) and then an important disulphide bond has to be formed in SOD1 which occurs into two sequential steps[138, 139]. In the first step, an intermolecular bond is formed between the Cys244 of CCS D3 with the Cys57 of SOD1[138, 139]. In the second step and with the presence of oxygen, an intramolecular disulphide bond will be formed in SOD1 between Cys57 and Cys149 (Step 4)[138-141]. It is worth mentioning that not only Cys244 but also Cys264 of D3 has an important role for the disulfide isomerase activity, since single site mutations reduce SOD1 oxidation rate in similar way to the double site mutations[138]. The mature SOD1 monomer will be released from the heterodimer (Step 5) and then will interact with another mature SOD1 monomer in order to form the final dimeric active SOD1 enzyme (Step 6)[138].

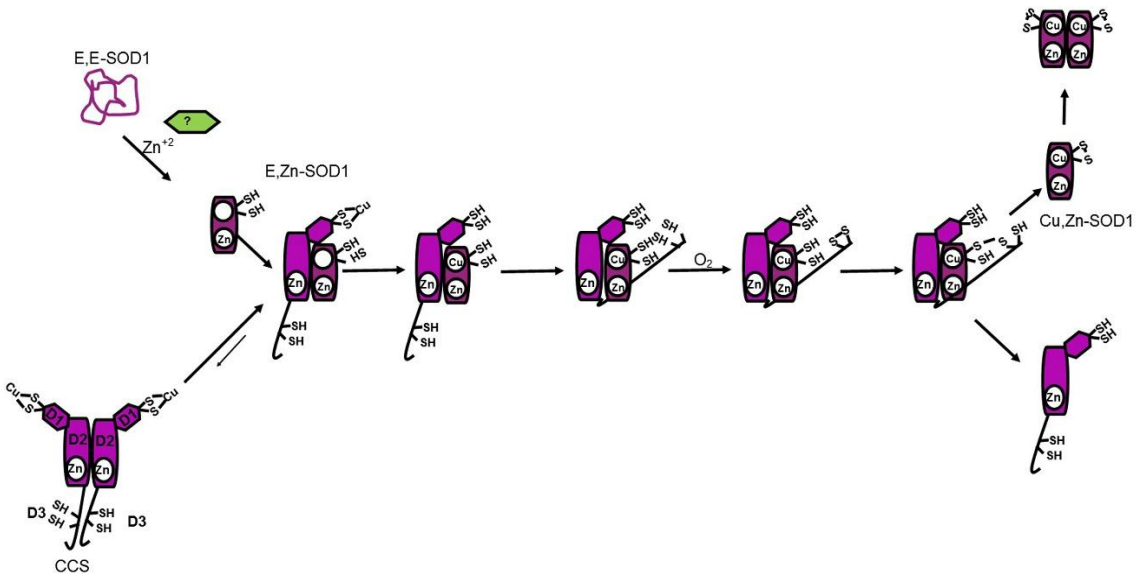

Figure 1.4 Proposed Mechanism of CCS Dependent Activation of SOD1.

SOD1 initially acquires zinc in the cytosol and then forms a heterodimer with copper loaded CCS. Copper will be transferred to SOD1 via D1 of CCS and then an intermolecular disulphide bond between Cys244 of CCS D3 and Cys57 of SOD1 will be formed. Consequently, in the presence of oxygen an intramolecular disulphide bond will be formed between Cys57 and Cys149 of SOD1 which will result in the formation of a mature SOD1. The final active enzyme will result after dimerization of the mature monomers. (Modified from Banci *et al.* 2012[130])

An *in vivo* study by Caruano-Yzermans proposed a slightly different mechanism based on experiments with CCS fibroblasts[127]. The proposed mechanism from that study supports that CCS delivers copper to SOD1 through a series of intra- and intermolecular transitions which includes copper movement from CCS D1 to the CXC motif on CCS D3, from where it will finally be transferred to SOD1[127]. Another major finding from the study from Caruano-Yzermans *et al.* was that the D1 in the human cells is required for the CCS-dependent copper delivery to SOD1 something which is not observed in yeast cells[126, 127]. Another study has tried to clarify the CCS-dependent activation of SOD1 by using in-cell NMR in transfected cells with SOD1 or CCS and found that only 25% of the cells overexpressing SOD1 had incorporated copper when grown in the presence of copper, and the remaining protein stayed unfolded and monomeric in the cytosol[121]. Copper loading into SOD1 and formation of the essential disulphide bond was only achieved in cells that co-express SOD1 and CCS[121]. The study from Banci *et al.* also established that CCS, promotes the formation of the disulfide bond in SOD1 in the absence of copper, a mechanism that is not observed in acellular systems[121].

CCS-independent activation of SOD1 was mainly studied by Culotta's group where they identified that mammalian or yeast cells that they did not express Ccs or CCS were still able

to maintain some of the activity of the human SOD1 and that the reduced GSH was required for the its activation[133]. Based on these studies, CCS-independent activation occurs rapidly *in vivo* within cells with pre-existing apo-SOD1 molecules and that the system used the same pool of available copper as the CCS-dependent activation pathway[141]. The formation of the important disulfide bond in SOD1 also occurred even under severe copper depletion conditions in the CCS-independent activation pathway[141]. Another difference between the two pathways is that in the CCS-dependent pathway, oxygen is essential for the activation of SOD1, but in the CCS-independent pathway, SOD1 can be activated under hypoxic or anoxic conditions indicating that oxygen is not required for activation of SOD1[141].

The importance of SOD1 in human development can be seen from knockout mice and disorders caused by mutations in the SOD1 gene. SOD1 knockout mice have reduced life span, develop liver cancers and exhibit peripheral neuropathy[142]. They also have increased oxidative stress and oxidative damage in all tissues which is accompanied by accelerated loss of skeletal muscle mass[143]. Mutations in the SOD1 gene are associated with the development of familial amyotrophic lateral sclerosis (FALS) a disorder characterized by selective degeneration of the motor neuron in the brain and spinal cord, leading to paralysis and death within five years[144]. More than 150 mutations, throughout the SOD1 gene have been linked with FALS where a toxic gain of function of the mutant protein is suggested since no loss of enzymatic activity is observed in the patients[145, 146]. The majority of SOD1 mutations in FALS will probably lead to protein misfolding and aggregation[147].

1.4 Alzheimer Disease (AD)

It has been more than 100 years since Alois Alzheimer first reported a case of a women who suffered from a peculiar type of dementia[148]. Clinically, dementia is defined as a syndrome characterized by decrease in cognitive abilities (memory, language, and learning), which are represented by a decline in the intellectual functions of the person sufficient to interfere with the everyday activities of that individual[149, 150]. Alzheimer's disease is considered to be the most common type of dementia and estimates that it contributes to more than 60 to 80% of the dementia cases in the elderly[151, 152]. AD is at the moment the fourth most common cause of death in the developing world and the estimated number of cases worldwide is around 30 million, a number which is expected to quadruple by 2050, making AD one of the most important global health issues[153]. In the UK the number of people affected by AD is more than half a million[154].

AD cases are divided into two broad categories arbitrarily based on the age of onset: the early onset or familial form of AD (EOAD) and late onset form of AD (LOAD). LOAD is the most common form of AD accounting for over 90% of cases with the clinopathological symptoms starting to appear after 65 years of age and its development has been correlated with genetic risk factors such as apolipoprotein E (ApoE) and advancing age[155]. EOAD is normally considered to be a much rarer disorder with the majority of symptoms starting to appear from 30 to 65 years and accounts for less than 10% of the AD cases[156]. Perhaps more than 20% of the EOAD cases belong to the familial AD cases which are due to the autosomal dominant inheritance of fully penetrant mutations in the presenilin 1 (PSEN1), presenilin 2 (PSEN2) or amyloid precursor protein (APP) genes[157]. Whilst both types show the classical symptoms and pathological features of AD, EOAD tends to be a more severe disease both clinically and pathologically[158, 159]. The main stratification criterion between the EOAD and LOAD cases is based on the age of onset where patients starting developing AD before the age of 65 will be categorised as EOAD cases whereas the rest as LOAD.

AD affects people in different ways but in both EOAD and LOAD the initial symptom is gradually worsening ability to remember new information. Some of the most common symptoms of AD are: memory loss that disrupts daily life, challenges in planning or solving problems, confusion with time or place, changes in mood and personality, including apathy and depression[160]. The above symptoms are correlated with the neuropathological findings of the disease which are progressive neuronal loss in key brain areas such as cortex and hippocampus, brain atrophy, amyloid containing senile plaques and neurofibrillary tangle (NFT) formation (Figure 1.5)[160].

Neurofibrillary tangles (NFTs) are intracellular structures composed mainly from the hyperphosphorylated, aggregated form of the microtubule-binding protein, tau (Figure 1.5B)[161]. Tau is synthesized and produced in all neurons and its normal function is binding to tubulin and stabilization of microtubules[162]. In AD, tau becomes hyperphosphorylated which causes tau proteins to fold from an unfolded monomer to a more structured form as paired helical filaments (PHF) which are capable of self-aggregating[161]. Ultimately that will lead to the formation of NFTs as large accumulations of PHF in the cell bodies and dystrophic neurites[161]. In the brain, NFTs are mainly detected in the trans-entorhinal and entorhinal layer, but at later stage of the disease they are spread throughout the brain from allocortex and into neocortex[163]. The aggregated forms of tau can cause cytotoxicity which leads to neuronal death, also the increased density of the NFTs is correlated with the severity of the clinical pathology of the disease[161].

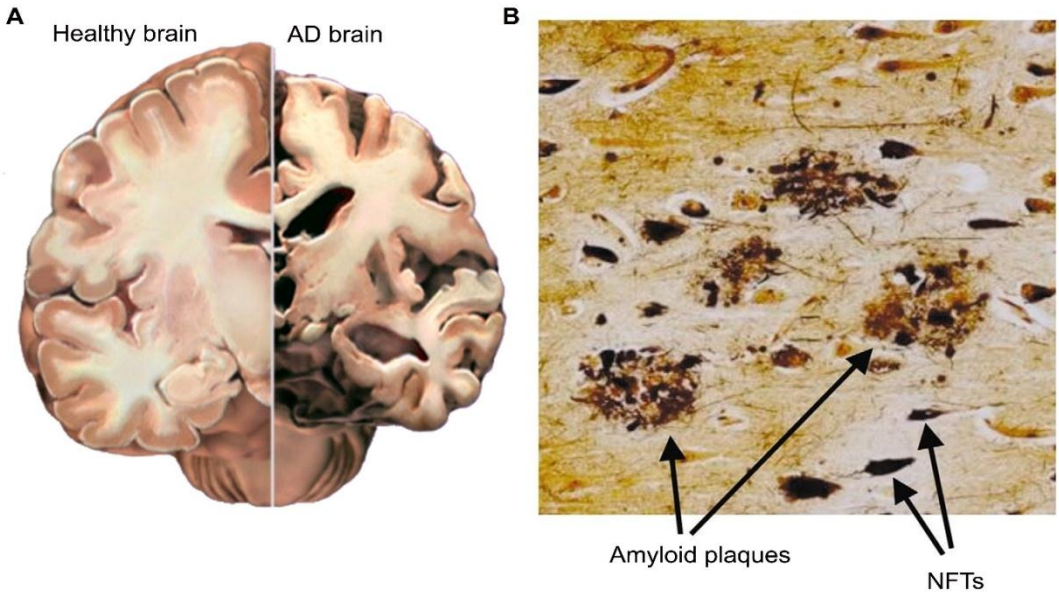

Figure 1.5 Pathological Characteristics of the AD Brain

(**A)** Cross sectioning of an AD brain that shows atrophy and shrinking relative to healthy brain. (**B)** Immunostaining for the identification of amyloid plaques and NFTs in AD. (Obtained from Blennow *et al.*[144])

Amyloid plaques are accumulations of a hydrophobic peptide in the extracellular space of the brain. The principal component of plaques is the amyloid beta (Aβ) peptide; a 38- to 43-amino acid peptide derived from the amyloid precursor protein (APP) which is formed by β-secretase (BACE1) and γ-secretase cleavage of APP (Figure 1.5B and 1.6)[164]. Within plaques, Aβ is present as aggregated insoluble forms including fibrils, as well as oligomers[165]. AD is considered as a disorder of protein aggregation in which the accumulation and aggregation of Aβ peptide and tau are the main pathological hallmarks of the disease. However, there are many additional cellular pathways, processes and molecules involved in AD pathogenesis, which may play an important role in the progress of the disease.

1.4.1 The amyloid pathway

It is more than twenty years since the amyloid cascade hypothesis was first used to explain the cause of AD pathogenesis[164]. According to that hypothesis, an imbalance between the production and clearance of Aβ in the brain is the initiating event for the pathogenesis of the disease, which will ultimately lead to neuronal degeneration and dementia[164, 166]. Aβ levels can be elevated by an imbalance between Aβ production and/or clearance, with increased Aβ production suggested to characterise more the EOAD cases and decreased Aβ clearance the LOAD[164-166]. The amyloid cascade hypothesis was initially based on finding from *in vitro*

and *in vivo* studies, but later it was further supported by the identification of genetic mutations associated with EOAD cases[166, 167].

The presence of Aβ in the brain is suggested to trigger various events which lead to neuronal damage, mitochondrial dysfunction, activation of oxidative stress, an inflammatory response, decreased neuroplasticity and apoptosis[166]. The above events are initiated by increased $A\beta_{42}$ oligomer formation, which causes subtle, then severe and ultimately permanent changes in synaptic function[168]. In parallel, $A\beta_{42}$ forms microscopic deposits in the brain parenchyma, which appear first as relatively benign diffuse Aβ accumulation and as they begin to acquire more fibrils of Aβ and a transformation into compact Aβ occur, the local inflammatory response (microgliosis and astocytosis) is initiated which further contributes to synaptic spine loss and neuronal dystrophy[168, 169]. Overtime, these events result in oxidative stress, altered metal (for example copper) homeostasis and other additional biochemical changes. The cascade culminates in widespread synaptic/neuronal dysfunction and cell death, leading to progressive dementia associated with Aβ pathology[164, 166, 170].

The amyloid cascade hypothesis seems to explain and incorporate several aspects of AD pathogenesis, such as pathology, phenotype occurring by gene mutations and genetic risk factors, but there are a few limitations regarding that hypothesis. First, neuropathological studies have failed to find any significant correlation between the Aβ amyloid plaque density and the severity of dementia[171]. The presence of the Aβ peptide in the non-demented elderly people which in some cases is comparable with those found in AD patients is not consistent with the hypothesis[171]. Second, the majority of the cell and animal studies concerning AD are based on mutations associated with EOAD cases which accounts for only a minority of the dementia cases and not with LOAD which is far more common but without any associated mutations and with only a few risk factors contributing to its progress[172]. This hypothesis does not consider the interaction of Aβ with NFTs which are also present in the AD brain[173]. Mutations in tau protein have been correlated with another type of dementia, autosomal dominant frontotemporal lobar degeneration, where tau pathology is similar to AD but the patients lacks the presence of Aβ plaques[173]. Thus, tau pathology can cause, on its own, neuronal loss and dementia.

1.4.1.1 Amyloid precursor protein (APP)

APP is a type I transmembrane glycoprotein which is expressed in both neuronal and extra-neuronal cells, and in most cells of the body[174]. APP is conserved between organisms and is member of a family that includes the APP-like proteins, APLP1 and APLP2[175]. APP has

three different major isoforms within the brain (APP_{695}, APP_{751}, APP_{770}) with all three containing the Aβ sequencing, but the APP_{695} is the most abundant and highest expressed in neuronal cells[176, 177].

Structurally, APP consists of a small cytoplasmic tail and a large extracellular domain, which consists of an E1 and E2 domain (Figure 1.7A)[178]. The E1 domain is a cysteine-rich region which is further subdivided to growth factor domain (GFD) and copper binding domain[179]. After the cysteine-rich region the next domains are, in order: an acidic-rich region, a Kunitz-type protease inhibitor (KPI) domain, an OX2 domain, a glycosylated E2/CAPPD domain, an unstructured domain immediately before the transmembrane domain and a small cytoplasmic tail which is involved in various cellular processes through a variety of protein interactions[176, 180, 181]. The range of APP isoforms occurs due to alternative splicing and in particular of exon 7 and 8 which contain the KPI and OX2 domains[176, 181]. The Aβ region itself includes 28 amino acids from the unstructured extracellular domain and 12-14 amino acids from the transmembrane domain[174].

The normal role of APP in the brain and other organs is not fully understood but is under intensive study attempting to explain its function. One proposed function of APP is related to cell-cell interaction and cell-substrate adhesion which are consistent with its role in developmental processes[182]. Some of the functions that APP is involved are: migration of neuronal precursor cells to the nascent cortical plate[183], cell cycle progression of neural stem cells [184], formation of neuromuscular junctions[185] and involvement in homeostasis of important metals such as calcium and copper[186, 187].

In cells, APP is metabolized by two alternative pathways, the non-amyloidogenic and the amyloidogenic[188]. In the non-amyloidogenic pathway, which accounts for more than 90%, α-secretase cleaves APP within the Aβ sequence and generates the soluble N-terminal ectodomain (sAPPα) and a C-terminal fragment C83 (CTFα)[189, 190]. Then γ-secretase cleaves the C83 fragment into a small nontoxic peptide, p3, and to the cytoplasmic polypeptide APP intracellular domain (AICD)[168]. In the amyloidogenic pathway, BACE1 cleaves APP in order to produce the N-terminal ectodomain (sAPPβ) and a C-terminal fragment, C99 (CTFβ) which is subsequently cleaved by γ-secretase to generate the Aβ peptide and AICD (Figure 1.6)[191].

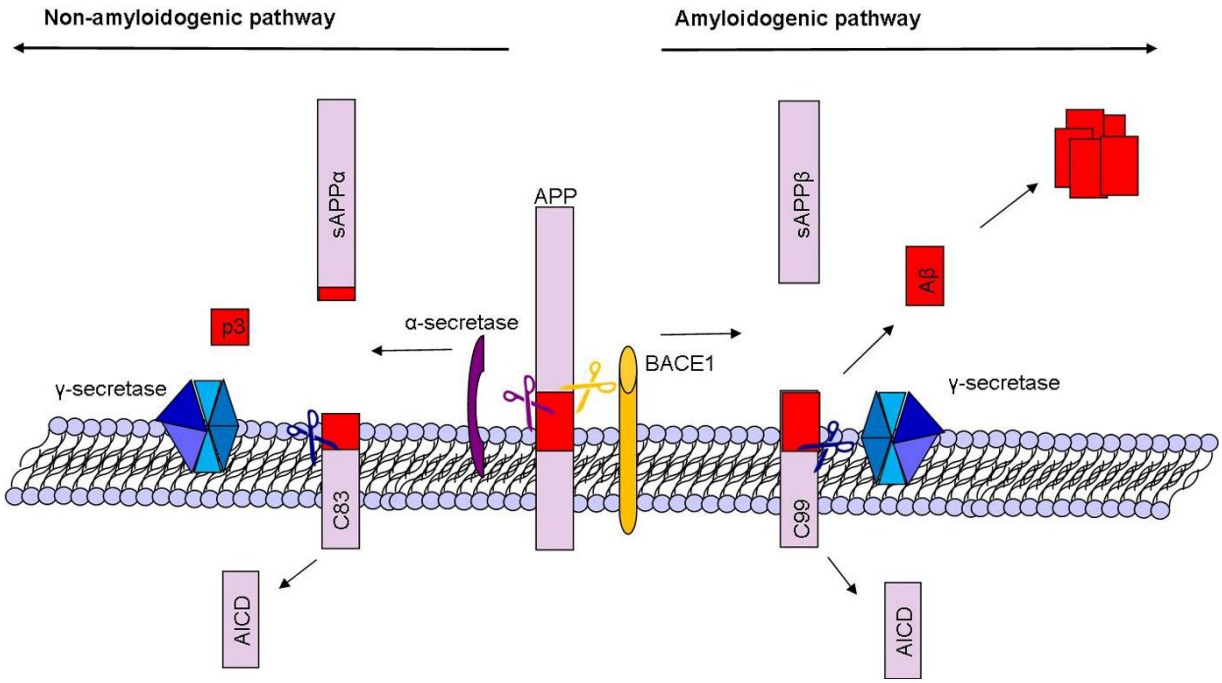

Figure 1.6 Diagram Representation of the Two APP Processing Pathways.

In the non-amyloidogenic pathway α-secretase cleaves APP within the Aβ sequence and produces the soluble extracellular sAPPα fragment and C83 membrane bound domains. Then γ-secretase will cleave C83 which will produce the intracellular AICD and the small p3 peptide. In the amyloidogenic pathway BACE1 cleaves initially APP and produces the soluble sAPPβ and the C99 fragment which will be further cleaved by γ-secretase in order to generate the different Aβ peptides and AICD. Different Aβ peptides aggregate under certain conditions and eventually will form the Aβ amyloid plaques. (Adapted from Zhang *et al*[178])

APP metabolism appears to involve an interaction with copper. APP structure has a copper binding site and several studies have shown that plays an important role in copper metabolism[179]. APP strongly bind Cu^{2+} (K_b around 10^8 M^{-1}) and reduce it to Cu^{1+} *in vitro*[192, 193]. Studies in mice and different cells have shown that copper can regulate both the expression and localization of APP in the cells[187, 194]. Knockout mice for APP contained higher copper levels in the cortex, and mice that overexpressing APP had lower copper levels in the brain relative to controls[195]. Further studies with mouse primary cortical neurons have shown similar results with the mice but when APP was overexpressed in Human Embryonic Kidney cell (HEK293) copper was accumulated in the cells which was attributed to increase APP-mediated capacity to reduce extracellular Cu^{2+}[196, 197]. Another point of conflict, about APP function in copper homeostasis, concerns the role of APP in copper induced toxicity where in primarily cortical neurons APP levels were correlated with increased sensitivity to copper but in HEK293 cells APP acted protectively against copper induced toxicity[195, 197, 198].

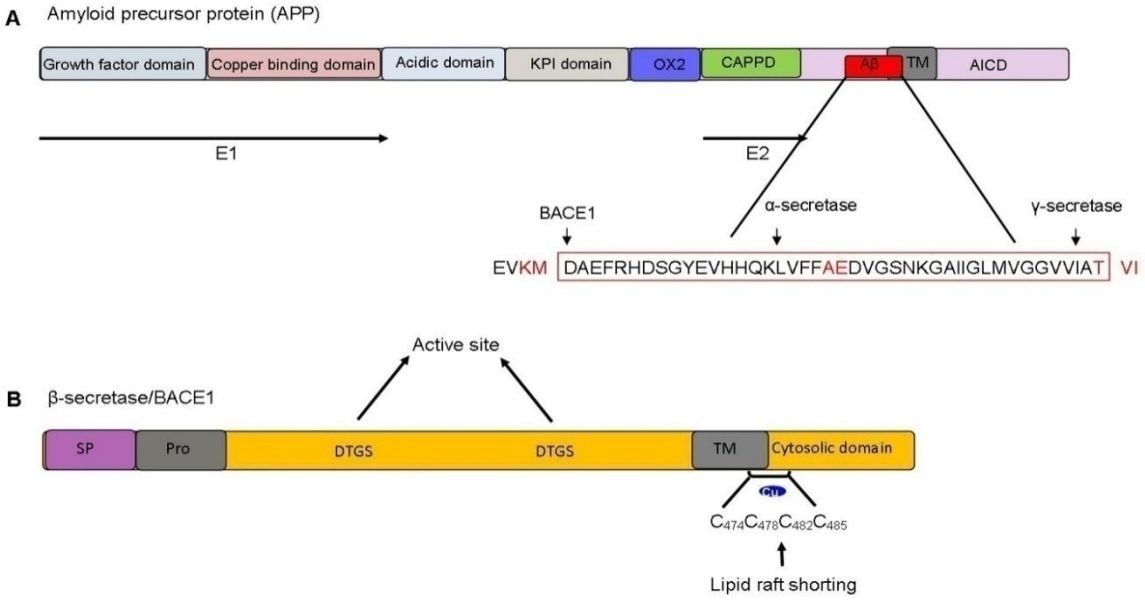

Figure 1.7 Schematic representation of APP and BACE1 structure.

(A) The APP family contains the conserved E1 and E2 domains in the extracellular region. The extracellular domains are subdivided into growth factor domain, copper binding domain, acidic domain, KPI domain, OX2 an unstructured domain, the glycosylated CAPPD domain and the Aβ domain. The inset displays the Aβ sequence along with the cleavage sites for each secretase. The amino acids highlighted in red are mutations that have been identified to correlate with increase/decrease activity of the respective secretase. (Adapted from Barnham *et al.*[169]) **(B)** Schematic representation of BACE1 structure. BACE1 is synthesized as a precursor protein with a signal peptide (SP) and a pro-domain (Pro), both of which are removed in the Golgi network. The mature BACE1 is inserted into membrane through a single transmembrane domain which places the two active sites (DTGS) on the extracellular part. The small cytoplasmic domain of BACE1 contains four cysteine residues that undergo palmitoylation where also copper is bound with high affinity. (Adapted from Kandalepas *et al.*[201])

A number of mutations have been identified in APP gene and are known to cause the inherited form of EOAD. The majority of them are missense mutations located in exons 16 and 17 which places them at either close to C-terminal γ-secretase cleavage site or to N-terminal BACE1 cleavage site[199]. Also, another mutation has been identified inside the Aβ sequencing close to α-secretase cleavage site[200]. The above mutations have different effects to Aβ production which can lead to selective increase of Aβ peptides ending at 42/43, increased heterogeneity of secreted Aβ peptides, increased hydrophobicity or enhanced protofibril formation[201, 202]. Recently, a coding mutation has been identified in APP gene, close to BACE1 cleavage site, that acts protectively against AD and cognitive decline in the elderly people without AD[203]. Studies in cells transfected with that protective mutated variant of APP showed decreased production of sAPPβ ectodomain which was also accompanied with slightly higher levels of sAPPα ectodomain[203].

1.4.1.2 The β-site APP-cleaving enzyme (BACE1) as β-secretase

Almost two decades ago, five independent groups identified the β-site APP-cleaving enzyme (BACE1) as β-secretase[204-208]. The five groups used different approaches, such as cloning, genomic strategies and biochemical purification, which established BACE1 as β-secretase. Some of the observations which characterized β-secretase as BACE1 was that both of these enzymes activities are predominantly expressed in the brain[206, 209], required a low pH range in order to be active[206], and for that reason they primarily localized within endosomes and the Golgi apparatus[206].

The specific role of BACE in the amyloid pathway was also confirmed with overexpression or gene silencing studies for BACE1. Accordingly, overexpression of BACE1 in cells which also co-expressed the wild-type or Swedish mutated APP, led to increase production of Aβ, which was accompanied by increased production of C99, sAPPβ and decreased levels of sAPPα[204-208]. Both gene interference experiments in cells and BACE1 knockout mice showed that BACE1 deletion was responsible for the decreased production of both Aβ and sAPPβ which was also consistent with increased levels of sAPPα[206, 207, 210]. The cleavage specificity of BACE1 was confirmed by sequencing and mass spectrometry which revealed that BACE1 cleaves APP only at Asp^{+1} or Glu^{+11} [205, 206]. The specificity of BACE1 was further demonstrated by experiments with APP carrying the Swedish mutation where BACE1 was able to cleave APP at higher rate relative to wild type APP[206, 208].

BACE1 gene encodes for a 70 kDa type I transmembrane aspartyl protease related to pepsins and retroviral aspartic proteases[204-208]. The structure of BACE1 consists of an N-terminal signal peptide, followed by a pro-domain, a protease domain, a single transmembrane domain and short cytosolic domain (Figure 1.7B)[204-208, 211]. The protease domain consists of two aspartic active site motifs which are spaced 200 residues apart and contain the highly conserved sequence defining the aspartic proteases, DT/SGS/T[206]. The N-signal peptide is responsible for BACE1 translocation to the endoplasmic reticulum where BACE1 is glycosylated at four asparagine residues and transiently acetylated on seven arginine residues[212]. After translocation into Golgi apparatus, complex cardohydrates are attached to BACE1 and the N-terminal signal peptide together with the pro-domain are removed[204, 213, 214]. After maturation, BACE1 is transferred from the trans-Golgi network to the cell surface where it undergoes recycling between the early endosomes and the plasma membrane[215, 216].

BACE1 is susceptible to other post-translation modifications which occur mainly in the cytoplasmic domain. The C-terminal domain is phosphorylated at Ser 498 which together

with a di-leucine motif regulates BACE1 recycling between the cell surface and the endosomal compartments[215, 216]. BACE1 also undergoes palmitoylation at four cysteine residues, which facilitates BACE1 targeting to lipids rafts[217]. Those cysteine residues are also responsible for binding Cu^{1+}[218]. BACE1 binds copper with high affinity (K_b 2.3 x 10^{17} M^{-1}) and it is postulated that BACE1 obtains copper through interaction with cytosolic CCS[130, 218]. BACE1 interaction with copper homeostasis has also been studied where it has been found that BACE1 overexpression causes reduced SOD1 activity in cells, which might correlate with reduced availability of CCS for SOD1 activation or by directly influencing copper loading into SOD1 by favouring copper transfer to BACE1[218]. A study with known copper chelator, trientine, has shown that copper chelation reduces BACE1 protein and activity levels without effecting BACE1 mRNA levels[219].

Several studies have measured BACE1 protein levels and activity in the AD brain and they showed that BACE1 levels were increased by 2-fold in frontal and temporal cortex, which was accompanied by higher levels of its proteolytic products and activity[220, 221]. Mutations in the APP gene, close to the BACE1 cleavage site, have been associated with both EOAD pathology and a decreased risk for AD which signifies the importance of BACE1 in AD progression[203]. Based on the role of BACE1 in AD pathogenesis, on its properties, and on the finding that initial analysis from BACE1 knockout mice did not reveal any effect on gross behaviour, neuromuscular function, tissue morphology or histology, BACE1 inhibitors have become one of the most promising therapeutic targets for AD[210, 222].

1.4.1.3 The γ-secretase complex

The γ-secretase complex belongs to a family of intramembrane proteases which are characterized by fact that they are able to cleave their substrates within the lipid bilayer, with a process termed as regulated intramembrane proteolysis[223]. γ-secretase is a 230 kDa complex consisting of four subunits, the presenilins (PS, PSEN1 and PSEN2), nicastrin, anterior pharynx defective (APH -1) and presinilin enhancer 2 (PEN-2)[224]. The catalytic core of γ-secretase consists of a PS, which are multi-transmembrane proteins with more than nine transmembrane domains, with the N-terminal domain located in the cytosol and the C-terminal domain exposed to the luminal/extracellular space[225]. Full length PS is inactive and requires endoproteolytic cleavage between the transmembrane domain 6 and 7 of the nascent protein which generates a 28 kDa N-terminal fragment (NTF) and a 17 kDa C-terminal fragment (CTF)[226]. PS, NTF and CTF bind to form the stable and active PS heterodimers at 1:1 stoichiometry[226].

In order to form a stable, mature and active PS the presence of the other components of the γ-secretase complex is necessary. Nicastrin is a 130 kDa type I transmembrane protein which acts as a scaffolding protein within the complex[227]. The proposed role of nicastin is to bind, with its free N-terminal ectodomain, the different substrates of γ-secretase, acting as substrate receptor[228]. PEN-2 is a transmembrane protein and its function is probably related to PS stabilization within the complex[229]. APH-1 function is still not clear but some studies suggest that one of its roles is to contribute to the assembly and activity of the mature complex and to present substrates to PS[230, 231].

Until now more than 150 mutations, responsible for EOAD, have been identified in both PSEN1 and PSEN2 genes, with the majority of them within the *PSEN1* gene[232]. Mutations in PSEN1/2 are most likely linked with APP processing and all appear to increase the production of $A\beta_{42}$, which is considered to be more prone to form aggregates[233]. These mutations also seem to affect APP trafficking in the cells which results in decreased delivery of APP to cell surface and enhancement of the amyloidogenic pathway by increasing the Aβ production[234].

1.4.1.4 The β-amyloid peptide (Aβ)

Amyloid fibrils are self-assembled, fibrillar structures of small peptides that are able to fold in an alternative, β-rich form[235]. Amyloid plaques in the AD brain are mainly composed by Aβ peptides ranging from 39 to 43 amino acids, with the two major forms being the $A\beta_{40}$ which is prevalent under normal conditions and the $A\beta_{42}$ which is the major component of the diffuse plaques[164]. These peptides are composed of the hydrophilic N-terminal and a hydrophobic C-terminal[164]. Normally, Aβ forms amyloid fibrils by conformational changes from the native random coil state to an α-helical intermediate which results in the formation of a β-sheet amyloid monomer that is able to self-aggregate into fibrils[236].

Changes in Aβ metabolism are considered as the initiating factors that lead to the final formation of plaques. One initial factor is the increased accumulation of the total Aβ which probably occurs due to either increased production and/or reduced clearance[164, 166]. The enhanced $A\beta_{42}$ accumulation in the AD brain has as a result, an increased $A\beta_{42}$/ $A\beta_{40}$ ratio which leads to oligomer formation and gradually to benign diffuse (non-fibrillar) Aβ plaque formation[164, 166]. Diffuse plaques start to acquire more Aβ fibrils and eventually form the final aggregated (insoluble) forms of Aβ[164, 166]. These amyloid plaques are also surrounded by swollen, degenerating neurites, and increased microgliosis and astocytosis[237].

Synchrotron based infrared imaging, X-ray imagining and X-ray emission studies have shown that inside senile plaques metals are also present including copper, zinc, iron and

manganese[238, 239]. Copper is able to bind to multiple sites in the first 16 amino acids of the Aβ peptide with affinities (K_b) varying from 0.025 to 40 nM^{-1}[238]. Because Aβ has strongly redox-active properties it makes able to reduce both iron and copper upon binding *in vitro*[240]. When bound to Aβ, metals can reduce molecular oxygen to H_2O_2 and the latter to $OH^{\bullet}$ which have as a consequence the generation of ROS directly (Figure 1.8A)[240, 241]. The amount of reduced ions and ROS are dependent on the length of the Aβ peptide, generally $Aβ_{42}$> $Aβ_{40}$>> $Aβ_{28}$, a chemical relationship which is possibly correlated with the neurotoxicity of these peptides[240]. *In vitro* studies have shown that Aβ binds copper with differing stoichiometry which affects both the H_2O_2 degradation and Aβ plaque formation[242]. Generally, in 1 copper: 1 Aβ stiochiometry, the highest H_2O_2 degradation was observed where Aβ plaques starting forming non-fibrillar aggregates (Figure 1.8B)[242]. These observations suggest that copper is potentially able to trigger Aβ plaque formation in the AD brain[238].

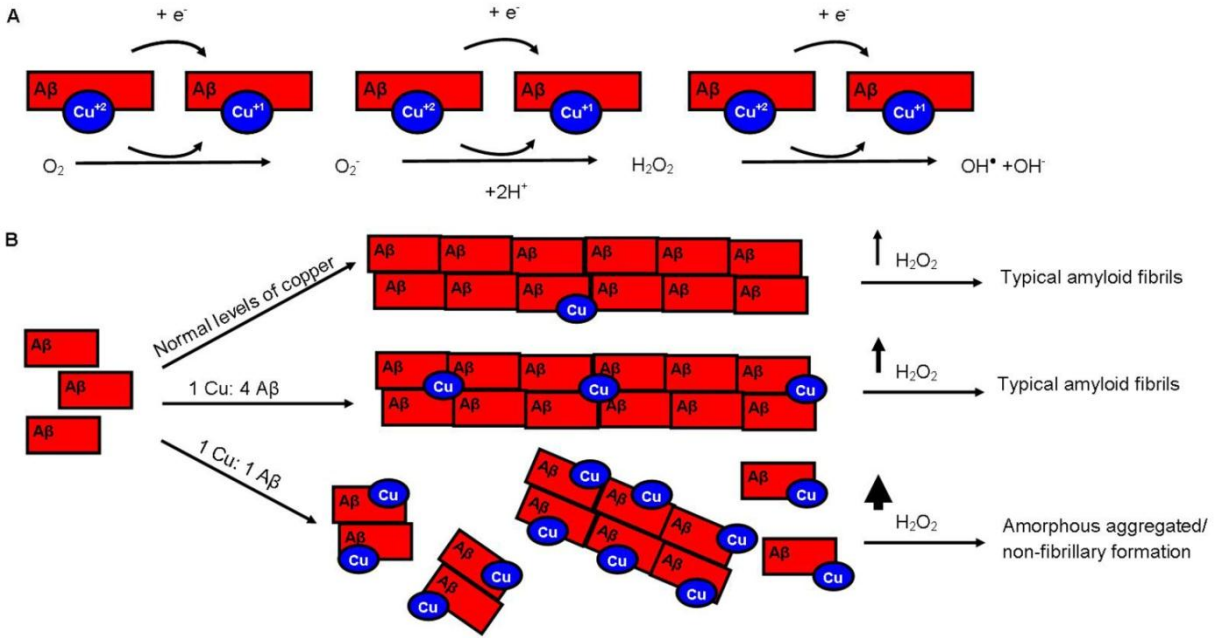

Figure 1.8 Copper and Aβ Interaction

(A) Proposed mechanism of ROS production by the redox active Cu-Aβ peptide. (Adapted from Pithadia *et al* 2012[231]). **(B)** Incubation of Aβ peptide with copper induces the formation of distinct aggregates which has a different capacity for H_2O_2 degradation. Without exogenous copper addition or at a ratio of 1 copper: 4 Aβ peptides, Aβ forms typical amyloid fibrils and H_2O_2 degradation is equivalent to copper concentration. In 1:1 ratio higher degradation of H_2O_2 is observed and Aβ forms amorphous/non-fibrillaly aggregates (Adapted from Mayes *et al.*[233])

1.5 The function of copper in the healthy brain and its association with AD

After absorption from the small intestine copper is delivered to the liver or kidneys for utilisation. In the liver, copper will be incorporated to Cp and secreted into blood in order to

be transferred to different tissues and organs. In serum, the majority of copper is tightly bound to Cp (60-70%) and the rest loosely bound to Ab, transcuprein and amino acids[243].

1.5.1 Copper metabolism and function in the healthy brain

Copper is the third most abundant metal in the brain after iron and zinc indicating the significance of this metal for the brain function[17]. In the brain copper will be delivered from these molecules and its transportation into the brain is regulated by the brain's vascular barrier system[50]. The brain barrier system consists of the blood-brain barrier (BBB) and the blood-cerebrospinal fluid barrier (BCB) [244]. The BBB functions to separate the blood circulation from the brain interstitial fluid, and BCB to separate the blood from the CSF[244]. The absence of any barrier between CSF and interstitial fluid allows the free exchange of fluids[244].

The BBB continues where the brain capillaries extended into the whole brain, is structurally composed by epithelial cells that line with the cerebral capillaries and have tight junctions between the adjacent cells[244]. The permeability across the BBB is highly dependent on the size and lipophilicity of the molecules; more complex molecules being transported through certain pathways at the BBB[244]. BCB is located within the choroid plexus, a vascularised and polarized tissue, which is located on top of the four brain ventricles, and its main structure is the tight junction of choroidal epithelial cells[244].

The exact mechanism of copper import-export in the brain is not completely understood but it is postulated that copper coming from the blood stream enters the brain mainly through the BBB[50, 243, 245]. Copper is primarily transported as free, unbound ions which are taken up by Ctr1 in cerebral capillary epithelial cells, and from there copper chaperone Atox1 delivers copper to ATP7a/b which then translocates copper to the abluminal membrane in order to release copper into the brain interstitial fluid for further transport and metabolism[50, 243, 245]. Copper may flow from the brain parenchyma to the CSF within the brain ventricles, where once again it can be imported to choroidal epithelial microvilli by either Ctr1 or DMT1[50, 243, 245]. Small amount of copper can also be removed by the CSF bulk flow to the arachnoid granulations for excretion from the brain (Figure 1.9)[50, 243, 245].

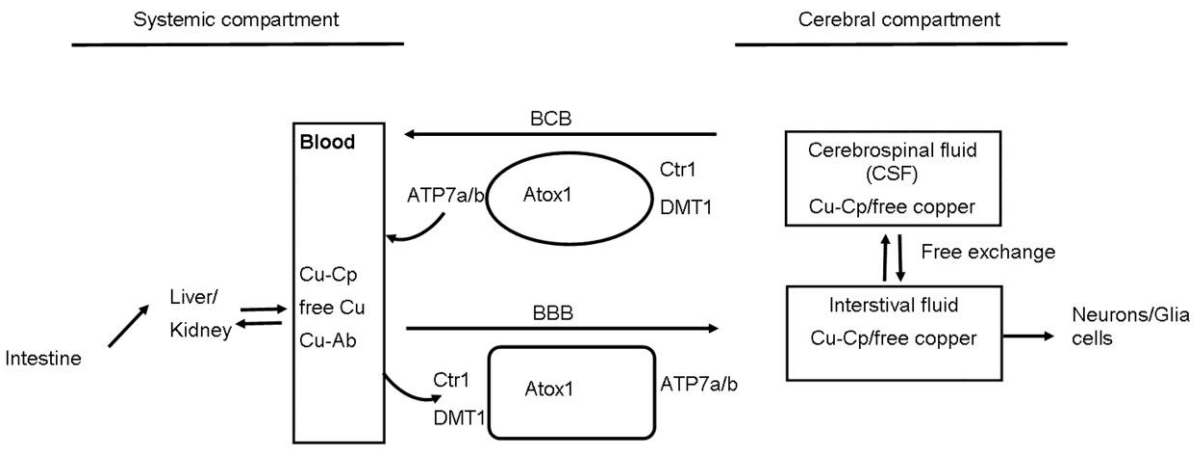

Figure 1.9 Copper Transportation in the Brain is Regulated by the Brain Barrier System. Free copper or bound to Cp and other proteins are transported, at the BBB, into cerebral endothelial cells by Ctr1 or DMT1. Atox1 will then deliver copper to ATP7a/b in order to export into interstitial fluids, where copper can be utilized by neurons or glial cells. Excess of copper is released to the CSF where is taken up by Ctr1 and DMT1, at the BCB, and within choroidal epithelial microvilli where is released back to the blood. (Adapted from Zheng *et al.*[(49)])

The normal healthy brain contains about 3.1 to 5.1 μg/ g wet tissue copper and the CSF contains about 0.3 to 0.5 μM of copper, but copper is not evenly distributed in the brain[(15, 48)]. Generally, grey matter has more than twice the amount of copper (1.6-6.5 μg/ g wet tissue) relative to the white matter (0.9-2.5 μg/ g wet tissue)[(16, 246)] . Substantia nigra and locus coeruleus are the highest copper containing regions amongst the other brain regions, since they both are pigmented tissues which contain catecholaminergic cells that require copper for their cellular processes[(16, 48)]. On the other hand, the thalamus is the brain region with the lowest copper levels[(247)]. A recent study that used Laser Ablation Inductively Coupled Plasma Mass Spectrometry (LA-ICP-MS) was able to identify differences in copper concentrations in the levels of individual cell populations in the brain, and they found that glial cells are most enriched in copper relative to neuronal cells[(248)].

1.5.2 Implications of copper homeostasis pathways in AD pathogenesis

As previously discussed, (see section 1.4.1.1-4) it is clear that copper amongst other metals plays an important role in AD pathogenesis, which has led to the "metal theory" in order to explain the disease pathogenesis. Further support to the theory that metal/copper homeostasis has a significant role in AD came from studies that showed decreased activity of two important copper binding enzymes necessary for cell function, COX and SOD1, in the AD brain[(249-253)].

Several studies have attempted to measure copper levels in the AD brain, but these are not always in agreement. In 2007 Magaki *et al.* measured the levels of copper in frontal cortex and hippocampus grey and white matter of controls, mild-moderate AD and severe AD cases using graphite furnace atomic absorption spectrometry (GFAAS)[(254)]. They showed that total copper levels in severe AD were higher in the frontal cortex compared to the hippocampus in normal brain. Compared to controls, total copper, in severe AD was significantly lower in the frontal cortex gray matter but there was no difference in the total copper concentration in the hippocampus in AD[(254)]. The findings from Magaki *et al.* are in agreement with a study from Deibel *et al.* who reported decreased copper levels in the AD brain[(14)]. Decreased copper was not seen in mild-moderate AD but only in severe AD, suggesting that this phenomenon of reduced copper may only occur at a later stage of the disease progress [(14, 254)]. This phenomenon might be explained based on the hypothesis that overproduction of APP and Aβ shift copper into the extracellular space from the intracellular compartment and thus cause a deficiency of intracellular copper in the AD brain[(255)].

In a study by James *et al*., the levels of both total copper and redox-active labile copper in the frontal and temporal lobe were measured[(256)]. A significant decrease was also observed in the mass fraction of copper (μmol copper per g wet tissue) in the frontal and temporal lobe in AD samples compared to controls (13% and 18% respectively)[(256)]. But when the total copper content was normalized with the protein levels there was no difference in copper between the two groups[(256)]. It was also reported that AD brain contains higher amounts of redox-active exchangeable copper which was significantly positively correlated with increased oxidative damage[(256)]. It is interesting to note, that in AD patients there are increased levels of copper in the CSF and plasma in contrast with the decreased copper levels found in the brain[(13)]. All the above mentioned studies that have measured copper levels or protein/activity of copper binding enzymes in the AD brain have mainly used cases that belong either to the LOAD subtype, based on the age criteria, or use a mixture of both EOAD and LOAD cases. That might explain why the results are quite controversial and also indicating the necessity of a study that will map these variables in both AD subtypes.

A better understanding of copper implication in AD has come from the usage of techniques that directly monitor metal distribution in the brain such as X-ray absorption and ICP-MS techniques that can directly measure copper-protein complexes. Two of these techniques have already mentioned above, X-ray imagining and LA-ICP-MS, where they have been used to detect/measure copper in correlation with protein or in the levels of a single cell population. The LA-ICP-MS works by laser ablate small particles of solid samples that are then carried by

a gas to an ICP-MS for metal specific detection[257, 258]. The LA-ICP-MS is a semi-quantitative technique with detection limit of 0.01 μg/g tissue, spatial resolution of 15-50 μm and 200 μm of analytical depth[258]. The synchrotron based X-ray fluorescence microscopy (SXRF) techniques are able to provide a more quantitative and highly sensitive probe for the detection of copper and other metals in biological systems[257, 258]. These techniques have a detection limit of 0.1-1 μg/g tissue, spatial resolution of 0.03-0.2 μm and more than 100 μm of analytical depth[258]. The implementation and development of these techniques will provide valuable information of how metal ions change in neurodegenerative disorder and how metals such as copper or iron contribute to the oxidative stress that has been found in the brain.

1.6 The "metal theory" of neurodegeneration

The evidences that were presented in the previous section of this chapter are suggesting that abnormal interactions with biological metals, such as copper, iron and zinc are upstream of the AD pathophysiology[259]. These metal interactions with AD was considered to be a novel drug target for the disease which led to the development of the "metal theory" of neurodegeneration[259]. The "metal theory" supports that by normalizing metal ion homeostasis and the same time disrupting the resistant dimeric Aβ can be a good target for intervening with AD progression[259]. Both copper supplementation and chelation therapy have been tested as potential treatments for AD however; the results from these types of clinical trials did not give any promising outcome. In the next sections, an overview of the up to now studies regarding these therapeutic approaches will be further analysed.

1.6.1 Copper chelation or supplementation as potential therapeutic agents for AD

An efficient treatment for AD is not yet available with the only approved FDA compounds being drugs that target symptomatic effects such as memory deficits and behavioural changes. The approved drugs are mainly based on the knowledge that in the AD brain there are neurotransmitter disturbances which have led to development of the acetylcholinesterase inhibitors (AChEIs) and memantine[260, 261]. AChEIs are used to enhance cholinergic neurotransmission by increasing the availability of acetylocholine and menantine, an N-methyl-D-aspartase (NMDA) receptor antagonist, is used to protect neurons against glutamate mediated excitotoxicity without preventing the normal function of the NMDA receptor[260, 261]. However, both strategies are not expected to change the course of the disease but to temporally alleviate some of the symptoms of AD.

The last few decades have seen a number of different therapeutic approaches tested in both animal and human trials but none of these have been able to obtain final FDA approval. The main drug candidates for AD are divided into two categories; the disease modifiers, which include secretase inhibitors, Aβ fibrilization inhibitors, Aβ immunotherapy or anti-tau drugs, and the epidemiology based drugs which are mainly anti-inflammatory drugs, cholesterol-lowering drugs, oestrogens and antioxidants. Given the fact that the majority of these drugs has failed to improve the clinical condition of the patients, the exploration of different pathways as potential therapeutic targets has been studied. The last two decades has seen the hypothesis of targeting metals in AD as an alternative and more tractable therapeutic approach which has led to clinical trials with two copper chelators, Clioquinol and PBT2, and the use of copper containing drugs.

1.6.1.1 Clioquinol and PBT2

5-Chloro-7-iodo-quinolin-8-ol, Clioquinol (CQ), is a derivative of 8-hydroxyquinoline which was used as antiparasitic agent for intestinal amoebiasis. CQ was explored as potential drug for AD since it has a moderate affinity for copper and zinc (K_{bCu} is 8×10^9 M^{-1} and K_{bZn} is 1.4×10^7 M^{-1})[262]. Initially, it was considered that CQ acts as a chelator but recent studies have shown that CQ acts as copper/zinc ionophore, with its role being to redistribute these metals into cells[263, 264]. The initial studies with CQ have shown that it rapidly clears aggregates of synthetic or AD derived Aβ *in vitro* and dramatically reduces Aβ plaque formation (by 49%) in 15 month old APPTg2567 mice which were treated with CQ for 9 weeks[265]. At the same time, the levels of copper and zinc were significantly increased in the APPTg2567 mice brain[265]. A small phase II clinical trial with 32 AD patients and a case study where AD patients were treated orally with CQ for 34 weeks, showed a lowering of $A\beta_{42}$ in the CSF which was also accompanied by a slower rate of cognitive decline[266, 267]. Even if the results from these studies were promising, large scale manufacturing of the compound made the development of the drug unviable.

White *et al.* proposed that CQ has dual role in the brain first in metal sequestration by removing copper and zinc from extracellular Aβ plaques and secondly as a stimulator of Aβ degradation pathways by activating an intracellular metal dependent signalling cascade[268]. This study used CHO and mouse neuroblastoma cells that overexpressed APP and they observed a decrease in Aβ levels, which was accompanied by increased copper and zinc uptake in the cells[268]. The proposed mechanism of action for CQ in the cells was suggested to initially activate the PI3K/Akt signalling pathway that leads to the phosphorylation of JNK

and ERK1/2 which stimulates intracellular neuroprotective pathways[268]. This pathway will eventually culminate in an upregulation of the activity of two matrix metalloproteinase (MMP2 and MMP3) which will start to degrade extracellular Aβ (Figure 1.10)[268].

PBT2 (Prana Biotechnology) is a second generation 8-hydroxyquinoline derived from CQ which has been shown to have better therapeutic effects in both AD mouse models and in a phase II clinical trial with AD patients. *In vivo* studies with an AD mouse model treated orally with PBT2 revealed that PBT2 crossed more effectively the BBB, reduced the Aβ amyloid burden and also restored cognitive function back to the levels of healthy mice[263]. The initial results from a phase II clinical trial with 78 AD patients showed that after 12 weeks of 250 mg PBT2 daily oral administration there was significant decrease in CSF Aβ levels and improvements in some of the performed cognitive performance tests[269]. Unfortunately, recently it has been announced by Prana Biotechnology that a 12 month phase II clinical trial with 56 AD patients failed to show any significant loss of Aβ plaques in AD brain relative to healthy controls (Prana Biotechnology, News Room).

As an 8-hydroxyquinoline, PBT2 is able to coordinate with copper and zinc in 2:1 ratio, which is accompanied by deprotonation of the phenol proton[263, 270, 271]. PBT2 eventually forms a neutral complex with metal ions, making it able to cross cell membranes and transfer these metals in the cells[263, 270]. The moderate affinity of PBT2 for these metals improves their bioavailability inside the cells which enables activation of neuroprotective pathways within cells[270]. The mechanism of action for PBT2 has been studied in SH-SY5Y cells where PBT2 in concert with zinc inhibited the dephosphorylating activity of calcineurin, which resulted in decreased tau phosphorylation, and increased phosphorylation of several downstream targets such as CREB, CaMKII and decreased caspase 3 activity and finally the activation of the MMP2/3 (Figure 1.10)[270, 271].

1.6.1.2 Copper supplementation therapy

It is well established that copper can enhance Aβ toxicity *in vitro* hinting at the important role of copper in AD pathogenesis. On the other hand, lower levels of copper in AD brain and mouse models for AD imply that copper deficiency contributes also to neurodegeneration[14]. The potential that copper deficiency might play a role in AD pathology was studied initially in an AD transgenic mouse model where they showed that copper supplementation can increased bioavailable copper in the brain, restore SOD1 activity, decrease Aβ in the brain and prevent premature death[272, 273]. The above observations lead Kessler *et al.* in 2008, into pilot clinical trial phase II study with AD patients that received 8 mg copper daily for 12

months but the results from the study showed no improvement in the cognitive abilities of the AD patients[262, 263]. However, they observed a statistical significant 10% decrease (non-parametric Wilcoxon test, p=0.04) in CSF $A\beta_{42}$ levels in the copper treated group but the same time the placebo group presented a much higher 30% decrease (non-parametric Wilcoxon test, p=0.001) in $A\beta_{42}$ levels[274, 275]. Kessler *et al.* study showed that long-term copper supplementation can be excluded as a risk factor for AD based on the decrease CSF $A\beta_{42}$ levels in both groups [274, 275]. The levels of $A\beta_{42}$ in the CSF is a biomarker of AD pathogenesis and the decreased levels are correlated with the severity of disease progress[276]. That indicates that copper supplementation in patients that have already developed AD might not be appropriate.

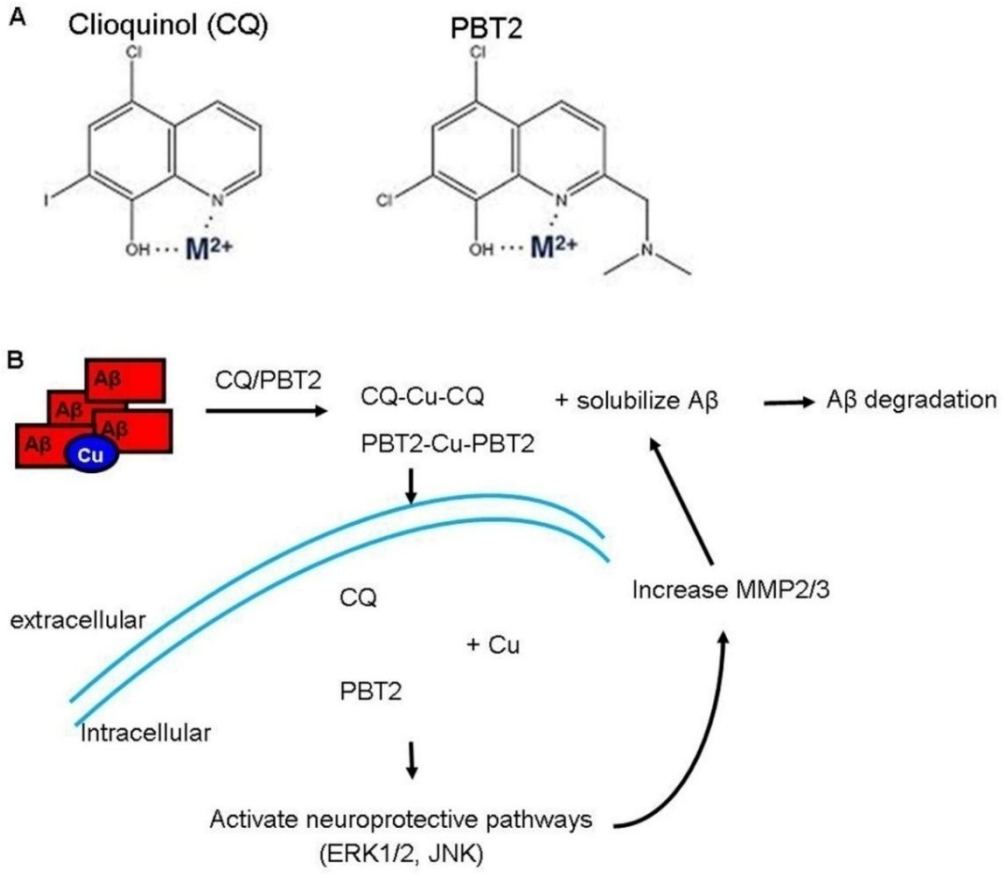

Figure 1.10 Schematic representation of Clioquinol (CQ) and PBT2 as well as their Mechanism of Action in Cells.

(A) Chemical structures of CQ and PBT2. **(B)** Proposed mechanism of action for CQ and PBT2 in AD brain. CQ and PBT2 remove copper from Aβ amyloid plaques in the process of solubilising Aβ. Additionally, the CQ-Cu/PBT2-Cu complexes are able to cross cellular membranes and make copper available to cells. In that process they also activate intracellular neuroprotective pathways and MMP2/3 proteinases that will start degrading Aβ. (Adapted from Barnham *et al.*[263])

1.7 Study aims and objectives

Alzheimer disease is a neurodegenerative disorder that mostly affects the elderly and whilst several aspects of the biology of the disorder are already known, there is still no available treatment. The last two decades have seen an increasing number of studies which have shown that copper plays an important role in AD pathogenesis and targeting copper levels may potentially lead to a new therapeutic strategy for AD. The aim of this thesis is to study the routes by which copper enters and is distributed around cells and to identify the potential role of copper in AD pathogenesis. To accomplish this we will examine the following questions:

1. Are changes of important copper homeostasis pathway components observed not only in affected brain regions of LOAD and EOAD brains but also in the healthy ageing brain?
2. How does copper normally distribute in a model mammalian cell line, HEK293 cells, and how does the balance of copper change when the levels of one of the cytosolic chaperones is changed?
3. Can different therapeutic and non-therapeutic copper chelators and copper containing compounds be used to alter the copper distribution inside mammalian cells and associated copper related enzyme activities, and can these compounds be used as possible targets for AD treatment?

The overall aim of the project is to identify if there is a link between AD and copper homeostasis and to explore the mechanism of copper prioritization in a cell. In order to achieve these goals different experimental techniques have been used. Initially, brain samples from post mortem LOAD, EOAD and healthy control were analysed in order to determine the levels of copper, the activity of two important cellular copper binding enzymes (SOD and COX) and the levels of various copper binding proteins. The usage of both EOAD and LOAD cases was consider important as to understand how copper homeostasis pathways are changing in the both AD subtypes. As mentioned above, the already published studies have only focused on the LOAD or used mixed AD cases and taking into consideration that the two AD subtypes are having significant pathological differences the separation into different groups was considered important in order to get a clear view of the copper homeostasis pathways in the AD brain.

In order to explore the mechanism of copper distribution and how different copper chelators affect copper homeostasis pathways, a model cell line was used to initially identify the toxic levels of the tested drugs, and then the effects on the intracellular copper levels, activity of

COX and SOD, and their respective protein levels. HEK293 cells were selected for the these experiments since it is a typical epithelial cell line which allows easy manipulation and can be grown in high quantities as was found necessary for several experiments.The HEK293 cell line was initially derived in 1973 by exposing a human embryonic kidney cell culture to sheared DNA of adenovirus type 5 (AD5)[277]. Since then HEK293 cells and derivatives have been the most frequently used cells after HeLa cells in cell biology studies[278]. HEK293 cells are often used as a model for studying the transforming/oncogenic properties of cancer related genes but sometimes this cell line is incorrectly used as a non-tumorigenic or even "normal" human cell line[279].

2 Material and Methods

2.1 Clinical material

To investigate the possible role of copper in ageing and AD, a study involving post-mortem human brain tissue was undertaken. Brain tissues from frontal and temporal cortex, and cerebellum were obtained from Newcastle Brain Tissue Resources (NBTR), Newcastle University. Ethical approval for the study was provided by the National Research Ethics Service. Three different groups were included in the present study: EOAD, LOAD, and aged matched healthy control cases for both AD groups which showed an absence of any clinically significant neurological or psychiatric history and who showed age related neuropathology according to standard accepted criteria. Cases of AD showed a clinical history compatible with typical symptoms of AD with progressive decline in cognition and activities of daily living on clinical review and showed abundant senile plaque and neurofibrillary tangle deposition in cortical grey matter sufficient to fulfil accepted neuropathological criteria for AD. Cases of AD were cognitively assessed during life and were known to have been severely demented at time of death. Approximately 0.4 g of snap frozen grey matter tissue was dissected by Dr Chris Morris from medial temporal cortex (Brodmann Area 21), lateral frontal cortex (Brodmann Area 9) and lateral cerebellar cortex. Tissue was rapidly thawed and the majority of the white matter dissected off and the remaining grey matter used partly for metal analysis (see section 2.3) and the remainder homogenised for protein analysis (see section 2.2). Brain tissue is divided into grey matter, which consists mainly from neuron cell bodies and dendrites and the white matter, which consist, by myelinated axons and supporting oligodendrocytes. In the present study, only the grey matter was used for the protein/enzyme and metal analysis since studies have shown that the AD brain presents more severe grey matter associated changes (e.g atrophy) and to lesser extend white matter changes[(280)]. Furthermore, studies have shown that the grey matter contains higher copper levels compare to the white matter possibly reflecting the requirement for copper in the neuronal cell bodies and dendrites processes (e.g. neurotransmission)[(247)].

Details about the groups that were used are shown in Table 2.1 for the control cases and in Table 2.2 for the AD groups where post mortem delay, age, sex and pH of the brain are presented. Determination of the brain's pH is a standard procedure, which is conducted by the NBTR staff during the processing of a new brain tissue. The pH is used as a surrogate measurement of pro-mortem agonal state which is correlated with prolonged death and hypoxia and normally low pH indicates high amount of lactic acid[(281)]. The majority of the cases had pH 6.0-7.2, which is in the acceptable range and only a few cases had pH below 6.0.

Case	Age of death (years)	Braak stage	Post mortem delay (hours)	Sex	pH
1	64	1	89	F	6.60
2	68	0	54	M	6.27
3	63	0	30	M	7.16
4	73	0	25	M	6.45
5*	69	1	48	M	6.70
6	54	0	9	M	6.81
7	69	0	45	F	6.43
8*	67	0	10	M	7.23
9*	65	1	28	M	6.67
10*	64	0	23	F	6.80
11*	67	0	20	M	6.95
12	66	0	9	M	7.22
13	67	0	22	M	6.89
14	51	2/3	9	F	5.69
15	87	2	8	M	6.39
16	88	3	22	F	5.90
17	89	3	34	F	6.20
18	96	3	29	F	5.53
19	74	1	49	F	6.1
20	81	2	43	M	6.05
21	94	2	50	F	N/A
22	89	2	24	F	6.36
23	80	2	16	M	6.10
24	88	2	26	M	6.30
25	88	2	28	M	N/A
26	80	2	31	F	6.10
27	80	2	25	F	N/A

Table 2.1 Demographic Information Regarding the Control Group.

Case 1-14 were used as control for the EOAD group and case 15-27 for the LOAD group.*, cases indicated are not included in the cerebellum analysis. F: female, M: male, N/A: data not available.

Case	Diagnosis	Age of onset (years)	Age of death (years)	Braak stage	Family history	Post mortem delay (hours)	Sex	pH
1*	EOAD	60	64	6	Neg	28	M	6.50
2*	EOAD	52	59	5	Neg	44	M	6.13
3	EOAD	51	63	6	Neg	11	F	6.50
4*	EOAD	N/A	64	N/A	Pos	N/A	F	6.04
5	EOAD	55	70	6	Neg	24	M	6.43
6	EOAD	52	62	6	Neg	48	M	6.22
7	EOAD	57	69	6	Neg	11	M	6.21
8	EOAD	65	71	6	Neg	31	F	6.35
9	EOAD	60	72	6	Neg	4	F	6.47
10	EOAD	N/A	64	6	Pos	39	M	6.94
11*	EOAD	61	64	6	Neg	10	M	5.96
12	EOAD	60	63	6	Neg	55	M	6.37
13	EOAD	N/A	64	6	Neg	48	M	6.00
14	EOAD	58	78	6	Neg	40	F	6.07
15	EOAD	62	76	6	Neg	37	F	5.53
16	EOAD	65	68	6	Neg	24	M	6.10
17	LOAD	68	80	6	Neg	24	M	5.95
18	LOAD	76	87	6	Neg	22	M	6.40
19	LOAD	72	75	6	Neg	33	F	6.20
20	LOAD	84	92	6	Neg	40	M	5.90
21	LOAD	85	93	5	Neg	34	F	6.80
22	LOAD	72	85	6	Neg	29	M	5.60
23	LOAD	67	78	6	Neg	37	M	5.70
24	LOAD	73	80	6	Neg	32	F	N/A
25	LOAD	78	87	6	Neg	21	M	6.23
26	LOAD	78	81	6	Neg	83	F	6.40
27	LOAD	93	96	6	Neg	74	M	5.90
28	LOAD	69	76	6	Neg	53	M	6.10
29	LOAD	71	76	6	Neg	23	M	6.50

Table 2.2 Demographic Information Regarding the EOAD and LOAD Groups.

Case 9 had a PSEN1 R269H mutation and case 10 had a PSEN1 A246G. *, cases indicated are not included in the cerebellum analysis. F: female; M: male; N/A: data not available; Neg: negative; Pos: positive.

In order to see if the pH is affected by age or post mortem delay Spearman rank test (see section 2.12.1) was conducted for the three different groups (controls, EOAD and LOAD). A significant correlation was observed between pH and age in the control group (r_s=0.785, p<0.0001, n=22) but not in the EOAD (r_s=-0.019, p=0.952, n=12) or LOAD (r_s=-0.198, p=0.462, n=16) group. Post mortem delay did not present any significant correlation with the pH in the control (r_s=-0.289, p=0.192, n=22), EOAD (r_s=-0.156, p=0.572, n=16) or LOAD (r_s=-0.252, p=0.428, n=12) group.

2.2 Tissue preparation

In order to determine the proteins and enzyme activity levels in the brain, frozen grey matter tissue was homogenised by using an ULTRA-TURRAX® Tube Drive homogeniser. Approximately 0.2 g frozen tissue from all groups' frontal and temporal cortex grey matter and cerebellum were homogenised in ice-cold 0.2 M triethylammonium bicarbonate (Sigma Aldrich, Poole, UK) which contained proteases inhibitor tablets also (Complete ethylenediaminetetraacetic acid (EDTA) free (Roche, Welwyn Garden City, UK)) in order to obtain a 10% w/v homogenate in the end. Aliquots were prepared and stored at -30^{o} C until used for analysis.

2.3 Metal analysis from brain tissue with inductively coupled plasma mass spectrometry (ICP-MS)

Frozen brain (0.05-0.2 g) tissue was initially weighed in a three place balance and then digested with 50% HNO_3 in order to obtain 10% w/v of brain digest [SpA Grade, 80% Nitric Acid (Romil, Cambridge UK) diluted with double distilled deionised water (>18MΩ, Milli-Q, Millipore, UK)] and incubated for 48 hours at 50^{o} C. In order to determine metal content samples were analysed by using inductively coupled plasma emission mass spectrometry (ICP-MS) Thermo Scientific X Series^{II} in both standard and collision cell technology (CCT) mode by using 7% (v/v) H_2 in He as the collision gas, with in-sample switching between CCT and normal modes. All the dilutions for the sample preparation were made with a diluter/dispenser (MICROLAB 530B, Hamilton. Bonaduz AG, CH). Prior to analysis the brain samples were diluted fifty times with a diluent containing, 0.5% HNO_3 (Romil), 0.1% triton X-100 (Romil) and 1 µg/ml Rb, 1 µg/ml Ir, 10 µg/ml Ga and 200 µg/ml Gold SPEX (SPEX CertiPrep) as internal standards. The samples were analysed based on a standard addition method which required four diluted samples for each brain and then in the respective sample 0, 10, 20 and 50 µl of standard A containing, 5% HNO_3, 200 mg/L Fe, 80 mg/L Cu, 400 mg/L Zn, 0.04 mg/L Sn, 50 mg/L Spex Hg and Spex custom mixed (50 mg/L Ba, Be, Cr,

Co, As, Mo, Cd, Cs, Pt, Tl, U, 100 mg/L Mn, 500 mg/L Pb, 1000mg/L Al, Se (SPEX CertiPrep)), was added.

ICP-MS measures both oxidised and reduced forms of copper in the brain. It is worth mentioning that brain pH could affect the oxidation state of copper since is well known that under acidic conditions of pH 5.0 to 6.0 copper exist mainly in the form of Cu^{2+}. Some of the brain samples had pH around that range and in order to determine if there is any correlation between these two variables Spearman rank test was conducted (see section 2.12.1). No significant correlation was observed between pH and copper levels for the control cases (Frontal cortex: r_s=0.280, p=0.205, n=22; Temporal cortex: r_s=0.310, p=0.152, n=22; Cerebellum: r_s=0.442, p=0.072, n=17), the LOAD group (Frontal cortex: r_s=-0.628, p=0.028, n=13; Temporal cortex: r_s=-0.287, p=0.364, n=13; Cerebellum: r_s=-0.574, p=0.053, n=13) and the EOAD group (Frontal cortex: r_s=-0.101, p=0.708, n=16; Temporal cortex: r_s=0.014, p=0.956, n=16; Cerebellum: r_s=0.531, p=0.075, n=12).

2.4 Protein concentration determination with Bradford assay

Protein concentration within homogenized samples was determined by using Bradford's method[282] using a bovine serum albumin (BSA) standard curve. Standards of BSA (Pierce, Thermo Scientific) were prepared with concentrations of 1, 0.8, 0.7, 0.6, 0.5, 0.4, 0.3, 0.2, 0.1, 0.05 and 0 mg/ml. Brain homogenates and HEK293 lysates were sonicated for 10 seconds with a sonic probe and then in a sonic bath on ice (40 min for brain and 20 min for cell samples) and then diluted from 1:5 to 1:20 v/v in water. Fifteen microlitres of BSA standards and 15 µl of sample were loaded into respective 1 ml plastic cuvettes in triplicate. In each cuvette, 1 ml of Bradford reagent (Thermo Scientific) was added and incubated for 20 min at room temperature. The absorbance was measured at 595 nm on a spectrophotometer (PerkinElmer). The sample concentration was determined based on the BSA standard curve and samples immediately assayed for mitochondrial enzyme activity. Brain samples for Western Blot analyses had sodium dodecyl sulfate (SDS) (Ambion, Thermo Scientific) added to a final concentration of 0.2% before sonication and protein determination followed the same protocol as above.

2.5 Western blot analysis

Western blot analysis was performed by using one-dimensional SDS gel electrophoresis of proteins with NuPAGENovex (Invitrogen, Thermo Scientific, Cramlington UK) pre-cast gels. Ten micrograms protein extract from brain or cell sample was prepared containing 1×

NuPAGE LDS sample buffer (Invitrogen) and 1× NuPAGE Sample reducing agent (Invitrogen). Samples were vortexed and heated for 10 min at 70^{o}C, and then loaded into NovexNuPAGE 4-12% precast gels (Invitrogen) along with SeeBlue pre-stained standard (Invitrogen) molecular weight marker. The gels were electrophoresed in 1× NuPAGE (3-(N-morpholino) propane sulfonic acid) MOPS or (2-(N-morpholino) ethane sulfonic acid) MES (pH 7.3-7.7, Invitrogen) running buffer. MOPS running buffer was used to resolve proteins at a molecular weight from10-200 kDa and MES for low molecular weight (5-50 kDa) proteins. To the inner chamber of the electrophoresis tank 0.25% antioxidant (a proprietary reagent, Invitrogen) was added and the samples electrophoresed for 20 min at 120 V and for 70 min at 160 V. Samples were transferred to nitrocellulose membranes with iBlot transfer stacks (Invitrogen) at 20 V for 8 min. Membranes were stained with Ponceau S (Sigma Aldrich) for one minute and were washed with MilliQ water. Membranes were cut in strips based on molecular weight of the protein of interest (Table 2.3) and washed twice for 10 min with 1× Tris buffered saline (TBS: 50 mM TrisHCl, pH 7.4 and 150 mM NaCl) (Santa Cruz Biotechnology, Texas USA) containing 0.2% Tween 100 (Sigma Aldrich) (TBS-T). Membranes were blocked for 1 h in 5% non-fat dry milk in TBS-T at room temperature and then incubated for one hour at room temperature (RT) or overnight (O/N) with the primary antibody. Primary antibodies were diluted (Table 2.3) in 5% non-fat dry milk in TBS-T for the incubations. Two 10 min washes followed with TBS-T and then incubation with appropriate horseradish peroxidase (HRP)-conjugated secondary antibodies (Table 2.4) for 30 min at RT.

Membranes were then washed with TBS-T for approximately 1 h and developed by using the enhanced chemiluminescence system Pierce ECL plus substrate (Thermo Scientific) according to the manufacturer's instructions. Substrate A and Substrate B were mixed in a 40:1 ratio and incubated with the membranes for 2 min and then the membranes were transferred to cassettes. Membranes were exposed to autoradiography film (Kodak, Sigma Aldrich) to detect the chemiluminescent signal. For proteins with a molecular weight close to that of glyceraldehyde 3-phosphate dehydrogenase (GAPDH) which was used as a loading control, membranes were stripped of the initial antibodies by incubating them with 60 mM TrisHCl (Sigma Aldrich) pH 6.8, 2% SDS (Santa Cruz Biotechnology) and 0.6% mercaptoethanol (Sigma Aldrich) for 1 h at 50^{o}C. Membranes were then washed with TBS-T followed by blocking in 5% non-fat dry milk and incubation with the new antibody as described previously.

Protein of interest	Molecular Weight	Dilution	Incubation	Supplier	Secondary Antibody
Atox1	7 kDa	1:5,000	1 h RT	Abcam	Mouse IgG-HRP
CCS	25/29 kDa	1:2,000	1 h RT	Santa Cruz Biotechnology	Rabbit IgG-HRP
SOD1	16 kDa	1:8,000	1 h RT	Abcam	Rabbit IgG-HRP
SOD2	25 kDa	1:10,000	1 h RT	Abcam	Mouse IgG-HRP
VDAC1	30/35 kDa	1:8,000	1 h RT	Abcam	Mouse IgG-HRP
COX1[1]	35 kDa	1:8,000	1 h RT	Abcam	Mouse IgG-HRP
COX2	25 kDa	1:8,000	1 h RT	Abcam	Mouse IgG-HRP
ATP7a	178 kDa	1:500	O/N	Santa Cruz Biotechnology	Mouse IgG-HRP
Sco2	28 kDa	1:2,000	1 h RT	Proteintech	Rabbit IgG-HRP
Ctr1	28 kDa	1:20,000	1 h RT	Abcam	Rabbit IgG-HRP
DDK		1:2,000	1 h RT	Cell signalling	Mouse IgG-HRP
NDAFV1	51 kDa	1:1,000	1 h RT	Abcam	Mouse IgG-HRP
NDAFS1	54 kDa	1:5,000	1 h RT	Santa Cruz Biotechnology	Goat IgG-HRP
GAPDH-HRP	36 kDa	1:2,000	1 h RT	Santa Cruz Biotechnology	

Table 2.3 Molecular Weight of the Analysed Proteins and Dilutions of the Primary Antibodies.

Secondary Antibodies	Dilution	Supplier
Horseradish peroxidase (HRP)–conjugated anti-mouse	1:4,000	Abcam
Horseradish peroxidase (HRP)–conjugated anti-rabbit	1:4,000	Dako
Horseradish peroxidase (HRP)–conjugated anti-goat	1:4,000	Dako

Table 2.4 Dilutions of Secondary Antibodies.

The X ray films of the western blots were scanned using a flatbed scanner and band intensity was analysed using ImageJ software[(283)]. The GAPDH band was used to normalise the results and the mean for the protein of interest/GAPDH ratio were calculated for all samples.

[1] Samples were heated at 50° C before loading into NovexNuPAGE 4-12% precast gels.

2.6 HEK293 cell culture

The HEK293 human embryonic kidney cell (CRL-1573) line was obtained from American Type Culture Collection (ATCC) and the culture method was according to supplier instructions for the cell line.

2.6.1 HEK293 culture method

The majority of the cell culture has been performed in T75 cm^2 tissue culture flasks. The initial culture was started from frozen stocks of cells. Cells were defrosted for a few seconds in water bath at 37ºC and then added, drop by drop, into pre-warmed fresh growth medium containing Dulbecco's Modified Eagle's Medium (Sigma Aldrich), 10% FBS (Sigma Aldrich), 1× non- essential amino acids (Sigma Aldrich), 3.5 µg/ml fungizone (Invitrogen) and 2 mM L-glutamine, 100U penicillin and 0.1 mg/ml streptomycin solution (Sigma Aldrich). Cells were then washed by centrifugation for 5 min at 200 rpm, resuspended into 5 ml fresh medium and seeded into a T25 cm^2 flask. Cells were incubated in 95% air, 5% CO_2 at 37º C for 24 hours and the spent medium was replaced with fresh medium. Cells were left to grown until reached maximum confluency. Generally cells were subcultured every three days using a 1:3 split ratio. The old culture medium was removed, discarded and 3 ml of 1× trypsin in 0.02% EDTA solution (Sigma Aldrich) added to the cells and incubated for 3 min. Cells were resuspended with 5 ml fresh medium and then pelleted by centrifuging for 5 min at 200 rpm at RT. The supernatant was discarded and the cells resuspended with 5 ml medium and aliquots of the cell suspension placed into new culture flasks.

2.6.2 Cell viability assays

2.6.2.1 Alamar Blue assay

For the determination of copper ($Cu(NO_3)_2$), bathocuproinedisulfonic acid (BCS) and D-penicillamine (D-pen) (Sigma Aldrich) toxicity, HEK293 cells were seeded into a 48-well plate at 60,000 cells per well in 350 µl growth medium. After 24 h cells were treated with different concentrations of $Cu(NO_3)_2$, BCS or D-pen (4 replicates for each concentration) including cell treated with the diluent that was used to dissolve the compound (or referred as vehicle). For toxicity determination a range of concentrations was used for exposure times ranging from 24-72 h. In order to measure cell viability 0.01% of Alamar Blue [resazurin (Sigma Aldrich) 1 mg/ml in 1× phosphate buffered saline (1× PBS: 137 mM NaCl, 2.7 mM KCl, 8 mM Na_2HPO_4, 1.46 mM KH_2PO_4) (Sigma Aldrich)] was added to each well and incubated for 2-4 h. After incubation, 100 µl of each sample medium was transferred to a 96-

well plate. Samples were measured using a fluorescence plate reader using an excitation wavelength of 530 nm and emission at 590 nm. For the determination of cell viability the emission mean of each 4 replicate set of samples was divided by the mean of the vehicle treated samples to provide a proportion of cells surviving. After incubation with Alamar Blue, the remaining spent medium was replaced with fresh containing the appropriate concentration of compound and incubated further to allow 48 or 72 h exposure.

2.6.2.2 MTT assay

Using Alamar Blue on cells treated with ammonium tetrathiomolybdate (TTM, Sigma Aldrich) showed abnormal results and therefore the assay was altered to reflect this. HEK293 cells were seeded into 48-well plates at 60,000 cells per well in 350 µl growth medium including wells with just medium for background correction. After 24 h cells were treated with different concentrations of TTM (4 replicates for each concentration) including cell treated with the diluent that was used to dissolve the compound (or referred as vehicle). For TTM toxicity a range of 1 µM to 333 µM was used for exposure times from 24 to 72 h. In order to measure cell viability, after 24 h, 0.5 mg/ml MTT (MTT 5 mg/ml in 1× PBS (Sigma Aldrich)) was added in each well and incubated for 4 h. After incubation the supernatant was removed and the formed crystals were resuspended with 400 µl Isopropanol/10% Triton/0.05 M HCl. The plate was incubated for 1 h in the dark and after incubation 100 µl of each sample was transferred to a 96-well plate. Samples were measured by using a plate reader and absorbance at 570 nm was determined. For the determination of cell viability the absorbance mean of each 4 replicate set of samples was divided by the mean of the vehicle treated samples. The same protocol was followed for 48 and 72 h plates.

2.6.3 HEK293 cell growth curve

HEK293 cells were seeded onto 6-well plates at 3×10^5 cells/ well in 3 ml grown medium. After 24 h cells were treated with 200 µM BCS, 10 µM $Cu(NO_3)_2$, 350 µM D-pen or 2 µM TTM. In each plate three wells were used as a control and the other three were treated with the test compound. Cell viability, cell number and medium pH were determined for five continuous days. The pH determination was performed in 900 µl cell medium by using a micro pH meter (Thermo Scientific), calibration of the pH meter was performed daily as a baseline before measuring the samples. In order to measure cell viability Alamar Blue assay was used for BCS, $Cu(NO_3)_2$ and D-pen and MTT assay for TTM (see section 2.6.2.1 and 2.6.2.2) . Afterwards, cells were washed twice with PBS, trypsinized, resuspended with 500 µl 1 × PBS and centrifuged for 5 min at 200 rpm. The cell pellets were resuspended in 1 ml

1× PBS and 20 µl of each sample was stained with 0.04% Trypan blue and the viable cells were counted by using a Neubauer counting chamber.

2.6.4 Copper manipulation in HEK293 cells

Stocks of cells were maintained in growth medium and subcultured into new T175 cm^2 tissue culture flasks (10^7 cells/ T175 cm^2 flask into 25 ml medium) and left to attach for 24 hours. The spent medium was replaced with fresh medium containing 50 µM BCS, 200 µM BCS, 10 µM $Cu(NO_3)_2$, 350 µM D-pen , or 2 µM TTM or medium (as control) and left to incubate for 24, 48 or 72 h. The experiment was performed in triplicate for each condition. After 24 and 48 h incubation, cells were rinsed twice with 1× PBS and then incubated with 5 ml 1× trypsin-EDTA solution. Cells were resuspended with 7 ml 1× PBS and pelleted by centrifugation at 200 rpm for 5 min. A second wash with 4 ml 1× PBS was followed and the pellets were resuspended with 4 ml 1× PBS, and 20 µl of each sample was used for cell counting with a Neubauer counting chamber. The 4 ml cell suspension was centrifuged at 200 rpm for 5 min and the final pellet was resuspended in 100 µl ice cold cell lysis buffer (1× TBS and 0.32 M sucrose (Sigma Aldrich)). After 72 h cells were rinsed with 1× PBS, trypsinazed, pelleted and washed twice with 4 ml 1× PBS. After the second wash and cell counting, 1 ml of the cell suspension was pelleted by centrifugation at 200 rpm for 5 min and resuspened with 100 µl ice cold cell lysis buffer for protein analysis and the remaining 3 ml centrifuged at 200 rpm for 5 min and the final pellet resuspended with 1 ml 65% HNO_3 (Millipore) and digested for 24 h at 50^o C. Additionally, 1 ml of the spent cell growth medium was digested with 1 ml 65% HNO_3. Cells after resuspension with lysis buffer were sonicated for 10 seconds with a sonic probe and then sonicated for 20 min in a sonic bath on ice and stored at -80^o C until use.

2.6.4.1 Metal analysis from cellular samples with inductively coupled plasma mass spectrometry (ICP-MS)

Digested HEK293 cell and spent cell culture medium were diluted 5 times with 2% HNO_3 containing 20 µg/L Co and Ag as internal standards (see section 2.6.4). For the cell digest, standard solutions were prepared in a range of 0 to 60 µg/L Cu, Zn, Fe, Mn in buffer that contained 14% HNO_3 and 20 µg/L Co and Ag. The above standards were used for a calibration curved from which the sample metal content was calculated. For the spent cellular medium, standards were also prepared in a range of 0 to 100 µg/L Cu, Zn, Fe, Mn in buffer that contained 7% HNO_3 and 20 µg/L Co and Ag. All the samples were analysed using a Thermo Electron Corp., Series X^{II} both in standard mode and collision cell technology (CCT) mode with He of high-purity grade as collision gas.

2.7 Activity assays

2.7.1 Mitochondrial activity assays

Cytochrome *c* oxidase (COX) and Citrate synthase (CS) activity assays were performed based on previously described protocols which are in use within the National Health Service Mitochondrial Disorders Diagnostic Laboratories[*(284)*]. The assays were performed with cell or brain homogenates on a PerkinElmer spectrophotometer at 30° C.

2.7.1.1 Cytochrome *c* oxidase (COX) activity assay

The specific activity of mitochondrial COX was measured by following the oxidation of the reduced cytochrome *c* (Fe^{2+}-cytochrome *c*) at 550 nm (extinction coefficient for the reduced Fe^{2+}-cytochrome *c* at 550 nm is $E_{550} = 29.0\ mM^{-1}\ cm^{-1}$). As the apparent affinity constant K_m for the substrate (reduced Fe^{2+}-cytochrome *c*) and the dissociation constant K_i for the product (oxidised Fe^{3+}-cytochrome *c*) are similar (see equation 1.3, section 1.3.3), the reaction rate decays pseudoexponentially during the assay as the substrate is oxidized, so the activity is expressed as an apparent first-order rate constant (K/sec) rather than an initial rate.

Initially, the Fe^{2+}-cytochrome *c* was prepared by reducing the oxidised Fe^{3+}-cytochrome *c* with ascorbic acid and in order to do that 50 milligrams of Fe^{3+}-cytochrome *c* (Sigma Aldrich) were diluted with 5 ml 20 mM potassium phosphate (KH_2PO_4, Sigma Aldrich) pH 7.4 (assay buffer). To 1 ml Fe^{3+}-cytochrome *c* solution (bark red colour), a few grains of solid L-ascorbic acid (Fluka, Sigma Aldrich) was added in order to reduce the Fe^{3+}-cytochrome *c* to Fe^{2+}-cytochrome *c*. The reaction is complete when the colour of cytochrome *c* has turned into bright red-pink. L-ascorbic acid was removed from the mixture by desalting on a PD10 column (GE healthcare, Amersham UK). The column has had been equilibrated with the assay buffer before loading the Fe^{2+}-cytochrome *c*. The bright red-pink fraction of the eluted Fe^{2+}-cytochrome *c* was collected and stored at -30° C, where it was stored for up to two weeks. The concentration of Fe^{2+}-cytochrome *c* was estimated by measuring the absorbance at 550 nm and the quality of Fe^{2+}-cytochrome *c* from the ratio of the absorbance at 550 nm and at 565 nm. In order to determine the Fe^{2+}-cytochrome *c* concentration the absorbance was zero by using the assay buffer and then a baseline measured was recorded from 600 nm to 500 nm. The reduced Fe^{2+}-cytochrome *c* was diluted 200 fold with assay buffer and then the absorbance was recorded from 600 nm to 500 nm. In order to determine the quality of the reduced Fe^{2+}-cytochrome *c*, the ratio of Delta A_{550}/ Delta A_{565} (Delta $A = Abs_{peak} - Abs_{baseline}$)

was calculated. If the ratio was <6 the Fe^{2+}-cytochrome *c* was too oxidized to be used. The concentration of the reduced Fe^{2+}-cytochrome *c* was calculated based on equation 2.1:

$$Fe^{2+}\text{-cytochrome } c \text{ concentration (mM)} = \frac{\text{Delta Abs}_{550}}{29} * \frac{1000}{\text{sample volume}} \quad \textbf{(2. 1)}$$

where Delta Abs_{550} is the difference in absorbance between the peak and baseline of the trace at 550 nm, 29 is the extinction coefficient for reduced Fe^{2+}-cytochrome *c* ($mM^{-1}\,cm^{-1}$) at 550 nm and sample volume is in µl.

One millilitre plastic cuvettes were filled with an appropriate volume of assay buffer which had been placed in a 30° C water bath to equilibrate. The following reaction reagents, 0.345 mM DDM (Melford, Ipswich UK), 15 µM Fe^{2+}-cytochrome *c* (kept on ice), were added, mixed gently and placed in the spectrophotometer. The absorbance was "zeroed" and baseline rate (nonenzymatic blank) was recorded for 30 to 50 seconds, then 10 µg of cell sample or 50 µg brain sample were added, gently mixed and the decrease in absorbance was recorded for about 5 min in order to allow the measurement of the enzyme-catalyzed oxidation of Fe^{2+}-cytochrome *c*. At the end of the reaction a few grains of potassium ferricyanide (Fluka) were added to oxidize the remaining Fe^{2+}-cytochrome *c*, the sample was gently mixed and the absorbance change was recorded until it became a flat line which was used as an endpoint reading for the final reaction calculation.

In order to calculate the activity, 6 time points were picked with their respective absorbance values ($AbsT_0$-$AbsT_5$) while the curve is in the exponential phase along with the end point absorbance value. The final COX activity was calculated based on the equation 2.2:

$$\text{COX activity } (10^{-3}\text{ K/sec}) = \left[\frac{\left(\log\frac{A}{X_5} - \log\frac{A}{X_1}\right)}{\text{time period}}\right] * 2.303 * \frac{1000}{\text{sample volume}} * \text{dilution factor} * 1000 \quad \textbf{(2. 2)}$$

where A (absorbance change) = $AbsT_{end}$ -$AbsT_0$, X_1=$AbsT_{end}$ –$AbsT_1$, X_5=$AbsT_{end}$ –$AbsT_5$, time period (sec) is the time difference between $AbsT_1$ and $AbsT_5$, 2.303 is the conversion factor for log10 to natural log, sample volume is in µl and K is the first-order rate constant.

2.7.1.2 Citrate synthase (CS) activity assay

CS is the most commonly assayed mitochondrial matrix marker enzyme to assess mitochondrial content. The activity of CS is routinely used as a reference when expressing activities of respiratory chain complex enzymes; the ratio of COX/CS is the preferred way of expressing the COX activity data. The specific activity of mitochondrial CS is measured by following the CoASH released from acetyl-CoA during the enzymatic synthesis of citrate,

which reacts with 5,5'-dithiobis-2-nitrobenzoic acid (DTNB) to yield the 5-thio-2-nitrobenzoate ion at 412 nm (extinction coefficient at 412 nm is E_{412}=13.6 mM^{-1} cm^{-1}).

The CS activity was determined by following the absorbance change at 412 nm. In 1 ml cuvettes 0.1 M TrisHCl pH 8 (assay buffer), 100 µM DTNB (10 mM DTNB stock solution was diluted in assay buffer (Sigma Aldrich), 1% Triton (Sigma Aldrich), 10 mM EDTA (Sigma Aldrich), 100 µM Acety-CoA (Sigma Aldrich) and 10 µg of cell sample or 50 µg brain sample were added. The content of the cuvette was mixed gently and placed in the spectrophotometer. The absorbance was "zeroed" and a base line rate was recorded for 10 to 50 seconds then 250 µM of oxaloacetate (Sigma Aldrich) (1 M oxaloacetate was freshly diluted with 2 M $KHCO_3$ (Sigma Aldrich) and then a working solution of 50 mM oxaloacetate was prepared by diluting it with assay buffer) was added into the cuvette and gently mixed to start the reaction and record the slope (Abs/min) of the increase in absorbance over 5 min. CS activity was calculated (equation 2.3) as the slope (Abs/min) of the enzyme-catalysed formation of 5-thio-2-nitrobenzoate ion activity and expressed as nmols 5-thio-2-nitrobenzoate ion/min as follows:

$$\text{CS activity (nmols/min)} = \frac{\text{slope (Abs/min)}}{13.6} * \frac{1000}{\text{sample volume}} * \text{dilution factor} * 1000 \qquad \textbf{(2. 3)}$$

where slope (Abs/min) = Abs_{T2} - Abs_{T1}/ $T_2 - T_1$, 13.6 is the is the extinction coefficient for DTNB in Tris buffer (mM^{-1} cm^{-1}) at 412 nm and sample volume is in µl.

2.7.2 SOD activity assay

SOD activity was measured based on the commercially available SOD assay kit from Sigma Aldrich with modifications. SOD activity of the cell or brain samples was determined based on an inhibition curve made with SOD from bovine erythrocytes (Sigma Aldrich). Initially, SOD standards were prepared containing 50, 25, 10, 5, 4, 3, 2, 1, 0.5 U/ml. The suggested assay volumes from the datasheet were adjusted to be compatible with 1 ml plastic cuvettes by increasing the volumes by 4. In order to measure the activity of the samples 10 µg brain 50 µg cell were used in the assay. The assay required the preparation of the next black samples in order to measure the percentage inhibition.

Blank 1: ddH_2O, WST working solution and enzyme working solution.

Blank 2: test sample, WST working solution and dilution duffer.

Blank 3: ddH_2O, WST working solution and dilution buffer.

The final mixtures were incubated at 37° C for 10, 20 and 30 min and the absorbance was measured at 450 nm. SOD activity was calculated based on the equation 2.4:

$$\text{SOD activity (inhibition rate \%)} = \left\{\frac{[(\text{Abs}_{\text{blank 1}} - \text{Abs}_{\text{blank 3}}) - (\text{Abs}_{\text{sample}} - \text{Abs}_{\text{blank 2}})]}{(\text{Abs}_{\text{blank 1}} - \text{Abs}_{\text{blank 3}})}\right\} * 100 \quad \textbf{(2.4)}$$

where $\text{Abs}_{\text{blank1}}$, $\text{Abs}_{\text{blank2}}$, $\text{Abs}_{\text{blank2}}$ and $\text{Abs}_{\text{sample}}$ is the measured absorbance at 450 nm of the respective sample.

In order to calculate the units of SOD in the cell or brain samples plots of the % inhibition versus Log (Units/ml) of SOD standards were made in Origin 7 software and a sigmoidal curve was fitted to the data. From the given equation the Units/ml of the unknown samples were able to be calculated which were finally transformed to U/mg of protein based on the protein amount that was used for the assay.

2.8 Seahorse Cell Mito Stress Test Kit

The Cell Mito Stress test (Seahorse Bioscience) measures the key parameters of mitochondrial function by directly measuring the oxygen consumption rate (OCR) of the cells (Figure 2.1). The kit uses modulators of respiration that target compounds of the electron transport chain (ETC) in the mitochondria to reveal key parameters of metabolic function. Oligomycin, carbonilcyanide p-triflouromethoxyphenylhydrazone (FCCP) and a mix of rotenone and antimycin A are serially injected onto live cells in order to measure ATP production, maximal mitochondrial respiration, and non-mitochondrial respiration, respectively. Proton leak and spare respiration capacity can then be calculated by using these parameters and the basal respiration rate. Each one of the above mentioned compounds targets a specific compound in the ETC. Oligomycin inhibits the ATP synthase (complex V) and the decrease in OCR following oligomycin injections correlates with the mitochondrial respiration associated with cellular ATP production. FCCP is an uncoupling agent that collapses the proton gradient and disrupts the $\Delta\Psi_m$. As a result, electron flow through the ETC is uninhibited and oxygen is maximally consumed by Complex IV. The FCCP-stimulated OCR can therefore be used to calculate the spare respiratory capacity, defined as the differences between maximal respiration and basal respiration. Spare respiratory capacity is a measure of the cells' ability to respond to increased energy demand. The last injection is a mix of rotenone, a Complex I inhibitor, and antimycin A, a Complex III inhibitor, which will shut down mitochondrial respiration and allow the calculation of non-mitochondrial respiration driven by processes outside of the mitochondria.

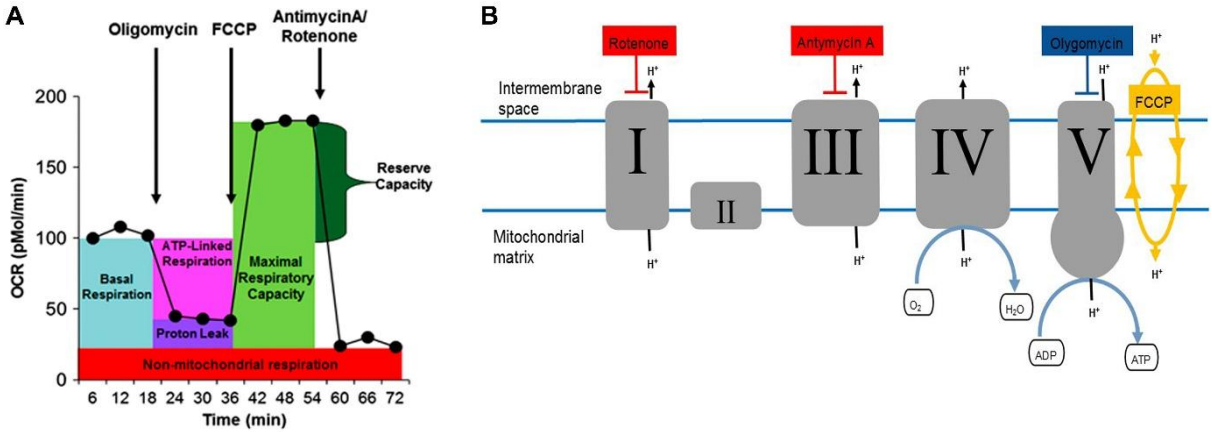

Figure 2.1 Cell Mito Stress Test

(A) Profile of the key parameters of the mitochondrial respirations and **(B)** modulators of the ETC. The figure copied and modified from the Seahorse Bioscience manual.

The assay was performed in the Institute of Genetic Medicine (IGM), Newcastle University under the guidance of Dr. Aurora Gomez-Duran. The experimental protocol was adjusted based on the manufacturer's instructions. Initially, 5,000 cells/ well were seeded into a 96-well XF Cell Culture Microplate by using 75 µl of growth medium. After 24 hours the medium was discarded and replaced with fresh medium containing the appropriate treatments. For the Seahorse assay, the following conditions were tested: 1× PBS, 50 µM BCS, 200 µM BCS, 0.5 µM TTM, 2 µM TTM and 10 µM $Cu(NO_3)_2$. For each condition, at least 9 wells per treatment were used. The plate was incubated with the treatments for 72 h before analysis. Twenty four h prior to analysis the sensor cartridge XF Calibrant was hydrated with XF Buffer and placed at 37° C in a non-CO_2 incubator O/N. On the analysis day, the assay was prepared by adding to the XF Base Medium 25 mM glucose, 1 mM sodium pyruvate, 2 mM glutamine and the pH was adjusted at 7.4. The cell culture microplate was removed from the CO_2 incubator and the old cell culture medium was replaced with warmed assay medium by using a multichannel pipette. The plate was incubated for 1 h at 37° C in a non-CO_2 incubator. For the assay, the following four injections were used: 1.5 µM oligomycin, 0.5 µM FCCP, 0.5 µM FCCP and 1 µM rotenone/antimycin A. Fresh stocks of the working concentrations were prepared prior to starting the assay and diluted with assay buffer. From each working solution, 25 µl were loaded into the appropriate port in the hydrated sensor cartridge which was then placed in the analyser for calibration. Following the use of the calibration plate within the sensor, the calibration plate was replaced with the cell culture microplate.

After the analysis, the spent medium was discarded and 20 µl of cell lysis buffer was added to each well. The plate was incubated on ice for 1 h and then a Bradford assay was used for the determination of the protein concentration. Due to the small volume of the samples the assay was performed in a plate reader. From each well 3 µl of lysate was loaded in duplicate in a

96-well plate together with BSA standards (0, 0.05, 0.1, 0.15, 0.2, 0.3, 0.4, 0.5, 0.6, 0.7 and 0.8 mg/ml). Two hundred and fifty microliters of Bradford reagent was added and the plate was incubated for 20 min at room temperature prior reading the absorbance at 595 nm in a plate reader (BioRad). The data were analysed on Wave software (Seahorse Bioscience) and the final results presented as pmoles/min/mg of protein.

2.9 Fluorescence Activated Cell Sorting (FACS)

2.9.1 Sample generation

To determine if treatments caused changes in mitochondrial morphology or mitochondrial production of ROS we used fluorescence activated cell sorting (FACS). HEK293 cells were seeded into 6-well plates in 3 ml growth medium at a density of 3×10^5 cells cells/well and incubated overnight to allow recovery before treatment. Cell were treated with 1× PBS, 200 µM BCS, 2 µM TTM, 350 µM D-pen, 10 µM $Cu(NO_3)_2$ and 5 µM H_2O_2 as a positive control in triplicate for 72 h before being rinsed twice with 1× PBS, trypsinized and centrifuged at 200 rpm for 5 min. Pellets were resuspended in 500 µl 1× PBS/0.5% BSA containing 5 µM MitoSOX Red (Invitrogen) and 200 nM MitoTracker Green FM (Invitrogen). Cells were then incubated for 15 min before being spun down and resuspend in 1 ml 1× PBS/0.5% BSA. Cells were washed once more with 1x PBS/0.5% BSA before the cell pellets were resuspended in 500 µl of 1× PBS/0.5% BSA.

2.9.2 FACS

Data was collected on a FACSCanto II flow cytometer (BD Bioscience, Oxford, UK) using FACSDiva v6.1.2 software. One thousand events were analysed and a signal threshold was applied for forward scatter (FSC-A), which measures approximate cell size, and side scatter (SSC-A), which measures cell granularity and internal complexity, to exclude debris and a single cell population was gated in order to measure the fluorescence of that specific cell population. Since MitoSOX red and MitoTracker green show spectral overlap over common wavelengths (510/580-42 nm and 490/516-30 nm, respectively), when the emission of one fluorochrome is detected by a detector designated for another, it is impossible to separate the two signals optically and for that reason a compensation correction was applied to the raw data to remove the effects of the spillover emission. For that reason unstained cell and single stained cells were initially analysed in order ensure that the positive stained population was aligned with the correct fluorescent channel. Analysis of the double stained cells was

followed, and collection and analysis of the data was performed with the FACSDiva software and the raw fluorescence values for each fluorochrome were used for statistical analysis.

2.10 Transfection of HEK293 cells

2.10.1 Transfection protocols

For the transfection of the HEK293 cells, the pCMV6-an-DDK mammalian expression vector was used which has DDK tag on its N-terminus for ease identification of the protein product using a DDK antibody. In order to determine the best transfection procedure the next two approaches were tested by using a plasmid caring the GFP protein (Origene plasmid PS100048/ pCMV6-an-mGFP). Initially, in 4-well culture slide HEK293 were seeded in density of 4,000 cells into 250 µl growth medium and left to attach overnight. After 24 hours the next transfection protocols were tested.

2.10.1.1 Polyethylenimine (PEI) transfection

In a sterile tube 1 ml of serum-free DMEM and 7 µg plasmid DNA (pCMV6-an-mGFP/pCMV6-an-DDK_CCS/pCMV6-an-DDK_Atox1) and 20 µg/ml PEI were mixed, vortexed and incubated at RT for 10 min. Thirty and sixty microlitres of the mixture were added in each chamber and incubate for 24 h.

2.10.1.2 Calcium phosphate transfection

Into a 5 ml aliquote of 2× Hepes Buffer Salina (HBS) Na_2HPO_4 (Sigma Aldrich) was added to final concentration of 1.73 mM which was mixed and filtered sterile. Five hundred microlitres of the HBS (Invitrogen) mixture was transferred to a 15 ml tube. In a sterile tube 10 µg of the plasmid DNA (pCMV6-an-mGFP/pCMV6-an-DDK_CCS/pCMV6-an-DDK_Atox1), 61 µl of 2 M $CaCl_2$ (Sigma Aldrich) and sterile H_2O up to 500 µl were added. The mixture with the DNA was added drop by drop to the HBS buffer whilst vortexing. Five min incubation at RT was followed and then 30 µl and 60 µl of the mixture was added to each chamber. Transfected cells were left for 24 h.

In all the above mentioned protocols prior to the addition of the transfection mixture the old medium was discarded and replaced with fresh. After 24 h the medium that contained the transfection reagents were removed from the cells and replaced with fresh growth medium which was left for 72 h in order to accomplish maximum expression. The transfection efficiency of each method was determined by checking the number of transfected cells with

GFP under a fluorescent microscope (Zeiss). The transfection efficiency was similar for the two protocols with PEI method giving a slightly better yield.

2.10.2 Copper manipulation in HEK293 transfected cells

HEK 293 cells were seeded into T25cm^2 flasks (800.000 cells/ 5 ml media) and left to adherent for 24 hours and transfection with PEI was followed (see section 2.11.1.1). Twenty four hours post-transfection the spent medium was replaced with fresh containing the appropriate treatment (200 μM BCS, 2 μM TTM, 10 μM $Cu(NO_3)_2$) and left to incubate for 72 h. After 72 h, cells were washed twice with 1× PBS, 50 μl cell lysis buffer was added, cell were scraped, incubated on ice for a few minutes and scraped again before collection. Lysed cell samples were sonicated for 10 seconds with a sonic probe, 20 min on a sonic bath on ice and stored at -80^o C.

2.11 Immunofluorescence

Immunofluorescence staining was performed on the transfected cells for Atox1. Seventy-two hours post-transfection the spent medium was removed and the cells were rinsed twice with 1× PBS for 5 min, fixed with 4% formaldehyde (Sigma Aldrich, diluted in 1× PBS) for 15 min and washed again twice with 1× PBS. Slides were taken immediately to the staining protocol where they were blocked for 1 h with 1× PBS/5% normal goat serum/0.3% triton. After 1 h incubation with mouse anti-Atox1 diluted 1:1000 in buffer containing 1× PBS/1% BSA/0.3% triton, cells were given 3 washes for 5 min with 1× PBS, followed by incubation with secondary goat anti-mouse Alex-Fluoro 488 (Invitrogen). Slides were washed three times with 1× PBS for 5 min before removing the slide chamber then placed for 30 sec in DAPI/PBS in order to stain the cell nuclei. Slides were visualized under a fluorescent microscope where images were captured with AxionVison software under identical exposure times.

2.12 Statistical analysis

Statistical analysis for both brain and cell study was performed in GraphPad Prism 5. All data are presented as mean (SD) as a preferred way of describing the variability around the sample population[*(285)*].

2.12.1 Statistical analysis for brain samples data set

A non-parametric t- test (Mann-Whitney U test) was used to analyse between two group variables (controls versus LOAD or EOAD) since in the majority of the data sets fail to pass the F test for equal variances and the D'Agostino & Pearson omnibus normality test. Spearman's rank test was used to define if there was any correlation between variables in the different groups, such as age versus metal levels or activity/protein levels. A Kruskal-Wallis test followed by Dunn's Multiple Comparison post-test was used in order to determine differences amongst the different brain regions. For the non-parametric test (Mann-Whitney U test and Kruskal-Wallis) p values less than 0.05 were consider as statistical significant whereas for the correlation analysis values less than 0.01 were consider as significant.

2.12.2 Statistical analysis for cell sample data set

The obtained data from the toxicity and growth curves were analysed with a two-way ANOVA since we wanted to determine the effects of variables between time and treatments. In order to determine if there was any significant difference between treatments, a Bonferroni post-test was performed and p values less than 0.05 were consider as statistical significant. A one-way ANOVA was used to analyse data set with different treatments and the in-between group variable difference was determined by a Tukey's post-test and p values less than 0.05 were consider as statistical significant.

3 The role of copper homeostasis pathways in the ageing brain

3.1 Introduction

Ageing is a natural process which is characterized by progressive decline in physiological functions, behavioural capacity, and increased susceptibility to disease and death[286]. In developing countries the average life expectancy is higher than 70 years with some people living to more than 100 years. The increasing life span has produced an increase in age associated health problems and some of these are correlated with changes in brain function. Over the years, a number of theories have been used to explain the natural process of ageing with one of the most accepted being the "free radical theory of ageing"[287]. This theory proposes that ageing is a combination of free radical induced damage to cellular macromolecules and the inability of the cell to balance these changes with an efficient mechanism of antioxidant defence[287]. The origin of this theory goes back to almost one century ago when Pearl introduced the "rate of living theory" suggesting that the lifespan of every individual depends on the rate they utilize energy and on the genetically determined amount of energy consumed during adult life[288]. Generally Pearl's theory supports that the longevity of an organism is inversely correlated with the metabolic activity: increase metabolic activity results in decrease longevity whereas factors that decrease the metabolic rate can contribute to longevity[288].

The "free radical theory of ageing" was originally proposed by Harman in the mid-1950s and suggests that free radicals which are produced during aerobic respiration have a significant impact on cell components, causing increased damage over the normal lifespan which eventually results in ageing and death[287]. Initially it was believed that the free radicals are mostly produced through reactions involving molecular oxygen which is catalysed within cells by oxidative enzymes and enhanced in the presence of transition metals such iron and copper[287]. Later, Harman expanded the theory by including mitochondria in the physiological process of ageing since they are responsible for generating a significant amount of cellular energy by consuming the majority of the intracellular oxygen[287]. This addition led to the new improved "mitochondrial free radical theory of ageing" which supports that oxidative stress attacks mitochondria, leading to increased oxidative damage and as the damage progresses mitochondria become less efficient [287]. Mitochondria will eventually lose their function and release more oxygen radicals which will increase the oxidative damage and will culminate in accumulation of dysfunctional mitochondria within cells with ageing[286, 287].

Several studies have shown that the brain is particularly susceptible to both structural and functional changes with ageing. Brain mass decreases by up to 3% by the age of 50 and

people of more than 80 years exhibit a 10% brain mass loss relative to younger persons brains[289]. Studies with magnetic resonance imaging (MRI) and voxel based morphometry (VBM) have shown that the brain's grey and white matter volume decreases with ageing especially in regions such as prefrontal, parietal and temporal cortex[290, 291]. At a cellular level, shortening of the telomeres, activation of tumour suppressor genes, accumulation of mitochondrial and nuclear DNA damage, oxidative stress, and mild chronic inflammation are some of the ageing characteristics of the brain[286].

Copper as a redox metal has the potential to generate free radicals in the brain and could contribute to the "free radical theory of ageing". Copper is also required for the activity of two central enzymes in the theory, the mitochondrial COX and the antioxidant defence enzyme SOD. Understanding how copper, copper binding enzymes and proteins correlate with ageing in different brain regions will allow us to understand better the natural process of ageing and if they are factors that can enhance brain longevity.

3.2 Aims

The aim of this chapter is to identify if there is a correlation between ageing, copper levels, activity levels of COX and SOD, and important copper binding proteins in two different brain regions, frontal and temporal cortex. Correlations between the above mentioned variables were also determined to establish if there were any linkages. Brain homogenates from healthy control samples were analysed by ICP-MS, COX and SOD activity and samples were arranged by increasing age for protein levels measurement by Western blot.

3.3 Results

3.3.1 Identifying changes in copper levels, COX and SOD activity in the healthy brain with ageing

Initially ICP-MS analysis was used in order to determine the copper levels in 27 brain samples coming from normally aged people in two different brain regions, frontal and temporal cortex. These two brain regions were selected since changes with aging have been observed in the cortex; also, they are two of the most affected brain regions in age related disorders such as AD. A partial analysis in cerebellum was conducted since due to time limitation it was not possible to finalise the protein analysis in that brain region[290, 291]. The obtained results regarding copper levels, SOD and COX/CS activity for cerebellum are reported in Appendix A. By arranging the measured copper levels by chronological order we observed that copper levels started to decline with increasing age at death, and similar findings were also observed for SOD and COX activity. In order to confirm our observation we used Spearman's rank statistical test since the data failed to pass the D'Agostino & Pearson omnibus normality test. Multiple statistical tests were performed which increases the possibility of obtaining false positive results by chance at $p<0.05$. In order to avoid this, statistical significance was set at p values of less than 0.01.

A significant negative correlation between age and copper levels in both frontal (r_s=-0.617, n=27, p=0.0006) and temporal cortex (r_s=-0.535, n=27, p=0.0041) was identified (Figure 3.1A). The result indicates that there is a moderate to strong correlation which shows that in the healthy brain copper levels are decreasing with age. In the same brain samples, total SOD activity was measured in the homogenates and the relative units per mg of protein calculated. SOD activity was also tested for correlation and a significant positive correlation between age of death and activity was observed in temporal cortex (r_s=0.5801, n=27, p=0.0025). In frontal cortex there was also a positive correlation (r_s=0.4564, n=27, p=0.0167) but the change was not significant based on the multiple comparison correction that we set. In temporal cortex and to a lesser extent in frontal cortex, there is a moderate increase in SOD activity during ageing in the healthy brain (Figure 3.1B).

In the same brain homogenates we also measured COX and CS activity. Both assays were conducted the same day and from the same brain aliquot in order to ensure comparability. The final activity of Complex IV is expressed as a ratio of COX relative to the CS. The COX/CS ratio was also examined in order to identify if there was a correlation with ageing and again

there was a significant positive correlation in temporal cortex COX/CS activity (r_s=0.522, n=27, p=0.0051) but not in frontal cortex COX/CS activity (r_s=0.346, n=27, p=0.076) (Figure 3.1C). Whilst the correlation in frontal cortex was not significant, as with temporal cortex, activity was increased with ageing

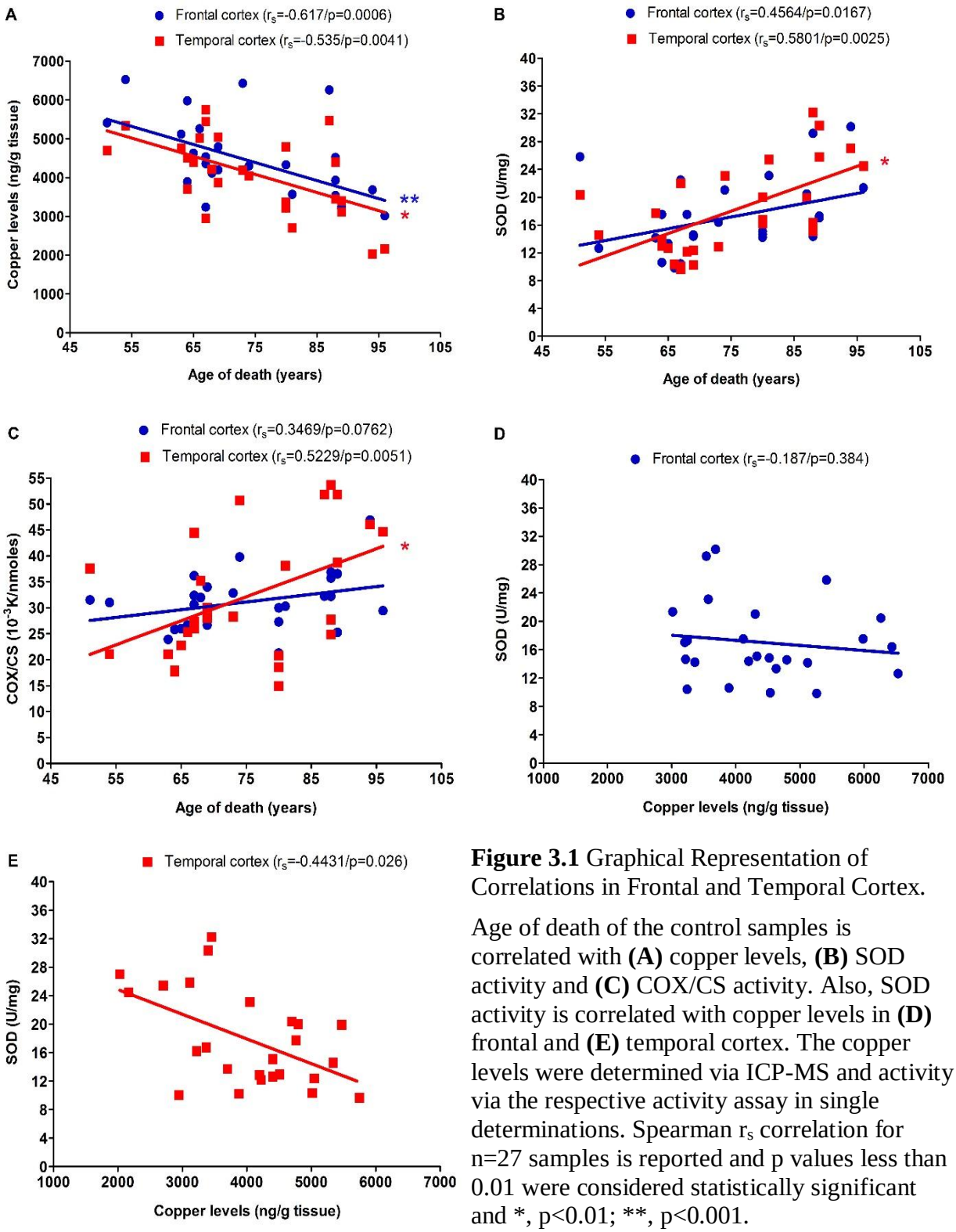

Figure 3.1 Graphical Representation of Correlations in Frontal and Temporal Cortex.

Age of death of the control samples is correlated with **(A)** copper levels, **(B)** SOD activity and **(C)** COX/CS activity. Also, SOD activity is correlated with copper levels in **(D)** frontal and **(E)** temporal cortex. The copper levels were determined via ICP-MS and activity via the respective activity assay in single determinations. Spearman r_s correlation for n=27 samples is reported and p values less than 0.01 were considered statistically significant and *, p<0.01; **, p<0.001.

Further COX/CS and SOD activity were correlated with copper levels in both brain regions. Correlating COX/CS with copper levels did not reveal any significant association for either of the brain regions (Table 3.1 and 3.2) although for SOD there was a negative correlation in temporal cortex (r_s=-0.4431, n=27, p=0.026) but this was not significant following correction for multiple testing. Whilst not significant, the correlation between SOD activity and copper levels suggests that in both frontal and temporal cortex when copper levels are increasing SOD activity is decreasing (Figure 3.1D, E).

3.3.2 Changes in COX complex proteins in the ageing brain

The two catalytic protein subunits of COX, COX1 and COX2, both bind copper and are necessary for complex activity. Western blotting was used to measure the protein levels of COX1, COX2 and VDAC1 in 25 brain samples. Two of the control cases were excluded from the analysis due to lack of space in the gels and based on the fact that there were 2 other cases with the same age. The brain samples from frontal and temporal cortex were loaded with increasing age at death order and the membranes were incubated with antibodies for the protein of interest. Representative Western blots from both brain regions for COX1, COX2 and VDAC1 are presented in Figure 3.2A, B, D and E. The measured relative protein levels were correlated with the age of death of control samples and the analysis showed that for COX1 protein levels there was a positive correlation with increasing age of the controls. In frontal cortex (r_s=0.7636, n=25, p<0.0001) there was a strong and significant increase in COX1 protein levels as the brain gets older. Similar increase was also observed in temporal cortex (r_s=0.441, n=25, p=0.0273) but the correlation was not statistical significant (Figure 3.2C). On the other hand, COX2 protein levels showed a negative correlation with ageing which means that as the brain gets older there is less COX2 protein especially in temporal cortex (r_s=-0.5702, n=25, p=0.0029). Similar trend was also observed in frontal cortex (r_s=-0.3079, n=25, p=0.1344) but again the changes was not considered significant (Figure 3.2F).

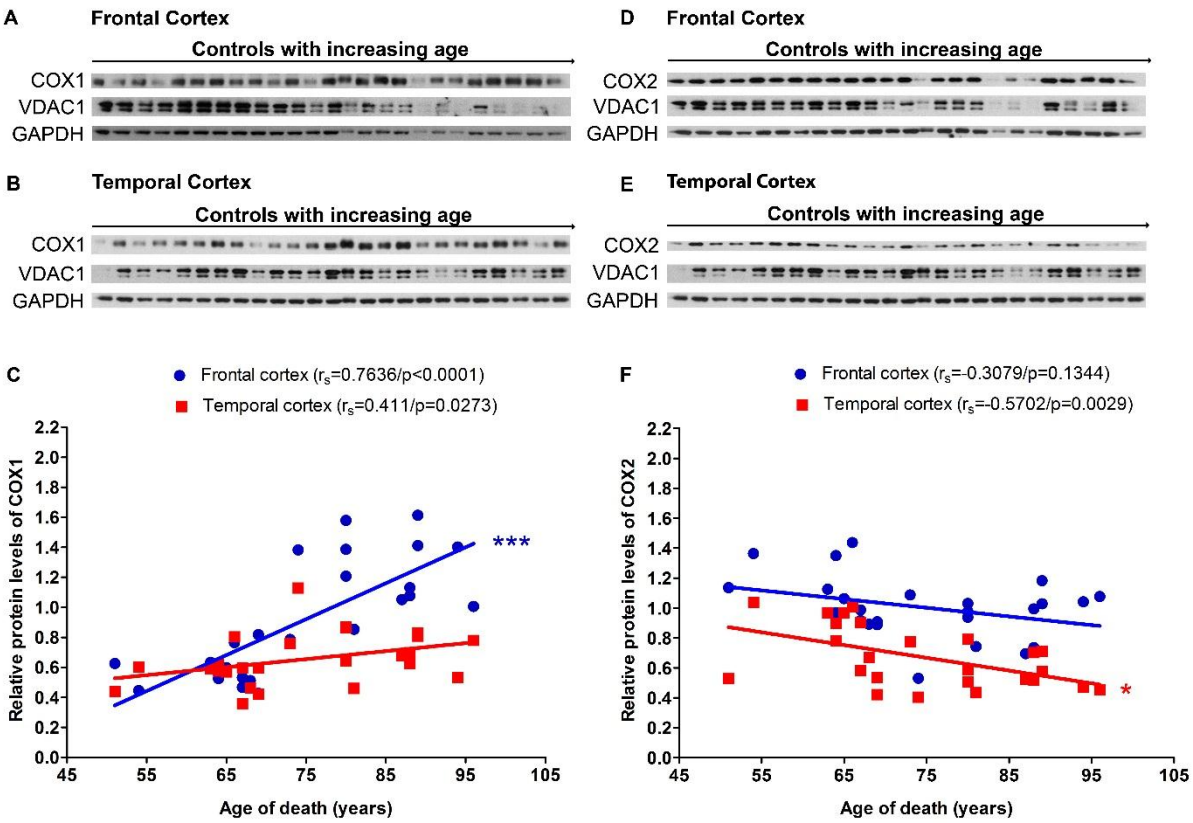

Figure 3.2 COX1, COX2 and VDAC1 Protein analysis in Frontal and Temporal Cortex and Correlation with Age of Death in Healthy Human Brain.

Western blot analysis for COX1 or COX2 in **(A, D)** frontal and **(B, E)** temporal cortex. Correlation with age of death for **(C)** COX1 and **(F)** COX2 protein levels normalised with GAPDH in both frontal and temporal cortex. The protein levels were measured by semiquantitate Western blot analysis in single determinations. Spearman r_s correlation is reported and p values less than 0.01 were considered statistically significant and *, $p<0.01$; ***, $p<0.0001$.

COX2 and COX1 protein were examined for potential correlations between their levels and COX/CS activity. For COX1, no significant correlation is observed in either frontal or temporal cortex and COX/CS (Table 3.1 and 3.2). However, for COX2 a negative correlation was detected in both frontal and temporal cortex. In temporal cortex, COX2 protein levels significantly decreased with increasing COX/CS activity (r_s=-0.5831, n=25, p=0.002) (Figure 3.3B). In frontal cortex (r_s=-0.376, n=25, p=0.065) a trend towards a similar correlation was observed although this failed to reach significance (Figure 3.3A).

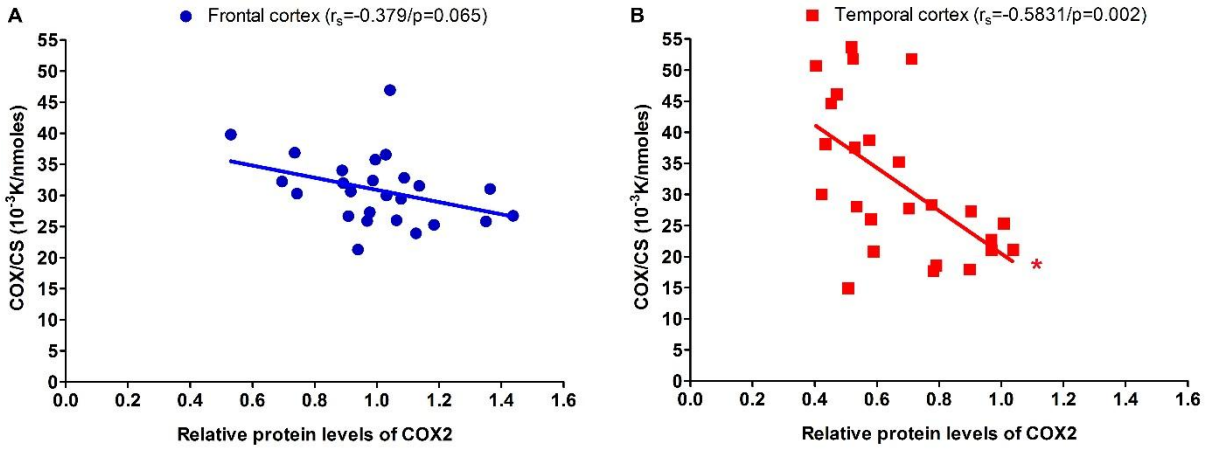

Figure 3.3 Graphical representation of COX2 Protein Levels Correlated with COX/CS Activity.

(A) Frontal and **(B)** temporal cortex COX/CS activity correlated with COX2 protein levels normalised with GAPDH. Spearman r_s correlation is reported and p values less than 0.01 were considered statistically significant and *, p<0.01.

COX1 and COX2 are mitochondrial DNA encoded proteins and for that reason mitochondrial mass levels were measured by using VDAC1, a mitochondrial loading control, however no significant change with ageing was observed, with only a moderate not significant trend towards a decrease in frontal cortex (r_s=-0.500, n=25, p=0.011) being present (Table 3.2 and 3.3). Since COX1 and COX2 are mitochondrial proteins, the normalized ratio with VDAC1 was analysed in order to determine changes with ageing. COX1/VDAC1 ratio showed a similar increase with ageing but the ratio of COX2/VDAC1 showed opposite results to that of COX2. COX2/VDAC1 ratio in frontal cortex showed a trend towards a positive correlation with increasing age at death (r_s=0.359, n=25, p=0.078) although this was opposite to the effect of what was observed in temporal cortex (r_s=-0.537, n=25, p=0.006). This finding is possibly due to the decreased VDAC1 levels in frontal cortex with ageing which is not observed in temporal cortex where mitochondria levels do not change. Tables 3.1 and 3.2 presents further correlations with different variables for the mitochondrial related proteins and activity.

Frontal Cortex	Copper levels (ng/g tissue)	COX/CS activity (10^{-3} K/nmoles)	VDAC1 protein levels	COX1 protein levels	COX1/VDAC1 protein levels	COX2 protein levels	COX2/VDAC1 protein levels
Age of death (years)	**r_s=-0.617, n=27 p=0.0006 (**) Decrease**	r_s=0.3469, n=27 p=0.076 NS	r_s=-0.500, n=25 p=0.011 NS	**r_s=0.7636, n=25 p<0.0001 (***) Increase**	**r_s=0.846, n=25 p<0.0001 (***) Increase**	r_s=-0.307, n=25 p=0.134, NS	r_s=0.359, n=25 p=0.078, NS
Copper levels (ng/g tissue)		r_s=0.101, n=27 p=0.632 NS		r_s=-0.485, n=25 p=0.021 NS	**r_s=-0.536, n=25 p=0.006 (*) Decrease**	r_s=0.305, n=25 p=0.138, NS	r_s=-0.245, n=25 p=0.239 NS
COX/CS activity (10^{-3} K/nmoles)			r_s=-0.068, n=25 p=0.748 NS	r_s=0.195, n=25 p=0.351 NS	r_s=0.173, n=25 p=0.408 NS	r_s=-0.376, n=25 p=0.064, NS	r_s=-0.320, n=25 p=0.119 NS
VDAC1 protein levels				**r_s= -0.529, n=25 p= 0.007 (*) Decrease**		r_s=0.486, n=25 p=0.014, NS	
COX1 protein levels						r_s=-0.119, n=25 p=0.470, NS	r_s=0.419, n=25 p=0.037, NS
COX1/VDAC1 protein levels						r_s=-0.160, n=25 p=0.445, NS	**r_s=0.592, n=25 p=0.002 Increase (*)**

Table 3.1 Correlations between Mitochondrial Enzymes and Copper in the Ageing Human Frontal Cortex.

Spearman rank (r_s) test was used to identify correlation in frontal cortex of control brain samples with variables being age of death, copper levels, COX/CS activity, VDAC1, COX1 and COX2 protein levels. Values highlighted with red indicate statistical significant changes where p values less than 0.01 were considered statistically significant. *, p<0.01; **, p<0.001; ***, p<0.0001; NS: non-significant.

Temporal cortex	Copper levels (ng/g tissue)	COX/CS activity (10^{-3} K/nmoles)	VDAC1 protein levels	COX1 protein levels	COX1/VDAC1 protein levels	COX2 protein levels	COX2/VDAC1 protein levels
Age of death (years)	**r_s=-0.535, n=27 p=0.0041 (*) Decrease**	**r_s=0.5229, n=27 p=0.0051 (*) Increase**	r_s=-0.007, n=25 p=0.975 NS	r_s=0.441, n=25 p=0.0273 NS	r_s=0.382, n=25 p=0.059 NS	**r_s=-0.570, n=25 p 0.0029 (*) Decrease**	**r_s=-0.537, n=25 p=0.006 (*) Decrease**
Copper levels (ng/g tissue)		r_s=-0.266, n=27 p=0.198 NS		r_s=-0.173, n=25 p=0.408 NS	r_s=-0.149, n=25 p=0.476 NS	r_s=0.356, n=25 p=0.081 NS	r_s=0.481, n=25 p=0.015 NS
COX/CS activity (10^{-3} K/nmoles)			r_s=-0.152, n=25 p=0.486 NS	r_s=0.056, n=25 p=0.790 NS	r_s=0.275, n=25 p=0.184 NS	**r_s=-0.583, n=25 p=0.002 (*) Decrease**	r_s=-0.341, n=25 p=0.096 NS
VDAC1 protein levels				r_s=0.372, n=25 p=0.067, NS		r_s=0.399, n=25 p=0.048, NS	
COX1 protein levels						r_s=0.074, n=25 p=0.726 NS	r_s=-0.245, n=25 p=0.239 NS
COX1/VDAC1 protein levels						r_s=-0.405, n=25 p=0.045 NS	r_s=0.275, n=25 p=0.184 NS

Table 3.2 Correlations between Mitochondrial Enzymes and Copper in the Ageing Human Temporal Cortex

Spearman (r_s) rank test was used to identify correlation in temporal cortex of control brain samples with variables being age of death, copper levels, COX/CS activity, VDAC1, COX1 and COX2 protein levels. Values highlighted with red indicate statistical significant changes where p values less than 0.01 were considered statistically significant. *, $p<0.01$; NS: non-significant.

3.3.3 Proteins related to SOD activity change in the ageing brain

Proteins that directly regulate SOD activity (SOD1, SOD2 and CCS) were also measured in order to see how they were affected by ageing, SOD activity or copper levels. Representative Western blots from both brain regions for CCS, SOD1 and SOD2 are presented in Figure 3.4A, B, C and D. The relative protein levels of each protein were correlated with the age of death which revealed that for CCS there was a significant positive correlation in temporal cortex (r_s=0.690, n=25, p=0.0001) and a trend towards a significance in frontal cortex (r_s=0.4419, n=25, p=0.027) with CCS levels increasing with ageing (Figure 3.4E)

Similar results were obtained for SOD1 protein levels where there was a significant positive correlation in temporal cortex (r_s=0.7047, n=25, p<0.0001) but not in frontal cortex (r_s=0.187, n=25, p=0.373). For SOD1, in temporal cortex, there was a strong increase in its levels as ageing progresses (Figure 3.4F). Whilst in frontal cortex there was no significant change of SOD1 levels with ageing, the pattern was similar to temporal cortex. SOD2 protein levels were also seen to be increasing with ageing but the correlation was not significant for either frontal (r_s=0.451, n=25, p=0.024) or temporal cortex (r_s=0.435, n=25, p=0.03) (Figure 3.4G).

CCS is responsible for delivering copper and activating SOD1 in the cytosol. A positive correlation between CCS and SOD1 protein levels was showing that CCS protein levels are increasing together with SOD1 protein levels. A significant correlation was observed in temporal cortex (r_s=0.795, n=25, p+0.0001) with a similar trend in frontal cortex (r_s=0.474, n=25, p=0.016) although this failed to reach significance following correction (Figure 3.5A and B). Total SOD activity consists of the combined activities of SOD1 and SOD2 and therefore possible correlations amongst them was examined. A positive correlation was observed between SOD activity and SOD1 protein levels with an increase in temporal cortex (r_s=0.6323, n=25, p=0.0007) although in frontal cortex (r_s=0.187, n=25, p=0.380), despite there being a similar positive association, the correlation was not significant (Figure 3.5C and D). In frontal cortex a positive correlation between SOD2 protein levels and SOD activity was observed (r_s=0.570, n=25, p=0.002) although this failed to reach significance within the temporal cortex (r_s=0.4277, n=25, p=0.03) (Figure 3.5E and F). Table 3.3 and 3.4 present a summary of the correlations and additional variables including copper, protein levels, and SOD activity where trend towards a significant correlation was seen in temporal cortex between CCS protein levels and SOD activity.

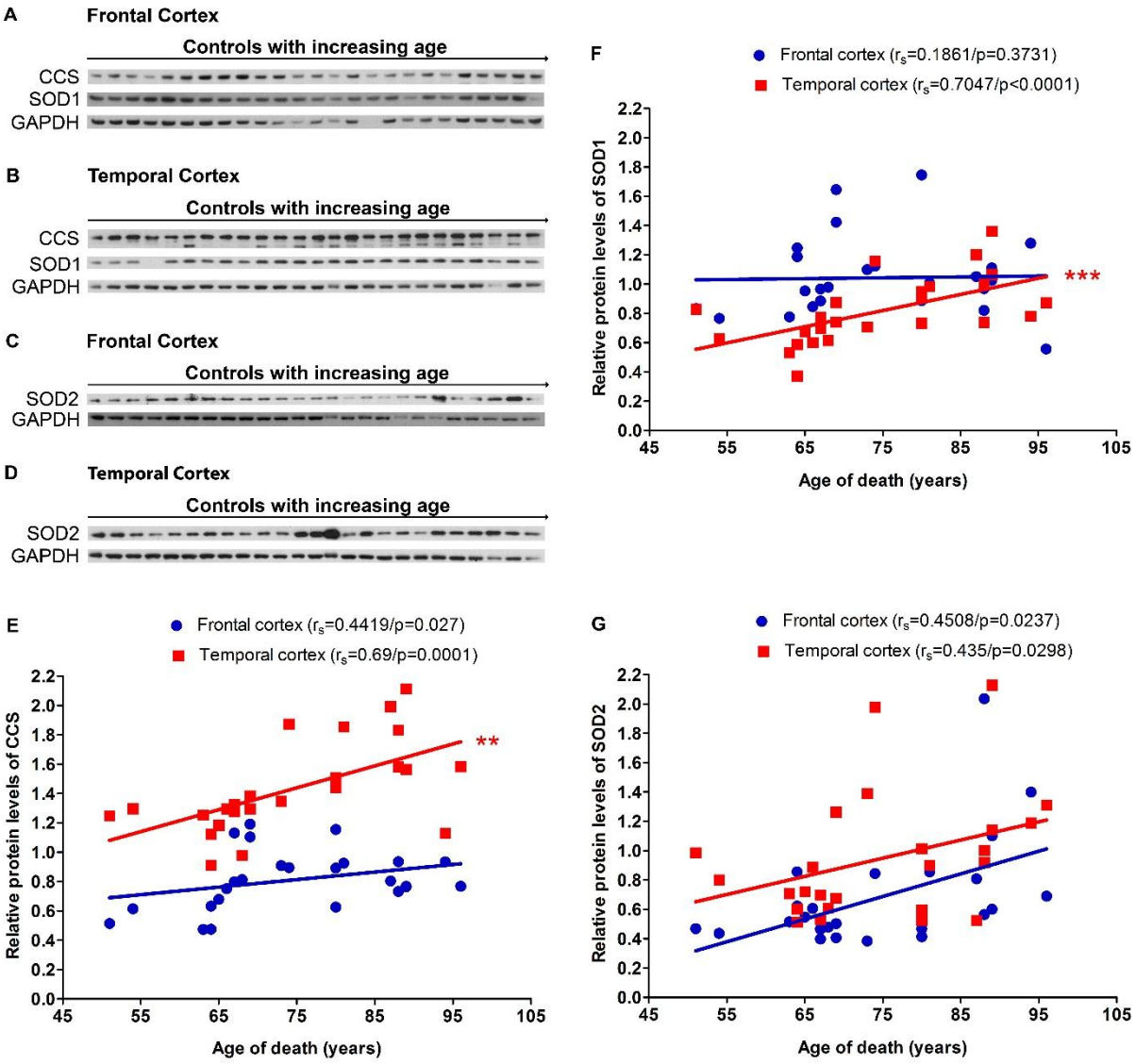

Figure 3.4 CCS, SOD1 and SOD2 Protein Analysis in Frontal and Temporal Cortex and Correlation with the Age of Death in Healthy Brain.

Western blot analysis for CCS and SOD1 or SOD2 in **(A, C)** frontal and **(B, D)** temporal cortex. Correlation with age of death for **(E)** CCS **(F)** SOD1 and **(G)** SOD2 protein levels normalised with GAPDH in both frontal and temporal cortex. The protein levels were measured by semiquantitate Western blot analysis in single determinations. Spearman r_s correlation for n=25 samples is reported and p values less than 0.01 were considered statistically significant. **, p<0.001; ***, p<0.0001.

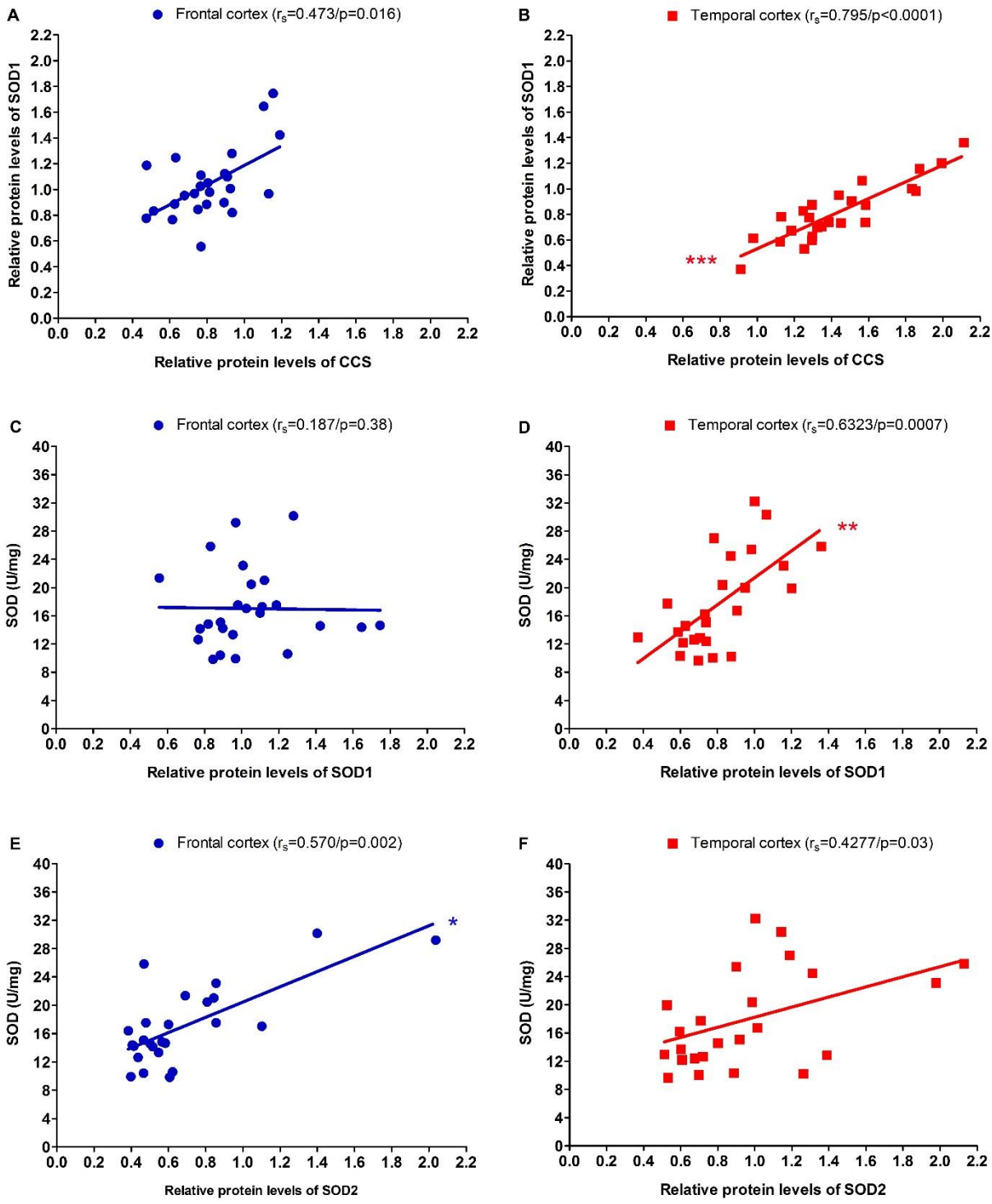

Figure 3.5 Graphical Representation of Correlations between CCS, SOD1 and SOD2 Protein Levels with SOD Activity or SOD1 Protein Levels.

CCS protein levels were positive correlated with SOD1 protein levels in **(A)** frontal and **(B)** temporal cortex. SOD activity is also positive correlated with either SOD1 or SOD2 protein levels respectively in **(C, E)** frontal or **(D, F)** temporal cortex. Spearman r_s correlation for n=25 samples is reported and p values less than 0.01 were considered statistically significant. *, p<0.01; **<0.001.

Frontal cortex	Copper levels (ng/g tissue)	SOD activity (U/mg)	SOD1 protein levels	CCS protein levels	SOD2 protein levels
Age of death (years)	r_s=-0.617, n=27 p=0.0006 (**) Decrease	r_s=0.4564, n=27 p=0.0167 NS	r_s=0.186, n=25 p=0.373 NS	r_s=0.4419, n=25 p=0.027 NS	r_s=0.4508, n=25 p=0.0237 NS
Copper levels (ng/g tissue)		r_s=-0.187, n=25 p=0.384 NS	r_s=-0.142, n=25 p=0.497 NS	r_s=-0.260, n=25 p=0.209 NS	
SOD activity (U/mg)			r_s=0.183, n=25 p=0.380 NS	r_s=0.024, n=25 p=0.908 NS	**r_s=0.570, n=25 p=0.002 (*) Increase**
SOD1 protein levels				r_s=0.473, n=25 p=0.016 NS	r_s=0.234, n=25 p=0.261 NS

Table 3.3 Correlation between Protein and Enzyme Activity in the Ageing Human Frontal Cortex.

Spearman (r_s) rank test was used to identify correlations in frontal cortex between age, copper, SOD activity and the protein levels of CCS, SOD1, SOD2 and as well as different combinations amongst these. Values highlighted with red indicate statistical significant changes where p values less than 0.01 were considered statistically significant. *, $p<0.01$; **, $p<0.001$; NS: non-significant.

Temporal cortex	Copper levels (ng/g tissue)	SOD activity (U/mg)	SOD1 protein levels	CCS protein levels	SOD2 protein levels
Age of death (years)	**r_s=-0.535, n=27 p=0.0041 (*) Decrease**	**r_s=0.5801, n=27 p=0.0025 (**) Increase**	**r_s=0.7047, n=25 p<0.0001 (***) Increase**	**r_s=0.690, n=25 p=0.0001 (**) Increase**	r_s=0.435, n=25 p=0.0298 NS
Copper levels (ng/g tissue)		r_s=-0.4431, n=27 p=0.026 NS	r_s=-0.356, n=25 p=0.078 NS	r_s=-0.191, n=25 p=0.361 NS	
SOD activity (U/mg)			**r_s=0.6323 n=25 p=0.0007 (**) Increase**	r_s=0.477, n=25 p=0.016 NS	r_s=0.427, n=25 p=0.03 NS
SOD1 protein levels				**r_s=0.795, n=25 p<0.0001 (***) Increase**	r_s=0.467, n=25 p=0.019 NS

Table 3.4 Correlation between Proteins and Enzyme Activity in the Ageing Human Temporal Cortex.

Spearman (r_s) rank test was used to identify correlations in temporal cortex between age, copper, SOD activity and the protein levels of CCS, SOD1, SOD2 and as well as different combinations amongst these. Values highlighted with red indicate statistical significant changes where p values less than 0.01 were considered statistically significant. *, p<0.01; **, p<0.001; NS: non-significant.

3.3.4 Effects of ageing brain on other copper binding proteins

The overall aims of the study was to measure the activity /protein levels of key components of the three copper pathways, however, we encountered some difficulties in the process. Initially, we wanted to study the expression/activity of a secreted copper binding enzyme in both the brain samples and the HEK293. However, the HEK293 did not express the majority of these enzymes and Cp activity/protein levels could not be used since the cell were grown in the presence of bovine serum (contains bovine Cp) and we would not be able to separate the different forms. Then, we attempted to measure the activity levels of the copper dependent ferroxidase Hephaestin but the assay was not giving reproducible results. Since we were not able to measure the activity levels of a copper secreted enzyme, we focused on measuring the protein levels of key components of the secretory copper pathway such as ATP7a, Atox1 and

Hephaestin. We attempted to measure Cp levels in the ageing brain but the used antibody did not work well when the analysis was conducted and due to time restrictions, we were not able to repeat the analysis. In the general attempt to measure representative proteins from all pathways, Sco2 protein levels were measured too, however, the results were not significant and for that reason they are presented in this section. The results from the Spearman rank tests frontal and temporal cortex are presented in Table 3.5. Generally, the results did not show statistical significance for the majority of these proteins after correction for multiple testing and also there were some inconsistencies between the two brain regions. For example ATP7a showed a trend towards positive correlation in temporal cortex (r_s=0.3882, n=25, p=0.0937) but negative in frontal cortex (r_s=-0.2404, n=25, p=0.247). Furthermore, the analysis showed that Sco2 protein levels were increasing with ageing in frontal cortex (r_s=0.5521, n=25, p=0.0042) but not changing at all in temporal cortex (r_s=-0.05, n=25, p=0.8092). Hephaestin protein levels were significantly increasing with ageing in temporal cortex (r_s=0.5421, n=25, p=0.0051) but not in frontal cortex (r_s=0.1399, n=25, p=0.5049). No significant correlation was observed between the above mention proteins and copper levels in either brain regions.

Protein of interest	Frontal cortex		Temporal cortex	
	Age of death (years)	Copper levels (ng/g tissue)	Age of death (years)	Copper levels (ng/g tissue)
ATP7a protein levels	r_s=-0.2404, n=25 p=0.247 NS	r_s=0.1862, n=25, p=0.373 NS	r_s=0.3425, n=25, p=0.0937 NS	r_s=-0.2877, n=25, p=0.1632 NS
Sco2 protein levels	**r_s=0.5521, n=25 p=0.0042 (*) Increase**	r_s=-0.3231, n=25 p=0.1152 NS	r_s= 0.0508, n=25 p=0.8092 NS	r_s=-0.1808, n=25 p=0.3872 NS
Hephaestin protein levels	r_s=0.1399, n=25 p=0.5049 NS	r_s=-0.2469, n=25 p=0.2341 NS	**r_s= 0.5421, n=25 p=0.0051 (*) Increase**	r_s=-0.4362, n=25 p=0.293 NS
Atox1 protein levels	r_s=0.3679, n=25 p=0.0707 NS	r_s=-0.0746, n=25 p=0.723 NS	r_s=-0.161, n=25 p=0.4419 NS	r_s=0.2192, n=25, p=0.2924 NS

Table 3.5 Correlation between Proteins and Copper in the Ageing Human Frontal and Temporal Cortex.

Spearman (r_s) rank analysis for the protein levels of ATP7a, Sco2. Hepahaestin and Atox1 in frontal and temporal cortex are correlated with age of death and copper levels Values highlighted with red indicate statistical significant changes where p values less than 0.01 were considered statistically significant. *, p<0.01; **, p<0.001; NS: non-significant.

3.4 Discussion

The aim of this chapter was to identify how copper homeostasis pathway associates with the process of healthy ageing in the brain. Copper can be toxic in high levels but under normal conditions is required for the activity of two important cellular enzymes, COX and SOD1. Both of these enzymes play a central role in the "mitochondrial free radical theory of ageing" since COX contributes directly to ROS production and SOD1 is responsible for the elimination of the superoxide free radical. It is known that in the ageing brain, mitochondria are potentially dysfunctional and produced ROS are elevated as a possible consequence. The main source of the mitochondrial derived ROS is Complex I and to lesser extent Complex III[(86)]. Complex I mainly releases superoxide anions into the mitochondrial matrix and Complex III to both sides of the inner membrane, which makes Complex III derived ROS more accessible to the cell cytosol[(292)]. In mitochondria, ROS production depends on the $\Delta\Psi_m$ which under normal conditions is around 100-140 mV although when $\Delta\Psi_m$ goes above 150-200 mV an increased production of ROS occurs[(293)].

ROS are also produced by other molecules in the cells such as from NADPH oxidase in the plasma membrane, peroxisomes, cytochrome P450, xanthine oxidase, monoamine oxidase, cyclooxygenase and lipoxygenase. Transition metals such copper and iron can produce ROS through Fenton or Haber-Weiss reactions where they form hydroxyl radicals by oxidizing H_2O_2. The role of iron has also been studied in the ageing brain and is well established that iron accumulates in the brain with ageing[(294)].

By analysing 27 healthy brain samples varying from age 51 to 96 we identified that copper levels significantly decrease as the brain ages (Figure 3.1A). Decreased copper levels in frontal and temporal cortex might be explained by low dietary copper uptake and gradual weight loss that is normally observed in the elderly people[(295)]. Few studies have attempted to measure copper in the normal fully developed brain with the first coming from Bonilla *et al.* who also showed a negative correlation between copper and age[(246)]. However, a more recent study from Ramos *et al.* showed that copper levels showed a small, non–significant decline[(296)]. Studies with animals have attempted to establish a correlation between copper levels and age in the brain however, these have found that copper accumulates in the brain with ageing[(297, 298)].

The differences amongst studies, especially in humans, might depend on different variables, such as number of samples, post-mortem delay, sample preparation or even the different copper determination procedure. It is worth mentioning that the mean copper concentration

from our study is 4.41±1.05 μg/g tissue is close to that of Bonilla *et al.* (5.43±0.71 μg/g tissue) but almost four times less than Ramos *et al.* reported (21±7 μg/g tissue)[246, 296]. This indicates that small differences in the sample preparation or alternative protocols for analysis can lead to large differences between studies. As far as it concerns the opposite effect that we observed between human and animal studies this can be attributed to the fact that 1-2 years old animals might not be consider as senescence/aged. The observation of accumulated copper in the animals' brain might reflect the events that happen in the human brain during the childhood and adolescent. Based on a study, where synchrotron X-ray microscopy was used in paraffin fixed post-mortem brain tissue, copper concentration seems to increase over the first 20 years of the human life and then a decrease seems to occur in copper levels[299]. The increased requirement for copper for the first 20 years possibly reflects developmental processes of the brain since in that stage copper is required for the function of COX and SOD1 in the developing neurons as well as for the myelination of the neuronal axons[300].

3.4.1 The "mitochondrial free radical theory" in the ageing brain

The "mitochondrial free radical theory" suggests that an imbalance between ROS production and the antioxidant defence mechanism is causative in ageing[286, 287]. A number of studies have tried to measure ROS levels, the activity of the mitochondrial respiratory complexes, and activity of the antioxidant defence enzymes in different human or animal tissues. In this study, we have focussed on measuring the enzyme activity of these two systems (mitochondrial and antioxidant defence) and determined the protein levels which regulate and contribute to the two systems.

3.4.1.1 Are mitochondria malfunctioning in the healthy human brain?

Two different brain regions were used and the results were similar between them with only small differences observed, probably related to local brain regional changes (further discussed in section 3.5.2). Mitochondrial levels were not significantly changed with ageing in either brain regions although there was a moderate increase in COX/CS activity with ageing (Table 3.1 and 3.2). The brain is the highest consumer of energy substrates in the body where normally it metabolizes 60% of glucose and 20% of oxygen[85, 301]. Neurons mainly produce ATP through the respiratory chain since they require ATP for maintaining ion homeostasis and membrane potentials. Given this high metabolic demand it is not surprising that COX/CS activity was found to be increasing with ageing, in order to maintain the energy demand in the non-dividing and long-living neurones. Another possible reason might be due to neuronal

atrophy which is typical in the ageing brain[302], the remaining "healthy" neurons increase metabolic activity to compensate for the neuronal loss in a specific brain region.

Numerous studies have tried to measure the activity of all the electron transport chain complexes, with the majority of these having been conducted in mice or rats and only a few studies in human tissues. COX activity has been measured in skeletal muscle mitochondria where no change in activity was observed with ageing[303]. However, the reported ageing studies in mice and rats using different tissues (liver, heart, skeletal muscles and brain) show variable changes from increases to decreases or no change in COX activity[304, 305]. It is worth mentioning that studies with isolated mitochondria from mouse brain have reported both a decrease and an increase in COX activity[305]. Once again, what these studies define as an aged animal might not be representative of the human ageing brain since they use animals from 1.5 to 2 years old. Other factors such as the tissue preparation or even the differences in the methodologies and substrates that they used to conduct the assays may contribute to the variability between studies. Another important factor that none of these studies took into consideration was to use a control of the variable degrees of mitochondrial enrichment in the brain tissue, such as CS activity. In the present study, by correcting COX activity with CS activity, using brain samples with small post-mortem delays and cases with a wide range of ages, we enhanced the accuracy and reliability of the results.

For the first time we report the protein levels of the two core catalytic subunits of COX, COX1 and COX2, in the ageing brain (Figure 3.2). Part of the mitochondrial free radical theory supports that mitochondria become deficient in enzyme activity with ageing because increased ROS production causes mutation in both the mitochondrial and nuclear DNA. Changes in the DNA consequently affect the protein synthesis of the respective gene products and in mitochondrial DNA this may be COX1 or COX2. We found that COX1 levels are strongly increasing, and COX2 levels are decreasing with ageing (Figure 3.2). COX1 is the first protein that enters in the assembly process of the complex, and contains three of the redox centres that are required for COX activity[96, 118, 119]. The fact that COX1 increases in the same way as COX/CS activity possibly signifies the importance of COX1 in the final complex activity (Figure 3.2). COX1 contains the Cu_B redox site although COX1 protein levels did not seem to correlate with copper levels, on the contrary, COX1 protein levels are increasing when copper levels are decreasing even if the correlation was not strong enough to be considered significant (Tables 3.1 and 3.2 as well as Figures 3.2 and 3.3)

While COX1 levels did not seem to be affected by either copper or COX/CS activity, COX2 levels were significantly dependent on COX/CS activity and possibly on copper levels (Tables 3.1 and 3.2 as well as Figure 3.3). COX2 contains the Cu_A site and becomes part of the complex at a later stage of COX assembly[96, 118, 119]. Whilst the correlation between copper levels and COX2 protein only showed a trend towards significance in the temporal cortex (Table 3.2) it indicates that COX2 protein levels are increasing when copper levels are higher. This may explain why COX2 decreases with age since copper levels are also decreasing in the ageing brain. COX2 is known to require insertion of copper at the Cu_A site before being assembled into the full COX complex and studies, mainly in yeast, have shown that unassembled copper deficient COX2 is rapidly degraded by the ATP-Zn^{2+} dependent YME1p protease[97, 306]. If, therefore, COX2 does not have copper it will not enter the complex and will be degraded. The current study shows that COX2 protein levels are decreasing when COX/CS activity is higher. In the brain, neurons are long-lived with a slow turnover of both mitochondria and mitochondrial components with a half-life of 4-6 weeks[307]. Under these conditions, the COX complex will continue being active but no assembly of new complexes may take place until necessary. It is possible that in the ageing brain decreased levels of copper leads to degradation of COX2 with only sufficient COX2 available to meet the demands of increased COX/CS due to the high metabolic demand in the brain. This might imply that copper pools within the brain could be redistributed during ageing to maintain certain key enzymes such as COX. Whilst the total copper pool might be depleted with age, certain enzymes are protected to maintain adequate brain function, and in this instance, copper availability to COX2 might be a rate limiting step.

3.4.1.2 How is the brain responding to ROS production?

It is well established from studies in both humans and animals that ROS levels increase with ageing[308-311]. The most commonly used markers for measuring the accumulation of oxidative stress are oxidative induced modifications to macromolecules such as proteins, DNA and lipids. In the ageing brain it has been shown that increased production of the oxidative DNA damage marker, 8-hydroxyl-2´-deoxyguanosine[312], and increased levels of lipid peroxidation malondialdehyde and protein oxidation carbonyl markers occur[309-311]. In a recent study Venkateshappa *et al.* reported that different brain region exhibit differences in protein oxidation[313, 314]. The study reported that in frontal cortex, protein oxidation was higher compared to hippocampus and substantia nigra or to cerebellum and striatum where no change with age was observed[313, 314].

Cells, in order to defend against oxidative stress, have evolved different antioxidant defence enzymes. The first defence line comes with SOD, both in the cytosol and the mitochondria, which degrade oxygen radicals derived from the mitochondria or other sources. Mitochondria produce increased ROS not only when respiratory chain enzymes are blocked, but also when they function at higher rates. Even if they are not producing ROS directly from COX, we can assume that increased COX activity will be accompanied by increased activity of the other mitochondrial enzyme complexes and increased membrane potential which will further enhance the production of oxygen radicals. The ageing brain in order to defend against the increased production of ROS has to increase the activity of SOD.

In the healthy brain we found that total SOD activity increases with ageing. The total SOD activity that we measured in this study represents the activity of both the Cu,Zn-SOD1 and the mitochondrial Mn-SOD2 and potentially the secreted Cu,Zn-SOD3. In human brain the concentration of SOD1 has been reported to be 6 to 7 times more than that of SOD2, therefore total SOD activity potentially reflects more SOD1 related activity[315]. The increased activity of SOD identified in ageing was perhaps not surprising if we consider that higher levels of ROS may be produced in the ageing brain, thereby requiring an increased antioxidant defence system of the brain. Several studies, predominantly in different mammalian species, have been conducted in order to investigate how SOD activity correlates with age[316, 317]. Such results are however quite contradictory since studies in mouse brain report both increase or decrease in SOD activity with ageing[318] or no change or a decrease in the rat brain[319, 320]. Variances in these studies may reflect differences in the procedures used to measure SOD activity and also the ages of the animals which were quite different.

One study conducted by Venkateshappa *et al.* which measured SOD activity in human frontal cortex showed no significant change in total SOD activity with ageing[313]. One possible reason for the difference between the current and Venkateshappa study is the usage of cases with a broader age range (0.01 to 80 years) where only 10 cases were between 50 to 80 years whereas the majority of our cases are between 50 and 100 years[313]. By using such a broad age range, particularly infant tissue where the brain is not fully developed, might have masked any real changes that occur later in life observed in our study.

SOD protein levels related to SOD activity have not been measured previously in animal studies. SOD1 and SOD2 protein levels in the current studies show increases with ageing, possibly reflecting the need for more active SOD (Figure 3.4). By correlating SOD1 and SOD2 protein levels with the total SOD activity this was confirmed showing a positive

correlation (Table 3.3, 3.4 and Figure 3.5). SOD1 requires copper for its activity however, correlating SOD1 levels with brain copper levels showed the absence of any correlation (Table 3.3 and 3.4). SOD1 is a relatively stable enzyme when active (35-40 hours half-life) which possibly indicates that the requirement for antioxidant defence is important with SOD1 being activate even at low copper levels[134, 321]. Furthermore, SOD1 protein is mainly as an apo-form, without bound metals, and the protein determination reflects both apo- and holo-SOD1[121]. Increased SOD activity might also occur due to increased levels of CCS, the protein which is responsible for the delivery of copper to SOD1 and its activation. CCS protein levels were not only strongly increased with age in the brain but a positive correlation with SOD1 protein levels was observed which may indicate that when there is more SOD1 protein CCS levels are higher (Table 3.3, 3.4 and Figure 3.5). Increased CCS levels might reflect either the requirement derived from an increased need for activation of SOD1 in the ageing brain, or by the presence of less copper in the brain. Studies in cells and mice have shown that CCS levels are regulated by copper availability, generally under copper depleting conditions CCS protein levels are increased[134]. The correlation between CCS and copper was not significant but it does show that at lower copper levels CCS protein levels were higher along with SOD1.

One possible assumption may be that since SOD is more active in the brain, the observed oxidative stress and ageing processes should be reduced due to lower levels free radicals. Unfortunately, SOD is also responsible for the production of another ROS product, since during the detoxification of superoxide, H_2O_2 is generated as by-product. Consequently cells contain two further enzymes in the first line of antioxidant defence: catalase (CAT) and glutathione peroxidase (GPx), which both detoxify H_2O_2. CAT monitors H_2O_2 in the extracellular space and also reduces peroxisomal H_2O_2 to oxygen and water while GPx acts in the cytosol and mitochondria. Even though the brain has a high demand for ROS detoxification due to high mitochondrial activity, it also contains lower concentrations of antioxidant defence enzymes compared to other tissues of the body[322]. Few studies have measured CAT or GPx levels in the human brain, with the majority of the studies having been performed in mice or rats. In the human brain, based on the studies of Venkateshappa *et al.*, CAT activity decreased with ageing in the substantia nigra, hippocampus, and striatum but increased in the frontal cortex[313, 314]. GPx activity on the other hand decreased in cerebellum and substantia nigra, but no change was observed in frontal cortex, striatum or hippocampus. These studies indicate that different brain regions may have different demands for antioxidant defence mechanisms which possibly dependent on the function of the brain region and its

metabolic demand. Studies coming from animals are again quite controversial since no change, increases or decreases of CAT activity have been reported in different brain regions in mouse or rat brain[316, 318]. Most animal studies however show that GPx activity increases in the brain with age which may be due to the increased formation of H_2O_2 with ageing[318, 319].

Figure 3.6 represents a proposed mechanism of ROS production and antioxidant defence in the brain during ageing based on our findings. According to that model increase activity of COX/CS indicates increase function of the respiratory chain which will elevate the production of oxygen radicals. Cells in order to defend against them increase the activity and the protein levels of SOD1/2 in the cytosol and mitochondria. SOD1 activity is mainly regulated by copper and CCS availability based in our findings copper depletion cause increase expression of CCS which was also positive correlated with SOD1 protein levels and activity. However, for an improved understanding of the ageing mechanisms in the brain it would be important to measure the activity levels of mitochondrial Complex I and III which are known to generate mitochondrial ROS. Also, measuring the activity and protein levels of other antioxidant defence enzymes (CAT, GPx) will provide better understanding of how the function of the SOD integrates with ageing mechanisms.

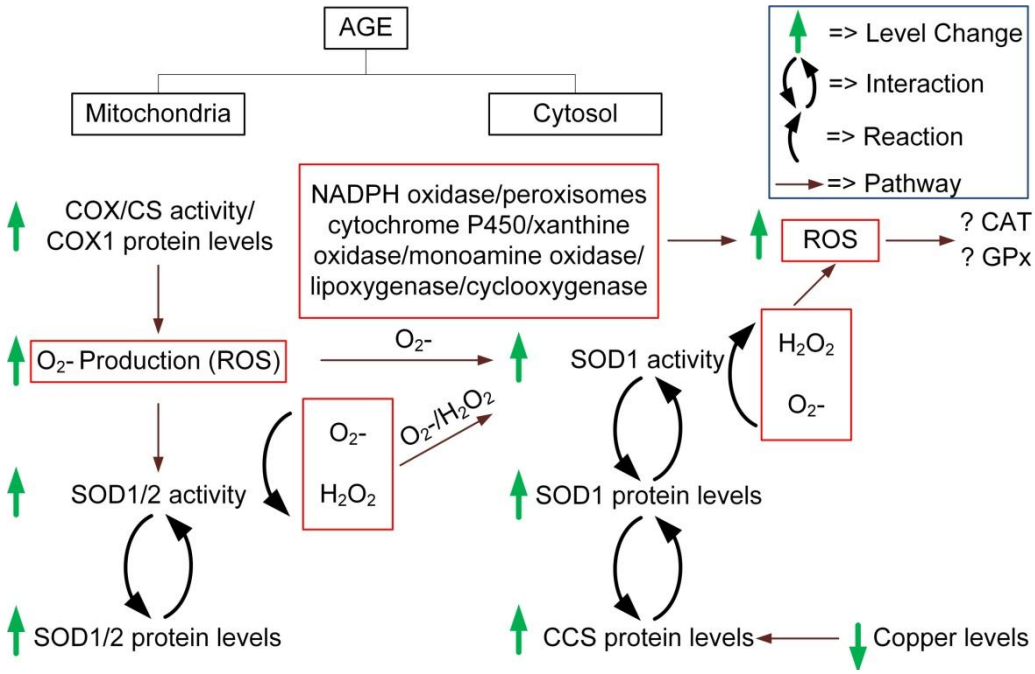

Figure 3.6 A Proposed Mechanism of ROS Production and Antioxidant Defence in the Ageing Brain.

The proposed mechanism suggest that increase COX/CS activity will generate higher levels of ROS which will require more active SOD in the mitochondria and the cytosol in order to defend against them. Copper availability seems to regulate mainly the protein levels of CCS rather than COX or SOD activity, signifying the importance of these enzymes in the brain function. Highlighted with red boxes are the different sources of ROS in the cell.

3.4.2 Differences between frontal and temporal cortex in the ageing brain

The brain faces not only biochemical and molecular changes with ageing but also morphological changes. According to morphological studies, each brain region faces different changes with the cortex being the most affected, although some cortical regions are relatively spared. Several studies with MRI scans in the age groups from 0.1 to 100 years have shown that the brain loses volume and weight with ageing which is more prominent after the age of about 50 to 60 [290, 291]. These changes are suggested to be occurring due to neuronal loss, reduction in neuron size, loss of synapses and pruning of dendritic trees. Changes in both grey and white matter are observed with ageing, with grey matter declining linearly with age and resulting in a final loss of about 10% of the neurons within the cortex[302]. On the other hand, white matter volume appears to increase through childhood and into adulthood and then starts to decrease after the age of about 60[302].

The cerebral cortex is one of the most affected areas in the brain but the changes are not globally and evenly distributed, different cortical regions are affected more than others. Frontal cortex is responsible for executive processes, speech and social functions and temporal cortex for visual memories, processes involved in hearing, language recognition and new memories. Studies have shown that frontal and temporal cortex are affected in slightly different ways. In frontal cortex there is an approximately 50% decrease in neuronal density whereas temporal cortex exhibits a 60% decrease which is also accompanied by a similar decrease in dendritic trees[323]. Also, in both brain regions, differences in the size of the neurons were observed with ageing, generally the density of the larger neurons was decreased although some changes in the smaller neurons were present[323, 324].

Based on the above observations the small differences in copper containing enzymes and protein levels with ageing could be attributed to the morphological neuronal changes in frontal and temporal cortex regions. Generally, we observed that in temporal cortex the majority of the studied proteins, COX/CS and SOD activity were significantly changed with ageing compared to frontal cortex where in some cases there was no significant change or the correlation was not as strong as in temporal cortex. One possibility is that the higher neuronal loss in temporal cortex has as a consequence the effect of making the mitochondria in the remaining neurons to increase their metabolic rate in order to compensate for the increased energy demands. A net effect being greater metabolic demand on the remaining neurones to maintain the same level of function for the specific anatomical region. However, the changes

in copper levels were quite similar in both brain regions possibly signifying that copper is evenly distributed in the cortex.

3.4.3 Do other copper binding proteins change with ageing in the brain?

The present study did not reveal any particular change in the levels of other copper binding proteins in the ageing brain. We only observed a small increase in the protein levels of Sco2 in frontal cortex and Hephaestin in temporal cortex. For the remaining of the studied proteins (ATP7a and Atox1), no significant change was observed with ageing or between different brain regions (Table 3.5). Hephaestin is a homologue of Cp and is a membrane bound multi-copper ferroxidase necessary for iron transportation[325]. It is more abundant in the intestine but is also expressed in brain regions such as cortex, hippocampus and substantia nigra[325]. Haphaestin levels showed increase with ageing (Table 3.5) in both frontal and temporal cortex although this was only significant in temporal cortex which might represent either the higher iron accumulation in that brain region[326] or differences in local demand for copper and iron. Sco2 is localized in the mitochondria and is responsible for copper insertion to COX2; the increased levels in frontal cortex (Table 3.5) might be correlated with the less severe changes that were observed in frontal cortex for both COX2 protein levels and COX activity generally. On the other hand, in temporal cortex where more severe changes in COX/CS activity and COX2 levels are observed Sco2 protein levels are not changing at all since there is reduced available COX2 to utilise copper.

3.4.4 Conclusions

In the current study, for first time we have identified that copper, two of the most important copper binding enzymes, COX and SOD1, and different copper binding proteins are playing an important role in the ageing brain. We show for first time that in the ageing brain mitochondrial respiration is increased possibly due to increased demands for energy which has as a result increased production of oxygen radicals in the neurones. The brain in order to defend against the increased ROS production increases the antioxidant defence mechanisms by increasing SOD activity. The higher activity of COX and SOD enzymes was accompanied also by increased protein levels of their respective proteins (COX1 or SOD1/2) or others proteins that are required for their activity (CCS). Decreased copper levels play a significant role in ageing since lower levels have an effect in the protein levels of CCS and COX2 in the brain. From the above data we can conclude that the major components of the copper homeostasis pathway play central role in the progression of ageing in the healthy brain.

In order to obtain a better understanding of how copper metabolism affects the ageing brain studying its pathway in other brain regions such as hippocampus, substantia nigra, locus coeruleus or cerebellum will provide a better overview. For cerebellum we have initial results that showed a tendency for decrease copper and activity levels (See Appendix A). Obtaining samples from substantia nigra and locus coeruleus which have the highest copper concentration in the brain will help us to better elucidate the copper metabolism in the ageing brain. By studying how other metals such as iron, manganese or zinc are correlated with ageing or proteins that act as cofactors will help us understand better how metals generally affect ageing in the healthy brain and potentially in neurodegenerative disorders.

4 An investigation of copper homeostasis in early onset and late onset Alzheimer's disease brain

4.1 Introduction

AD cases are classified in two subtypes based on the year of onset of dementia, EOAD and LOAD, and while these show common clinicopathological characteristics they often differ in the neuropathological features and clinical symptoms. The differences between EOAD and LOAD, typically include an earlier age of symptom onset, unusual behaviours, marked psychiatric changes, seizures, myoclonous, bradykinesia and aphasia, although these are not always universal[158, 327].

In both subtypes, the neuropathological progression of the disorder is similar and is suggested to follow certain stages. Braak and Braak classified these stages based on the topographical distribution of amyloid plaques, NFTs and neuritic plaques (NPs)[163, 328]. NPs are composed of abnormal, dystrophic neuronal processes filled with AT8-ir non-argyrophilic material, and cellular processes composed by argyrophili tau aggregates, along with astrocytes and microglia cells. Aβ deposits accompany NPs in the form of peripheral infiltrations and, frequently, compact cores. The main staging system introduced by Braak and Braak is based on the presence of NFTs and NPs in the brain[163, 328]. According to the system in stage I and II the lesions start to affect the allocortex and specifically the transentorhinal region and only mild lesions in hippocampus CA1 region are observed. In stage III, the lesions extend into the cortex of the fusiform and lingual gyri and the already affected regions present a more severe phenotype[163, 328]. Also, lesions in the hippocampus start to become more apparent and appear in other hippocampal sub-regions (CA2, CA3 and CA4)[163, 328]. In stage IV, the pathology extends into the neocortex where dense NPs start to appear in the middle temporal gyrus and a rapid decrease in the severity of the lesions occurs at the transition to the superior temporal gyrus[163, 328]. Lesions in stage V extend widely into the first temporal gyrus and in other areas such as frontal and parietal cortex[163, 328]. In stage VI, the pathology reaches secondary and primary cortex areas, the occipital lobe and extends into the striate area (Figure 4.1A)[163, 328].

A phase system has been introduced in order to monitor the development and progression of Aβ deposits in the brain. In phase 1, isolated plaques start to develop at one or more sites in the basal temporal and the orbitofrontal cortex[329]. In phase 2, additional plaques are found in the allocortex and amygdala with Aβ deposits starting to develop in all high order association areas of the neocortex[329]. A further expansion of Aβ deposits signifies phase 3 where they extend into secondary neocortical fields, striatum, in the perforant pathway and presubiculum[329]. In phase 4, Aβ plaques can been seen in all areas of the neocortex and reach

the mesencephalon, particularly the inferior colliculi[329]. At phase 5, Aβ deposits reach the lower brainstem and cerebellar cortex (Figure 4.1B)[329].

Whilst EOAD and LOAD have a common neuropathology, EOAD frequently shows a more severe and extensive degeneration in the affected brain areas with lesions often extending into the cerebellum. Histopathology studies from post-mortem brain tissues and pre-mortem studies with neuroimaging (VBM, PET, and MRI) have revealed the presence of metabolic differences between the two subtypes[159, 280, 330, 331]. A greater burden of NFTs and NPs throughout the EOAD brain have been confirmed by histopathological studies[159, 332]. Greater atrophy in different brain regions but especially in the EOAD temporal cortex has been observed and occurs probably due to more marked neuronal loss, cell shrinkage and/or synaptic loss[159, 333-335]. The cerebellum is often less affected in AD however studies have shown Purkinje cell loss and increased astrocytosis in the EOAD cerebellum relative to LOAD[336]. Similar observation has also been observed in pre-mortem MRI based neuroimaging studies using VBM which have shown increased cortical atrophy in the parietal, posterior cingulate and precuneal regions of EOAD relative to LOAD[330]. Topographic studies with MRI scans have shown that grey matter in EOAD patients is often more atrophic than in LOAD patients which reveals the presence of topographic specificity where cortical areas were more atrophic in EOAD, and hippocampus in LOAD brain[280].

Certain common characteristics of the AD brain are oxidative stress, lipid peroxidation, mitochondrial malfunction and neuronal death which are mainly induced by the increased accumulation of Aβ and NFTs[337, 338]. A better understanding of how all these characteristics correlate with AD clinicopathological features and pathogenesis may eventually lead to either a new therapeutic route or ways to prevent the disorder initiation. The last few decades have shown that metals and especially copper play an important role in AD pathogenesis but until now there has not been a study investigating the different aspects of its pathways in these two AD subtypes.

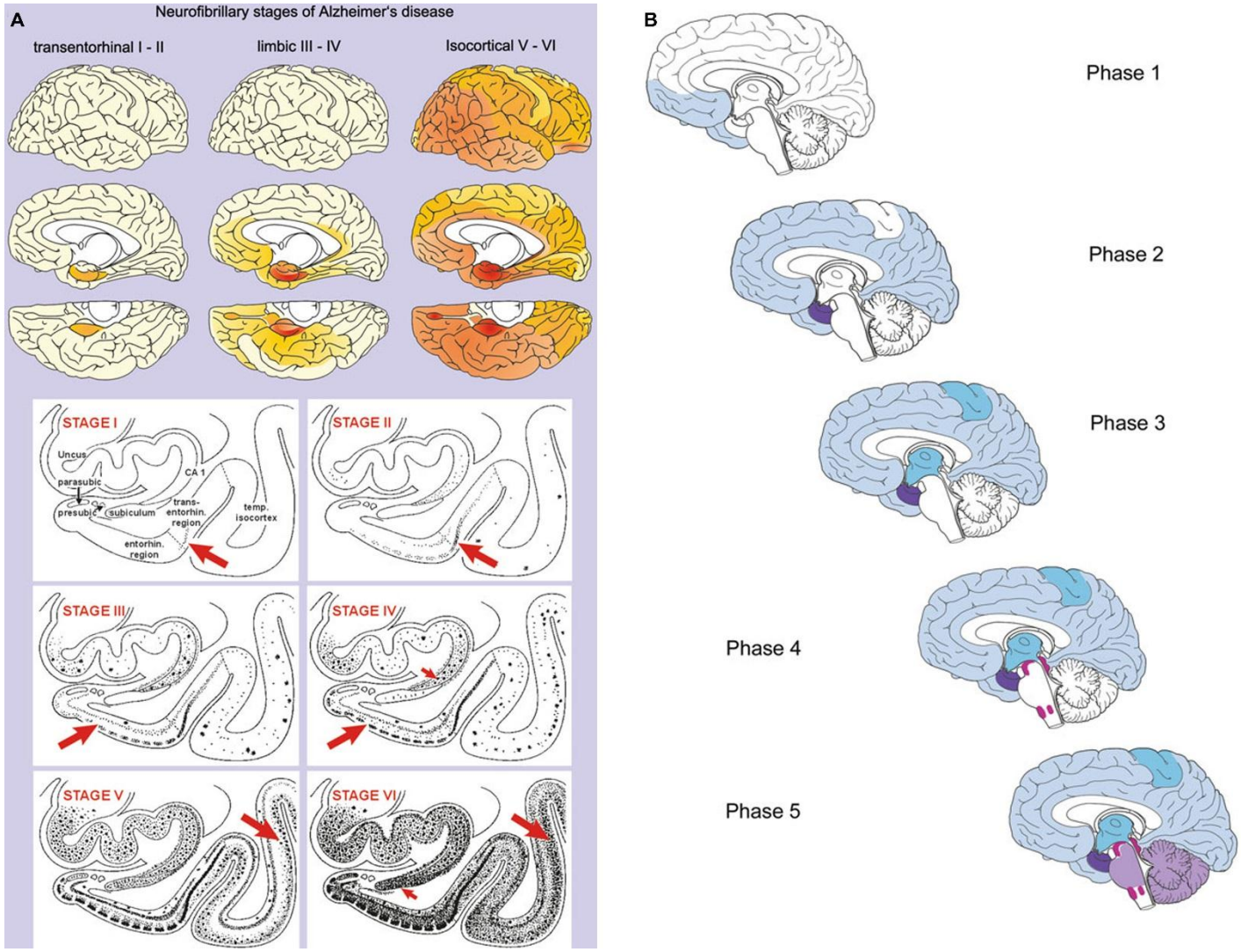

Figure 4.1 NFT Staging and Aβ Phases in the AD Brain.

A) The six NFT stages can be distinguished in the top part of the figures and the bottom shows a diagram of the development of intraneuronal tau lesions. **B)** Representation of the 5 phases of Aβ plaques development and progression in the brain. (Copied from Braak H et al, 2015[310]).

4.2 Aims

The purpose of this chapter is to identify the role of copper homeostasis pathways in EOAD and LOAD brain. Levels of copper, COX and SOD activity as well as various copper binding proteins were measured in frontal, temporal cortex and cerebellar brain samples from EOAD, LOAD and aged matched controls for both subtypes. The changes between the two AD subtypes and their aged matched controls were identified and a comparison between EOAD and LOAD as well as changes between different brain region were examined in order to determine if changes related to possible pathological changes.

4.3 Results

Brain samples from three different regions (frontal, temporal cortex and cerebellum) were analysed for the determination of a range of metals by ICP-MS, for COX and SOD activity and for protein levels by Western blot as previously. The brains were separated into different groups. Group one contained EOAD cases, clinically and neuropathologically verified, and their respective age matched controls. A second group contained pathologically and clinically verified LOAD cases with their respective age matched controls. In the first group (EOAD group) we obtained matched frontal and temporal cortex from 16 EOAD and 14 control cases but with matched cerebellum for only 12 EOAD and 9 control cases. In the LOAD group, we acquired 13 LOAD and 13 controls with matched frontal, temporal cortex and cerebellum. A nonparametric t-test (Mann Whitney test) was used to identify the in-between group differences since in some cases the samples were not normally distributed since they failed to pass the D'Agostino & Pearson omnibus normality test and the F-test for variances.

4.3.1 Levels of copper and other metals in the EOAD and LOAD brain compared to aged matched controls

Initially in order to identify if there were variances amongst the four subgroups a Kruskal-Wallis test was performed in the next groups: controls for EOAD and LOAD cases, EOAD, and LOAD. For copper levels the statistical analysis showed that there were significant variances amongst the groups in frontal ($p<0.0001$), temporal ($p<0.0001$) cortex and cerebellum ($p=0.0178$). The above only indicates that they are significant changes amongst the groups and in order to further identify them we conducted a nonparametric t-test between the EOAD or LOAD cases and their respective age matched controls.

The analysis revealed that in the EOAD brain there was a decrease in copper levels in all three regions relative to healthy controls. In frontal and temporal cortex there was a 41% (nonparametric t-test, $p=0.0004$) and 43% (nonparametric t-test, $p<0.0001$) decrease of copper respectively, which was statistically significant. In EOAD cerebellum, whilst there was a 25% decrease in copper levels this failed to reach significance (nonparametric t-test, $p=0.0507$) (Figure 4.2A). In the LOAD brain, copper levels decreased in the neocortex relative to healthy controls but not in the cerebellum. In frontal cortex, there was 14% (nonparametric t-test, $p=0.111$) decrease in copper although the difference was not statistically significant. In temporal cortex copper levels were significantly decreased by 24% (nonparametric t-test, $p=0.04$) whereas in cerebellar copper levels did not change significantly (nonparametric t-test, $p=1$; Figure 4.2B).

During the analysis we were able to determine also the concentration of other metals such as zinc, manganese and iron where we also observed small changes. In EOAD frontal cortex manganese levels decreased by 12% with the change showing a trend towards significance (nonparametric t-test, p=0.088) and in temporal cortex iron levels were significantly increased by 17% (non-parametric t-test, p=0.026). In the LOAD brain no change in the rest of the studied metals was observed in any of the brain regions. For more details, see supplementary data Table B.1 and B.2.

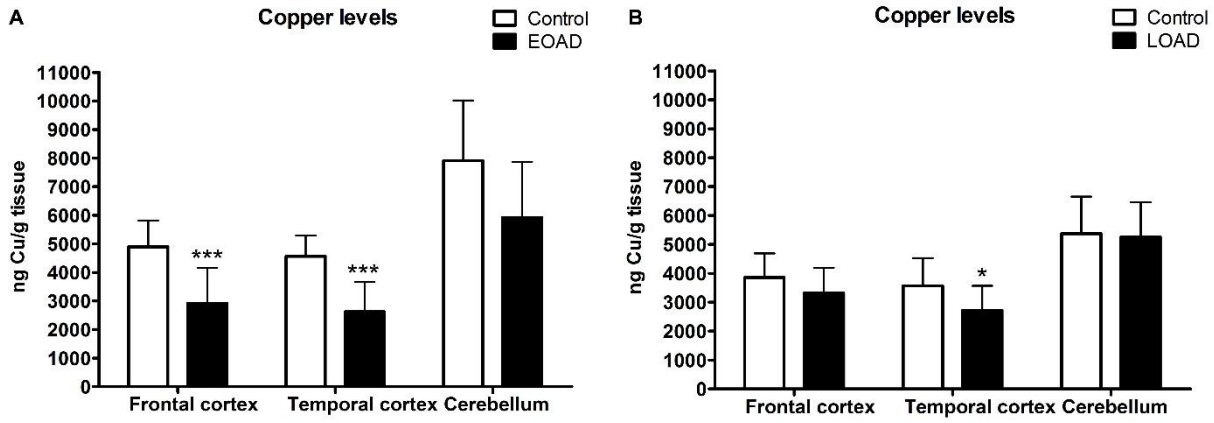

Figure 4.2 Copper Levels in Frontal, Temporal Cortex and Cerebellum.

Copper was determined by using ICP-MS in **(A)** EOAD and (**B)** LOAD brain and values compared to their respective age matched controls. Data were analysed with nonparametric t-test and *, $p<0.05$; ***, $p<0.001$.

4.3.2 Activity levels of copper binding enzymes in EOAD and LOAD brains

The activity levels of COX, CS and SOD were measured in the same brain samples as used for copper determination where COX and CS activity was measured in brain homogenates that were not freeze-thawed and SOD activity from the same aliquots that had been frozen. The independent COX and CS activities are presented as well as the ratio of COX/CS.

The determined activity levels of COX, CS and COX/CS in all three brain regions in the EOAD and LOAD groups where initially analysed by Kruskal-Wallis test in order to identify the presence of variances amongst the different groups. The analysis revealed that COX/CS ratio did not significantly changes amongst the different groups with the change in temporal cortex (p=0.085) and cerebellum (p=0.088) being in the margins of significance. However, for COX activity the analysis identified the presence of significant changes amongst the groups in temporal cortex (p=0.016) and cerebellum (p=0.029) but not in frontal cortex (p=0.19). Significant changes were also identified amongst the different groups in frontal ($p<0.0001$), temporal ($p<0.0001$) and cerebellum (p=0.0171) for CS activity. Consequently, a

nonparametric t-test was used to identify changes between the EOAD or LOAD cases and their respective control group.

In all three EOAD brain regions COX activity was decreased by 14% but the change was not statistically significant in the majority of these except EOAD frontal cortex which showed a trend towards significance (nonparametric t-test, p=0.07) (Figure 4.3A). In LOAD brain COX activity was reduced by 14% in frontal cortex but not significantly (nonparametric t-test, p=0.329) however in temporal cortex a significant 50% decrease was observed (nonparametric t-test, p=0.012; Figure 4.3B). CS activity in all three brain regions in both groups showed lower levels compared to controls. In the EOAD frontal and temporal cortex CS was significantly decreased by 25% (nonparametric t-test, p<0.0001) and 30% (nonparametric t-test, p<0.0001) respectively relative to age matched controls whereas in cerebellum the 11% decrease was not statistically significant (nonparametric t-test, p=0.308; Figure 4.3C). A similar trend was also observed in LOAD frontal and temporal cortex where CS was significantly decreased by 16% (nonparametric t-test, p=0.0183) and 33% (nonparametric t-test, p=0.001) respectively however in cerebellum there was no change (nonparametric t-test, p=0.959; Figure 4.3D)

The final COX/CS ratio in all EOAD brain regions was increased compared to age matched controls. In frontal cortex a small 14% increase was present but the difference was not statistically significant (nonparametric t-test, p=0.119) although in temporal cortex the 25% increase relative to age matched control was significant (nonparametric t-test, p=0.016). The COX/CS activity in EOAD cerebellum was higher by 7% although this was not significant (nonparametric t-test, p=0.441; Figure 4.3E). However, in LOAD brain regions, COX/CS did not significantly change in frontal cortex (nonparametric t-test, p=0.608), in temporal cortex there was a 23% loss of COX/CS (non-parametric t-test, p=0.1) and a 6% decrease in cerebellum (nonparametric t-test, p=0.441) compared to age matched controls (Figure 4.3F).

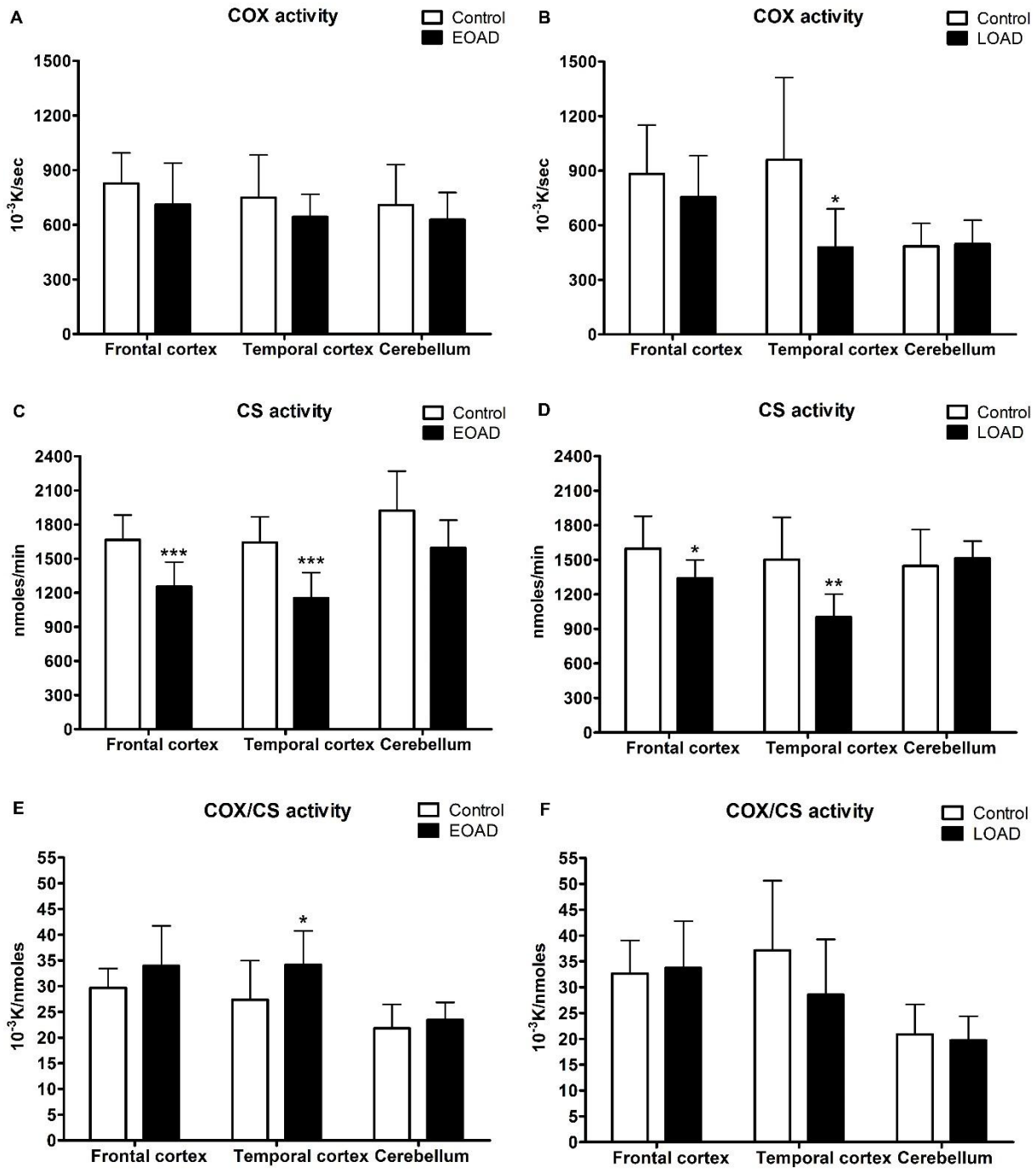

Figure 4.3 Activity of COX, CS and COX/CS in EOAD and LOAD brain tissue.

Activity of COX, CS and the final COX/CS ratio was measured in frontal, temporal cortex and cerebellum of **(A, C and E)** EOAD and **(B, D and F)** LOAD brains compared to age matched controls, respectively. Data were analysed with a nonparametric t-test and *, $p<0.05$; **, $p<0.01$; ***, $p<0.001$.

Kruskal-Wallis test was also performed regarding SOD activity and the presence of significant variances were identified in frontal ($p=0.0032$) and temporal ($p<0.0001$) cortex but not in cerebellum which was in the margins of significance ($p=0.0563$). Generally total SOD activity was higher in the AD brain in both EOAD and LOAD groups. In EOAD frontal cortex and cerebellum a small non-significant increase of 8% (nonparametric t-test, $p=0.289$) and 4% (nonparametric t-test, $p=0.1551$) was observed, respectively. However, in EOAD temporal cortex SOD activity was significantly increased by 54% compared to age matched controls (nonparametric t-test, $p=0.0016$; Figure 4.4A). In LOAD frontal and temporal cortex total SOD activity increased by 11% (nonparametric t-test, $p=0.199$) and 12% (nonparametric t-test, $p=0.174$) respectively and a similar non-significant change was observed in the cerebellum (nonparametric t-test, $p=0.626$; Figure 4.4B).

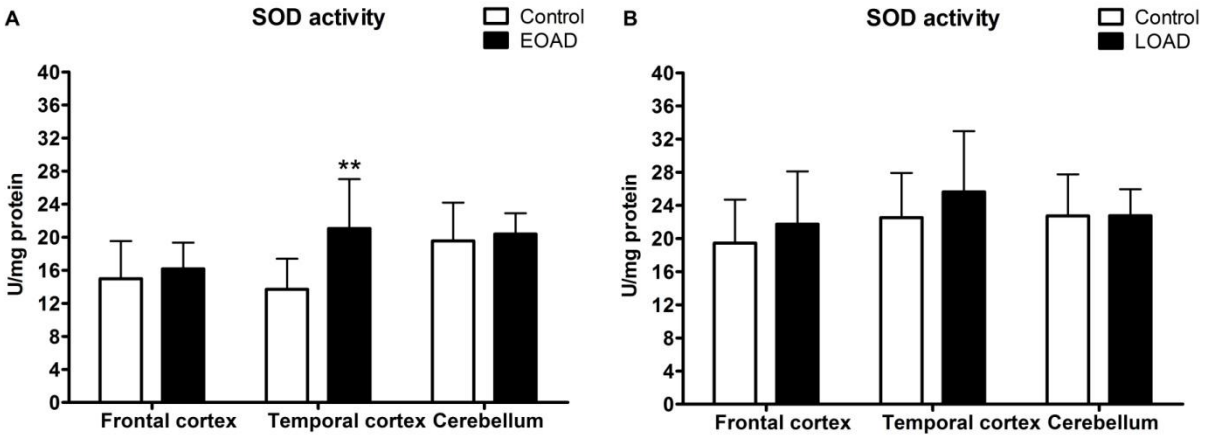

Figure 4.4 Total SOD activity in EOAD and LOAD brain.

Total SOD activity was determined in frontal, temporal cortex and cerebellum from **(A)** EOAD and (**B)** LOAD brains and compared to age matched controls. Data were analysed with a nonparametric t-test and **, $p<0.01$.

4.3.3 Comparison of copper and activities of COX, CS and SOD in EOAD and LOAD brain

In order to examine if there are changes in copper or activity of COX, CS and SOD between the EOAD and LOAD brains which might indicate differences due to pathology we compared results from the three studied brain regions. The analysis revealed that copper levels did not differ in the EOAD brain compared to LOAD in any of the three regions. Frontal cortex copper levels increased by 14% (nonparametric t-test, $p=0.160$) in LOAD brain, also a small increase in LOAD temporal cortex compared to EOAD was present (nonparametric t-test,

p=0.982) and in LOAD cerebellum copper levels decreased by 12% compared to EOAD (nonparametric t-test, p=0.341; Figure 4.5A).

Comparison of EOAD and LOAD tissues showed changes in the COX, CS and the COX/CS ratio. In LOAD frontal cortex, COX activity was non-significantly increased by 7% compared to EOAD (nonparametric t-test, p=0.323) but in LOAD temporal cortex a significant 26% decrease was observed compared to EOAD (nonparametric t-test, p=0.041). Similarly, in LOAD cerebellum COX activity decreased by 21% showing a trend towards significance (nonparametric t-test, p=0.0685; Figure 4.5B). A similar trend was also present for the CS activity however the changes were smaller and not significant (nonparametric t-test, p=0.469 for frontal cortex, p=0.100 for temporal cortex, p=0.187 for cerebellum; Figure 4.5C). The ratio of COX/CS did not show any change between EOAD and LOAD although it is worth noting that LOAD temporal cortex showed a non-significant 17% decrease (nonparametric t-test, p=0.30). In cerebellum, COX/CS activity decreased by 11% in LOAD brain compared to EOAD cerebellum which was significant (nonparametric t-test, p=0.027; Figure 4.5D).

Differences in SOD activity levels were observed between the EOAD and LOAD brains. A general increase in SOD was observed in all three LOAD brain regions compared to EOAD with in frontal cortex the 35% change being significant (nonparametric t-test, p=0.004). In LOAD temporal cortex, SOD activity was higher by 22% compared to EOAD with the change showing a trend towards significance (nonparametric t-test, p=0.083). Similarly, in cerebellum a 12% increase in LOAD brain SOD activity compared to EOAD cerebellum was observed showing a trend towards significance (nonparametric t-test, p=0.077; Figure 4.5E).

In order to identify if variables such as age of death, age at onset of dementia, or duration of the disease showed any correlation with copper levels or SOD and COX/CS activity, Spearman's rank correlation was performed on variables. We identified that in EOAD brain a positive correlation between the activity levels of SOD and the age of death was present, with an increase of SOD activity with increasing age of death in both frontal (r_s=0.6229, n=16, p=0.0099) and temporal (r_s=0.6946, n=16, p=0.0028) cortex. However, in EOAD cerebellum, the change was not statistically significant (r_s=0.4912, n=12, p=0.1048; Figure 4.6A). In all LOAD brain regions, no significant correlation between age of death and SOD activity was observed (Figure 4.6B).

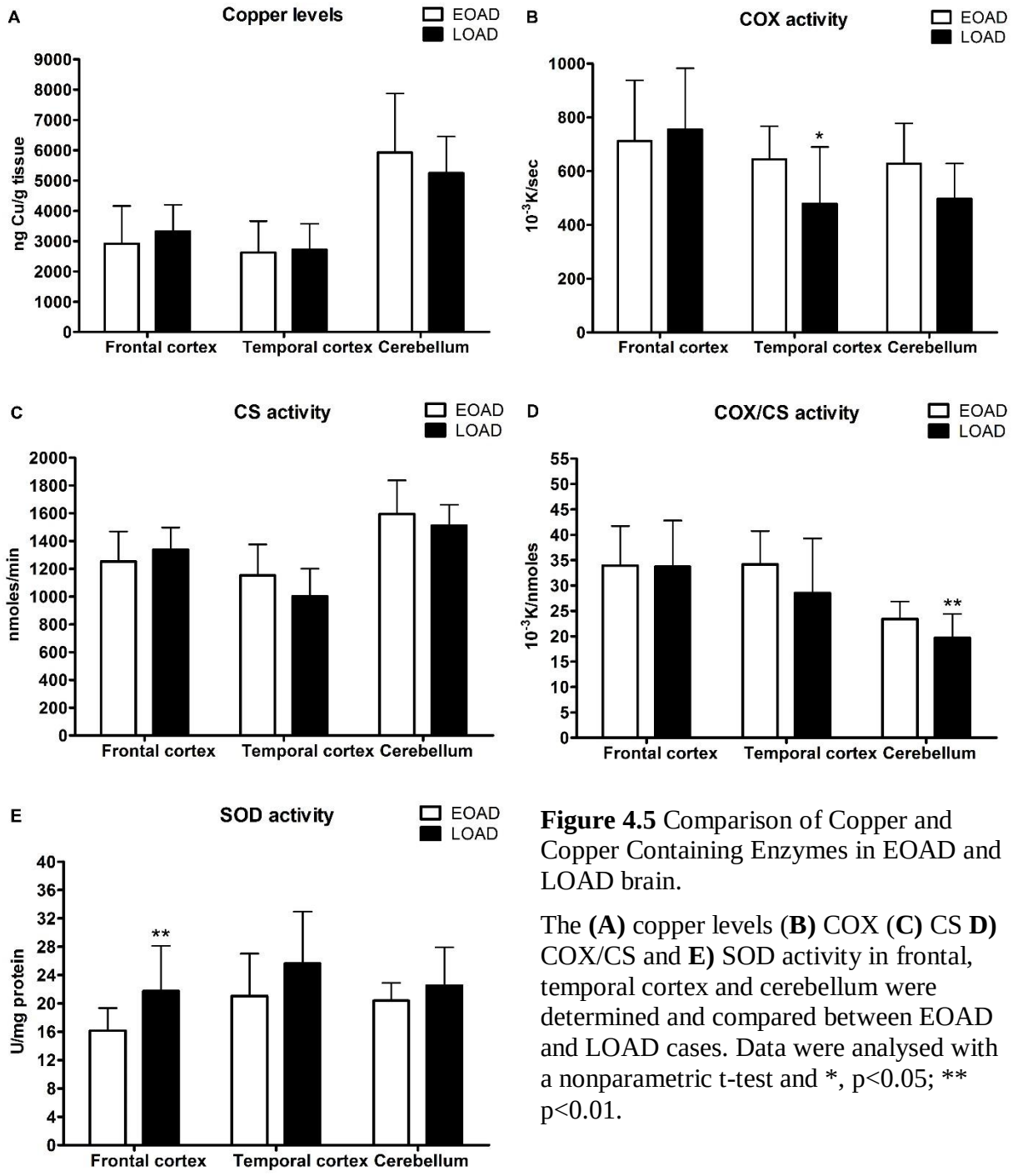

Figure 4.5 Comparison of Copper and Copper Containing Enzymes in EOAD and LOAD brain.

The **(A)** copper levels (**B)** COX (**C)** CS **D)** COX/CS and **E)** SOD activity in frontal, temporal cortex and cerebellum were determined and compared between EOAD and LOAD cases. Data were analysed with a nonparametric t-test and *, $p<0.05$; ** $p<0.01$.

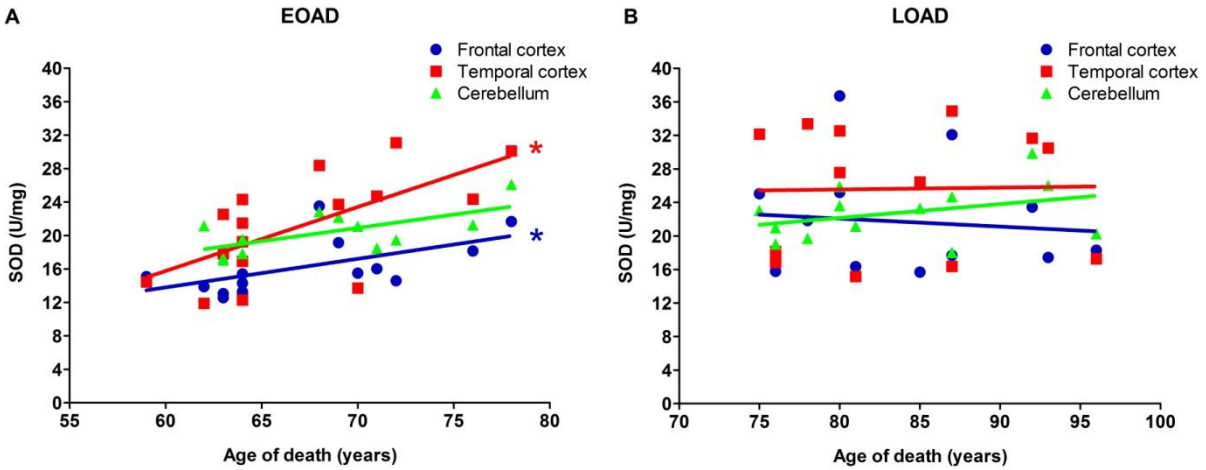

Figure 4.6 Graphical Representation of the Correlation between SOD activity and Age of Death in the EOAD and LOAD brain.

Comparisons were made between SOD activity and age at death in (**A)** EOAD cases where in frontal cortex (r_s=0.6229, n=16, p=0.0099), temporal cortex (r_s=0.6946, n=16, p=0.0028) and cerebellum (r_s=0.4912, n=12, p=0.1048) a positive correlation was present. In (**B)** LOAD cases in frontal cortex (r_s=0.011, n=12, p=0.97), temporal cortex (r_s=0.08, n=12, p=0.78) and cerebellum (r_s=0.325, n=12, p=0.277) non-significant correlations between SOD activity and age at death were observed.

4.3.4 Comparison of copper binding protein levels in EOAD and LOAD brains and healthy controls

The levels of selective copper binding proteins were measured in frontal and temporal cortex of the EOAD and LOAD groups. Due to lack of space in the gels for Western blotting it was only possible to load 12 controls and 12 AD cases and the criteria for the exclusion were based on the lack of any item of clinical information or if there were cases with similar characteristics. Cerebellum was not analysed for protein levels since no significant change was observed in copper/activity levels in both groups. In the following sections, the changes in the protein levels are presented as percentage change of the respective control group.

4.3.4.1 Levels of mitochondria-associated copper binding proteins

The protein levels of the two copper binding subunits of COX, COX1 and COX2, as well as Sco2 were measured in both the EOAD and LOAD groups along with VDAC1 as a mitochondrial mass marker. Figures 4. 7A and B show representative Western blots for COX1 and VDAC1 in frontal and temporal cortex of the EOAD group. The analysis revealed that in the EOAD brain COX1 levels relative to total protein levels (total COX1) decreased by 26% in frontal cortex (nonparametric t-test, p=0.002) and by 15% in temporal cortex (nonparametric t-test, p=0.193; Figure 4.7C). Significant mitochondrial loss was also observed in EOAD frontal and temporal cortex as indicated by VDAC1 protein levels where a 26% (nonparametric t-test, p=0.001) and 20% decrease (nonparametric t-test, p=0.014) was

measured in EOAD frontal and temporal cortex, respectively (Figure 4.7D). Since COX1 is encoded by mitochondrial DNA and localized to mitochondria, COX1 levels were normalized with VDAC1 where we found a small decrease in frontal's cortex COX1/VDAC1 ratio (7%, nonparametric t-test, p=0.7) but in temporal cortex the COX1/VDAC1 ratio increased non-significantly by 13% (nonparametric t-test, p=0.518; Figure 4.7E).

In the LOAD group, COX1 and VDAC1 levels were also determined in frontal and temporal cortex (see Figure 4.7F and G). In LOAD brain, total COX1 protein levels decreased by 18% in frontal cortex (nonparametric t-test, p=0.236) but no major change in temporal cortex (nonparametric t-test, p=0.505; Figure 4.7H). VDAC1 levels showed a significant decrease in both LOAD frontal and temporal cortex; where a 45% (nonparametric t-test, p=0.0005) and 39% (nonparametric t-test, p=0.0006: Figure 4.7I) mitochondrial/VDAC1 loss was measured, respectively. The normalized protein levels of COX1 with VDAC1 increased in both LOAD frontal and temporal cortex by 22% (nonparametric t-test, p=0.549) and 41% (nonparametric t-test, p=0.001), respectively (Figure 4.7J).

Protein levels of COX2 were also measured in EOAD (Figure 4.8A and B) and LOAD (Figure 4.8E and F) frontal and temporal cortex. COX2 was significantly decreased by 19% (nonparametric t-test, p=0.001) and 33% (nonparametric t-test, p=0.0003) in EOAD frontal and temporal cortex, respectively (Figure 4.8C). The normalized levels of COX2 with VDAC1 were non-significantly increased by 12% (nonparametric t-test, p=0.23) in EOAD frontal cortex but only in temporal cortex the 19% decrease was statistical significant (nonparametric t-test, p=0.0073; Figure 4.8D). In LOAD brain COX2 protein levels were statistically significant decrease in both brain regions with frontal cortex losing 34% (nonparametric t-test, p=0.001) and temporal cortex 21% (nonparametric t-test, p=0.0019) of COX2 (Figure 4.8G). In LOAD brain the COX2/VDAC1 ratio increased in both frontal (20%; nonparametric t-test, p=0.141) and temporal cortex (16%; nonparametric t-test, p=0.441) but the change was not significant (Figure 4.8H).

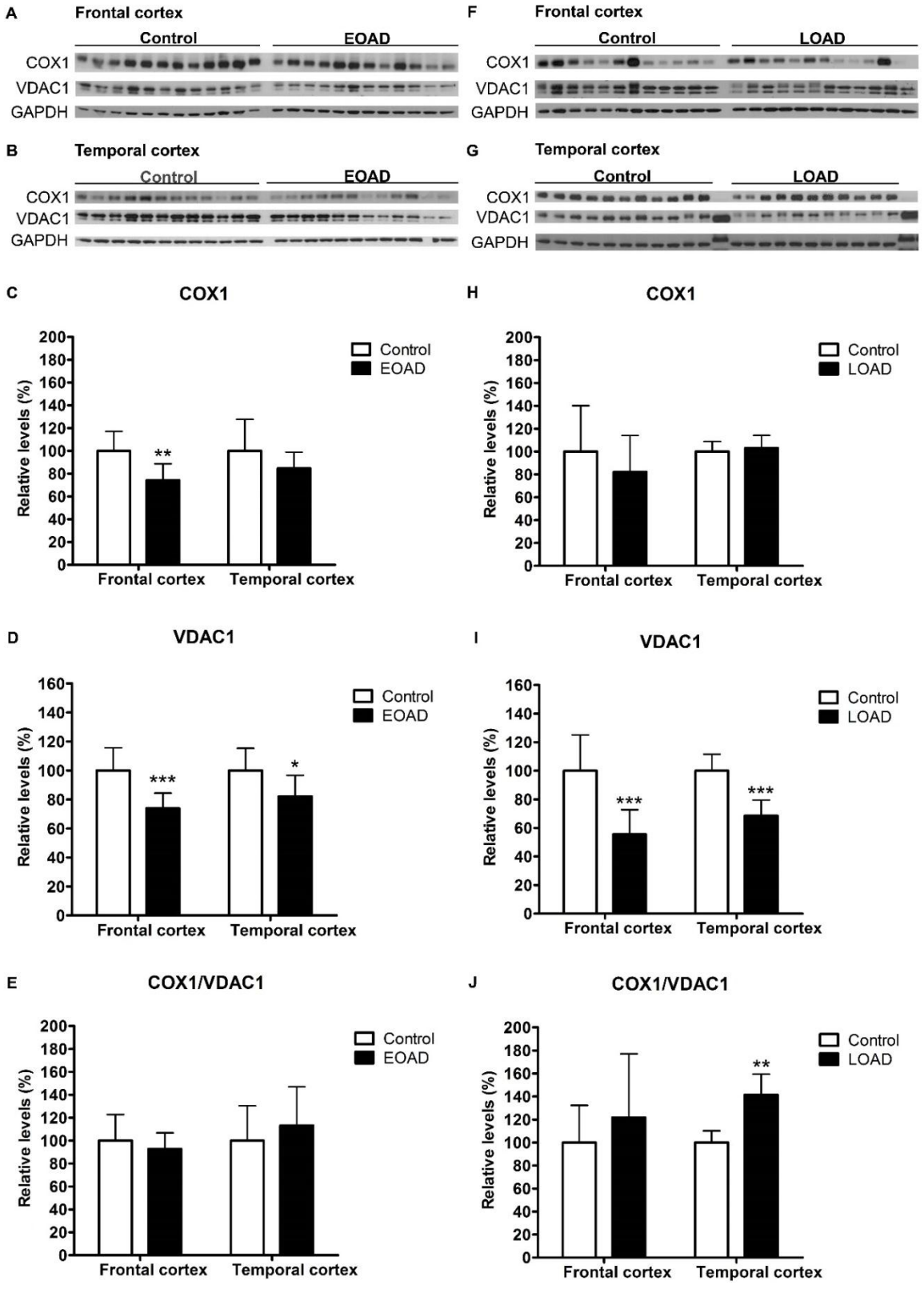

Figure 4.7 COX1 and VDAC1 Protein Levels in EOAD and LOAD Frontal and Temporal Cortex.

Representative Western blots from EOAD or LOAD and their age matched control in **(A, F)** frontal and **(B, G)** temporal cortex as well as their respective densitometric analysis of **(C, H)** COX1 and (**D, I)** VDAC1 normalized with GAPDH and **(E, L)** COX1 normalized to VDAC1. Data were analysed with a nonparametric t-test and *, $p<0.05$; **, $p<0.01$;***, $p<0.001$.

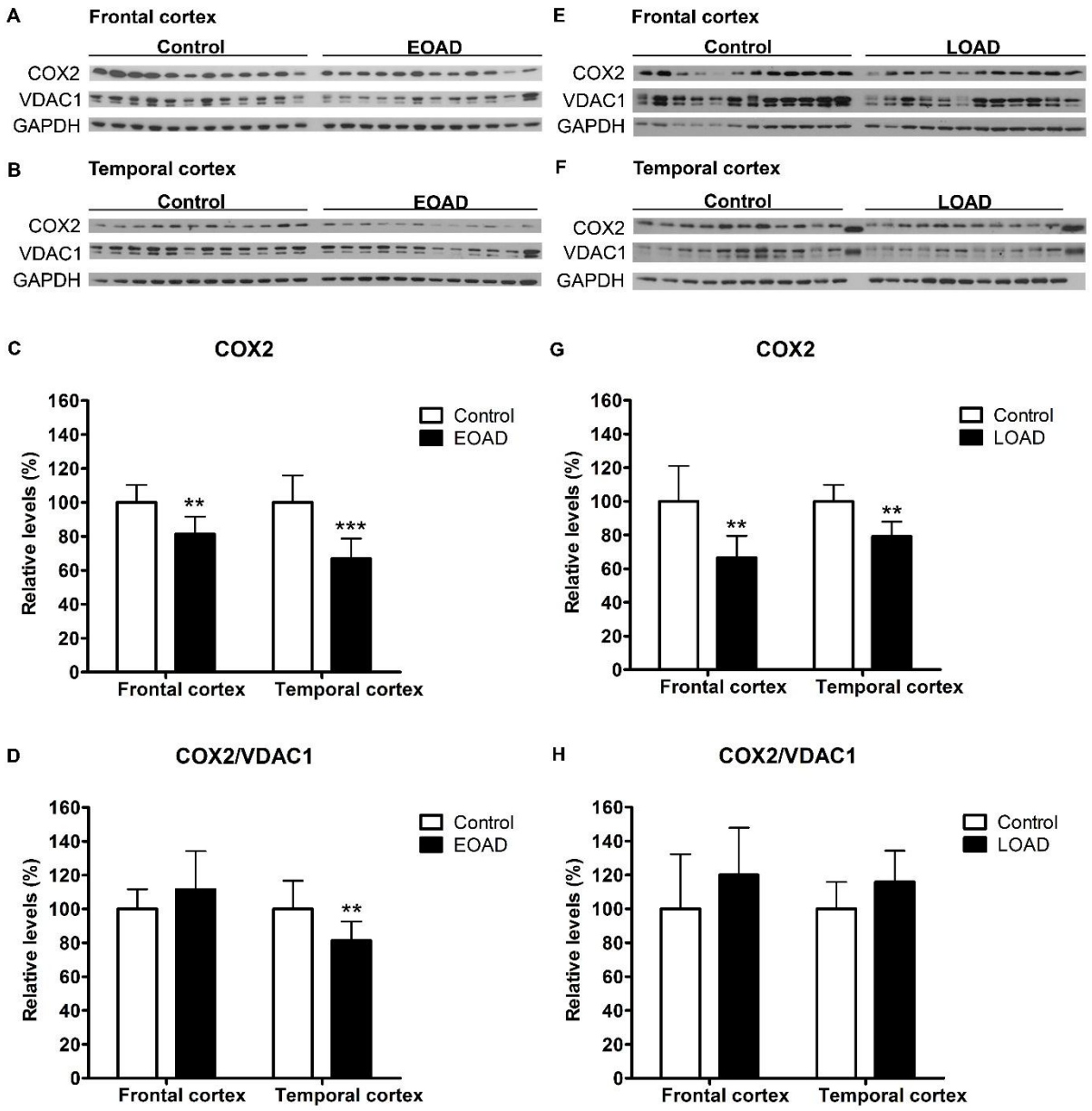

Figure 4.8 COX2 Protein Levels in EOAD and LOAD Frontal and Temporal cortex.

Representative Western blots from EOAD or LOAD and their age matched control in **(A, E)** frontal and **(B, F)** temporal cortex along with their respective densitometric analysis of COX2 normalized with **(C, G)** GAPDH or **(D, H)** VDAC1. Data were analysed with a nonparametric t-test and **, $p<0.01$; ***, $p<0.001$.

Sco2 protein levels were also determined in EOAD (Figure 4.9A and B) and LOAD (Figure 4.9D and E) frontal and temporal cortex. Sco2 protein levels were significantly decreased by 42% (nonparametric t-test, p=0.0001) in the EOAD frontal cortex whereas temporal cortex showed only a 19% decrease (nonparametric t-test, p=0.03; Figure 4.9C). In LOAD frontal and temporal cortex Sco2 was decreased by 14% but the difference was statistically significant only in temporal cortex (nonparametric t-test, p=0.037) and close to pass the statistical test in frontal cortex (nonparametric t-test, p=0.088: Figure 4.9F).

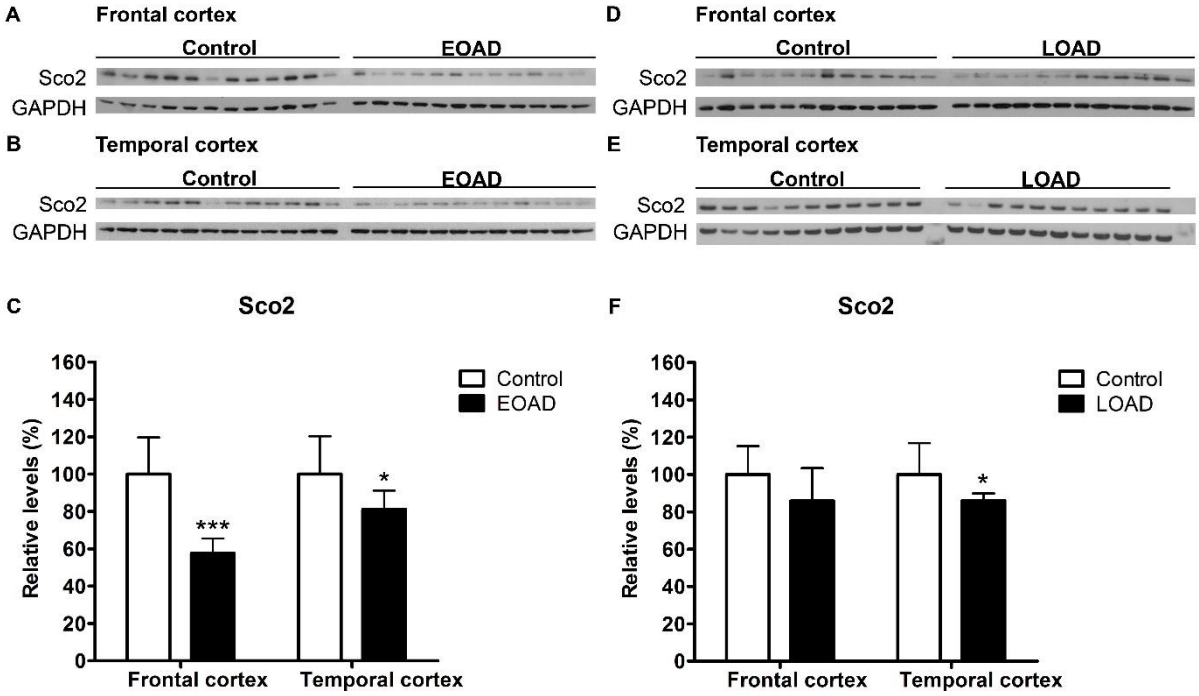

Figure 4.9 Sco2 Protein Levels in EOAD and LOAD Frontal and Temporal Cortex.

Representative Western blots of Sco2 from EOAD or LOAD and their age matched control in **(A, D)** frontal and **(B, E)** temporal cortex along with their respective **(C, F)** densitometric analysis of Sco2 normalized with GAPDH. Data were analysed with a nonparametric t-test and *, $p<0.05$; ***, $p<0.001$.

4.3.4.2 Levels of copper binding proteins related to the cytosolic pathway

In the cytosolic pathway the protein levels of the two major components, CCS and SOD1 were measured and significant changes were observed for both. The protein levels of the cytosolic chaperone CCS were measured in EOAD (Figure 4.10A and B) and LOAD (Figure 4.10D and E) frontal and temporal cortex. In EOAD frontal cortex, CCS was significantly decreased by 25% (nonparametric t-test, $p<0.0001$) but in temporal cortex only a small 13% decrease was measured which showed a trend towards statistical significance (nonparametric t-test, p=0.053; Figure 4.10C). On the other hand, CCS protein levels increased in LOAD frontal and temporal cortex and similarly the change was only significant in frontal cortex

where a 26% (nonparametric t-test, p=0.014) increase was observed and not in temporal cortex (8%; nonparametric t-test, p=0.26; Figure 4.10D).

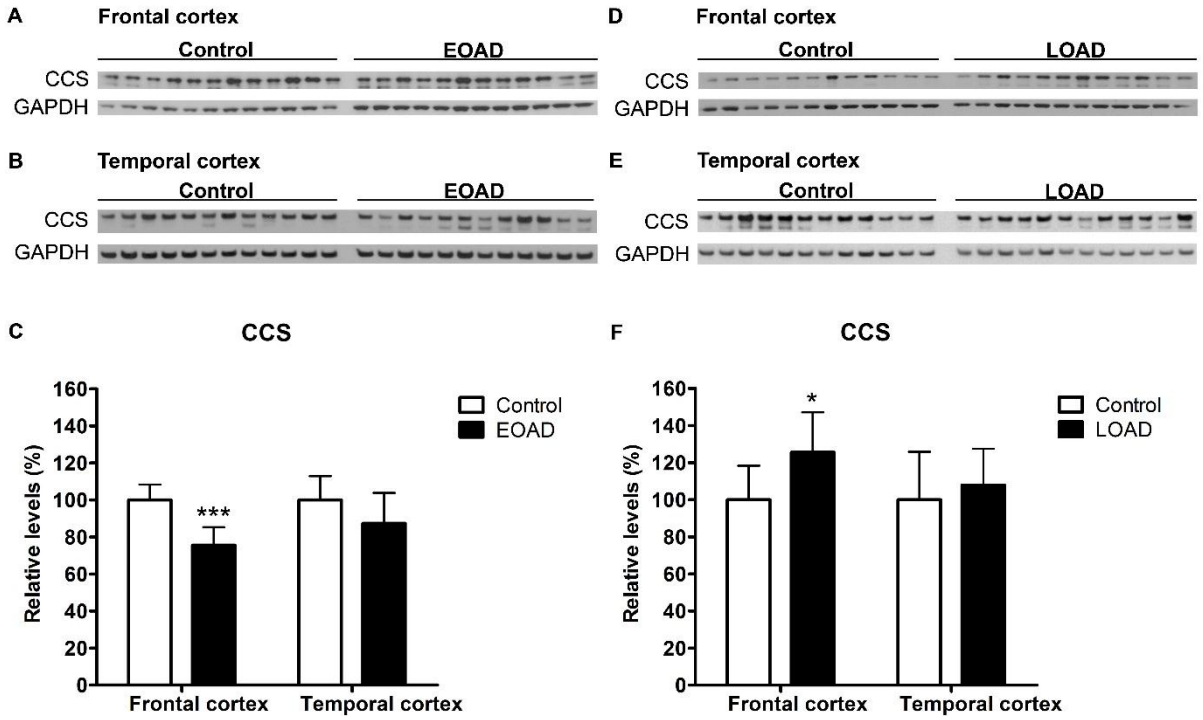

Figure 4.10 CCS Protein Levels in EOAD and LOAD Frontal and Temporal Cortex. Representative Western blots from EOAD or LOAD and their age matched control in **(A, D)** frontal and **(B, E)** temporal cortex as well as their respective **(C, F)** densitometric analysis of CCS normalized with GAPDH. Data were analysed with a nonparametric t-test and *, $p<0.05$; ***, $p<0.001$.

SOD1 protein levels were also determined in both EOAD (Figure 4.11A and B) and LOAD groups (Figure 4.11D and E). Similar to CCS, SOD1 protein levels decreased in EOAD frontal and temporal cortex where a statistical significant 28% loss (nonparametric t-test, $p<0.0001$) was observed in frontal cortex but no change in temporal cortex (nonparametric t-test, $p=0.665$) was observed (Figure 4.11C). In the LOAD brain, a significant increase in both brain regions was present for SOD1 protein levels where a 30% (nonparametric t-test, $p<0.0001$) and 41% (nonparametric t-test, $p=0.0009$) increase was measured in frontal and temporal cortex respectively (Figure 4.11F).

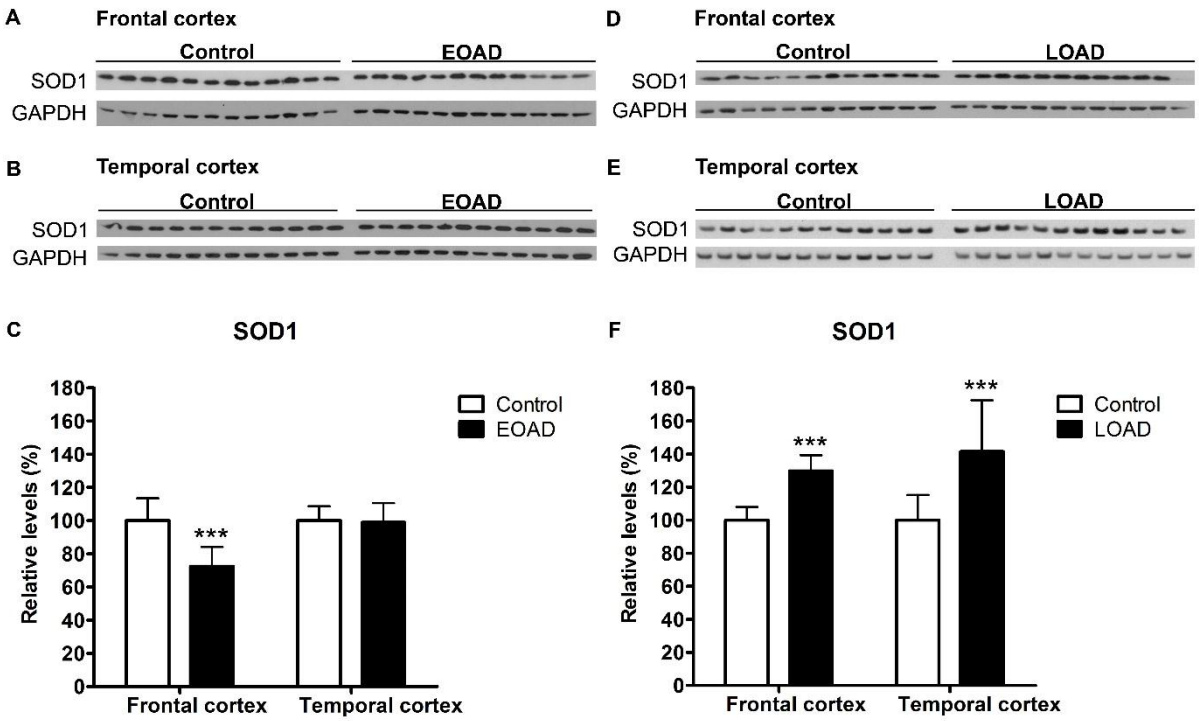

Figure 4.11 SOD1 Protein Levels in EOAD and LOAD Frontal and Temporal Cortex.

Representative Western blots from EOAD or LOAD and their age matched control in (**A, D)** frontal and (**B, E)** temporal cortex along with their respective **(C, F)** densitometric analysis of SOD1 normalized with GAPDH. Data were analysed with a nonparametric t-test and ***, $p<0.001$.

Measuring the protein levels of SOD2 was also important in order to understand how the levels of SOD2 might contribute to the total SOD activity. SOD2 protein levels were determined in both brain regions of the EOAD (Figure 4.12A and B) and LOAD (Figure 4.12E and F) groups. In EOAD frontal cortex SOD2 protein levels were significantly decreased by 16% (nonparametric t-test, $p=0.04$) but in temporal cortex its levels were increased by 16% though not significantly (nonparametric t-test, $p=0.078$; Figure 4.12C). Since SOD2 localized in the mitochondria SOD2 levels were also measured relative to VDAC1 where a non-significant increase of 14% (nonparametric t-test, $p=0.185$) and 16% (nonparametric t-test, $p=0.425$) was observed in frontal and temporal cortex respectively for EOAD (Figure 4.12D). A statistically significant protein loss of SOD2 was observed in LOAD frontal (28%; nonparametric t-test, $p=0.008$) and temporal (17%; nonparametric t-test, $p=0.007$) cortex, however, the SOD2/VDAC1 ratio did not change statistically even if there was a 29% increase (nonparametric t-test, $p=0.193$; Figure 4.12G and H).

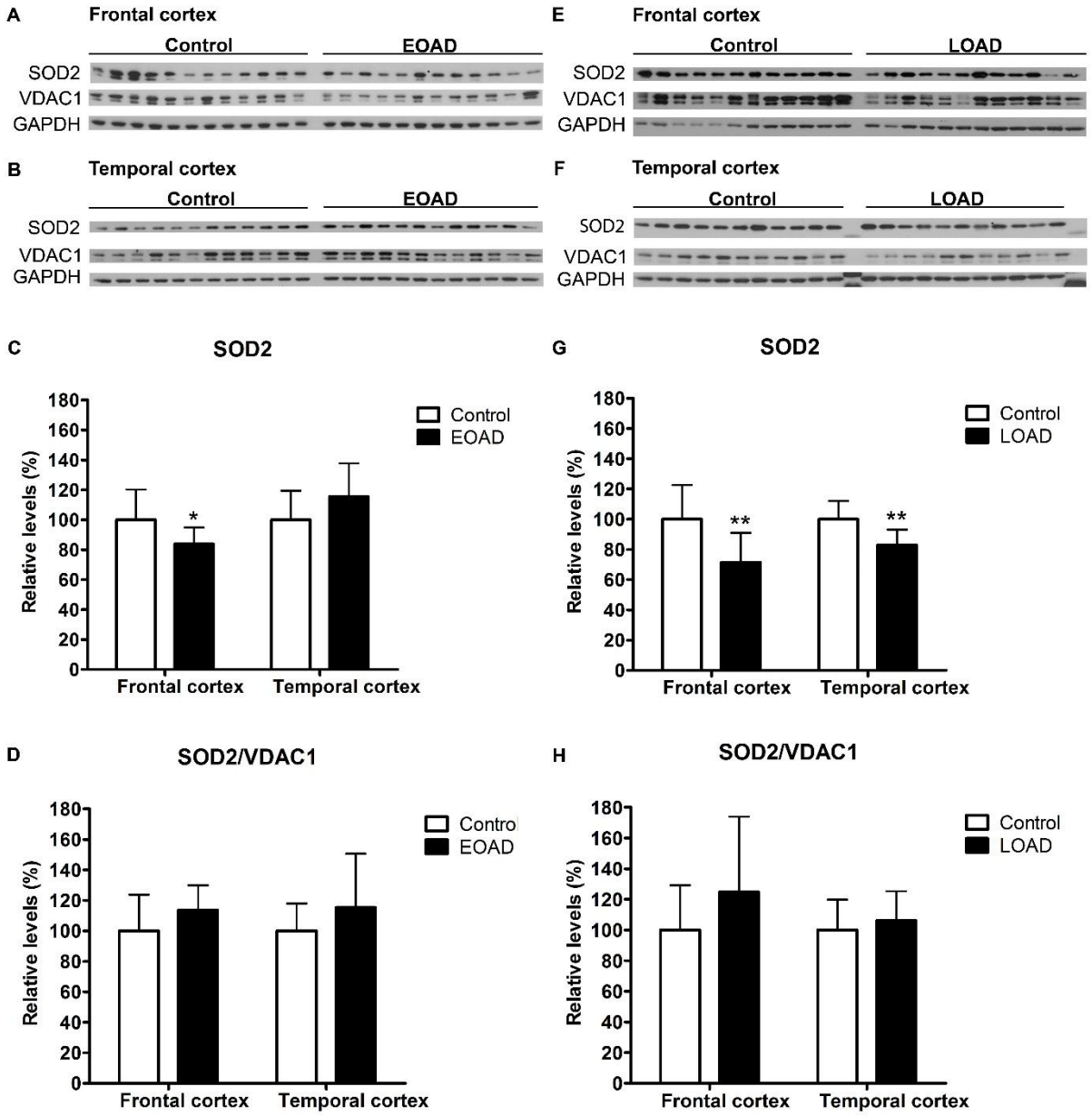

Figure 4.12 SOD2 Protein Levels in EOAD and LOAD Frontal and Temporal Cortex.

Representative Western blots from EOAD or LOAD and their age matched control in (**A, E)** frontal and (**B, F)** temporal cortex as well as their respective densitometric analysis of SOD2 normalized with (**C, G)** GAPDH and (**D, H)** VDAC1. Data were analysed with a nonparametric t-test and *, $p<0.05$; **, $p<0.01$.

4.3.4.3 Levels of copper binding proteins related to the secretory pathway

In the secretory pathway of copper metabolism we measured the levels of a key copper binding proteins (Atox1, ATP7a, Cp and Ctr1). For the protein levels of Ctr1, Atox1 and ATP7a we did not observe any statistically significant change in the studied brain regions with the exception of the EOAD temporal cortex where all three proteins decreased by 23% (nonparametric t-test, p=0.0007), 43% (nonparametric t-test, p=0.0003) and 24% (nonparametric t-test, p=0.0017) respectively. See supplementary figures B.1 to B.3 for more details. However, for the levels of the secreted enzyme Cp we observed various changes in both brain regions and groups. In the brain, we were also able to identify the two different isoforms of (GPI-Cp and sCp) where we determined their levels in EOAD (Figure 4.13A and B) and LOAD (Figure 4.13E and F) frontal and temporal cortex. In EOAD, the protein levels of GPI-Cp were significantly increased by 37% in frontal (nonparametric t-test, p=0.035) and by 50% in temporal cortex (nonparametric t-test, p=0.026; Figure 4.13C). The levels of sCp decreased by 25% (nonparametric t-test, p=0.112) and 4% (nonparametric t-test, p=0.623) in frontal and temporal cortex respectively, but the changes were not statistically significant (Figure 4.13D). In LOAD frontal cortex, the protein levels of Cp were significantly decreased by 27% for the GPI-Cp (nonparametric t-test, p=0.006) although there was no decrease in temporal cortex (nonparametric t-test, p=0.505). A decrease of 30% for the sCp (nonparametric t-test, p=0.015) was observed in frontal cortex however, in LOAD temporal cortex sCp did not show any significant change (nonparametric t-test, p=0.328).

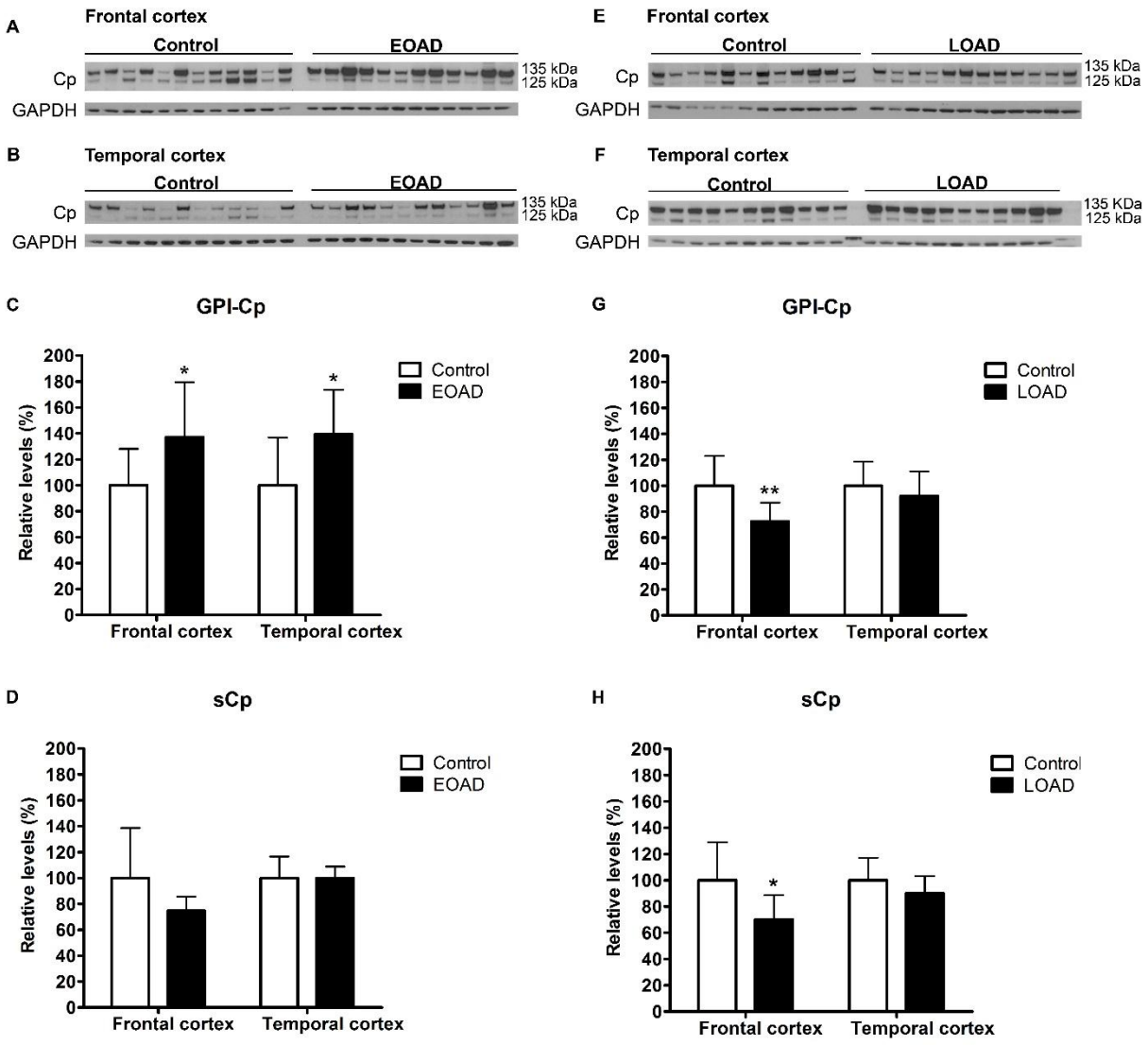

Figure 4.13 Cp Protein Levels in EOAD and LOAD Frontal and Temporal Cortex.

Representative Western blots from EOAD or LOAD and their age matched control in (**A, E)** frontal and (**B, F)** temporal cortex along with their respective densitometric analysis of (**C, G)** membrane bound GPI-Cp (135 kDa) and (**D, H)** secreted sCp (125 kDa) normalized with GAPDH. Data were analysed with nonparametric t-test and *, $p<0.05$; **, $p<0.01$.

4.3.5 Identifying regional differences in the EOAD and LOAD brains

In order to investigate if the levels of copper, SOD and COX/CS activity differed between the EOAD or LOAD brain regions, a Kruskal-Wallis test was used with Dunn's Multiple Comparison post-test in order to determine which regions differ from each other. In both the EOAD and LOAD brains copper levels were significantly higher in cerebellum compared to frontal (Kruskal-Wallis, $p<0.001$ in EOAD and $p<0.01$ in LOAD) and temporal cortex (Kruskal-Wallis, $p<0.001$ in both LOAD and EOAD). No difference was observed between frontal and temporal cortex in either EOAD or LOAD brains (Kruskal-Wallis, $p>0.05$; Figure 4.14A and B).

On the other hand, the COX/CS activity in EOAD cerebellum was significantly lower compared to either frontal (Kruskal-Wallis, $p<0.001$) or temporal cortex (Kruskal-Wallis, $p<0.001$). Between frontal and temporal cortex in EOAD brain no change was identified (Kruskal-Wallis, $p>0.05$). COX/CS activity was also significant lower in LOAD cerebellum but only compared to frontal cortex (Kruskal-Wallis, $p<0.01$). The activity in LOAD temporal cortex was lower relative to frontal (Kruskal-Wallis, $p>0.05$) but the change was not statistically significant compared to the other two brain regions (Kruskal-Wallis, $p>0.05$; Figure 4.14C and D).

SOD activity in the EOAD temporal cortex (Kruskal-Wallis, $p<0.05$) and cerebellum (Kruskal-Wallis, $p<0.05$) was higher compared to frontal cortex although no significant change was observed between the temporal cortex (Kruskal-Wallis, $p>0.05$) and cerebellum (Kruskal-Wallis, $p>0.05$). In LOAD brain even if SOD activity appeared to be higher in temporal cortex relative to frontal cortex (Kruskal-Wallis, $p<0.05$), the change was not statistically significant. SOD activity in LOAD cerebellum did not also seem to differ significantly from frontal (Kruskal-Wallis, $p>0.05$) or temporal cortex (Kruskal-Wallis, $p>0.05$; Figure 4.14E and F).

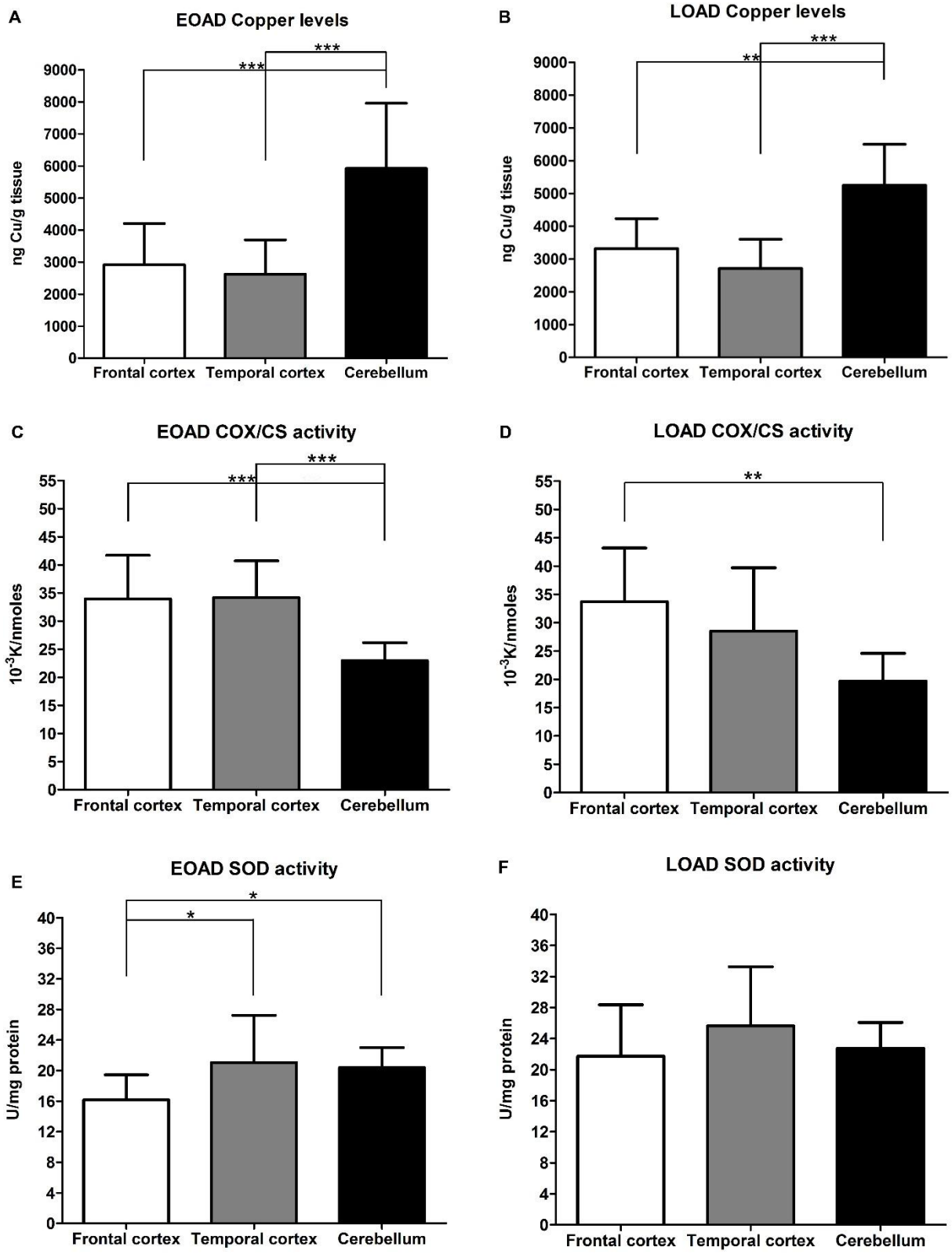

Figure 4.14 Regional Differences in Copper, COX/CS or SOD Activity in the AD Brain.

For copper levels in the (**A)** EOAD and (**B)** LOAD brain cases, cerebellar, frontal and temporal cortex were compared. For COX/CS or SOD activity in (**C, E)** EOAD and (**D, F)** LOAD brain cases were compared. Data were analysed with Kruskal-Wallis test followed by post-test Dunn's Multiple Comparison test to determine if regional differences in levels were apparent and *, $p<0.05$; **, $p<0.01$;***, $p<0.001$.

4.4 Discussion

The aim of this chapter was to study if there is any connection between the copper homeostatic pathway and AD. For many years, the role of certain metals in AD has gained considerable acceptance in relation to the classic amyloid cascade hypothesis but until now the reported results from different studies studying this "metal hypothesis" have proved quite controversial, particularly in relation to the role of copper in AD pathogenesis. In the current study we aimed to answer the question of whether copper is altered and consequently implicated in AD pathology. To achieve this we measured in the same brain samples copper, activity and protein levels of major components of the three intracellular copper pathways. Further, in order to gain a better understanding of all different aspects of AD pathology we examined the role of copper homeostasis in the two AD subtypes: early onset and late onset.

Copper as a redox-active metal is required for a number of metabolic processes in the brain (energy production, antioxidant defence, and neurotransmitter synthesis). Furthermore, copper has a strong potential to participate in free radical chemistry and for that reason its distribution and delivery is carefully regulated by intracellular proteins (chapter 1). This handling system manages to maintain free copper ions to less than one per cell[339]. Several studies have tried to measure copper levels, activity of SOD and COX as well as copper binding proteins in the AD brain, mainly in the age range of the LOAD cases, but the results are quite controversial since some reports showed decrease, no change or increased levels of the studied variable.

4.4.1 Differences in the two AD subtypes for copper demand

In order to obtain a better understating of the role of copper homeostasis in the AD brain we initially measured copper levels in frontal, temporal cortex and cerebellum from both EOAD and LOAD cases and compared these with suitably age matched controls. In all three EOAD brain regions, a marked loss of copper was observed especially in temporal cortex where the decrease reached almost 45%. On the other hand, in LOAD brain the changes were not as severe as in EOAD brain since only in temporal cortex the observed decrease was significant different (Figure 4.2). Comparing copper levels between EOAD and LOAD brain regions failed to show any significant difference with only a small increase in LOAD frontal and temporal cortex and a small decrease in cerebellum (Figure 4.5).

The marked copper loss that we observed in the EOAD frontal and temporal cortex compared to age matched control and to LOAD brain can be either attributed to the greater neuronal/synaptic loss and atrophy in the EOAD brain or to the decline of copper

concentration with increasing age in the brain (as discussed in chapter 3). Studies have shown that the EOAD temporal cortex exhibits 40-60% greater atrophy compared to healthy controls whereas the LOAD temporal cortex faces only 70-80%[334]. Similarly, frontal cortex in the EOAD brain shows 29-46% atrophy in terms of volume loss whereas the LOAD brain only 18% loss compared to healthy controls[334]. Also, in the EOAD brain the synaptic loss can reach more than 50% in frontal and temporal cortex relative to LOAD brain[159]. The severity of change found in the EOAD brain has been further established by studies which counted neurons and demonstrated that the EOAD frontal cortex exhibits more than 20% neuronal loss compared to LOAD and almost 40% relative to healthy controls[335, 340, 341]. In the EOAD temporal cortex the neuronal loss can reach the 50-60% in certain regions compared to healthy controls and 15-25% relative to LOAD brain[335, 340, 341]. However, cerebellum appears to be less affected especially in the LOAD brain where normally only a few amyloid plaques are present, although in EOAD the cerebellum may have slightly increased AD pathology since a lower Purkinje cells density and higher astrocytosis has been observed compared to both controls and LOAD[336].

From the above mentioned results and observations we can conclude that the considerable copper loss that we identified in the EOAD brain is an effect of the greater atrophy, neuronal and synaptic loss which occurs in these brain regions. On the other hand, the changes in the LOAD brain compared to age matched controls are a combination of reduced copper levels with ageing and increased AD pathology. The controls from the EOAD group had on average in frontal and temporal cortex 5892 and 4503 ng Cu/g tissue compared to control from the LOAD group where copper levels were 3860 and 3568 ng Cu/ g tissue respectively, which makes them to differ by more than 30%. The small increase in copper levels in LOAD brain relative to EOAD probably occurs from the small differences in pathology between the two subtypes of the disease.

In cerebellum, copper levels were higher than those found in control, EOAD and LOAD frontal and temporal cortex which is also in agreement with previous studies that measured copper in different brain region of either healthy controls or AD cases[14, 342]. Our study showed that copper levels decreased by 25% in EOAD cerebellum but the change was only marginally significant. On the other hand, in LOAD cerebellum copper did not change relative to age matched controls (Figure 4.2). That difference probably reflects the pathology in EOAD cerebellum which is more severe and relative absence in the LOAD cerebellum. In LOAD cerebellum copper levels were slightly lower compared to EOAD which probably occurs due to the normal decrease of copper with ageing since the controls for the EOAD

cases contained more than 32% copper compared to the LOAD controls (7915 ng Cu/g tissue for the EOAD controls and 5372 Cu/g tissue for the LOAD controls; Appendix A).

Several studies have measured copper levels in different AD brain regions where they used frozen brain tissue for the determination, however, the results are controversial. The majority of the studies were mainly focused on LOAD cases with Plantin *et al.* in 1987 reporting a 40% decrease in copper levels in temporal and frontal cortex[(343)]. Unfortunately, in this study details about the sample age were not apparent and so we cannot place them in an AD subtype (e.g. EOAD or LOAD), however, even if they used different determination technique for copper levels (gamma spectrum and Ge(Li) detector) the copper levels determined by Plantin and colleagues are quite close to the current determinations for the LOAD group (around 3.51-3.06 μg Cu/g for the controls and 2.14-1.81 μg Cu/g for the AD)[(343)]. Deibel *et al.* in 1996 used LOAD cases and showed 20% decrease of copper in temporal cortex and 11% in cerebellum but the change was not statistically significant[(14)]. The reported percentage change in Deibel and colleague study is close to that found in the current study for temporal cortex (24%) although in the current study this change was statistically significant[(14)]. The difference between the studies might due to either the different determination technique for copper (instrumental neutron activation analysis (INAA)) or sample preparation[(14)].

In a study, Loeffler *et al.* used similar cohort of AD samples and measured copper with AAS, copper levels were higher in frontal cortex but the difference was again not statistically significant[(344)]. A recent studies from Magaki *et al.* showed that copper levels were significantly decreased in frontal cortex but they used cases with an age range of 50-94 years which includes both of our AD subtypes[(254)]. Despite the use of GFAAS to determine copper levels in the AD brain and ages of cases which include both EOAD and LOAD the reported copper concentration was from 3.9 to 6.9 μg Cu/g which is quite close to the current levels of copper for the same brain region. Rembach *et al.* measured copper in LOAD frontal cortex with ICP-MS and showed again that copper levels were significantly decreased in AD brain[(345)]. The reported concentration from Rembach *et al.* is close to ours for that region (3.33 μg/g wet weight for the controls and 2.29 μg/g wet weight for the AD) but our current study failed to see any significant change in LOAD frontal cortex, possibly due to the different number of cases since they used almost 3 times as many[(345)].

From the above we can conclude that our results from the LOAD group are in good agreement with the majority of the above mentioned studies. Especially with the studies that reported similar copper concentration to ours and percentage changes in the same brain

regions. In relation to copper levels in the EOAD brain, our study seems to be the first to report the decrease copper levels in EOAD and also to identify small changes between EOAD and LOAD brains.

4.4.2 How is the mitochondria copper pathway affected in the AD brain?

One of the common characteristics of patients with AD is a decrease in glucose metabolism as seen with PET scans, a feature which occurs early in the disease course and which may precede cognitive deficits[346, 347]. The main source of energy in the brain is via aerobic metabolism, by breakdown of glucose via glycolysis and eventually through mitochondrial oxidative phosphorylation. The terminal enzyme of the respiratory chain, COX, requires copper for its activity and based on our observation of copper deficiency in both EOAD and LOAD brain and already published data from PET studies, this led us to investigate COX activity and protein levels in EOAD and LOAD subtypes.

4.4.2.1 COX/CS activity is not affected in the AD brain

Our results showed a general decrease in COX activity in all brain regions in the EOAD and LOAD brains but only in LOAD temporal cortex the change was statistically significant. However, when COX activity was corrected for mitochondrial content in the brain homogenates, by using CS activity as a reference, these differences were no longer present. This change appears to be due to the significant decrease of CS activity in both EOAD and LOAD frontal and temporal cortex which implies that the decrease COX activity is due to mitochondrial loss in the brain rather than copper deficiency (Figure 4.3). The mitochondrial loss was further supported by a decrease in protein levels of VDAC1 in these two brain regions (Figure 4.7D and I). The fact that in the EOAD temporal cortex the ratio of COX/CS is higher comes as a result of the greater mitochondrial loss (as indicated by the CS activity) relative to the smaller decrease of COX activity which indicates that the remaining mitochondria have to increase their function in order to compensate for the general energy deficiency in that specific brain region. In LOAD temporal cortex the ratio of COX/CS is lower since the remaining mitochondria have an even higher deficiency in COX activity.

The last three decades numerous studies have tried to determine COX activity in different brain regions by using frozen tissue with the observed results dividing into two categories the first one where they reported significant loss of COX activity in the AD brain[249-251, 348-350] and a second where no significant change was observed[351-355]. The majority of the studies followed similar methodology to determine COX activity but they differed in the number of

cases that they used, age of the groups, post-mortem delay and in some cases if they used CS to normalize the COX activity. Table 4.1 presents information about known studies that measured COX activity in AD brain (age range, COX and CS activity, brain region etc.).

Studies from Mutisya *et al.* and Maurer *et al.* measured COX and CS activity in frontal and temporal cortex and showed decreased activity of both COX and COX/CS ratio, however, these studies only noted that CS did not change between AD and controls[249, 250, 348]. Parker et al, Wong-Riley *et al.* and Bosetti *et al.* measured only COX activity in either brain hemisection or different regions and observed a marked decrease in COX activity especially in affected brain regions such temporal cortex and hippocampus but these studies lack any correction for differences in mitochondrial enrichment[251, 349, 350]. However, studies from Kish *et al.* and Cooper *et al.* showed that both COX and CS activity decreased in affected brain regions such as frontal and temporal cortex but when they normalized COX with CS activity no change was observed[351-353]. Reports from Reichmann *et al.* and Cavelier *et al.* showed a small decrease of COX activity in the AD brain but the changes were not statistically significant[354, 355]. It is worth mentioning that the majority of the above studies did not separate their AD cases into EOAD or LOAD, based on the age of onset, but mainly used cases that included both subtypes.

The above mentioned studies differed in the age of the samples or post-mortem delay. Our study has the unique characteristic that subdivided the AD cases into two groups where no statistical significant difference was observed for either age (controls for EOAD 64.7 ± 5.6; EOAD 66.9 ± 5.1, p=0.815; controls for LOAD 85.6 ± 6.0 and LOAD 83.5 ± 6.7, p=0.302) or post-mortem delay (controls for EOAD 30.0 ± 21.6; EOAD 30.6 ± 15.4, p=0.526; controls for LOAD 29.9 ± 11.6 and LOAD 38.8 ± 19.8, p=0.304). Few of the above mentioned studies have determined if there was any significant correlation of post-mortem delay with mitochondrial enzyme activities which might have affect the final measured activity[249, 351].

We conducted Spearman rank test in order to identify possible correlation between COX, CS activity and post-mortem delay where we found that the controls for the EOAD cases presented a negative and marginally significant correlation between post-mortem delay and COX activity in frontal cortex (r_s=-0.541, n=14, p=0.046). A significant negative correlation between post-mortem delay and CS activity was also observed in the controls of the EOAD cases both in frontal (r_s=-0.695, n=14, p=0.006) and temporal cortex (r_s=-0.638, n=14, p=0.014). No other significant correlation for COX, CS or COX/CS activity in both groups and brain regions was observed.

Author	Case	Age (years)	PM (hours)	Brain region	Activity (% changes to controls)		
					COX	CS	COX/CS
Parker *et al.* [a(251)]	Controls (n=8)	72.9 ± 5.2	11.8 ± 2.5	Brain hemisection	53% decrease (p<0.001)	NE	NE
	AD (n=9)	77.2 ± 3.4	9.9 ± 1.7				
Mutisya *et al.* [a,b(250)]	Controls (n=15-23)	75.9 ± 2.7[2] 70.1 ± 3.5 72.8 ± 3.6 73.9 ± 3.0	9.4 ± 1.3 11.8 ± 1.3 2.4 ± 1.3 12.3 ± 1.6	Parietal cortex	12-16% decrease (NS)	NR	20-30% decrease (p<0.001)
				Frontal cortex	22% decrease (NS)	NR	26% decrease (p<0.05)
	AD (n= 19-23)	73.5 ± 3.0 75.3 ± 2.6 73.2 ± 2.0 74.3 ± 2.2	10.7 ± 1.5 8.7 ± 1.2 9.2 ± 1.1 11.7 ± 1.3	Temporal cortex	15-21% decrease (p<0.05)	NR	25-27% decrease (p<0.01)
				Occipital cortex	40% decrease (p<0.001)	NR	29% decrease (p<0.001)
Maurer *et al.* [b(348)]	Controls	___	___	Frontal cortex	NS	NR	35% decrease (NS)
				Temporal cortex	53.6% decrease (p<0.07)	NR	63% decrease (p<0.01)
	AD	___	___	Hippocampus	60% decrease (p<0.002)	NR	65% decrease (p<0.002)
				Cerebellum	NS	NR	NS
Wong-Riley *et al.* [b(349)]	Controls (n=18)	73	11	Prefrontal cortex	40% decrease (p<0.01)	NE	NE
				Superior temporal gyrous	50% decrease (p<0.001)	NE	NE
	AD (n=51)	76	8	Hippocampus	~35% decrease (p<0.05)	NE	NE
				Cerebellum	~35% decrease (p<0.05)	NE	NE

[2] In this study they used different cohort of cases for the respective brain region that they studied. The age and post-mortem delays are arranged based on the mentioned brain regions.

Maurer *et al.* [b(249)]	Controls (n=13)	69.4 ± 8	28.2 ± 13.9	Frontal cortex	22% decrease (p=0.11)	NS	NS
				Temporal cortex	37% decrease (p=0.006)	NS	63% decrease (p=0.001)
	AD (n=23)	74.6 ± 7.3	28.6 ± 6.7	Hippocampus	52% decrease (p=0.003)	NS	56% decrease (p<0.001)
				Cerebellum	NS	NS	NS
Bosetti *et al.* [a(350)]	Controls (n=20)	63.4 ± 9.1	Within 24 hours	Motor cortex	10% decrease (NS)	NE	NE
	AD (n=20)	65.2 ± 8.5	Within 24 hours	Hippocampus	35-40% decrease (p<0.05)	NE	NE
Kish *et al.* [b(351)]	Controls (n=30)	69 ± 2	12 ± 1	Frontal cortex	26% decrease (p<0.01)	16% decrease (p<0.01)	NR
				Temporal cortex	17% decrease (p<0.05)	NR	NR
				Parietal cortex	16% decrease (p=0.055)	NR	NR
	AD (n=19)	73 ± 2	10 ± 1	Occipital cortex	5% decrease (NS)	NR	NR
				Putamen	NS	NR	NR
				Hippocampus	20% increase (NS)	NR	NR
Cooper *et al.* [b(353)]	Controls	___	___	Temporal lobe	9% decrease	5% decrease	NS
	AD	___	___				
Reichmann *et al.* [b(354)]	Controls (n=7)	77 ± 9	Within 6 hours	Parietal cortex	25% decrease (NS)	NE	NE
				Temporal cortex	24% decrease (NS)	NE	NE
	AD (n=7)	77 ± 9	Within 6 hours	Entorhinal cortex	26% decrease (NS)	NE	NE
				Hippocampus	10% decrease (NS)	NE	NE

Cavelier *et al.*[b] (*355*)	Controls (n=5)	___	___	Frontal cortex	NS	NE	NE
	AD (n=6)	___	___	Occipital cortex	NS	NE	NE
				Parietal cortex	NS	NE	NE
Kish *et al.*[b](*352*)	Controls (n=13)	69 ± 3	11 ± 1	Temporal cortex	32% decrease (p<0.001)	26% decrease (p<0.001)	8% decrease (NS)
	AD (n=15)	72 ± 2	8 ± 1	Parietal cortex	32% decrease (p<0.001)	23% decrease (p<0.001)	8% decrease (NS)
				Occipital cortex	NS	NE	NE

Table 4.1 Summary of Studies Measuring COX Activity in AD brain.

The numbers of studied cases, age, post-mortem delay (PM) and percentage change as well as the statistical change are presented. a, studies that conducted the assays in isolated mitochondria from frozen tissue. b, studies that conducted the assay in total brain homogenates from frozen tissue. NR: not reported; NE: not examined; NS: non-significant

Another factor which might affect the COX and CS activity is the pH of the brain which is used as an index of the agonal status of the person and is normally altered in brain of patients who died with protracted illness[281, 356, 357]. In our study groups we observed that there was a statistical significant difference between the pH of the EOAD and their age matched controls (controls 6.78 ± 0.29 and EOAD 6.23 ± 0.30, $p<0.0003$) but no difference in the LOAD and their respective controls (controls 6.06 ± 0.25 and LOAD 6.13 ± 0.32, $p=0.557$). The significant pH change between the controls and the EOAD cases might occur from the post-mortem delay since there was a strong negative correlation between the pH and post-mortem delay of the controls. It is worth mentioning that the EOAD controls had the highest pH value relative to the rest of the groups. In order to check if the pH effects the COX and CS activity we correlated pH with activity and only temporal cortex of the controls for the LOAD cases showed a negative and marginally significant correlation ($r_s=-0.615$, $n=11$, $p=0.044$) with COX activity. Taking into consideration that the observed correlations between post-mortem delay or pH with COX or CS activity occur only in certain brain regions or groups and the absence of any particular pattern we can conclude that these changes possibly represents minor characteristics of the studied specimens. The absence of a significant effect of post-mortem delay, pH or the agonal stage of the patients in COX or CS activity has also been confirmed by studied from Yates *et al.* and Perry *et al.*[356, 357]. Finally, our results are in agreement with studies of Cooper *et al.*, and Reichmann *et al.*, and particularly with the results of Kish *et al.* who measured COX and CS activity in AD brain and took into consideration how post-mortem delay and pH could affect COX and CS activity[351, 352].

In relation to the differences between the EOAD and LOAD brains for COX and CS activity, we only observed small changes in temporal cortex and cerebellum. Normally the EOAD brain is considered more atrophic with greater neuronal/synaptic loss[159, 334]. Based on these facts it was expected that COX and CS activity would be higher in the LOAD brain than in the EOAD but we showed that temporal cortex, the most affected brain region in AD, COX activity and COX/CS ratios were lower in the LOAD brain compared to EOAD (Figure 4.5). Since mitochondrial oxidative phosphorylation takes place mainly in neurons and the EOAD temporal cortex exhibits the greatest neuronal loss, it is possible that in order to compensate for the high energy demands the remaining mitochondria have to increase their respiration to maintain energy levels. This can also be seen in cerebellum where in LOAD brain normally there is negligible AD pathology but in EOAD an increased neuronal loss and astrogliosis is observed. In agreement with the findings in the temporal cortex in EOAD, cerebellar COX activity and COX/CS ratio were higher which possibly represents an attempt by the remaining

mitochondria in the neurons to fulfil that region's energy demands (Figure 4.5). Based on electron microscopy studies the majority of the mitochondria are localised in neurons since they require energy for various processes such as neurotransmission and synaptic development[358-360]. The same electron microscopy studies have also shown that the neuronal dendrites in AD brain are facing extensive mitochondria loss compare to healthy controls[358, 359]. Manczak *et al.* made a similar conclusion in a study where they measured mRNA levels of COX1 and COX2 in AD brain and found increased expression for both genes[361]. These authors suggested that the increased COX gene expression was either a functional compensation mechanism by the remaining neurons or a mitochondrial alteration related to increased oxidative damage in the AD brain[361]. Taking into consideration our results, Manczak *et al.* study and the results from the electron microscopy studies of reduced mitochondria number in the synaptic cliff, we can conclude that a functional compensation mechanism could happen in the AD brain. Since our finding showed that the EOAD brain regions, which exhibits the greatest neuronal loss, had higher COX activity compared to LOAD which has at least 10-20% more neurons.

4.4.2.2 COX subunits in the AD brain

In order to further understand how copper and COX activity is regulated in the AD brain we measured the protein levels, by Western blotting, of the two core subunits, COX1 and COX2 as well as the levels of Sco2 which together with Sco1 incorporate copper into COX2 (section 1.3.3). During the Western blot analysis, gels that contain samples from EOAD or LOAD are only compared with their respective age matched controls and for one brain region at a time. For that reason, any comparison of protein levels between EOAD and LOAD are not able to be performed with the given data. In relation to the regional differences of the studied groups, since the brain specimens are obtained from the same individual, we can only assume that the differences between frontal and temporal cortex represents regional brain changes.

As already noted, the mitochondrial loss was further supported by measuring VDAC1 levels in the brain extracts where a 20-45% decrease was observed in the different regions of the EOAD and LOAD brain tissue (Figure 4.7D and I). In the IMS, COX assembly initiates around a seed formed by COX1 which has already obtained the three redox centres (heme *a* and heme a_3-Cu_B). Our analysis showed that there was a small protein loss of COX1, relative to total protein levels, especially in the EOAD frontal cortex. However, in LOAD temporal cortex no change in COX1 protein levels was observed. The small decrease of total COX1 levels likely represents mitochondrial loss in the EOAD frontal cortex since when we

normalised COX1 levels with VDAC1 no change or in some cases higher COX1/VDAC1 ratio was observed in both AD subtypes. For example in LOAD temporal cortex, COX1/VDAC1 levels increased by 45% since in that brain region there was a 30% mitochondrial loss but at the same time the total COX1 protein levels remained unchanged (Figure 4.7).

It is well know that in temporal cortex, in both LOAD and EOAD brain, there is higher neuronal and synaptic loss compared to frontal cortex[362] but in our cases we showed that frontal cortex lost more mitochondria and COX1 protein which might suggest that the remaining neurons in temporal cortex are attempting to maintain mitochondria in order to fulfil the local energy demand by increasing protein synthesis in a functionally important brain region. The higher ratio of COX1/VDAC1 in temporal cortex in both AD subtypes furthers supports this concept (Figure 4.7E and J). The total protein levels COX2 and its assembly protein Sco2, were significantly decreased in both brain regions in EOAD and LOAD (Figure 4.8 and 4.9). Once again when COX2 protein levels were normalized with VDAC1 a non-significant change was present in the majority of the studied brain regions and groups. The only exception was the EOAD temporal cortex where the COX2/VDAC1 ratio decreased possibly due to the higher total COX2 protein loss in that region compared to mitochondria loss (Figure 4.8D). A possible reason for seeing greater loss of COX2 in EOAD temporal cortex might be correlated with the marked copper decrease. In order for COX2 to take part in COX biogenesis, it requires the Cu_A centre, a process which is coupled with the function of Sco1 and Sco2 in the IMS[363]. However, Sco2 seems to have a second role in addition to metalation, that of regulating COX2 protein synthesis which has been demonstrated in studies with human Sco2 deficient fibroblasts[111]. Combining these facts with our observations that Sco2 protein levels decreased in the EOAD temporal cortex we might conclude that Sco2 deficiency affects either COX2 synthesis or lower copper levels induce COX2 degradation since without the Cu_A centre, COX2 cannot enter the assembly pathway and remains in the IMS where dedicated mitochondrial proteases will begin degrading COX2.

It is worth mentioning that LOAD frontal cortex had the highest mitochondrial percentage change compared to age matched controls which was followed by the highest loss in COX2 protein levels. In chapter 3 we have shown that in frontal cortex there was a (non-significant) decline of mitochondrial levels with ageing which might have contributed to the higher percentage change in the LOAD frontal cortex compared to temporal cortex. In relation to Sco2 protein, we can see that Sco2 levels decreased in a similar way to that of COX2. Sco2 is

localized in the mitochondria but is nuclear encoded and multiple factors such as copper levels or mitochondria availability can affect its protein synthesis.

Our results of decreased total COX1 and COX2 protein levels in the AD brain are in agreement with a study by Kish *et al.* who used different cohort of samples and experimental approaches for protein determination but reported a decrease of COX1 and COX2 levels in temporal cortex[352]. Taking into consideration the above mentioned results about COX activity and protein levels we can conclude that the observed changes in the AD brain are a combination of neuronal and consequent mitochondria loss with the remaining mitochondria trying to increase their function rate in order to compensate and fulfil the great energy demand of the affected brain regions.

4.4.3 Cytosolic copper binding pathway proteins in AD

Oxidative stress has been proposed to play an important role in the pathogenic mechanism of AD pathology[364]. Several studied have reported increased markers of oxidative cellular damage such as lipid peroxidation, oxidative damage of proteins and DNA in the most affected AD brain regions[253, 365, 366]. Accordingly, one of the main sources of ROS production in the AD brain is the Aβ peptide which in the presence of metals such copper and iron can mediate an O_2-dependent cell free H_2O_2 generation[240, 367]. Nonetheless, cells have evolved an antioxidant defence mechanism with the first line of defence being SOD1 in the cytosol and SOD2 in the mitochondria matrix[368].

4.4.3.1 SOD activity is increased in the affected AD brain

Our study showed that the most severely affected brain region in the AD brain exhibited the highest percentage increase of total SOD activity. Generally no statistical significant change was observed in EOAD and LOAD frontal cortex and cerebellum. However, in EOAD temporal cortex a greater than 50% increase in SOD activity was observed compared to age matched controls. Total SOD activity was higher in LOAD temporal cortex but the change was not statistically significant (Figure 4.4). The general increase in SOD activity in the AD affected regions indicates an attempt by the brain to defend against increased oxidative stress occurring from either the increased of ROS generation from the accumulated Aβ or even from the increased function of the remaining mitochondria.

EOAD temporal cortex showed the highest percentage change in SOD activity compared to age matched controls amongst the rest of the studied regions and AD cases (Figure 4.4). Multiple factors could induce high activity in this severely affected brain region in AD[369].

During the progress of AD pathogenesis temporal cortex is affected in the intermediate stages (Braak stage III-IV) and also in the final stages (Braak stage V-VI) the amount of lesions and the long-lasting severe oxidative damage is higher relative to the other brain regions[163, 328]. Potentially, the increase of COX/CS activity that we identified in EOAD temporal cortex could also induce higher ROS production coming from the mitochondrial respiratory chain which will require more active SOD. Several studies have shown that within plaques metal such as copper and iron are "trapped" and in the presence of Aβ they generate ROS via the Fenton reaction[239]. Our findings showed that EOAD temporal cortex might have the lowest copper levels in the AD brain but at the same time had the highest iron levels which can increase the production of ROS and further trigger the activation of SOD in the brain (see table B.1 in supplementary data).With an increase in SOD activity in the AD brain the logical assumption will be that oxidative stress should be less. However, during its catalytic activity SOD generates another ROS product, H_2O_2. Another possibility for not seeing a decrease in oxidative stress in the AD brain might be due to the balance between ROS production and degradation by SOD where the brain produces more ROS which SOD is able to eliminate.

Several studies have tried to determine SOD activity in the AD brain by using frozen tissue archived and the majority of these show either a small non-significant or significant increase in the affected AD brain regions. Our results are not completely comparable with these studies since the majority of the previous studies used a mixture of EOAD and LOAD cases or just LOAD. Of these, Ramassamy *et al.* who measured SOD activity in LOAD frontal cortex, did not observe any change in total SOD which is in agreement with our observation[370]. Similarly, Karelson *et al.* measured SOD activity in LOAD frontal and temporal cortex where they observed a significant increase only in temporal cortex[365]. We also showed a 12% increase in LOAD temporal cortex but the change was not significant. The differences between the Karelson *et al.* study and ours might be either due to a smaller cohort of samples (7 cases vs. 13 cases), sample preparation or post-mortem delay. A study from Schuessel *et al.* who used frontal and temporal cortex and cerebellum from LOAD cases reported a significant increase of SOD1 activity in all three brain regions, even in the less effected LOAD cerebellum[371]. The total SOD activity that we measured contains the activities from both SOD1 and SOD2 but in the brain the amount of SOD2 is less and therefore the majority of the measured activity may represent SOD1. However, we cannot directly infer an increase in SOD1 activity over SOD2 without measuring these separately.

Studies that used mixed cases of EOAD and LOAD, based on age criteria, from Gsell *et al.* and Lovell *et al.* reported increased total SOD activity in the AD frontal, temporal cortex and

cerebellum but the change was not significant[372]. Their observed changes might not be significant but both studies reported that AD temporal cortex had higher SOD activity compared to age matched controls. On the other hand, a study from Marcus *et al.* reported a marked decrease (more than 80%) in total SOD activity in frontal, temporal cortex and cerebellum[253]. In this study they potentially used EOAD cases and quercetin as substrate in order to measure SOD activity, although these differences may not explain the considerable change in SOD activity not only compared to our study but also to the other published reports.

Our observation on SOD activity in LOAD brains is consistent with already published reports which suggests that the regional oxidative damage in the AD brain induces the increased activity of SOD. Our finding is further supported by the increased activity of SOD in all LOAD brain regions compared to EOAD (Figure 4.5). The difference between the two AD subtypes can be attributed to different factors but the most likely are higher neuron loss which leads to less protein generally in the EOAD brain compared to LOAD especially in cerebellum which is less affected in LOAD[334-336]. Further, SOD1 requires copper for its activity but in the EOAD brain copper levels are lower compared to LOAD. The lower copper levels could possibly effect the activation of SOD1 in the brain. Additionally, as discussed in Chapter 3, SOD activity increases with ageing in the healthy brain, the EOAD cases being younger compared to LOAD suggesting that the observed difference may be a simple effect of different age groups. The most likely explanation is the general impact of ageing on the brain. This is further supported by the fact that in the EOAD frontal and temporal cortex, SOD activity increases as the AD brain gets older (Figure 4.6). The same trend was also present in the LOAD brain regions and EOAD cerebellum although the correlation was not significant. Taking into consideration all the above, we might conclude that the increased activity in the AD brain is due to higher oxidative stress and that the differences between LOAD and EOAD reflects both the normal ageing impact on SOD activity and the decrease of SOD1/2 protein levels that we observed in the EOAD brain.

4.4.3.2 Levels of SOD and CCS proteins in the AD brain

To further understand how SOD activity is regulated in the AD brain we determined the proteins directly involved in SOD activity, SOD1, SOD2 and CCS. SOD1 requires CCS in order to be activated and we observed that their protein levels follow the same trend in all studied brain regions and groups. For example in EOAD frontal cortex both protein levels decreased by more than 25% relative to age matched controls (Figure 4.10 and 4.11). Similarly in LOAD frontal and temporal cortex both SOD1 and CCS increased compared to

controls. In EOAD temporal cortex, where we observed the highest percentage change of SOD activity, the protein levels of SOD1 and CCS did not however change. One possible assumption is that the CCS and SOD1 protein levels are correlated more with neuronal loss in the affected brain regions since both are mainly localized in neurons[131, 373]. Even if the EOAD temporal cortex exhibits higher neuron loss compared to frontal cortex, SOD1 and CCS protein levels still do not change compared to age matched controls in the current study. Combining the observations that in frontal cortex a 25% decrease of SOD1/CCS protein levels caused an 8% increase in SOD activity and in temporal cortex no change in the proteins had as a result a 54% increase in activity shows that the mechanism which regulates both the protein levels and the activity of SOD may be the oxidative stress in the respective brain region (Figures 4.5A and 4.11 C)

In relation to the increased protein levels of SOD1 and CCS in the LOAD frontal and temporal cortex, the change is possibly due to a combination of the increased oxidative stress that occurs normally with ageing and which is further enhanced by AD pathology. The higher SOD1 protein levels in the LOAD frontal (30%) and temporal (41%) cortex might suggest that the final activity should be significantly higher, however, studies have shown that SOD1 remains in apo-SOD1 form if there is reduced available copper in the cells (Figure 4.11F)[321]. Based on our results copper levels are lower in both brain regions which will result in lower activation rate of SOD1 and accumulation of nascent protein in the brain.

Several studies in mice and different cell lines have shown that CCS protein levels are regulated by copper availability and that lower levels induce a higher expression rate[134]. Our results in the LOAD brain are in agreement with that observation since we showed higher expression of CCS in the copper deficient frontal and temporal cortex. However, in EOAD frontal and temporal cortex CCS levels were lower relative to age matched controls even if these brain regions exhibited the highest copper loss (Figure 4.10). A possible reason for this discrepancy might be due to either higher neuronal loss in these brain regions or by the fact that there was less SOD1 protein to activate.

Previous studies have shown that CCS is implicated with the amyloid pathway by regulating BACE1 through interaction with the small cytoplasmic domain of BACE1 in order to transfer copper and possibly regulate its activity or localization[218]. Also, studies have shown that higher levels of BACE1 results in lower SOD1 activity and that CCS deficiency induced higher levels of Aβ[218, 374]. In the present study, we were not able to measure BACE1 protein levels or activity but it is well established that in AD brain BACE1 levels and activity are

higher[220, 221, 375, 376]. Combining the published data about BACE1 and the current study for SOD activity we can conclude that increased BACE1 levels do not seem to have any impact on SOD activity in the AD brain, on the contrary, higher activity was observed. In relation to the interaction of CCS with BACE1 we cannot draw any conclusion with the given data since no direct comparison can be made from our samples as to how these two proteins interact.

SOD2 is also directly implicated with SOD activity and our analysis showed that SOD2 protein levels decreased in all brain regions of the EOAD and LOAD brain except in EOAD temporal cortex where SOD2 levels were non-significantly increased (Figure 4.12). This specific result could be attributed to the higher observed percentage change of SOD activity in the EOAD temporal cortex. In the other brain regions, SOD2 protein decreased which potentially correlates with the mitochondrial loss in these regions. However, when normalized with VDAC1 the final ratio for SOD2 was higher in all brain regions of both AD subtypes. The increased antioxidant defence in the mitochondria matrix by SOD2 may be expected since the respiratory chain function is increased (based on the COX/CS activity) which will induce higher production of ROS and will require more active SOD2 protein within mitochondria to neutralise ROS. It is also worth noting that we did not observed any change in manganese levels in any of the study brain regions and AD subtypes (Table B.1 and B.2 supplementary data).

The current study appears to be the first to report the protein levels of SOD1 and SOD2 in the EOAD brain since the previous studies determined SOD protein levels only in LOAD brains where they observed results are variable. Kurobe *et al.* determined SOD1 and SOD2 protein levels by using an immunoassay in the cerebral cortex and found no change in SOD1 levels and a non-significant increase in SOD2 protein levels[315]. Also, Kato *et al.* reported a small but non-significant increase in SOD1 and SOD2 levels in frontal and temporal cortex in LOAD cases[377]. Murakami *et al.* used Western blotting in order to determine SOD1 and SOD2 protein levels in LOAD frontal cortex where a significant decrease in SOD1 protein levels was reported[378]. Our study and the ones from Kurobe *et al.* and Kato *et al.* are in agreement in the trend for higher SOD1 in the cortex and the small differences might occur due to the experimental approach (immunoassay vs. Western blot)[315, 377]. Other possible factors such as the different cohorts of cases or post-mortem delay, which might have affected protein degradation, can contribute to small differences between studies. It is worth mentioning our specimens did not show any correlation between post-mortem delay and SOD1/2 protein levels. Murakami *et al.* also used Western blot in order to determine SOD

protein levels but differences in the antibodies or type of membrane and even the clinicopathological features of the cases could contribute to the final result.

From the above we can conclude that the decrease copper levels in AD does not seem to effect either SOD activity or its protein levels. In contrast, the long-lasting severe oxidative stress in the AD brain seems to regulate both the activity of SOD and the levels of proteins associated with its activity. The majority of the current results are in good agreement with already published data although we report for first time CCS protein levels in the EOAD and LOAD brains as well as SOD activity and its protein levels in the EOAD brain.

4.4.4 The copper secretory pathway in the AD brain

The major components of secretory pathway consist of the cytosolic chaperone Atox1 and the transporters ATP7a and ATP7b in the Golgi membrane which are responsible for the incorporation of copper into newly synthesized enzymes such Cp, Hephaestin or PAM, and also for the efflux of excess copper from the cells. In the present study we were able to determine only the protein levels of the Atox1, ATP7a and Cp in the studied brain regions. In addition to the above mentioned proteins we also determined the protein levels of Ctr1.

Our results showed that Ctr1, Atox1 and ATP7a protein levels were significantly decreased only in EOAD temporal cortex (Figures B.1 to B.3). These three proteins play a regulatory role in copper influx-efflux in the cells and the fact that all of them decreased in the most affected brain region in AD might indicate that either the neuron loss or the highest copper loss in EOAD temporal cortex associates with protein changes. However, studies with cells have shown that copper levels do not affect the total Ctr1 or ATP7a protein levels but their localization in the cells[41, 68, 69]. Based on these studies we can conclude that the loss in protein levels in EOAD temporal cortex is due to extensive neuronal loss in that brain region.

In the AD brain we observed extensive changes in the protein levels of the secreted sCp and on astrocyte membrane bound GPI-Cp[82, 83]. In our study both isoforms of Cp were present in frontal and temporal cortex where we observed that their levels changed in a non-consistent way between the two AD subtypes. Studies have shown that sCp levels are lower in the brain, compared to GPI-Cp [82, 83], (which can also be seen from our analysis) and sCp is mainly located in the CSF. Our study has shown that sCp levels were generally decreased only in frontal cortex of the EOAD and LOAD brains compared to their respective age matched controls with the change being significant only in the LOAD brain (Figure 4.13D and H). The fact that sCp decreases by more than 20% in frontal cortex and not in temporal cortex could

indicate that there is a local regulatory mechanism of Cp degradation in the CSF or plasma which might also correlate with iron concentrations in the respective brain regions.

In order to further investigate if iron levels change between brain regions and if there is a correlation with sCp initially we compared iron levels between frontal and temporal cortex. No significant change was observed for iron levels in the different groups (non-parametric t-test, control group: p=0.315; LOAD group: p=0.6.444; EOAD group: p=0.174). Copper levels also did not present any significant change between these two brain regions in the different study groups (Figure 4.14 and supplementary data appendix A.2). The expression levels of sCp were then correlated with iron levels where a non-significant positive trend was observed in the frontal and temporal cortex of the both AD subtypes (LOAD frontal cortex: r_s=0.083, p=0.795, n=12; LOAD temporal cortex: r_s=0.269, p=0.539, n=8; EOAD frontal cortex: r_s=0.406, p=0.190, n=12; EOAD temporal cortex: r_s=0.239, p=0.354, n=12). These results indicate that there is a correlation between sCp and iron levels which seems to approach significance in temporal cortex. The failure to reach significance it might be due to the small sample number.

The expression levels of GPI-Cp in the two AD subtypes appear more complicated. In the EOAD brain we showed that GPI-Cp levels increased in both frontal and temporal cortex which matches with the increased astrocytosis in these two brain region and which is generally higher compared to LOAD (Figure 4.13C and G)[(379)]. However, the decreased GPI-Cp levels in LOAD cortex and especially in frontal cortex can possibly be explained more by less astrocytosis in the LOAD brain rather than change in iron homeostasis since no significant change in iron concentration was observed.

The current study appears to be the first to identify the protein levels of Ctr1, Atox1 and ATP7a in the AD brain, however, previous studies have determined Cp levels. In the first study Connor *et al.* used Western blot in order to measure Cp levels in temporal cortex and reported a 35% decrease by using cases consisting of both EOAD and LOAD. In the second, Loeffler *et al.* used ELISA in order to determine Cp levels in different LOAD brain regions and showed increased levels in frontal and temporal cortex and cerebellum however in the same study they also reported increased copper levels in frontal cortex which is in contrast to our observations[(344)]. These studies present quite contradictory results which could be either due to the different type of assay that they used to determine Cp levels or even the cohort of samples. Both of the above mentioned studies fail to identify the two different isoform of Cp in the brain and based on our results these isoforms change in a different way in the AD brain.

4.4.5 Differences in regional brain copper, COX/CS and SOD activity in AD

One of the most common pathological characteristic in AD brain is the differences in atrophy, neuronal/synaptic loss, amyloid burden and neuroinflammation amongst different brain regions. Temporal cortex is the most severely affected area in AD with perhaps slightly reduced pathology in frontal cortex and a generally limited pathology in cerebellum[362]. These gradients in the severity can be seen in the copper levels amongst the brain regions in the EOAD and LOAD brain where in the most affected, frontal and temporal cortex, copper levels were significantly lower compared to cerebellum where normally there is no pathology. The difference between frontal and temporal cortex whilst not significant, showed that the most severely affected temporal cortex had lower copper (Figure 4.14A and B).

COX/CS activity follow a different pattern where the most affected brain regions, frontal and temporal cortex, had higher levels compared to cerebellum. As mentioned previously, frontal and temporal cortex shows a higher neuronal and mitochondrial loss, so the increased activity under these conditions suggests an attempt of the remaining mitochondria to fulfil the energy demand of the brain. This trend is observed in both EOAD and LOAD brains with the only exception being in the LOAD temporal cortex where COX/CS was higher relative to cerebellum although the change was not statistically significant, possible due to the variability (higher standard deviation) of the samples. In EOAD and LOAD cortex there was no difference in the activity between both regions and both exhibited similar mitochondrial loss based on the CS activity (Figure 4.14C and D).

SOD activity in AD brain showed some variability. In the LOAD brain SOD activity levels do not significantly vary amongst brain regions however its levels were higher in temporal cortex possibly due to higher oxidative stress in that region. In the EOAD brain, SOD activity was higher in temporal cortex and cerebellum compared to frontal cortex (Figure 4.14E and F). The increased SOD activity in EOAD temporal cortex was perhaps expected due to the higher oxidative stress in that brain region relative to the rest. The increased SOD activity in the EOAD cerebellum can be attributed either to the higher copper levels which can trigger the ROS production in the presence of Aβ or due to the different cell types in cerebellum which could produce more ROS and further require more active SOD in order to eliminate ROS.

To summarise, our results confirm that regional changes in the AD brain pathology can affect copper molecules and pathways. Changes in copper levels, SOD and COX/CS activity are highly correlated with the atrophy and neuronal loss as well as to the energy demand and the

by-products occurring during the evolution of the disease (e.g. ROS production) in the specific brain regions.

4.5 Conclusions

The main finding from this chapter is that in LOAD and EOAD brains we observed decrease copper levels relative to age matched controls, however the lower levels of copper did not seem to have any impact in the activity or protein levels of important for the neuronal enzymes, COX and SOD1. The identified changes in the AD brain for COX mainly occur due to mitochondrial loss and the efforts of the remaining mitochondria to compensate for the neuronal loss and fulfil the energy demands of the diseased brain. Similarly, the increased SOD activity correlates more with the higher oxidative stress observed in the AD brain since more ROS may be produced from the deposition of amyloid-beta, the increased mitochondrial oxidative phosphorylation and also the astrocytosis found in the AD brain. Generally no major differences were observed between the EOAD and LOAD brains for copper levels, COX/CS and SOD activity which suggests that the small variations are possibly due to either pathological changes or the impact of the normal ageing process as discussed in chapter 3.

In order to get a full picture of how copper homeostasis pathways are implicated with AD we need to study its effects in BACE1 protein and activity levels. Then we will be able to draw conclusion of how and if CCS protein levels or copper availability affects BACE1 function. Also, identifying the effects of copper deficiency on one of the enzymes that belong to the secretory copper pathway such as PAM or lysil oxidase might give better indication of how the available copper is prioritized inside the neurons/brain. Extending the present study into other affected brain regions such as hippocampus or parietal and occipital cortex could further enhance our understanding about how copper homeostasis is implicated with AD pathogenesis.

The strategy of using copper chelators as way of treating AD might not be the best way forward since our results showed a copper deficient brain where the copper dependent enzymes still function in response to other factors. Taking into consideration that clinical trials with copper chelators fail to have any beneficial effect in the AD patients a reconsideration of this approach may provide better results (see sections 1.6.1). Combining our results from the healthy ageing brain and the AD brain, we can conclude that a strategy of increased copper consumption may be beneficial in both the elderly and AD patients.

The best approach of treating AD and ageing generally might be the consumption of products with high copper (beef liver, seafood and goat cheese etc.) or even vitamin copper containing supplements from early in life. Copper supplementation maybe more beneficial in early stage of human life or in the early stages of the AD pathogenesis since based on Kessler *et al.* study a significant decrease of $A\beta_{42}$ in the CSF of AD patients was observed when copper was used to treat AD patients[274, 275]. Decreased levels of $A\beta_{42}$ are correlated with the severity of the disease and as Kessler *et al.* study showed that by supplemented copper in cases were amyloid plaques are already present it will not improved the progress of the disease. That suggests that copper needs to be supplemented way before symptoms of AD or ageing start to appear.

By using the copper supplementation approach a few variables need to be taken into consideration such as delivery into the brain, copper induce toxicity to other organs and interaction with other metal pathways. Initially, it is of major significance that supplemented copper should target mainly the brain in order to avoid copper overload in peripheral tissues, which could cause toxicity. Now days the majority of the drugs/compounds can be modified in order to be able to cross the BBB or even target specific organs only. The dose of supplemented copper should be non-toxic in order to avoid intoxication of other organs or enzymes/proteins. One of the mechanisms of copper toxicity is occurring due its ability to replace iron from the iron-sulfur clusters[22]. A number of important for the cell survival enzymes require iron for their function (Complex I of the ETC) whereas other enzymes require both of these metals for their function (COX, Cp). For that reason the levels of the supplemented copper needs to be properly regulated in order to avoid malfunction of other iron-dependent enzymes and to avoid the release of free iron in the cells which can generated more reactive superoxide anions. Finally, the copper supplementation approach should be considered at the early stages of the AD pathogenesis, before the accumulation of copper in amyloid plaques, since the supplemented copper could potentially increase formation of aggregates.

5 Manipulation of copper levels in HEK293 cells and the effect on copper the homeostasis pathways

5.1 Introduction

The essential role of copper in biological systems is well established. However, copper can be toxic if its levels are not properly regulated since imbalance in copper levels can cause serious health problems including neurodegenerative symptoms[255], cardiovascular structural and functional defects[380] and deregulation of inflammatory response[381]. The effects of copper overload or deficiency are most evident in the two rare disorder Wilson's and Menkes disease.

Combined approaches are required in order to understand the diverse metabolic functions of copper in cells. Both copper supplementation and chelation strategies have been used throughout the years in order to study copper related biological functions[382]. The effects of copper supplementation or overload, as already discussed in chapter 1, is normally used to study the effects of copper on different cell lines. However, copper chelators have been proven to be useful in clinical approaches to manipulate disease conditions due to alterations in copper metabolism[383]. Three main aspects exists around the copper chelator usage: 1) understanding the molecular basis of copper and copper binding proteins in biological systems, 2) treatment of disease due to alterations of copper metabolism and 3) the diagnostic implications for copper metabolic disorders[384]. A number of copper chelating agents have been widely used in clinical and experimental studies such as EDTA, tetraethylenepentamine (TEPA), D-penicillamine (D-pen), tetrathiomolybdate (TTM), CQ, trientine and bathocuproine disulfonate (BCS). In the present study we focused on BCS, TTM and D-pen as chelating agents given their existing and potential therapeutic use and their main characteristics will be discussed in the next sections.

5.1.1 Bathocuproine disulfonate (BCS)

One of the most well-known and commonly used chelator in cell biology experiments is BCS which selectively chelates Cu^{1+} (Figure 5.1A)[385]. BCS is can bind Cu^{+2}, forcing copper into a tetrahedral geometry and inducing the reduction from Cu^{2+} to Cu^{1+}, when the reduced state of copper has been achieved, the complex is stabilized and cannot participate in redox cycles[385]. BCS is a sulfonated derivative of bathocupreine which gives BCS water soluble characteristics, and inhibits copper mediated toxicity by forming hydrophilic complexes with Cu^{2+}[385]. BCS has been used in experimental setting to inhibit copper dependent redox cycling mainly because: 1) BCS is charged and cannot form lipophilic complexes with copper which makes BCS/copper complexes cell membrane impermeable, and 2) since Cu^{2+} is the dominant form of copper in the extracellular environment, the use of BCS promotes the

reduction of Cu^{2+} to Cu^{1+} and the consequent stabilized BCS/copper complex which suppress the copper dependent redox cycle[385, 386]. BCS binds copper in 2:1 stoichiometry.

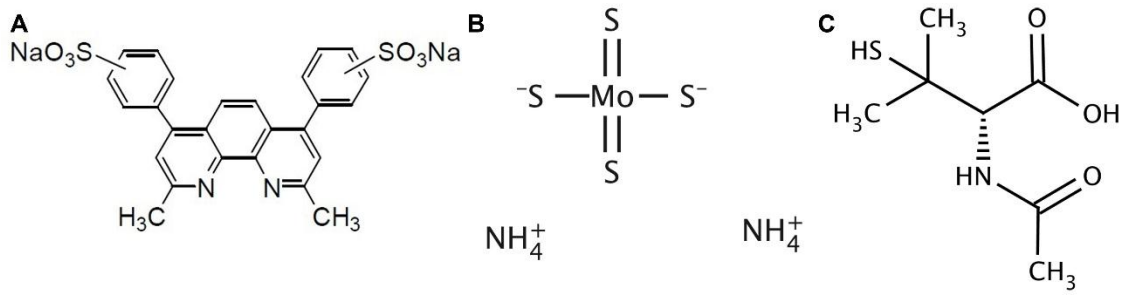

Figure 5.1 Chemical structure of the copper chelators.
(A) bathocuproine disulfonate (BCS), **(B)** tetrathiomolybdate (TTM) and **(C)** D-penicillamine (D-pen).

5.1.2 Tetrathiomolybdate (TTM)

TTM has a simple structure involving a molybdenum atom surrounded by four sulfhydryl groups (Figure 5.1B) and can be mainly found in ammonium or choline salts but the compound is quite unstable when exposed to air and moisture since oxygen can replace the sulfur within TTM. TTM chelation properties are based on the fact that it reacts with inorganic copper forming a heterobimetalic complex through the Mo-S-Cu cluster[387]. TTM is the third most commonly used medication for Wilson disease although only the Europe Medicines Agency (EMA) has approved its marketing authorization (EU/3/12/1089).

The mechanism of action of TTM is unique compared to some of the other copper chelators which depends on the route of administration. When TTM is orally administered with food, TTM forms tripartite complexes with food proteins and copper in the digestive bolus, preventing TTM/copper complexes being absorbed[388, 389]. If taken between meals, TTM will be absorbed in the blood stream where it will form tripartite complexes with albumin and serum copper, resulting in depletion of endogenous copper and making it unavailable for intracellular processes[388, 389]. This complex is so stable that is accumulated in the blood and reaches a plateau after 1 or 2 weeks of continued drug administration[390], then will slowly start degrading in the liver and the components will excreted in the bile[390]. The majority of the studies agree that TTM is able to cross the cell membrane and form complexes with intracellular copper storage proteins such as MTs[391, 392].

5.1.3 D-penicillamine (D-pen)

D-pen is an aminothiol which contains amino, thiol and carboxylate groups within the molecule (Figure 5.1C) that makes it able to chelate both Cu^{1+} and Cu^{+2}. D-pen binds Cu^{2+}

and reduces it in the process of chelation to Cu^{1+}[393]. Even if the metal binding ability of D-pen is low, it is believed that it constitutes an effective treatment for Wilson's disease. Experiments have shown that D-pen is only poorly chelates copper bound to albumin in the human serum compared to treintine or TTM[394]. D-pen has a unique feature that exhibits reductive activity through its thiolate group[395]. The hypothesized mechanism of action for D-pen supports that the reduction of the D-pen/copper complex would be accompanied by a change in conformation from preferred square planar geometry to a tetrahedral geometry which is also accompanied by charge change[395]. The above mentioned changes are less favourable for protein interaction and based on the fact that D-pen is able to reduce Cu^{2+} to Cu^{1+} and then chelate both of them simultaneously[395]. During the process of D-pen/copper complex formation H_2O_2 is produced which contributes to cytotoxicity in cells and also explain the suggested use of D-pen as a potential therapeutic agent for cancer[396, 397].

The strategy of copper chelation therapy has been studied as extensively as the investigation of copper function in the cells. Chelation is an important strategy which allows the study of how copper deficiency can affect cellular processes related to copper transport, storage and usage. A typical approach is to change the availability of copper and then observe the changes in subsequent copper dependent processes[384]. Studies with copper chelators are focused on one of the respective intracellular pathways however in the present study we tried to measure the effects of copper chelation or supplementation in all three intracellular pathways at multiple levels (copper availability, activity of copper binding enzymes and protein levels).

5.2 Aims

The aims of this chapter are to understand how copper is prioritized in a model cell line. The present study has the unique characteristic that copper levels, activities of COX and SOD as well as protein levels of the three intracellular copper pathways were determined in the same batch of cells. Also, we tested how copper supplementation, different copper chelators (BCS, TTM and D-pen) and exposure times affected the different pathways.

Furthermore, by using the Seahorse Mito Stress test we were able to identify how the different chelators affect the energy production of cells since copper is required for the function of the terminal enzyme of the mitochondrial respiratory chain, COX. Mitochondrial derived ROS and mitochondria function was further determined in cell samples since some of the studied chelators can contribute to the generation of ROS or target mitochondrial function.

5.3 Results

All the experiments have been performed in HEK293 cells and the presented results are aggregated from more than two independent experiments. The number of technical replicates will be stated in the figure legend together with the statistical test which was used for the respective analysis.

5.3.1 Toxic levels of selective copper chelators and copper supplementation as well as their effects in HEK293 cell growth

Both high and low levels of copper can cause problems to cell viability and therefore before culturing cells under excess or depleted copper conditions it was necessary to identify the concentrations which were not toxic for the HEK293 cells. Cell were cultured in the presence of $Cu(NO_3)_2$ as copper supplementation and BCS, TTM and D-pen as copper chelators. Generally, the minimum toxic dose is considered to be the concentration at which the cells still retained at least 80% of their viability in the absence of any treatment. Afterwards the selected concentration of each compound was further used to study its effects in cell growth.

In order to determine the levels of viable cells in the presence of different concentrations of $Cu(NO_3)_2$, BCS and D-pen, an Alamar Blue assay was used, and for TTM the MTT assay was used. The Alamar Blue assay monitors the reducing environment of the living cells by utilizing the ability of the non-fluorescent dye resazurin which can be reduced to the highly fluorescent resorufin. Alamar Blue acts as intermediate electron acceptor in the electron transport chain without interfering with the normal transfer of the electrons[*(398)*]. Therefore, Alamar Blue can be reduced by NADPH, FADPH, FMNH, NADH and cytochromes[*(398)*]. Utilizing these properties of Alamar Blue, we were able to identify the toxic levels of $Cu(NO_3)_2$, BCS and D-pen at three different time points, 24, 48 and 72 hours after exposure. Prior to the addition of Alamar Blue the cells were checked visually under the microscope for general viability and growth levels.

5.3.1.1 Toxicity of $Cu(NO_3)_2$ and its effects in HEK293 cell growth

Initially we determined the toxic levels of $Cu(NO_3)_2$ by using a range of concentrations from 1 to 120 µM, and the results were analysed with two-way ANOVA for variances followed by Bonferroni post-test. The statistical analysis revealed that both time and different concentrations (two-way ANOVA, $p<0.001$) have an effect on cell viability and that when copper levels increased by more than 10 µM after 48 hours, they caused a significant change

in cell viability compared to the 72 hour treatment (two-way ANOVA, $p<0.05$). As can be seen from figure 5.2A, the concentration of copper demonstrating at least 80% cell viability was 40 µM $Cu(NO_3)_2$. The basal growth medium of the HEK293 contains around 300 nM copper based on our ICP-MS determination (data not shown) which is over 100 times less than the toxic dose. However, in order to avoid any potential toxic effects of copper, for further experiments 10 µM $Cu(NO_3)_2$ was used.

During the experimental procedures with different chelators a change in the colour of the medium was noticed. The normal pink colour of the medium was turned yellow after 72 hours incubation with TTM and BCS indicating a possible metabolic shift from oxidative phosphorylation to glycolysis for energy production. To further identify the effects of this change, cell growth curves were performed where cell number, pH of the spent cell medium and viability were measured for 5 continuous days for all of the chelators and $Cu(NO_3)_2$. The results from each variable were analysed with two-way ANOVA followed by Bonferroni post-test in order to identify differences with variables of time and treatments.

Figure 5.2B-D presents the effects of 10 µM $Cu(NO_3)_2$ in cell number, pH of the growth medium and viability as determined by the Alamar Blue assay. We observed that 10 µM $Cu(NO_3)_2$ has no significant effect in cell growth rate since no change was observed between treated and control cell (two-way ANOVA, $p>0.05$), however the statistical analysis revealed that time has a significant effect on the cell number which resembled normal cell growth (two-way ANOVA, $p<0.001$, Figure 5.2B). Also, from all growth experiments we were able to determine the doubling time for the HEK293 as ~36 hours. No significant change in the medium pH in the copper treated cells was observed compared to untreated cells (two-way ANOVA, $p>0.05$) though a significant decline with time was observed (two-way ANOVA, $p<0.001$) since the pH of the medium normally decreased overtime because cells have utilized the majority of the important nutrients for their growth and survival (Figure 5.2C). Cell viability was measure at 30 min and 1 hour after the addition of the dye and the analysis revealed that there was a significant increase in fluorescence absorbance of the Alamar Blue with time in both time points (two-way ANOVA, $p<0.001$) and that at Day 5 the copper treated cells exhibited a significantly higher absorbance compared to the controls (two-way ANOVA, $p<0.05$) possibly due to the slightly higher cell number in the copper treated cells at that time point (Figure 5.2D). The increase in Alamar Blue absorbance during time in the control cells signified an increased cell number.

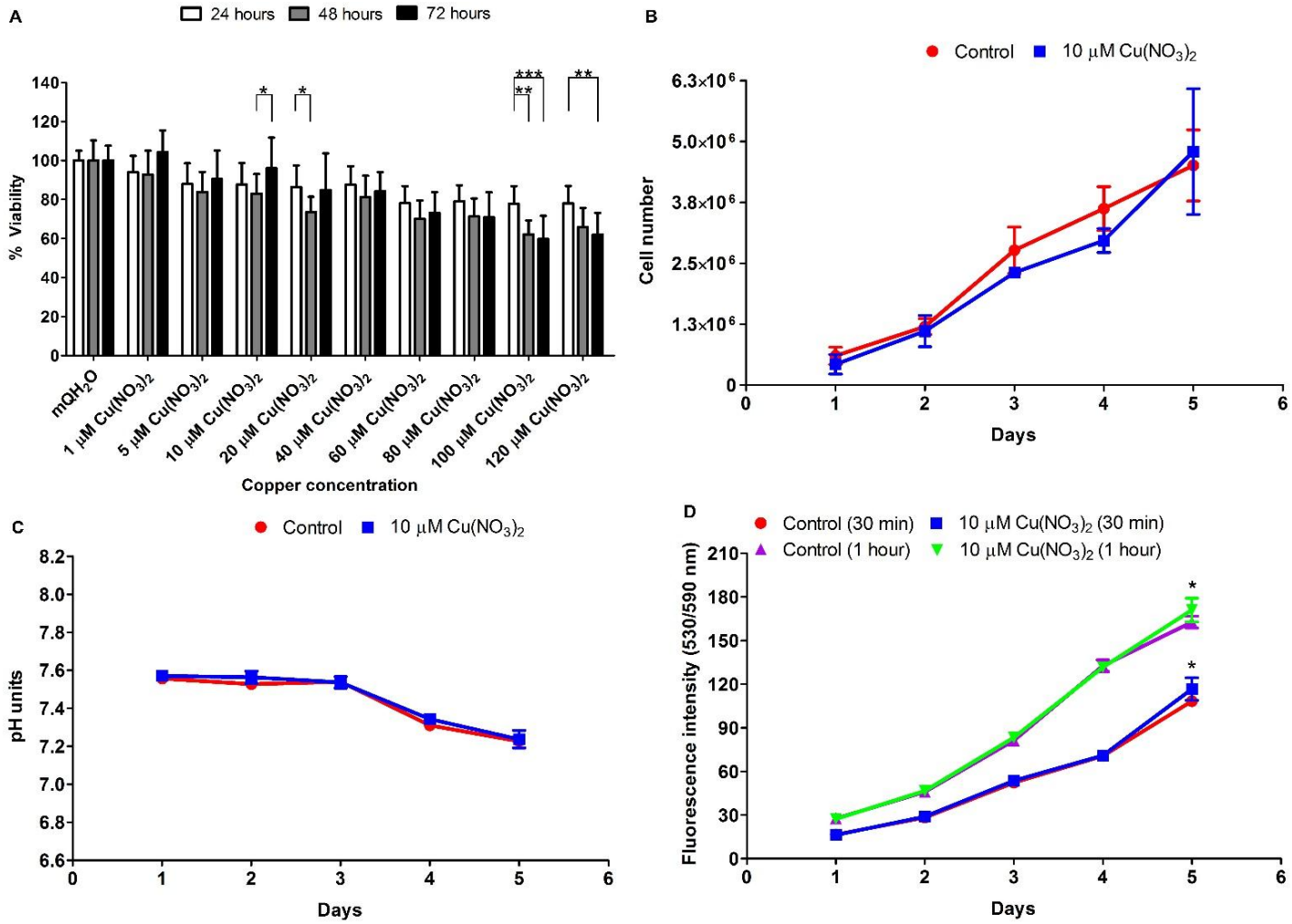

Figure 5.2 Toxicity and Growth Curve of Copper on HEK293 cells.

(A) Alamar Blue assay was used for the determination of copper toxicity (n=3). Effects of 10 µM $Cu(NO_3)_2$ on **(B)** cell number, **(C)** medium pH and **(D)** viability by Alamar Blue were measured for 5 continuous days (n=1). The growth curve for copper supplementation in cells has been repeated by more than 3 times however the presented results are from one experiment which contained all the studied variables. A repetition was not necessary since there was no significant effect. Data were analysed with two-way ANOVA followed by Bonferroni post-test and *, $p<0.05$; **, $p<0.01$; ***, $p<0.001$.

5.3.1.2 Toxicity of BCS and its effect in HEK293 cell growth

To determine toxic levels of the copper chelator BCS, a range of concentrations from 50 µM to 1.2 mM were used. The statistical analysis revealed that after 48 hours, concentrations above 400 µM BCS caused a significant decrease in cell viability (two-way ANOVA, $p<0.01$ between 48 hours and 72 hours as well as $p<0.05$ between 24 hours and 72 hours; Figure 5.3A). However, 80% of the cells were still viable when BCS reach the 1 mM (two-way ANOVA, $p<0.001$ after 72 hours). The concentration that was selected for further use was 200 µM BCS since there was no significant change in cell viability (two-way ANOVA, $p>0.05$), corresponding with previous studies also.

One of the compounds that induced the pH change in the cell growth medium was BCS which we further established by conducting growth curves. Figure 5.3B-D presents the results from the growth rate of cells treated with 200 µM BCS which showed that at Day 4 the BCS treated cells stopped growing and reached the plateau phase compared to controls (Figure 5.3B). The statistical analysis showed that there was a significant difference between BCS treated and control cells at Day 4 and Day 5 (two-way ANOVA, $p<0.001$) where the untreated cells had double the cell number relative to BCS treated cultures.

The 200 µM BCS also caused a significant decrease in the medium pH from Day 3 where we initially detected a significant decrease of 0.2 pH units which by Day 5 of treatment was more than 0.5 pH units change (two-way ANOVA, $p<0.001$; Figure 5.3C). In relation to cell viability of the BCS treated cells, an increase in Alamar Blue fluorescence from Day 3 was seen in both 30 min and 1 hour of incubation which continued until Day 5 (Figure 5.3D). The statistical analysis showed that the increase in the fluorescence was significant only from Day 3 to Day 5 (two-way ANOVA, $p<0.001$). At Day 5 after 1 hour incubation with Alamar Blue the change in the fluorescence absorbance was not as significantly different as compared to 30 min incubation or previous time points which suggests that the treated cells had metabolized the majority of the substrate (two-way ANOVA, $p<0.05$).

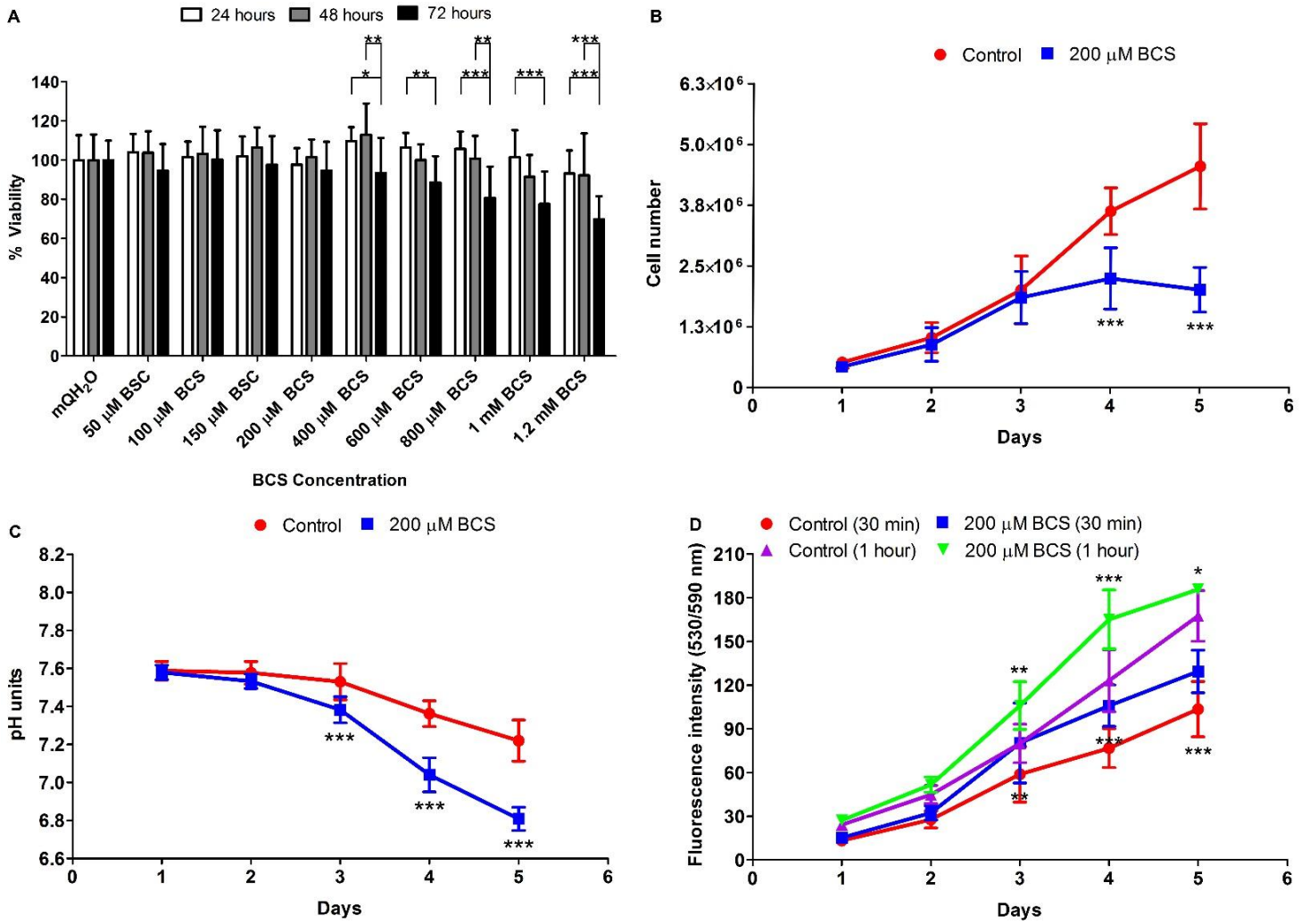

Figure 5.3 Toxicity and Growth Curve of BCS on HEK293 cells.

(A) Alamar Blue assay was used for the determination of BCS toxicity (n=3). The effects of 200 µM BCS on the **(B)** cell number, **(C)** pH of the cell medium and **(D)** viability by Alamar Blue were measured for 5 continuous days (n=3). Data were analysed with two-way ANOVA followed by Bonferroni post-test and *, $p<0.05$; **, $p<0.01$; ***, $p<0.001$

5.3.1.3 Toxicity of TTM and its effects in HEK293 cell growth

For the determination of TTM toxicity we were not able to use Alamar Blue since there was a positive correlation between TTM concentrations and measured fluorescence absorbance since during the visual inspection of the plate we showed that cells treated with the highest TTM concentrations were dead whereas the assay indicated that they were still viable. The above observation indicated that TTM has some sort of auto-fluorescence property and in order to eliminate it different approaches were tested. Initially, we modified the Alamar Blue protocol by replacing the spent medium, which contained the TTM, with fresh medium containing Alamar Blue or washing the cells with PBS before adding Alamar Blue. These approaches improved to a small degree the final results however there was still background coming from TTM (data not shown).

In order to accurately measure TTM toxicity we used the MTT viability assay. The assay relies on the reductive colouring reagent (tetrazolium salt) and the mitochondrial dehydrogenase activities to determine the cell viability with a colorimetric method. In viable cells MTT is mainly reduced by the NADH, FADH, FMNH and NADH to an insoluble formazan[(399)]. For the determination of TTM toxicity a range of 1 to 333 μM concentrations was used. After 24 hours of treatment an increase in viability was observed for the majority of the tested concentrations however at 48 hours a significant decrease occurred which was further enhanced at 72 hours (Figure 4.4A). The lowest toxic concentration for TTM was estimated to be around 6 μM and therefore we used 2 μM TTM since more than 90% of the cells were still viable and a significant change was due to increased viability at 24 hours compared to the other two time points (two-way ANOVA, $p<0.001$ between 24 and 48 hours/ $p<0.05$ between 24 and 72 hours).

Cell growth curves were conducted with 2 μM TTM and figure 5.4B presents the effects of TTM on cell number where an inhibition of the growth rate in the treated cells from Day 3 was seen which progressed to approximately three times fewer cells by Day 5. The statistical analysis revealed that the decrease in cell number in the TTM treated cells was significant only from Day 3 to Day 5 (two-way ANOVA, $p<0.01$ at Day 1 and $p<0.001$ for Day 4 and 5). The TTM treated cells presented similar pH change to the BCS treated cells where at Day 3 a decrease of 0.2 pH units was identified although the change was not significant (two-way ANOVA, $p>0.05$). At Day 4 and 5 the decrease was more than 0.5 pH units, and statistically significant (two-way ANOVA, $p<0.001$; Figure 5.4C). The effects on viability determined by the MTT assay showed a gradual decrease in absorbance from Day 2, in the treated cells,

although the change was significant only at Day 4 and 5 compared to untreated cells (two-way ANOVA, $p<0.001$, Figure 5.4D).

5.3.1.4 Toxicity of D-pen and its effects on HEK293 cell growth

In order to determine the toxic levels of D-pen in HEK293 cells we performed Alamar Blue assays. Initially a range of 1 to 400 µM of D-pen was tested which did not show any major change in the viability (data not shown). Then a range of 250 to 650 µM of D-pen was further examined however the results were variable for each repetition and it was not able to accurately determine the toxic dose for D-pen. The aggregated data from 3 independent experiments are presented at Figure 5.5A were no significant change was observed for any of the tested concentrations of D-pen, however, the two-way ANOVA identified a small difference amongst the different concentration which indicates that different concentration of D-pen had a small impact on cell viability ($p=0.039$). The selection of the D-pen concentration for further experiments was based on the Alamar Blue assays and an MTT assay after 72 hours of treatment (data not shown) where concentrations above 400 µM D-pen showed less than 80% viability. Based on the above criteria 350 µM D-pen was selected for subsequent experiments.

The effects of 350 µM D-pen on cell growth using cell number, pH of the medium, and viability were determined for 5 continuous days. The analysis revealed that the D-pen treated cells did not show any significant change in the cell number (two-way ANOVA, $p>0.05$; Figure 5.5B) or pH (two-way ANOVA, $p>0.05$; Figure 5.5C) compared to untreated cells. However, a small but significant increase in viability by using Alamar Blue assay was identified at Day 4 and 5 after 1 hour incubation with the substrate (two-way ANOVA, $p<0.01$; Figure 5.5D).

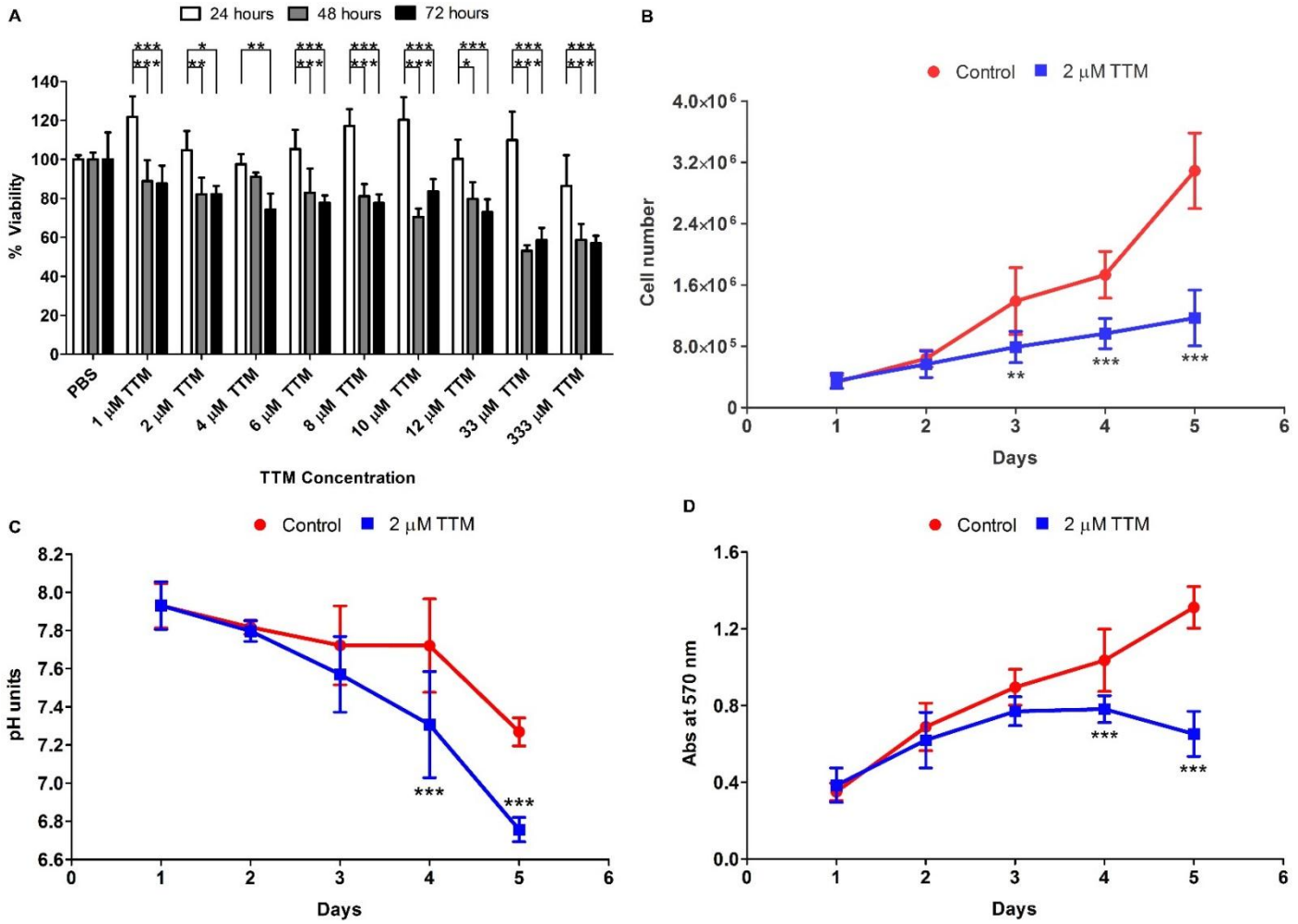

Figure 5.4 Toxicity and Growth Curve of TTM on HEK293 cells.

(A) MTT assay was used for the determination of TTM toxicity (n=1). The presented results are representative of only one experiment in that range of concentrations. The effects of 2 μM TTM on the **(B)** cell number, **(C)** pH of the cell growth medium and **(D)** viability by MTT assay were measured for 5 continuous days (n=2). Data were analysed with two-way ANOVA followed by Bonferroni post-test and *, $p<0.05$; **, $p<0.01$; ***, $p<0.001$.

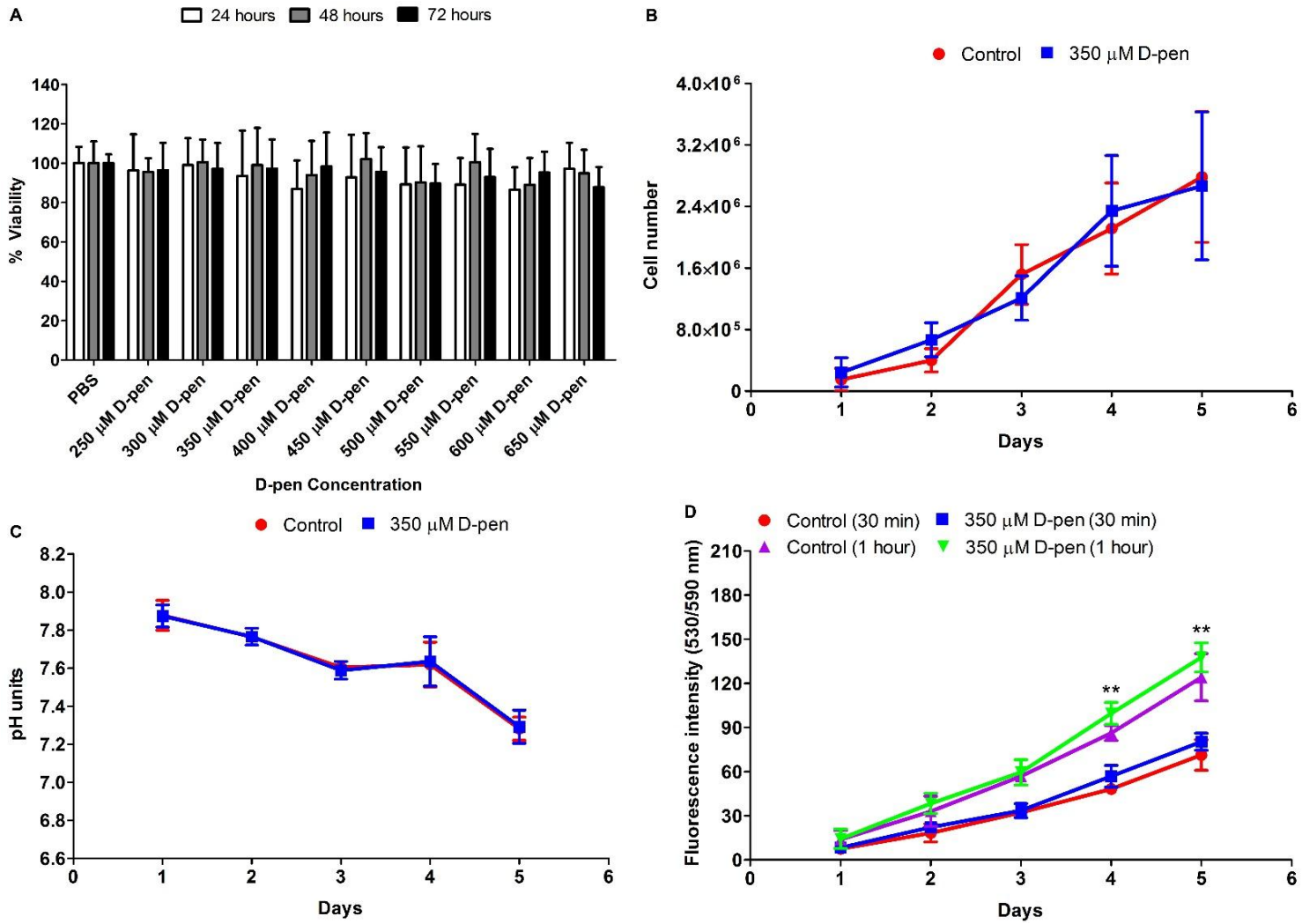

Figure 5.5 Toxicity and Growth Curve of D-pen on HEK293 cells.

(A) Alamar Blue assay was used for the determination of D-pen toxicity (n=3). The effects of the 350 µM D-pen on the **(B)** cell number, **(C)** pH of the cell growth medium and **(D)** viability by Alamar Blue assay were determined for 5 continuous days (n=2). Data were analysed with two-way ANOVA followed by Bonferroni post-test and *, $p<0.05$; **, $p<0.01$; ***, $p<0.001$.

5.3.2 Effects of copper supplementation and chelation in cellular copper levels

In the next stage we wanted to determine the effects of copper supplementation and chelation on the cellular copper levels and on the three intracellular copper pathways during a set time period. All the cell experiments were performed in T175 cm^2 flasks in order to be able to obtain enough cell/protein to conduct all the desired experiments. After treatment cells were harvested at Day 1, 2 and 3, however in the first two time points the cell quantity was not enough in order to conduct both metal analysis by ICP-MS and activity/protein analyses. For that reason we were able to measure the intracellular copper levels only at Day 3.

Figure 5.6 presents the intracellular copper levels expressed two different ways as either copper atoms per cell or as nmoles of copper per mg of total protein. Copper levels in the spent medium are presented too. The results are aggregates from three independent experiments and each treatment is presented compared to its respective experimental controls. In order to identify statistical differences between controls and treated cells as well as amongst different treatments, one-way ANOVA analysis was conducted followed by Tukey post-test. The only exception was cell treated with 10 μM $Cu(NO_3)_2$/copper where a non-parametric t-test (Mann-Whitney) had to be conducted in order to compare its levels with the respective control cells since the copper treated samples failed to past an F-test for variances. Any comparison amongst the other treatments and the copper treated cells was not possible since the statistical test could not detect any difference due to the large standard deviation in the copper treated cells which was masking any specific difference.

As can been seen from figure 5.6A and B, the copper atoms/cell or nmoles/mg protein in the different experimental controls was similar which indicates the reproducibility and consistency of our experimental approach. Initially, by treating the HEK293 cells with copper we were able to demonstrate a statistically significant increase in the intracellular Cu atoms/cell and in the nmoles Cu/mg protein (nonparametric t test, $p<0.0001$). The concentration of copper in the medium of the treated cells was around 10 μM, almost 60-times more than in the medium of the untreated cells and in agreement with the initial added copper concentration (nonparametric t-test, $p<0.0001$; Figure 5.6C).

The intracellular copper levels were also determined in the presence of different copper chelators. For BCS we tested two different concentrations a 50 μM and 200 μM where both of these showed a decrease by more than 80% of the intracellular copper levels, based on the two determination methods, (one-way ANOVA, $p<0.001$; Figure 5.6A and B). The measured intracellular copper levels were lower in the BCS treated cells however the copper

concentration in the spent medium of the treated cells had higher copper levels compared to untreated cells. The medium from the 50 µM BCS treatment showed a non-significant 40% increase in copper levels (one-way ANOVA, $p>0.05$), whereas the 70% increase in copper that was observed in the medium from the 200 µM BCS treated cells was significant (one-way ANOVA, $p<0.01$). The medium from the 200 µM BCS treated cells had 20% more copper than the 50 µM BCS treated cells however, the difference was not significant (one-way ANOVA, $p>0.05$; Figure 5.6C).

Similar effects on the intracellular copper levels were observed when cells were treated with 2 µM TTM for 3 days. Both of the analyses showed that intracellular copper was significantly decreased by more than 85% (one-way ANOVA, $p<0.001$ for Cu atoms/cell and $p<0.01$ for nmoles Cu/mg protein; Figure 5.6A and B). However, the copper concentration in the spent medium in the TTM treated cells was non-significantly decreased by over 60% (one-way ANOVA, $p>0.05$; Figure 5.6C). At this point, we have to mention that even if the experiments have been repeated three times in one of the repetitions a few samples were contaminated with copper, for unknown reason, and for that reason we had to exclude the contaminated samples from the final analysis. Also, one of the medium analysis for copper levels was excluded as the ICP-MS machine was unable to detect any copper in the medium samples which may be due to the performance of the machine or that particular batch of medium.

The last copper chelator, D-pen, was tested at a concentration of 350 µM over 3 days. The ICP-M analysis for D-pen showed a small but non-significant 30% increase in intracellular copper levels when calculated as Cu atoms/cell and a small non-significant 13% increase when calculated as nmoles/mg protein (one-way ANOVA, $p>0.05$) compared to controls (Figure 5.6A and B). The copper concentration in the medium of the D-pen treated cells was reduced non-significantly by over 60% which may correlate with the slightly higher intracellular copper levels (one-way ANOVA, $p>0.05$; Figure 5.6C). The D-pen treatments were conducted and analysed at the same time as the TTM treated cells and similar problems occurred during the analysis and for that reason the same exclusion criteria should be applied. We identified differences in the intracellular copper levels amongst the tested copper chelators or concentrations. In both ways of analyzing copper levels there was no difference amongst the cell treated with 50, 200 µM BCS or 2 µM TTM (one-way ANOVA, $p>0.05$). However, the copper levels in the D-pen treated cells were significantly higher compared to the other chelators (one-way ANOVA, $p<0.001$; Figure 5.6A and B). No significant difference was observed amongst the spent medium of the treated cells (one-way ANOVA, $p>0.05$; Figure 5.6C).

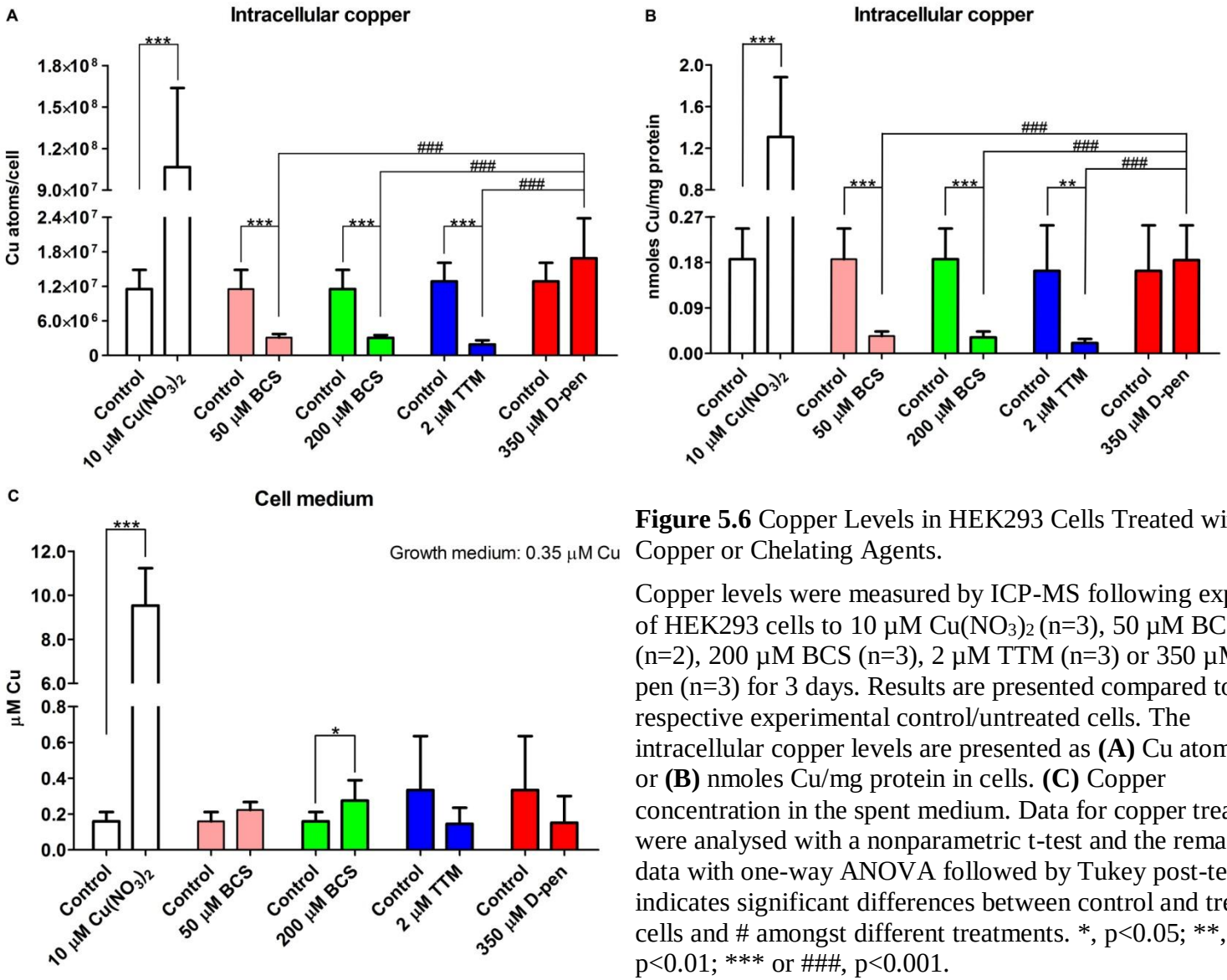

Figure 5.6 Copper Levels in HEK293 Cells Treated with Copper or Chelating Agents.

Copper levels were measured by ICP-MS following exposure of HEK293 cells to 10 µM $Cu(NO_3)_2$ (n=3), 50 µM BCS (n=2), 200 µM BCS (n=3), 2 µM TTM (n=3) or 350 µM D-pen (n=3) for 3 days. Results are presented compared to their respective experimental control/untreated cells. The intracellular copper levels are presented as **(A)** Cu atoms/cell or **(B)** nmoles Cu/mg protein in cells. **(C)** Copper concentration in the spent medium. Data for copper treatment were analysed with a nonparametric t-test and the remaining data with one-way ANOVA followed by Tukey post-test. * indicates significant differences between control and treated cells and # amongst different treatments. *, $p<0.05$; **, $p<0.01$; *** or ###, $p<0.001$.

5.3.3 Effects of copper supplementation and chelation in the mitochondrial copper pathway

Following copper or chelators exposure we analysed the cell lysates obtained from Day 1, 2 and 3 for activity levels of COX and CS as well as for the levels of mitochondrial-associated proteins. In first instance we determined the activity levels of COX and CS by using 10 µg cell extra for each assay and with all the samples representing a particular day assayed together. In the next sections we only present results from Day 1 and 3 since no major difference was observed between Day 2 and the other two time points.

5.3.3.1 Copper chelation causes significant inhibition of COX/CS activity

Figure 5.7 presents the COX/CS activity from Day 1 and 3 from the different treatments that we tested compared to their respective experimental controls. We identified significant decrease in COX/CS activity overtime only in the BCS and TTM treated cells. Supplementation with copper did not have any major effect in the COX/CS activity with activity increased non-significantly by 10% at Day 1 and 3 (one-way ANOVA, $p>0.05$). In the BCS treated cells, COX/CS activity gradually decreased overtime since at Day 1 activity was significantly reduced by 30-40% which led to further reductions by Day 3, to approximately 80%, of control values compared to untreated cells (one-way ANOVA, $p<0.001$). The two BCS concentrations (50 µM and 200 µM) showed similar activity on both days with no significant difference observed between them (one-way ANOVA, $p>0.05$; Figure 5.7A and B). Similar effects on COX/CS activity was also observed when cells were treated with 2 µM TTM. At Day 1 in the TTM treated cells, COX/CS activity was significantly reduced by 48% and by Day 3 the decrease reached over 80% of control activity (one-way ANOVA, $p<0.001$). Treatment of cells with 350 µM D-pen did not show any significant impact on the COX/CS activity either at Day 1 or 3 (one-way ANOVA, $p>0.05$).

We also compared the COX/CS activity amongst the different treatments where we identified that the activity of the D-pen treated cells was significantly higher compared to BCS and TTM treated cells on both days (one-way ANOVA $p<0.001$; Figure 5.7A and B). The copper treated cells showed significantly higher activity only compared to BCS and TTM treated cells but not to D-pen only at Day 3 (one-way ANOVA, $p>0.05$ at Day 1 and $p<0.001$ at Day 3, data not shown).

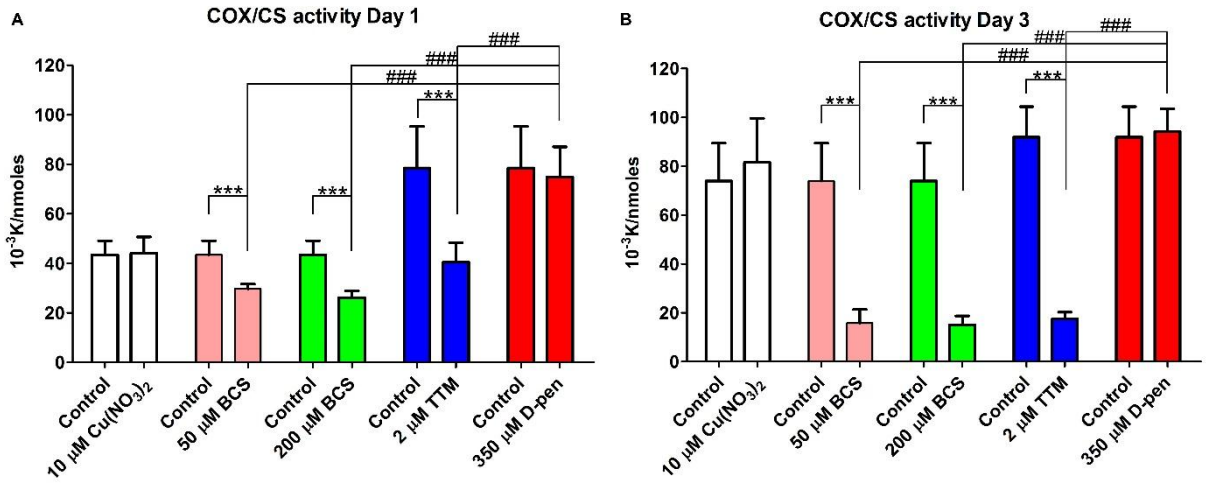

Figure 5.7 COX/CS Activity in HEK293 cells Treated with Copper or Chelating Agents. HEK293 cells were treated with 10 μM $Cu(NO_3)_2$ (n=3), 50 μM BCS (n=2), 200 μM BCS (n=3), 2 μM TTM (n=3) or 350 μM D-pen (n=3) for 1 or 3 days. The final COX/CS activity from **(A)** Day 1 and **(B)** Day 3 is presented compared to respective experimental controls for each treatment. Data were analysed with one-way ANOVA followed by Tukey post-test. * indicates significant differences between control and treated cells and # amongst different treatments. *** or ###, $p<0.001$.

In an attempt to identify the lowest BCS and TTM concentration that had the lowest impact in COX/CS, we treated cells with 0.5 and 5 μM BCS and 0.5 μM TTM and measured the activity at Day 3. We found that 0.5 μM BCS did not show any significant change in COX/CS activity (one-way ANOVA, $p>0.05$) and 5 μM BCS only reduced by COX/CS activity by 40% (one-way ANOVA, $p<0.001$). The 0.5 μM TTM had a similar effect to the 2 μM treatment since the COX/CS activity was significantly reduced to 80% of control (one-way ANOVA, $p<0.001$, supplementary data Figure B.4A).

5.3.3.2 Changes in mitochondrial copper containing proteins after copper supplementation or chelation

In order to further understand how copper supplementation and chelation effect both COX and mitochondrial function we measured the protein levels of COX1 and COX2 and the levels of mitochondria via VDAC1. We further decided to analyze Complex I protein levels since several studies have shown that COX interacts and forms supercomplexes with Complex I[(400)] and so we determined the levels NDUFS1 and NDUFV1. Western blot analysis was performed on two different data sets, the first one which contained control, 50 μM BCS, 200 μM BCS and 10 μM $Cu(NO_3)_2$/copper treated HEK293 cells and the second one with control, 2 μM TTM and 350 μM D-pen from Day 1 and Day 3, respectively. The separation was based on the way that the initial experiments were conducted. Since the two sets of treatments were run on different gels, we were only able to compare with one-way ANOVA followed by

Tukey post-test treatments that were run on the same gel. The results from the Western blot analysis are presented as percentage change of the control/untreated cells and aggregates from two independent experiments are shown. The third experimental replicate was not analysed since no major difference was noticed between the first two analysed experiments.

The protein levels of COX1 and VDAC1 were measured from Day 1 and Day 3 in the copper/BCS (Figure 5.8A) and TTM/D-pen (Figure 5.8B) treated cells. The densitometric analysis showed that at Day 1 total COX1 protein levels did not change in the presence of any of the treatments (one-way ANOVA, $p>0.05$; Figure 5.8C) compared to control cells. At Day 3 COX1 protein levels were significantly increased by 31% in the presence of copper (one-way ANOVA, $p<0.05$) whereas a non-significant 22% and 15% decrease was observed in cells treated with 50 and 200 µM BCS, respectively (one-way ANOVA, $p>0.05$). COX1 protein levels, at Day 3, were significantly decreased by 21% in cells treated with 2 µM TTM (one-way ANOVA, $p<0.01$), whereas 350 µM D-pen did not show any significant effect (one-way ANOVA, $p>0.05$; Figure 5.8D). The statistical analysis also showed that in the copper treated cells at Day 3, COX1 protein levels were significantly higher compared to 50 and 200 µM BCS (one-way ANOVA, $p<0.001$). Similarly, the D-pen treated cells had higher COX1 protein levels relative to the TTM treated cells (one-way ANOVA, $p<0.001$; Figure 5.8D) whereas at Day 1 no significant change was observed amongst the different treatments (one-way ANOVA, $p>0.05$, Figure 5.8C).

Mitochondria levels, based on VDAC1 protein levels, did not seem to show any significant change under the majority of the treatments. At Day 1 no change in VDAC1 protein levels was observed in any of the treatments relative to the untreated cells (one-way ANOVA, $p>0.05$; Figure 5.8E). However, at Day 3 in the D-pen treated cells, VDAC1 protein levels were significantly increased by 12% relative to control cells (one-way ANOVA, $p<0.05$; Figure 5.8F). No other significant change in VDAC1 levels amongst cells treated with copper, BCS or TTM and their respective controls was observed. Next, changes amongst the different treatments were examined at Day 1 and a significant increase in VDAC1 protein levels was observed in cells treated with D-pen compared to TTM (one-way ANOVA, $p<0.01$) whereas at Day 3 there was a significant increase in VDAC1 protein levels in copper treated cells compared to cells treated with 50 µM BCS (one-way ANOVA, $p<0.01$; Figure 5.8E and F).

For the COX1/VDAC1 an opposite trend was observed between the two time points for the tested conditions. At Day 1 the ratio of COX1/VDAC1 was significantly increased by 21%, 13% and 21% in cells treated with copper, 50 and 200 µM BCS, respectively, compared to

controls (one-way ANOVA, $p<0.001$ for copper treated and $p<0.01$ in the BCS treated; Figure 5.8G). In TTM and D-pen treated cells no change was observed in the COX1/VDAC1 ratio (one-way ANOVA, $p>0.05$). At Day 3 the COX1/VDAC1 ratio was significantly decreased by 19% and 25% in the 200 µM BCS and 2 µM TTM treated cells (one-way ANOVA, $p<0.05$ in the BCS and $p<0.001$ in the TTM) respectively, whereas in the copper, 50 µM BCS and D-pen treated cells no change was observed (one-way ANOVA, $p>0.05$; Figure 5.8H). We also examined if the COX1/VDAC1 ratio changed amongst treatments where at Day 1 a significant increase in cells treated with copper was seen compared to cells treated with 200 µM BCS (one-way ANOVA, $p<0.05$; Figure 5.8G). Similarly, at Day 3 the VDAC1/COX1 ratio was significantly higher in copper treated cells compared to both 50 and 200 µM BCS treated cells (one-way ANOVA, $p<0.01$). Furthermore, cells treated with 350 µM D-pen showed a higher COX1/VDAC1 ratio relative to TTM treated cells (one-way ANOVA, $p<0.001$, Figure 5.8H).

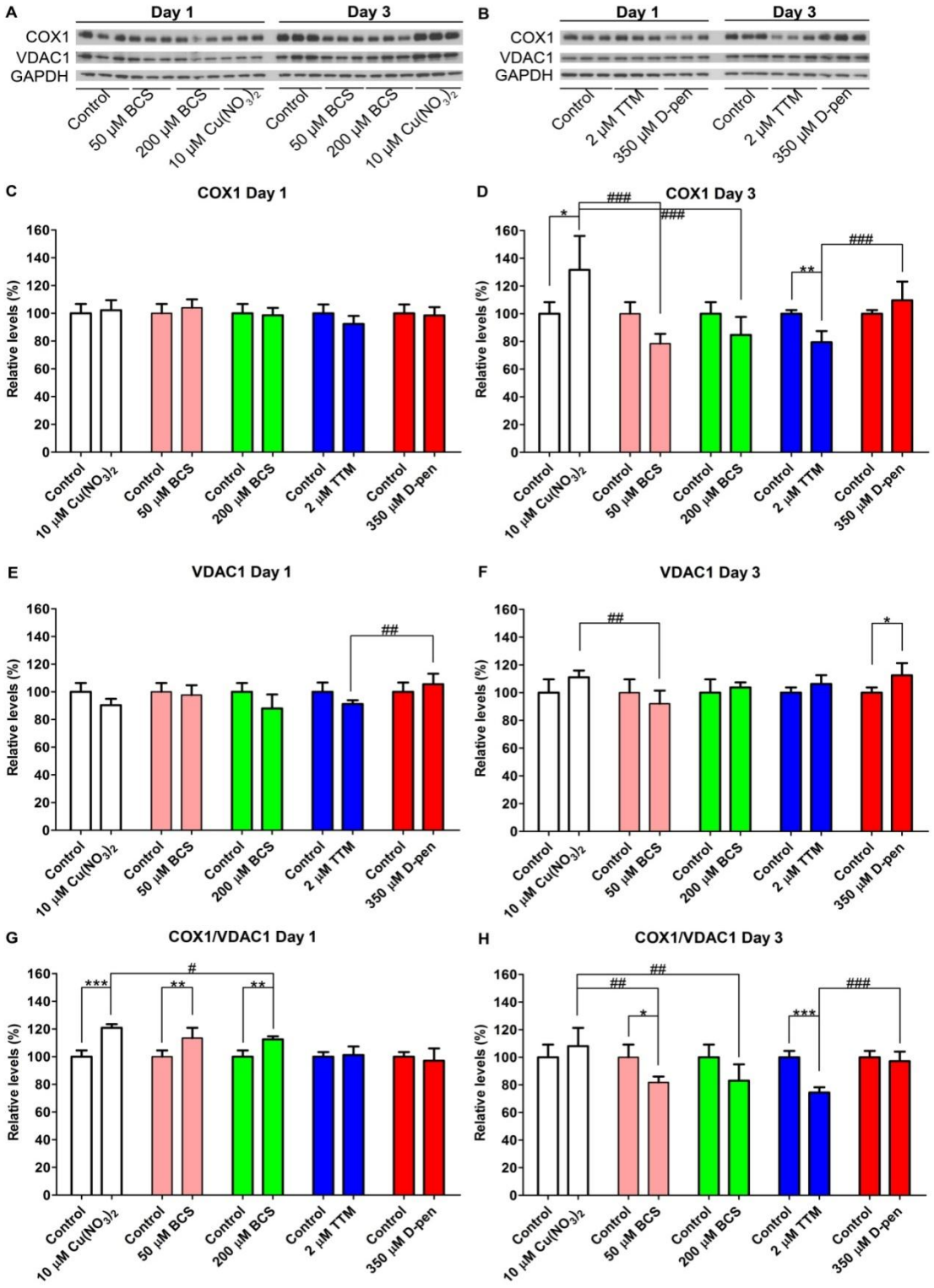

Figure 5.8 COX1 and VDAC1 Protein Levels in HEK293 Cells Treated with Copper or Chelating Agents.

HEK293 cells were treated with 10 µM $Cu(NO_3)_2$, 50 µM BCS, 200 µM BCS, 2 µM TTM and 350 µM D-pen for 1 or 3 days and proteins extracted. Representative Western blots from cells treated with **(A)** 50, 200 µM BCS or 10 µM $Cu(NO_3)_2$ (n=2) and **(B)** 2 µM TTM or 350 µM D-pen (n=2) at Day1 and 3. Densitometric analysis of COX1 and VDAC1 normalized with GAPDH at **(C, E)** Day 1 and **(D, F)** Day 3. Densitometric analysis of COX1 normalized with VDAC1 at **(G)** Day 1 and **(H)** Day 3. Data were analysed with one-way ANOVA followed by Tukey post-test. * indicates significant differences between control and treated cells and # amongst different treatments. *, $p<0.05$; ** or ##, $p<0.01$; *** or ###, $p<0.001$.

The protein levels of COX2 were also measured and representative Western blots from the copper, BCS, TTM, or D-pen treated cells are presented in figure 5.9A and B. COX2 protein levels showed a more than 65% protein loss at Day 1 in the BCS and TTM treated cells relative to their respective controls (one-way ANOVA, $p<0.001$; Figure 5.9C). At Day 3 the protein levels of COX2 disappeared completely from cells treated with 200 µM BCS and 2 µM TTM whereas in cell treated with 50 µM BCS only 12% of COX2 protein remained (one-way ANOVA, $p<0.001$; Figure 5.9D). At Day 1 the copper treated cells showed a significant 26% decrease in COX2 protein levels compared to untreated cells (one-way ANOVA, $p<0.001$) with at Day 3 presenting a non-significant increase of 11% (one-way ANOVA, $p>0.05$; Figure 5.9C and D). By comparing the protein levels of COX2 amongst different treatments we found that at Day 1 COX2 was significantly higher in the copper treated cells relative to the BCS treated (one-way ANOVA, $p<0.05$ for the 50 µM BCS and $p<0.001$ for the 200 µM BCS) and in the D-pen compared to TTM treated cells (one-way ANOVA, $p<0.01$). Similar effects were also observed at Day 3 (one-way ANOVA, $p<0.001$; Figure 5.9C and D).

The normalized levels of COX2 with VDAC1 were also examined where similar results with COX2 protein alone were obtained. At Day 1 the ratio of COX2/VDAC1 was significantly decreased by 33%, 36% and 63% in the 50 µM BCS, 200 µM BCS and 2 µM TTM treated cells compared to their respective controls (one-way ANOVA, $p<0.001$; Figure 5.9E). A small non-significant 19% decrease in the COX2/VDAC1 ratio was observed in cells treated with 350 µM D-pen (one-way ANOVA, $p>0.05$, Figure 5.9E). At Day 3 the COX2/VDAC1 ratio was negligible in cells treated with 200 µM BCS and 2 µM TTM whereas cells treated with 50 µM BCS retained 10% of the normal COX2/VDAC1 ratio (one-way ANOVA, $p<0.001$, Figure 5.9F). The COX2/VDAC1 ratio did not change in the copper or D-pen treated cells at Day 3 (one-way ANOVA, $p>0.05$; Figure 5.9F). Comparing differences in the COX2/VDAC1 ratio amongst the tested treatments showed that at both Day 1 and 3 the COX2/VDAC1 ratio was significantly higher in the copper treated cells compared to the BCS treated cells (one-way ANOVA, $p<0.001$) and also in the D-pen relative to the TTM treated cells (one-way ANOVA, $p<0.01$ at Day 1 and $p<0.001$ at Day 3; Figure 5.9E and F).

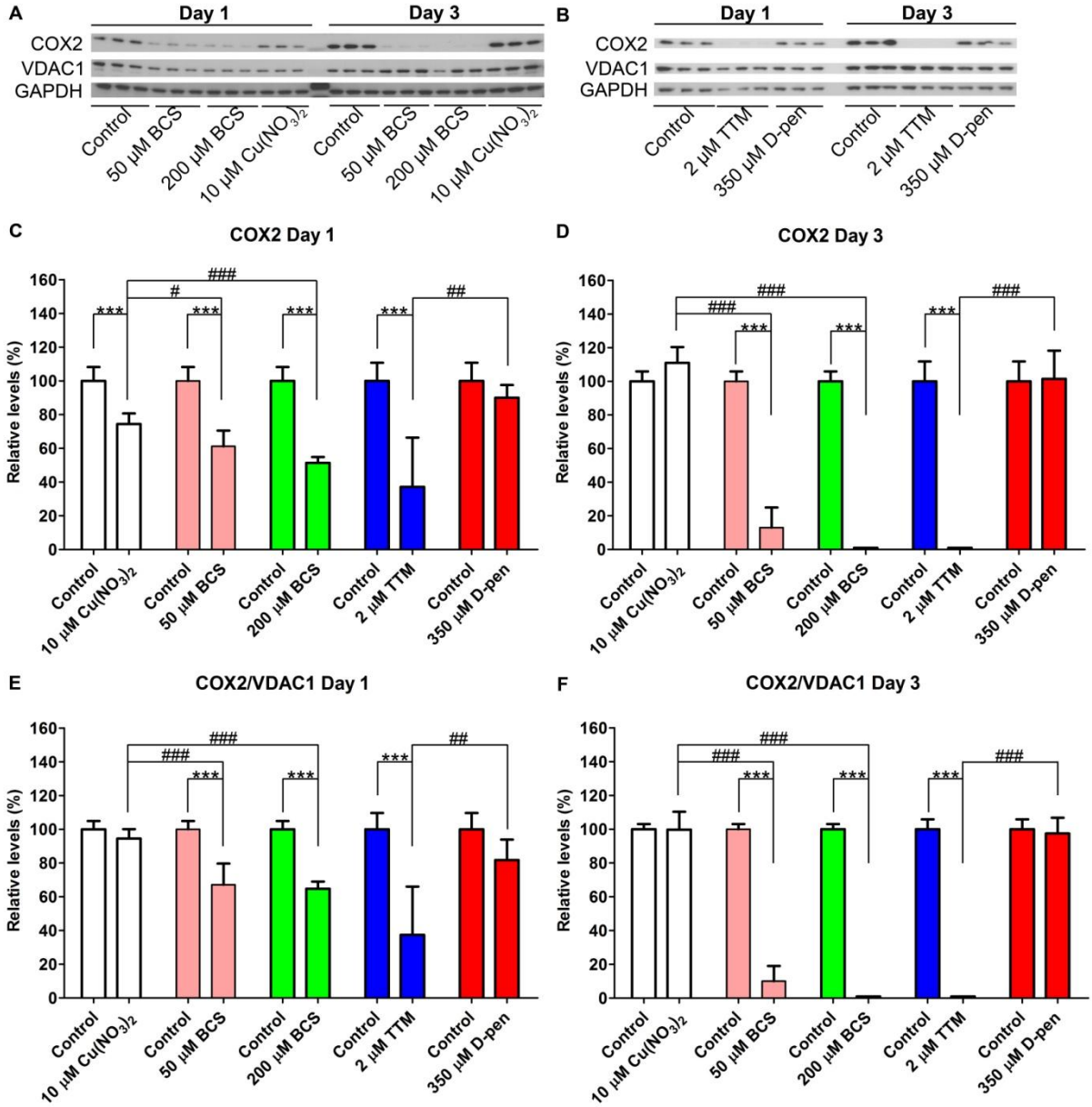

Figure 5.9 COX2 Protein Levels in HEK293 cells Treated with Copper or Chelating Agents.

HEK293 cells were treated with 10 µM $Cu(NO_3)_2$, 50 µM BCS, 200 µM BCS, 2 µM TTM and 350 µM D-pen for 1 or 3 days and proteins extracted. Representative Western blots from cells treated with **(A)** 50, 200 µM BCS or 10 µM $Cu(NO_3)_2$ (n=2) and **(B)** 2 µM TTM or 350 µM D-pen (n=2) from Day 1 and 3. Densitometric analysis of COX2 normalized with GAPDH at **(C)** Day 1 and **(D)** Day 3 as well as with VDAC1 at **(E)** Day 1 and **(F)** Day 3. Data were analysed with one-way ANOVA followed by Tukey post-test.* indicates significant differences between control and treated cells and the # amongst different treatments. #, $p<0.05$; ##, $p<0.01$; *** or ###, $p<0.00$.

Complex I is the largest enzyme of the oxidative phosphorylation system which catalyzes the oxidation of NADH and reduction of ubiquinone, utilizing the energy generated by this process to translocate protons across the mitochondrial inner membrane[401]. Complex I consists of over 44 different subunits, with seven encoded by the mitochondrial DNA and the remaining from the nucleus[401]. Complex I is organized into three functional modules, the dehydrogenase, the hydrogenase and the proton-translocation modules[401]. NDFUS1 and NDUFV1 are nuclear encoded subunits which form the dehydrogenase module with NDUFS1 being the largest protein of the complex (75 kDa) and a component of the four iron-sulfur clusters of the enzyme[401]. It may also form part of the active site where NADH is oxidized. NDUFV1 is 51 kDa protein that carries the NADH-binding site as well as flavin mononucleotide (FMN) and an iron-sulfur binding site[401].

Initially, we determined the protein levels of NDUFV1 in copper/BCS (Figure 5.10A) and the TTM/D-pen (Figure 5.10B) treated groups of the cells from Day 1 and 3 where only small changes were observed between treated and control cells. At Day 1 NDUFV1 protein levels were significantly decreased by 22% and 19% in cells treated with copper (one-way ANOVA, $p<0.01$) and 200 µM BCS (one-way ANOVA, $p<0.05$), respectively, however no significant change was present in the other treatments compared to their respective controls (one-way ANOVA, $p>0.05$; Figure 5.10C). At Day 3 NDUFV1 protein levels were higher by 17%, 27% and 12% in the copper, 200 µM BCS and 350 µM D-pen treated cells, respectively, but the changes were not significant (one-way ANOVA, $p>0.05$; Figure 5.10D). The rest treatments did not show any significant difference relative to their control cells. When we examine if NDUFV1 protein changed compared to different treatments no significant change was present at Day 1 or 3 (one-way ANOVA, $p>0.05$; Figure 5.10C and D).

As a mitochondrial protein and also a major subunit of Complex I, NDUFV1 protein levels were normalized to VDAC1. The NDUFV1/VDAC1 ratio was significantly decreased by 10% and 20% in cells treated with 2 µM TTM (one-way ANOVA, $p<0.05$) and 350 µM D-pen (one-way ANOVA, $p<0.001$), respectively, at Day 1. A non-significant 13% decrease was identified in cells treated with copper although no other significant changes were seen for any other treatment (one-way ANOVA, $p>0.05$; Figure 5.10E). At Day 3 a non-significant increase of 15% and 21% in the NDUFV1/VDAC1 ratio was observed in cells treated with 50 or 200 µM BCS (one-way ANOVA, $p>0.05$), respectively. A 10% increase was also observed in the D-pen treated cells though the change was not significant (one-way ANOVA, $p>0.05$; Figure 5.10F). By comparing the NDUFV1/VDAC1 ratio amongst different treatments we identified a significant change between the TTM and D-pen treated cells at Day 1, with the

TTM treated cells presenting higher NDUFV1/VDAC1 ratio (one-way ANOVA, $p<0.05$; Figure 5.10E). No significant change was observed amongst the other treatments at Day 1 or 3 (one-way ANOVA, $p>0.05$; Figure 5.10E and F).

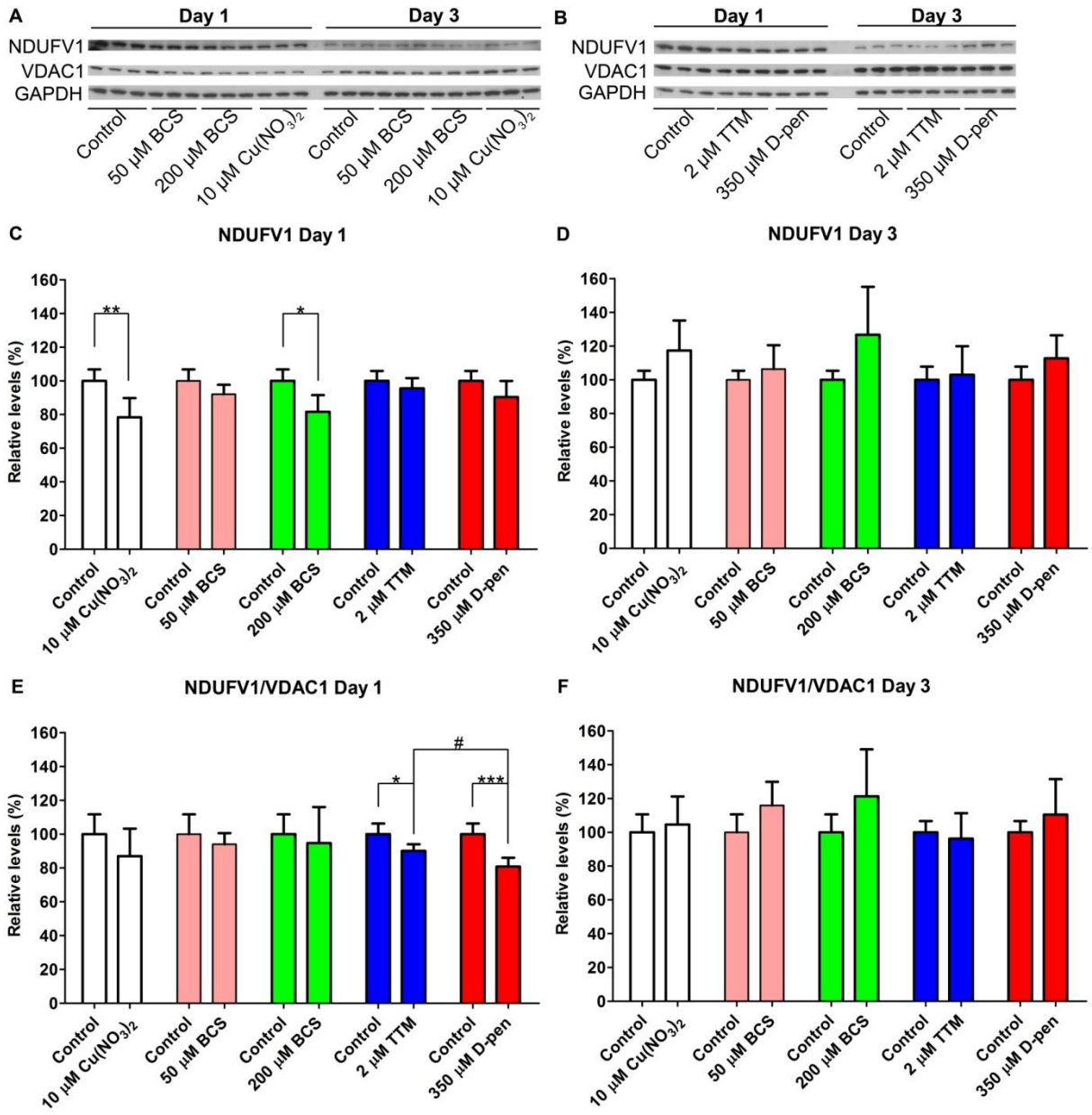

Figure 5.10 NDUFV1 Protein Levels in HEK293 cells Treated with Copper or Chelating Agents.

HEK293 cells were treated with 10 µM $Cu(NO_3)_2$, 50 µM BCS, 200 µM BCS, 2 µM TTM and 350 µM D-pen for 1 or 3 days and proteins extracted. Representative Western blots from cells treated with **(A)** 50, 200 µM BCS or 10 µM $Cu(NO_3)_2$ (n=2) and **(B)** 2 µM TTM or 350 µM D-pen (n=2) at Day 1 and 3. Densitometric analysis of NDUFV1 normalized with GAPDH at **(C)** Day 1 and **(D)** Day 3 as well as with VDAC1 at **(E)** Day 1 and **(F)** Day 3. Data were analysed with one-way ANOVA followed by Tukey post-test. * indicates significant differences between control and treated cells and # amongst different treatments. * or #, $p<0.05$; **, $p<0.01$; *** , $p<0.001$.

By visually examining the bands in the Western blot films it was obvious that the protein levels of NDUFV1 in the controls were lower at Day 3 compared to Day 1. In order to examine if there was an actual decrease in NDUFV1 protein levels throughout the experimental period, the band intensity from Day 1 and Day 3 were plotted next to each other for all the tested conditions and two-way ANOVA followed by Bonferroni post-test was used. The statistical analysis revealed that time and different treatments had an impact of NDUFV1 or NDUFV1/VDAC1 protein levels (two-way ANOVA, $p<0.0001$). Figure 5.11 demonstrates the relative protein levels of NDUFV1 and NDUFV1/VDAC1 ratio where we can see that under all conditions the levels of NDUFV1 or NDUV1/VDAC1 were significantly decreased at Day 3 compared to Day 1. NDUFV1 protein levels and NDUFV1/VDAC1 ratio were decreased by more than 50%, particularly in controls (two-way ANOVA, $p<0.001$) and in the treated cells were decreased by 30-40% between Day 1 and 3.

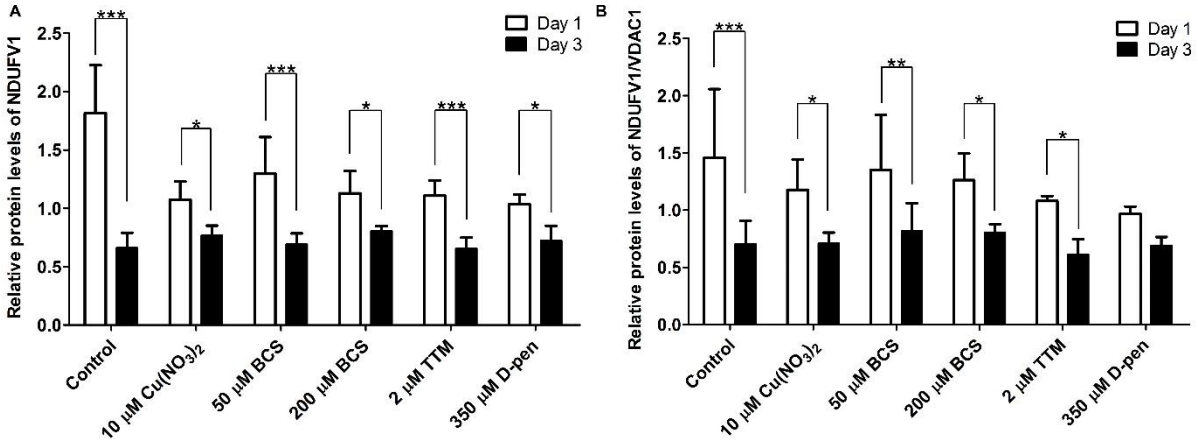

Figure 5.11 Change of NDUFV1 Protein Levels Overtime in Controls, Copper or Chelating Agent Treated HEK293 Cells.

Comparison of the relative protein levels of **(A)** NDUFV1 and **(B)** NDUFV1/VDCA1 between Day 1 and Day 3 for the next conditions: controls (n=2), 10 μM $Cu(NO_3)_2$ (n=2), 50 μM BCS (n=2), 200 μM BCS (n=2), 2 μM TTM (n=2) or 350 μM D-pen (n=2). Data were analysed with two-way ANOVA followed by Bonferroni post-test and *, $p<0.05$; **, $p<0.01$; ***, $p<0.001$.

NDUFS1 protein levels were also determined in both copper/BCS (Figure 5.12A) and TTM/D-pen (Figure 5.12B) treated cell groups where no major changes were observed. At Day 1 the NDUFS1 protein levels were significantly decrease by 14% in cells treated with copper compared to controls (one-way ANOVA, $p<0.05$; Figure 5.12C). At Day 3 the change in the copper treated cells was not apparent whereas in the 350 μM D-pen treated cells NDUFS1 protein levels were significantly increased by 20% (one-way ANOVA, $p<0.01$; Figure 5.12D). In the remaining treatments no significant change was observed compared to controls or amongst the different treatments at Day 1 and 3 (one-way ANOVA, $p>0.05$). Also,

the NDUFS1/VDAC1 ratio did not present any change between treated and controls cells (one-way ANOVA, $p>0.05$) except at Day 3 where a significant increase in cells treated with 50 µM BCS was seen compared to copper treated cells (one-way ANOVA, $p<0.01$; Figure 5.12E and F).

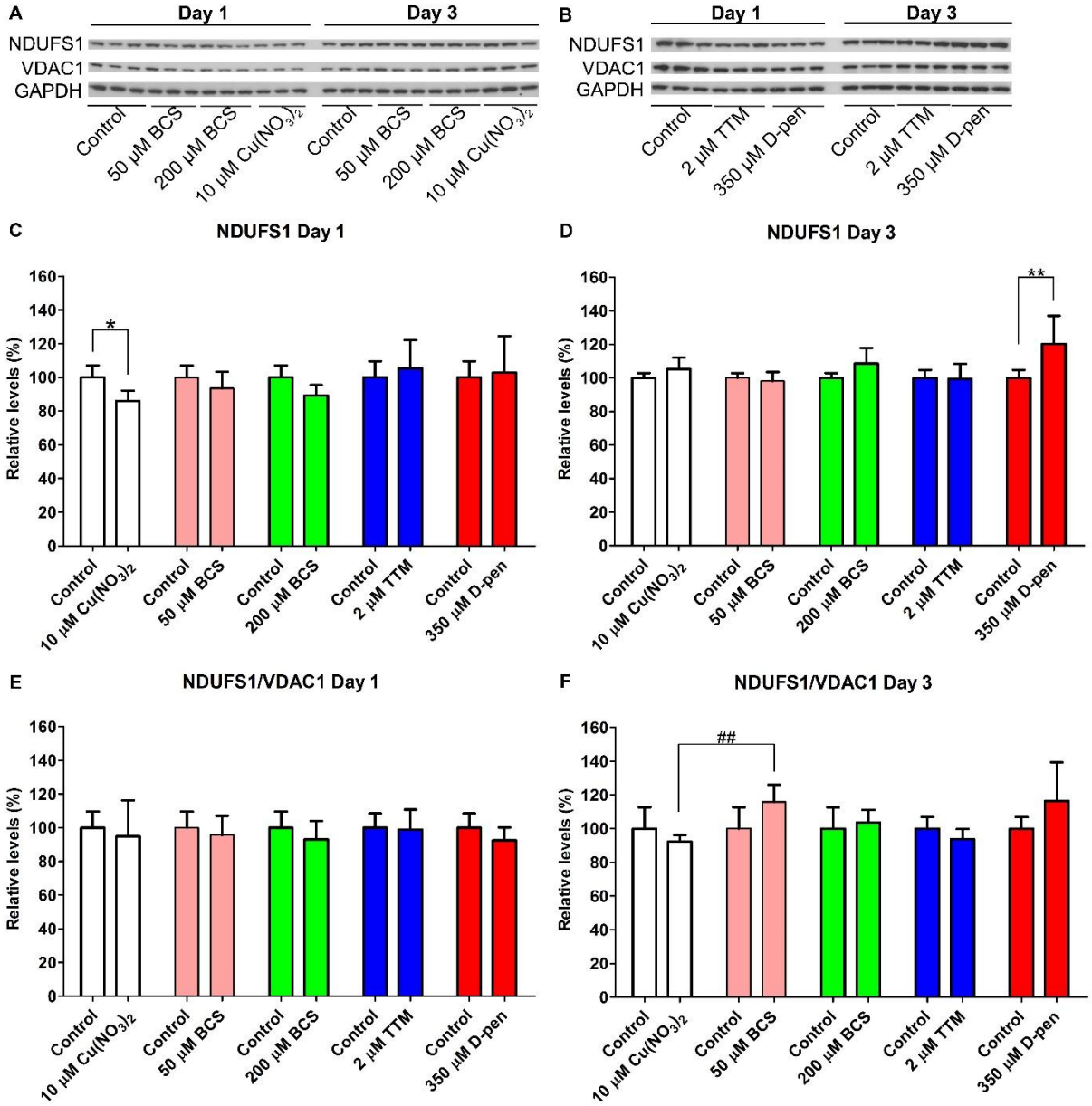

Figure 5.12 NDUFS1 Protein Levels in HEK293 cells Treated with Copper or Chelating Agents.

HEK293 cells were treated with 10 µM $Cu(NO_3)_2$, 50 µM BCS, 200 µM BCS, 2 µM TTM and 350 µM D-pen for 1 or 3 days and proteins extracted. Representative Western blots from cells treated with **(A)** 50, 200 µM BCS or 10 µM $Cu(NO_3)_2$ (n=1) and **(B)** 2 µM TTM or 350 µM D-pen (n=2) at Day 1 and Day 3. Densitometric analysis of NDUFV1 normalized with GAPDH at **(C)** Day 1 and **(D)** Day 3 as well as with VDAC1 at **(E)** Day 1 and **(F)** Day 3. Data were analysed with one-way ANOVA followed by Tukey post-test. * indicates significant differences between control and treated cells and # amongst different treatments. *, $p<0.05$; ** or ##, $p<0.01$.

5.3.3.3 Mitochondrial bioenergetics in HEK293 cells treated with copper chelators

The reduced COX activity and subunit protein levels indicate the presence of possible dysfunction in the mitochondrial respiratory chain. In order to provide a better understanding we utilized an available Seahorse assay in order to monitor the cellular respiration rate in a multi-well format with attached cells. The Seahorse analyser can measure simultaneously the proton and oxygen levels in a very small volume of medium above a monolayer of cultured cells[402-404]. By measuring the oxygen consumption rate (OCR) in the cells, an indicator of mitochondrial respiration, valuable knowledge about the physiological state of the cells and the alterations of the state of those cells can be obtained. Cells have a second source of ATP production via glycolysis where glucose is converted into lactate independently of oxygen. The measurement of the produced lactic acid can be indirectly measured via the protons released into the extracellular medium. Therefore, the extracellular acidification rate (ECAR) obtained from a Seahorse assay reflects the glycolytic function in the cells.

The cell respiratory control was measured in the presence of 50 µM BCS, 200 µM BCS, 0.5 µM TTM, 2 µM TTM and 10 µM $Cu(NO_3)_2$/copper after three days of treatment since this time point showed the highest loss of COX/CS activity and protein levels. The OCR (pmoles/min/µg protein) and the ECAR (mpH/min/µg protein) for all the treatments were analysed and plots were generated in order to identify changes in mitochondrial respiration and glycolysis. Figure 5.13 presents the graphical representation of OCR and ECAR under the studied conditions. The basal ECAR was calculated as the average rate of the three time points before the addition of oligomycin which blocks the mitochondrial ATP synthase[405] where a non-significantly increase of 0.5 mpH/min/µg protein in cells treated with 200 µM BCS was observed (one-way ANOVA, $p>0.05$) whereas in the 2 µM TTM treated the 1.5 mpH/min/µg protein increase was statistical significant (one-way ANOVA, $p<0.05$; Figure 5.14D). The higher ECAR indicates the preference of the cells for using glucose for glycolysis which is also in agreement with the results we obtained by measuring the medium pH under the same conditions (Figure 5.3C, 5.4C and 5.13D, E). Cells treated with copper did not present any significant change in the ECAR levels (Figure 5.13F and 5.14D).

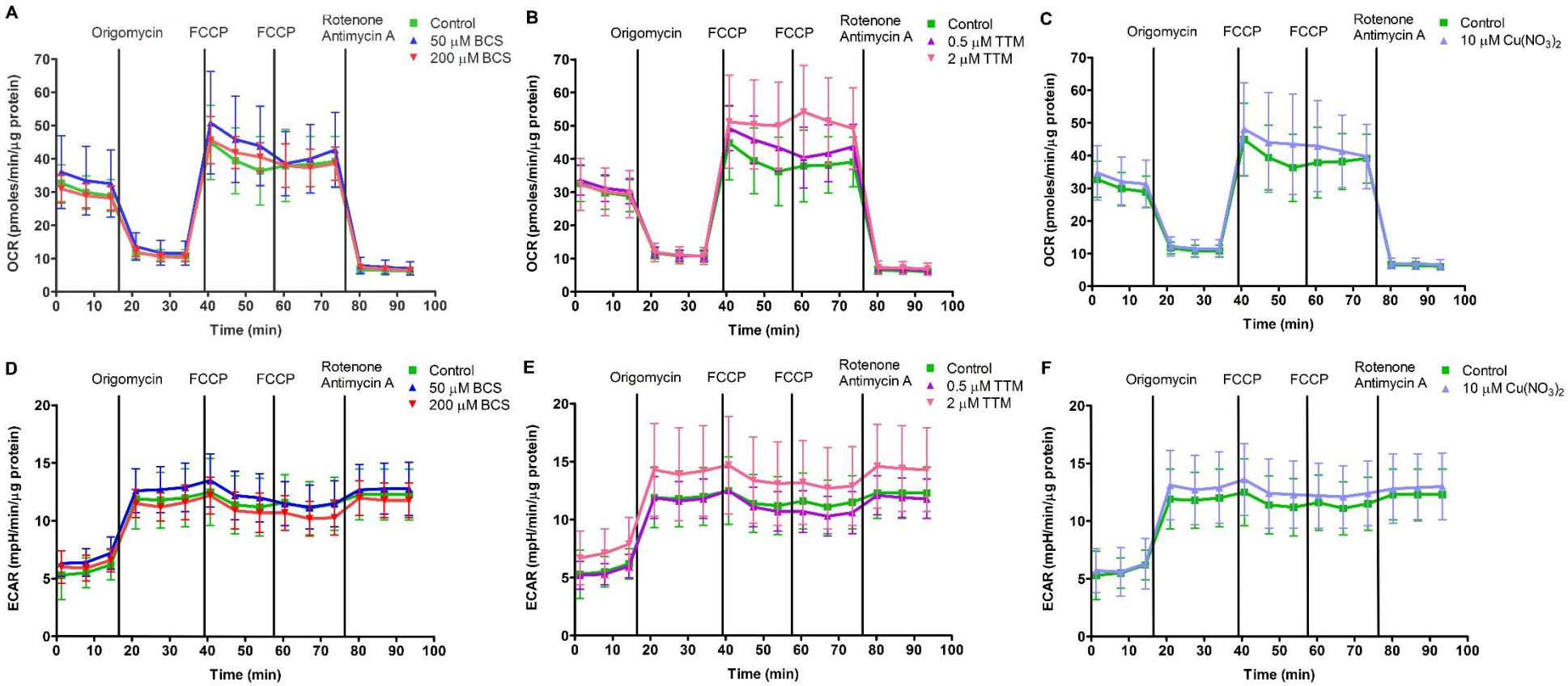

Figure 5.13 Cell Respiratory Control in HEK293 cells after 3 Days Treatment with Copper or Chelating Agents as Determined by the Seahorse Mito Stress Kit.

Graphical representation of the OCR and ECAR in cell treated with **(A and D)** 50 or 200 µM BCS, **(B and E)** 0.5 or 2 µM TTM and **(C and F)** 10 µM $Cu(NO_3)_2$, respectively. The assay was repeated once under the present condition however a pilot study had been conducted before which showed similar results with the one that is currently reported.

By visually inspecting the graphical representation of the OCR small changes in the areas that correspond to maximal respiration or spare capacity in the TTM and copper treated cells were seen (Figure 5.13A to C). The data from the Seahorse analyser were subjected to the XF Stress Test Report Generator where we were able to calculate the basal respiration, proton leak, maximal respiration, spare respiratory capacity, non-mitochondrial respiration, ATP production and coupling efficiency. All the above measured modules provide indications of mitochondrial function and are presented in Figure 5.14.

The results were analysed with one-way ANOVA followed by Tukey post-test where significant changes were only observed in the spare respiratory capacity and in the coupling efficiency. Basal respiration is mainly controlled by the ATP production and proton leak[406] and showed a non-significant increase of 12% and 8% in cells treated with 50 µM BCS and copper, respectively (one-way ANOVA, $p>0.05$; Figure 5.14A). The ATP production in the cells is estimated by the decrease in respiration on inhibition of the ATP synthase after the addition of oligomycin. Our results showed that when cells were treated with 50 µM BCS and copper, a non-significant increase of 15% and 9%, respectively, occurred in the ATP production (one-way ANOVA, $p>0.05$; Figure 5.14A). By measuring respiration in the presence of oligomycin we were able to directly measure the proton leak rate across the mitochondrial membrane *in situ*. The analysis revealed the presence of a non-significant decrease of 14% and 16% in proton leak when cells were grown in the presence of 200 µM BCS and 2 µM TTM (one-way ANOVA, $p>0.05$; Figure 5.14A).

The maximal respiration which depends on the addition of the uncoupler FCCP was determined by using two injections of FCCP (0.5 µM each) in order to achieve a gradually and fully uncontrolled respiration and yet limiting the drop of the $D\psi_m$. The calculated maximal respiration was increased by 22% in the cells treated with 2 µM TTM with the change not being significant possibly due to the high standard deviation (one-way ANOVA, $p>0.05$; Figure 5.14B). A small non-significant increase in maximal respiration was observed in the cells treated with 50 µM BCS and 0.5 µM TTM (one-way ANOVA, $p>0.05$). The spare respiratory capacity reflects the ability of substrate supply and electron transport in response to an increased energy demand[407] which under the experimental conditions presented a significant 55% increase in cells treated with 2 µM TTM (one-way ANOVA, $p<0.05$; Figure 5.14B). A small non-significant increases were present in the remaining treatments such as in the 0.5 µM TTM treated cells where the spare capacity was higher by 18% (one-way ANOVA, $p>0.05$). Significant changes in spare capacity were observed with cells treated with

2 µM TTM compared to cells treated with 200 µM BCS and copper (one-way ANOVA, $p<0.05$; Figure 5.14B).

In cells, non-mitochondrial respiration accounts for 10% of the total respiration and is due to various desaturase and detoxification enzymes[408]. A small non-statistical increase in the non-mitochondrial respiration rate was present with all treatments for example, cells treated with 50 µM BCS and 2 µM TTM showing up to an 13% increase (one-way ANOVA, $p>0.05$; Figure 5.14B).

From the data we were also able to calculate the coupling efficiency which shows the fraction of the basal mitochondrial oxygen consumption that is derived from the ATP synthase. The coupling efficiency is different amongst cell types for example hepatocytes have approximately 70% and pancreatic β-cells 30%[409, 410]. The coupling efficiency of the HEK293 was determined as 79% and a significant increase of 2-3% was observed in the cells treated with BCS (one-way ANOVA, $p<0.01$) and TTM (one-way ANOVA, $p<0.001$) with the changes in all four treatments being significant. In the copper treated cells no change was observed compared to the untreated cells (one-way ANOVA, $p>0.05$), however, its coupling efficiency was significantly lower when compared to the TTM treated cells (one-way ANOVA, $p<0.05$ for 0.5 µM TTM and $p<0.01$ for 2 µM TTM; Figure 5.14C).

In order to obtain a full understanding of mitochondrial function under the tested experimental conditions we measured the mitochondrial mass by staining the cells with MitoTracker green. MitoTracker green is mainly used in flow cytometry to identify mitochondrial mass due to its ability to become fluorescent when it is accumulated in the mitochondrial lipid environment[411] with accumulation being independent of the $D\psi_m$[412]. HEK293 were treated with 200 µM BCS, 2 µM TTM, 350 µM D-pen and 10 µM $Cu(NO_3)_2$/copper for 3 days and by using flow cytometry, we determined their effects on MitoTracker green fluorescence intensity. The emission of MitoTracker green was measured in single cell populations (Figure 5.15A) and initially histograms were plotted for MitoTracker green fluorescence emission (488/530-30) where no major differences were observed (Figure 5.15B-F). The measured mean fluorescence intensity was used to conduct statistical analysis in order to identify if there was any significant change in mitochondrial mass after the cell treatment. Figure 5.15G presents the percentage change of MitoTracker green intensity where no significant change was observed in any of the used treatments compared to untreated cells or amongst the different treatments (one-way ANOVA, $p>0.05$). However, it is worth mentioning that the mitochondrial mass as indicated by the MitoTracker green intensity, was lower by 22% and

17% in cells treated with 200 µM BCS and 2 µM TTM, respectively. Under the same experimental conditions the mitochondrial levels as determined by VDAC1 protein analysis did not present any major change (Figure 5.8F). The small variation between the two methods might be due to the fact that Western blotting is a semi-quantified method whereas FACS is fully quantified.

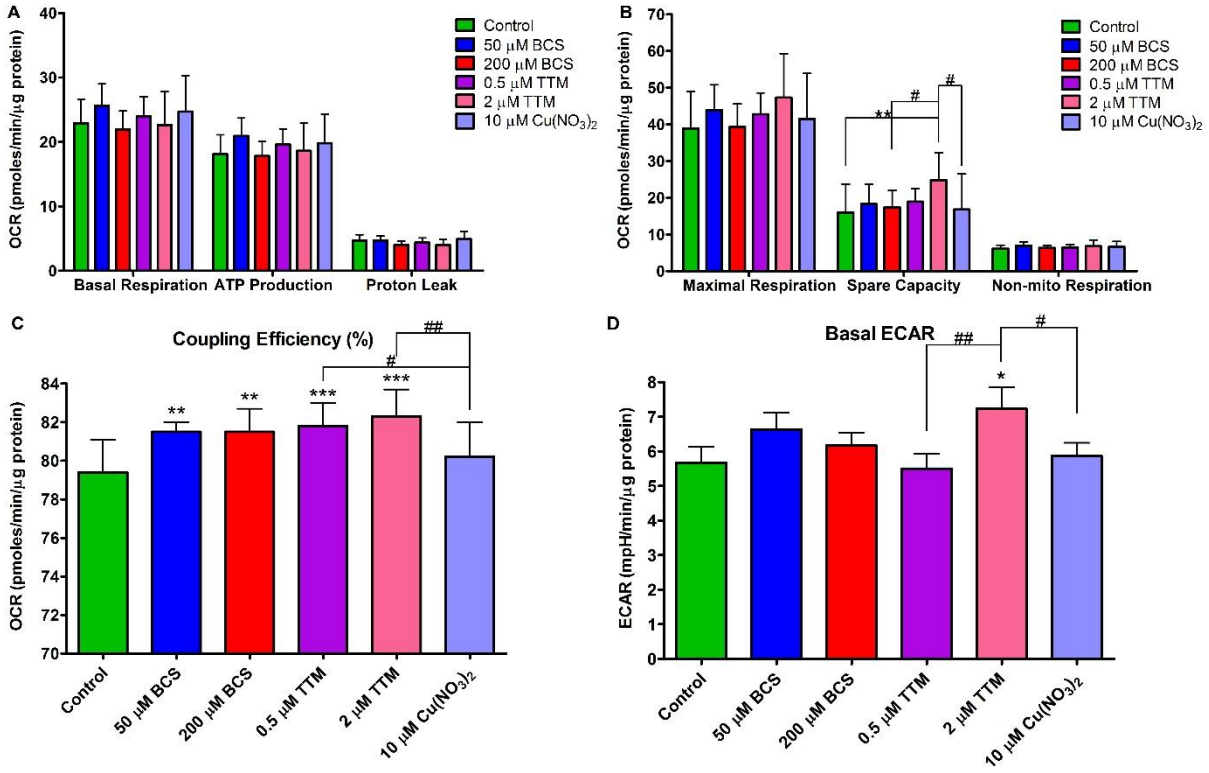

Figure 5.14 OCR and ECAR Comparison in HEK293 cells after 3 Days Treatment with Copper or Chelating Agents for the Different Respiratory Chain Modules.

Graphical representation of (**A)** the basal respiration, ATP production and proton leak, (**B)** maximal respiration, spare (respiratory) capacity and non-mitochondrial/non-mito respiration as well as (**C)** coupling efficiency in cells treated with 50 µM BCS, 200 µM BCS, 0.5 µM TTM, 2 µM TTM or 10 µM $Cu(NO_3)_2$. The reported values were calculated from the obtained data from the analyser which subsequently applied to the XF Mito Stress Test Report Generator. **(D)** Basal ECAR was calculated by combining the average of the three time points before the addition of oligomycin. Data were analysed with one-way ANOVA followed by Tukey post-test. * indicates significant differences between control and treated cells and # amongst different treatments. #, $p<0.05$; ** or ##, $p<0.01$; ***, $p<0.001$.

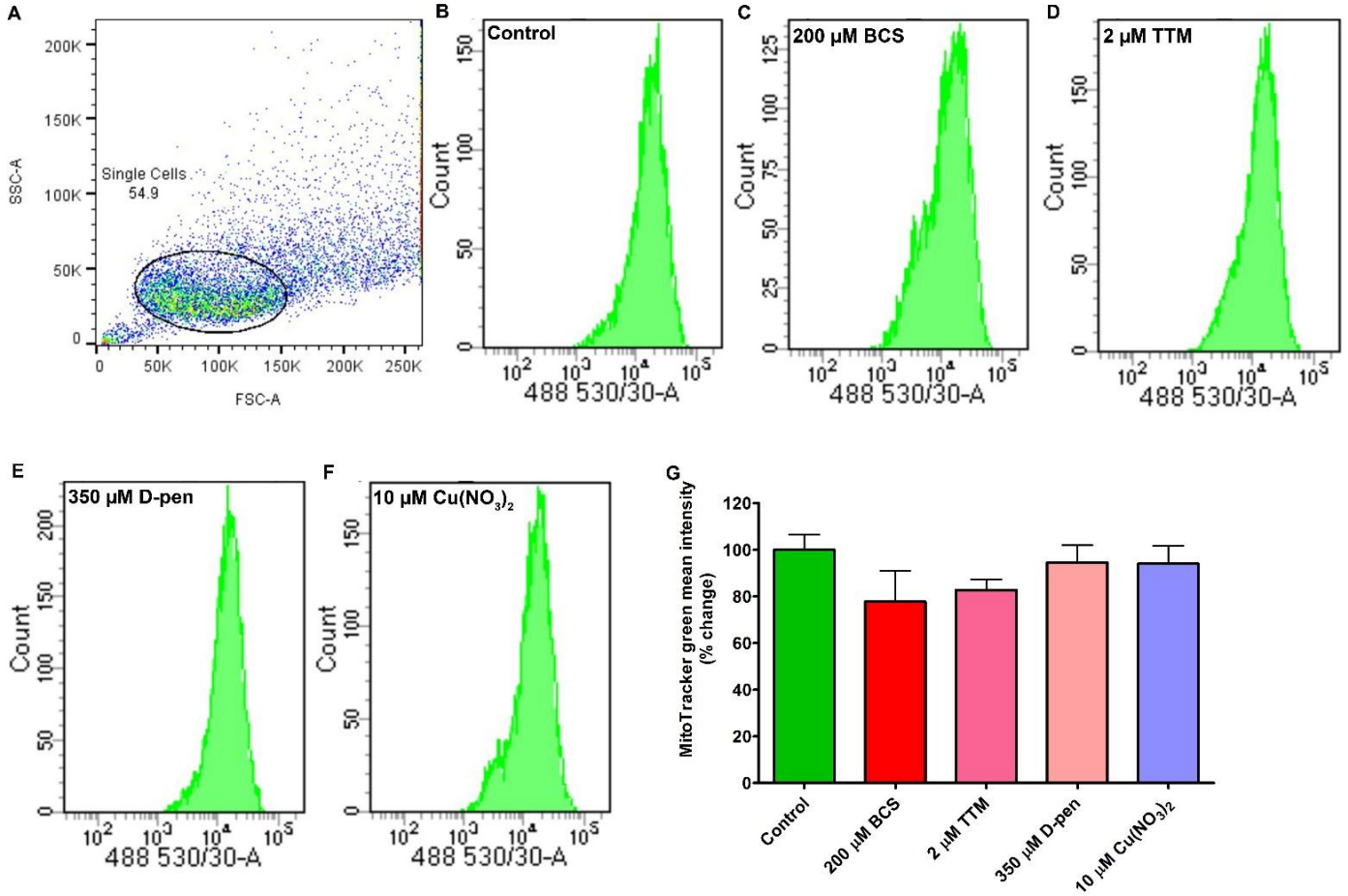

Figure 5.15 Flow Cytometry Analysis using MitoTracker green in HEK293 cells Treated with Copper or Chelating Agents.

HEK293 cells were treated with 200 µM BCS, 10 µM $Cu(NO_3)_2$, 2 µM TTM or 350 µM D-pen for 3 days and then treated with MitoTracker Green and analysed by using flow cytometry. **(A)** Single cell populations were gated for the analysis by using the forward scatter light (FCS) and side scatter light (SCS). In the single cell population the MitoTracker fluorescence intensity was determined. Representative histograms of MitoTracker emission for (**B)** control cells and cell treated with (**C)** 200 µM BCS, (**D)** 2 µM TTM, (**E)** 350 µM D-pen and (**F)** 10 µM $Cu(NO_3)_2$. (**G)** Percentage change of the MitoTracker mean intensity amongst the different treatments. Data were analysed with one-way ANOVA followed by Tukey post-test were no statistical change was observed.

5.3.4 The effects of copper supplementation and chelation in the cytosolic copper pathway

5.3.4.1 Copper chelation severely affects SOD activity in HEK293 cells

After the determination of COX and CS activities, the same cell extracts were used for the determination of SOD activity. The total SOD activity was measured at Day 1 and 3 in cells treated with 10 µM $Cu(NO_3)_2$/copper, 50 µM BCS, 200 µM BCS, 2 µM TTM or 350 µM D-pen with significant activity loss found in cells grown in the presence of BCS or TTM.

At Day 1 SOD activity was significantly decreased by 55% in the BCS treated cells (one-way ANOVA, $p<0.001$) compared to control whereas the TTM treated cells showed a much more severe loss of SOD activity with activity decrease by 87% (one-way ANOVA, $p<0.001$). D-pen showed a minor effect on SOD activity with a significant 8% decrease (one-way ANOVA, $p<0.05$) probably due to the small standard deviation in both D-pen treated cells and controls. The impact of a small or higher standard deviation in the statistical analysis can be seen in the case of copper treated cells since the 8% increase was not significant due to a higher standard deviation (one-way ANOVA, $p>0.05$). The difference in SOD activity amongst the different copper chelators was examined where we found that cells treated with 350µM D-pen had significantly higher SOD activity compared to the BCS or TTM treated cells (one-way ANOVA, $p<0.001$). At Day 1 SOD activity was significantly higher in cells treated with 200 µM BCS relative to TTM treated cells (one-way ANOVA, $p<0.05$; Figure 5.16A). The copper treated cells also had higher SOD activity relative to the BCS and TTM treated cells but not to D-pen treated cells (one-way ANOVA, $p<0.001$, data not shown).

SOD activity at Day 3 exhibited an even greater loss in the TTM and BCS treated cells since 67% decrease in the 50 µM BCS and an 82% decrease in the 200 µM BCS treated cells was observed with both changes being significant compared to untreated cells (one-way ANOVA, $p<0.001$). In TTM treated cells there was only 10% of SOD activity remaining (one-way ANOVA, $p<0.001$). The copper and D-pen treated cells did not show any change in total SOD activity (one-way ANOVA, $p>0.05$). Next we examined if there were changes in SOD activity amongst the different copper chelators with the analysis showing that D-pen treated cells had higher activity relative to the BCS and TTM treated cells (one-way ANOVA, $p<0.001$). No significant difference was observed amongst the BCS and TTM treated cells (one-way ANOVA, $p>0.05$; Figure 5.16B). SOD activity in the copper treated cells was also significantly higher than the BCS and TTM treated cells (one-way ANOVA, $p<0.001$) but not compared with the D-pen treated cells (one-way ANOVA, $p>0.05$, data not shown).

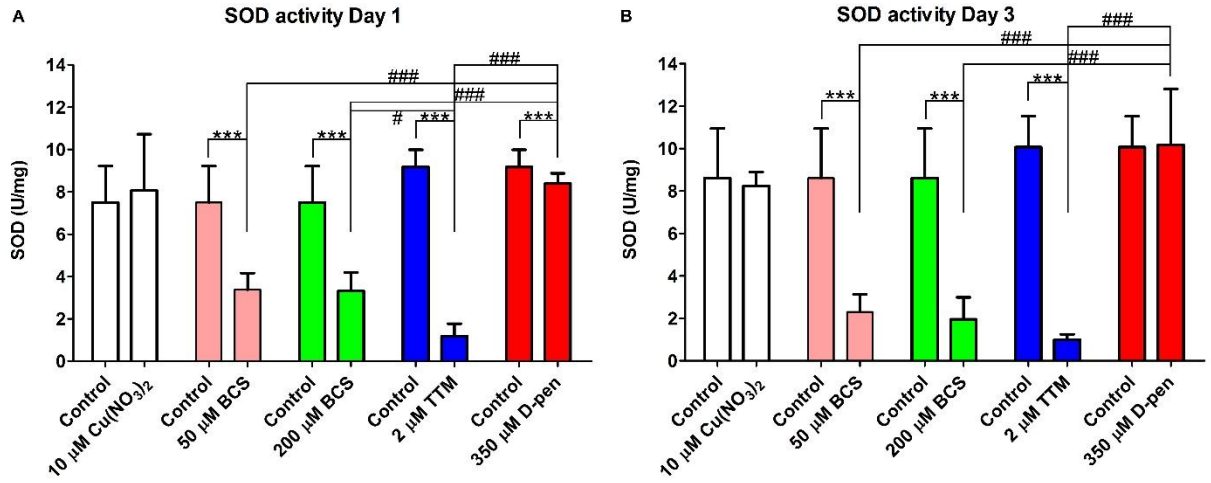

Figure 5.16 Total SOD Activity in HEK293 cell Treated with Copper or Chelating Agents. Total SOD activity was determined in HEK293 cells treated with either 10 µM $Cu(NO_3)_2$ (n=3), 50 µM BCS (n=2), 200 µM BCS (n=3), 2 µM TTM (n=3) or 350 µM D-pen (n=3) at **(A)** Day 1 or **(B)** Day 3. Data were analysed with one-way ANOVA followed by Tukey post-test. * indicates significant differences between control and treated cells and # amongst different treatments. #, $p<0.05$; *** or ###, $p<0.001$.

In order to determine the concentration of BCS and TTM that had the lowest impact in SOD activity a test experiment was run where cells were grown in the presence of 0.5 and 5 µM BCS and 0.5 µM TTM for 3 days. The measured SOD activity in the cell lysates showed that when BCS concentration was decreased an order of magnitude it induced an approximate doubling of SOD activity. For example at 50 µM BCS SOD activity was approximately 2.8 U/mg but at 5 µM BCS SOD activity was around 6 U/mg and at 0.5 µM BCS around 10 U/mg. The 35% decrease in SOD activity in cells treated with 5 µM BCS was also significant (one-way ANOVA, $p<0.01$) whereas in the 0.5 µM BCS it was not considered significant (one-way ANOVA, $p>0.05$). Cells treated with 0.5 µM TTM still showed greater than 80% decrease in total SOD activity even if the TTM concentration was quartered (one-way ANOVA, $p<0.001$, see supplementary Figure B.4B).

5.3.4.2 No change in the cytosolic copper binding protein levels following copper or copper chelator treatment

The protein levels of CCS, SOD1 as well as SOD2 were determined using the established experimental conditions and in general, no significant changes were observed for SOD proteins with only mirror changes to CCS protein. CCS protein levels from Day 1 and 3 were determined in the copper/BCS (Figure 5.17A) and TTM/D-pen (Figure 5.17B) treated cell groups. At Day 1 CCS protein levels were significantly increased by 43% in cells treated with 200 µM BCS (one-way ANOVA, $p<0.01$) with a smaller non-significant 12% increase in cells treated with 50 µM BCS (one-way ANOVA, $p>0.05$) being present too. TTM and D-pen

did not seem to have similar effects on CCS levels since no significant changes was seen (one-way ANOVA, $p>0.05$). Supplementing cells with copper showed a significant 32% increase of CCS protein levels (one-way ANOVA, $p<0.05$). By examining if there were changes amongst the different treatments we found that at Day 1 cells treated with 200 µM BCS had higher CCS protein levels compared to cells treated with 50 µM BCS (one-way ANOVA, $p<0.01$; Figure 5.17C). At Day 3 no significant change was seen between control and treated cells or amongst different treatments (one-way ANOVA, $p>0.05$; Figure 5.17D).

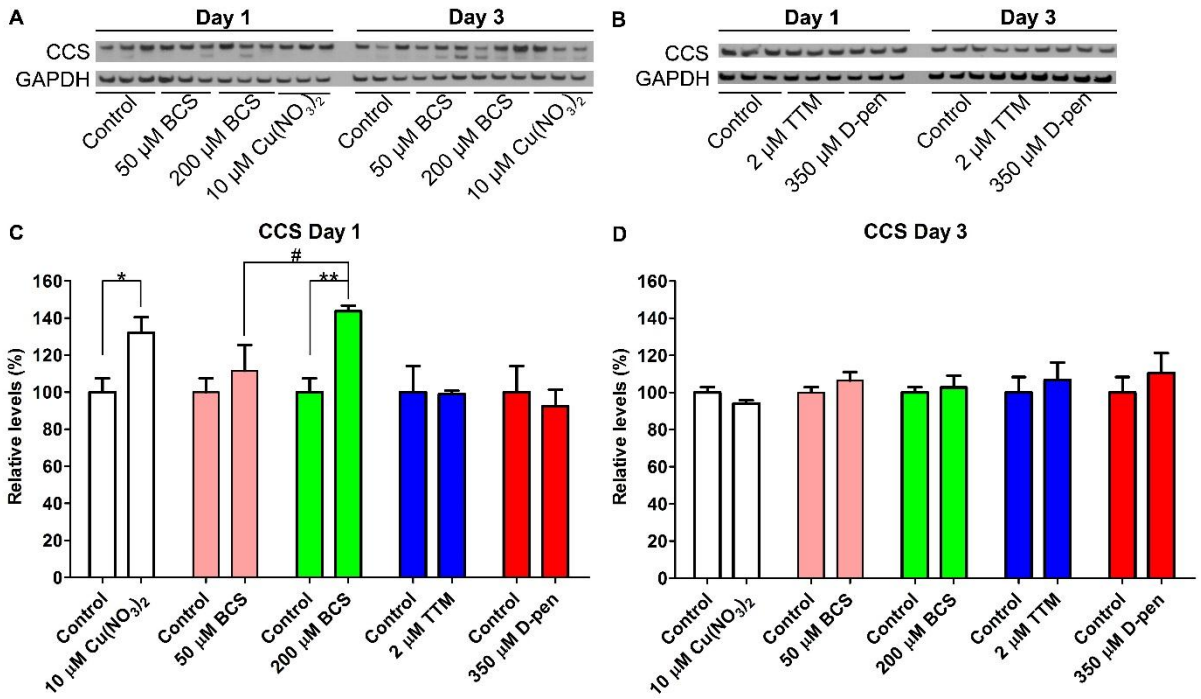

Figure 5.17 CCS Protein Levels in HEK293 cell Treated with Copper or Chelating Agents. HEK293 cells were treated with 10 µM $Cu(NO_3)_2$, 50 µM BCS, 200 µM BCS, 2 µM TTM and 350 µM D-pen for 1 or 3 days and proteins extracted. Representative Western blots from HEK293 cells treated with **(A)** 50, 200 µM BCS or 10 µM $Cu(NO_3)_2$ (n=1) and **(B)** 2 µM TTM or 350 µM D-pen (n=1) at Day 1 and 3. Densitometric analysis of CCS normalized with GAPDH at **(C)** Day 1 and **(D)** Day 3. Data were analysed with one-way ANOVA followed by Tukey post-test. * indicates significant differences between control and treated cells and # amongst different treatments. * or #, $p<0.05$; **, $p<0.01$.

Next we determined the protein levels of SOD1 at Day 1 and 3 in copper/BCS (Figure 5.18A) or TTM/D-pen (Figure 5.18B) treated cell groups. The statistical analysis revealed the absence of any significant change in SOD1 protein levels with any of the treatments compared to untreated cells or amongst the different treatments at Day 1 (one-way ANOVA, $p>0.05$; Figure 5.18C). At Day 3 SOD1 protein levels were significantly decreased by 10% in cells treated with 350 µM D-pen (one-way ANOVA, $p<0.05$). Cell treated with 200 µM BCS also showed a 13% loss of SOD1 protein levels compared to controls but the change was not

significant (one-way ANOVA, p>0.05). At Day 3 no other changes were observed in SOD1 protein levels (one-way ANOVA, p>0.05; Figure 5.18D).

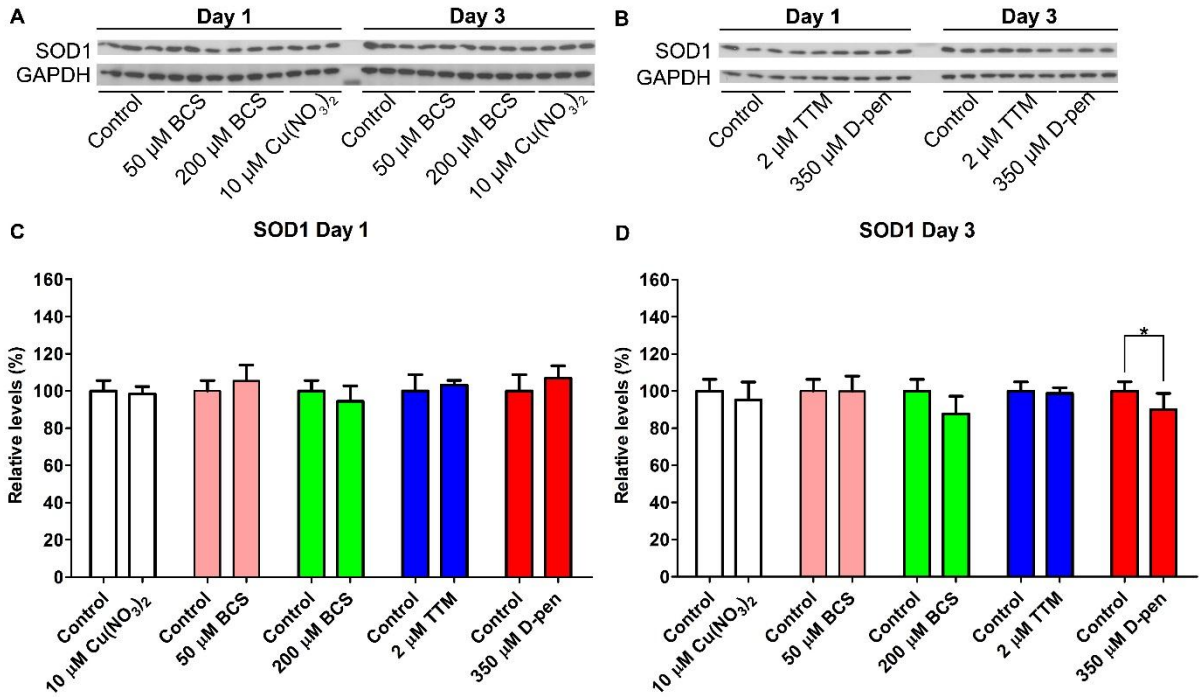

Figure 5.18 SOD1 Protein Levels in HEK293 cells Treated with Copper or Copper Chelators. HEK293 cells were treated with 10 µM $Cu(NO_3)_2$, 50 µM BCS, 200 µM BCS, 2 µM TTM and 350 µM D-pen for 1 or 3 days and proteins extracted. Representative Western blots from cells treated with **(A)** 50, 200 µM BCS or 10 µM $Cu(NO_3)_2$ (n=1) and **(B)** 2 µM TTM or 350 µM D-pen (n=1) at Day 1 and 3. Densitometric analysis of SOD1 normalized with GAPDH at **(C)** Day 1 and **(D)** Day 3. Data were analysed with one-way ANOVA followed by Tukey post-test. * indicates significant differences between control and treated cells. *, p<0.05.

SOD2 protein levels were also determined at Day 1 and 3 in cells treated with copper/BCS (Figure 5.19A) and TTM/D-pen (Figure 5.19B). No significant change was observed in SOD2 protein levels at Day 1 or 3 either compared to controls or amongst different treatments (one-way ANOVA, p>0.05; Figure 5.19C and D). Since SOD2 is so important for the mitochondria antioxidant defense system its levels were also normalized with VDAC1. At Day 1 the SOD2/VDAC1 ratio did not change under any of the tested conditions however in the TTM treated cells the ratio was non-significantly lower by 29% (one-way ANOVA, p>0.05; Figure 5.19E). At Day 3 SOD2/VDAC1 ratio seemed to be significantly higher by 22% in cells treated with 200 µM BCS (one-way ANOVA, p<0.01), however, no other treatment showed any change relative to their control (one-way ANOVA, p>0.05). Also, by comparing the different treatments we identified that cells treated with 200 µM BCS had higher SOD2/VDCA1 ratio compared to ones treated with 50 µM BCS (one-way ANOVA, p<0.01; Figure 5.19F).

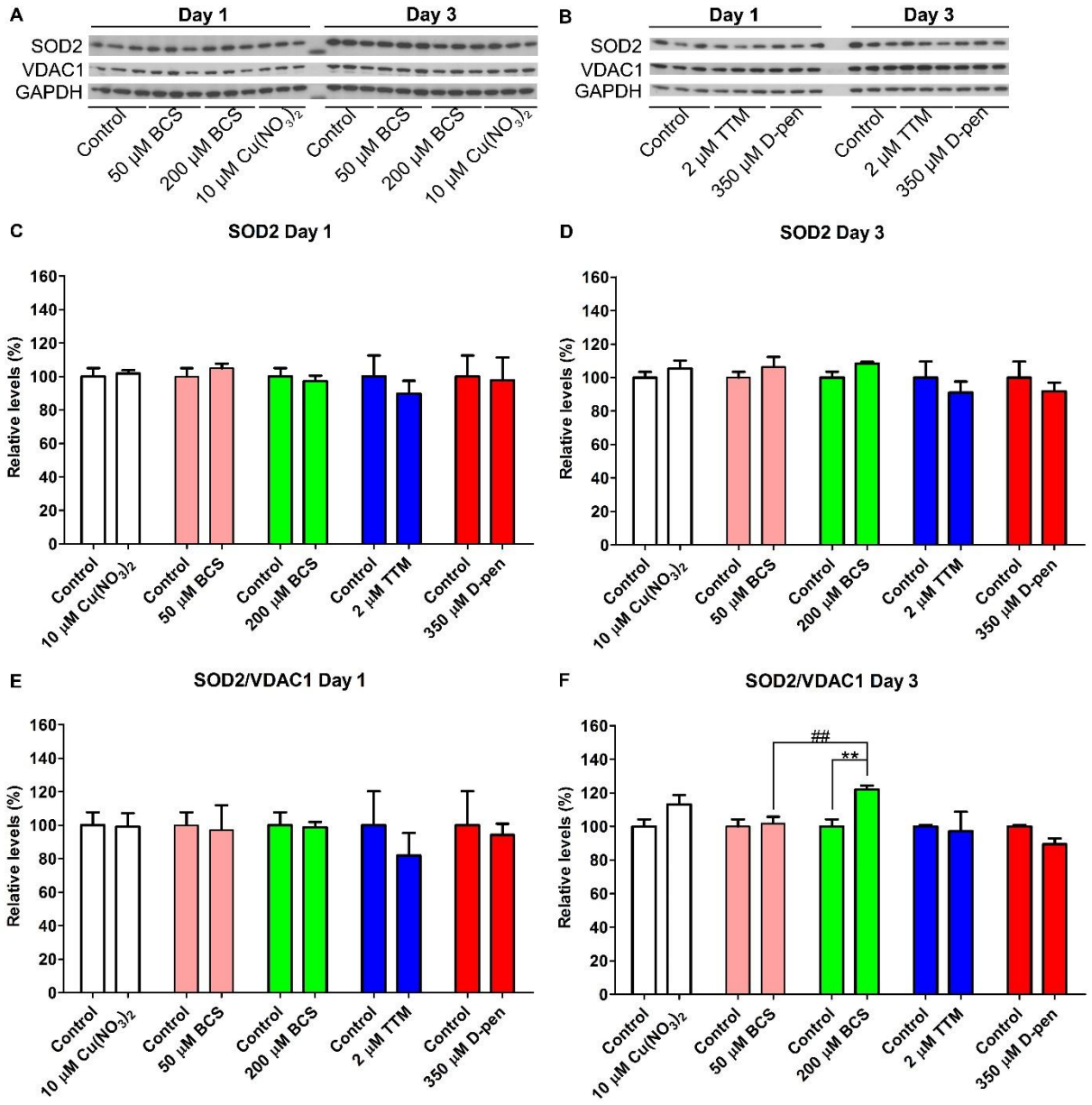

Figure 5.19 SOD2 Protein Levels in HEK293 cells treated Copper or Chelating Agents.

HEK293 cells were treated with 10 µM $Cu(NO_3)_2$, 50 µM BCS, 200 µM BCS, 2 µM TTM and 350 µM D-pen for 1 or 3 days and proteins extracted. Representative Western blots from cells treated with **(A)** 50, 200 µM BCS or 10 µM $Cu(NO_3)_2$ (n=2) and **(B)** 2 µM TTM or 350 µM D-pen (n=2) at Day 1 and 3. Densitometric analysis of SOD2 normalized with GAPDH at **(C)** Day 1 and **(D)** Day 3 as well as with VDAC1 at **(E)** Day 1 and **(F)** Day 3. Data were analysed with one-way ANOVA followed by Tukey post-test. * indicates significant differences between control and treated cells and # amongst different treatments. ** or ##, $p<0.01$.

5.3.5 Increased production of mitochondrial derived superoxide anions in BCS and TTM treated cells

The mitochondrial dysfunction and the decrease in SOD activity in the BCS and TTM treated cells led us to investigate if the mitochondria produced superoxide anions change under these conditions. In order to measure the superoxide anions in the treated cell flow cytometry was employed along with staining cells with MitoSOX red, a fluorogenic dye selective for mitochondrial superoxide in live cells[(413)]. MitoSOX red localizes into cellular mitochondria where it is readily oxidized by superoxide anions but not by other sources of reactive oxygen or nitrogen species[(413)].

The mitochondrial superoxide anions were measured in cells treated with 200 µM BCS, 2 µM TTM, 350 µM D-pen and 10 µM $Cu(NO_3)_2$ as well as in cells treated with 5 µM H_2O_2 as a positive control. Cells were stained with MitoSOX red after 3 days of treatment prior to analysis with flow cytometry. Figure 5.20A to F presents the histograms from the different treatments where a shift and a second peak is observed in the BCS and TTM treated cells. The mean fluorescence of MitoSOX red (488/ 585-42) was then applied and analysed in order to identify changes amongst the different treatments and the control. Mitochondrial superoxide anions were significantly higher by 52% and 83% in the BCS (one-way ANOVA, $p<0.05$) and TTM (one-way ANOVA, $p<0.001$) treated cells, respectively, compared to control cells. In the copper treated cells a non-significant 19% increase was observed (one-way ANOVA, $p>0.05$), but in the D-pen treated cells no change in the mitochondrial superoxide anions was observed (one-way ANOVA, $p>0.05$). We also determined if the levels of superoxide anions were different amongst the treatments where we found that in the BCS (one-way ANOVA, $p<0.05$) and TTM (one-way ANOVA, $p<0.001$) treated cells superoxide anions were significantly higher compared to copper treated cells. Also, the TTM treated cells produced higher levels of mitochondria derived superoxide anions relative to D-pen treated cells (one-way ANOVA, $P<0.01$; Figure 5.20G).

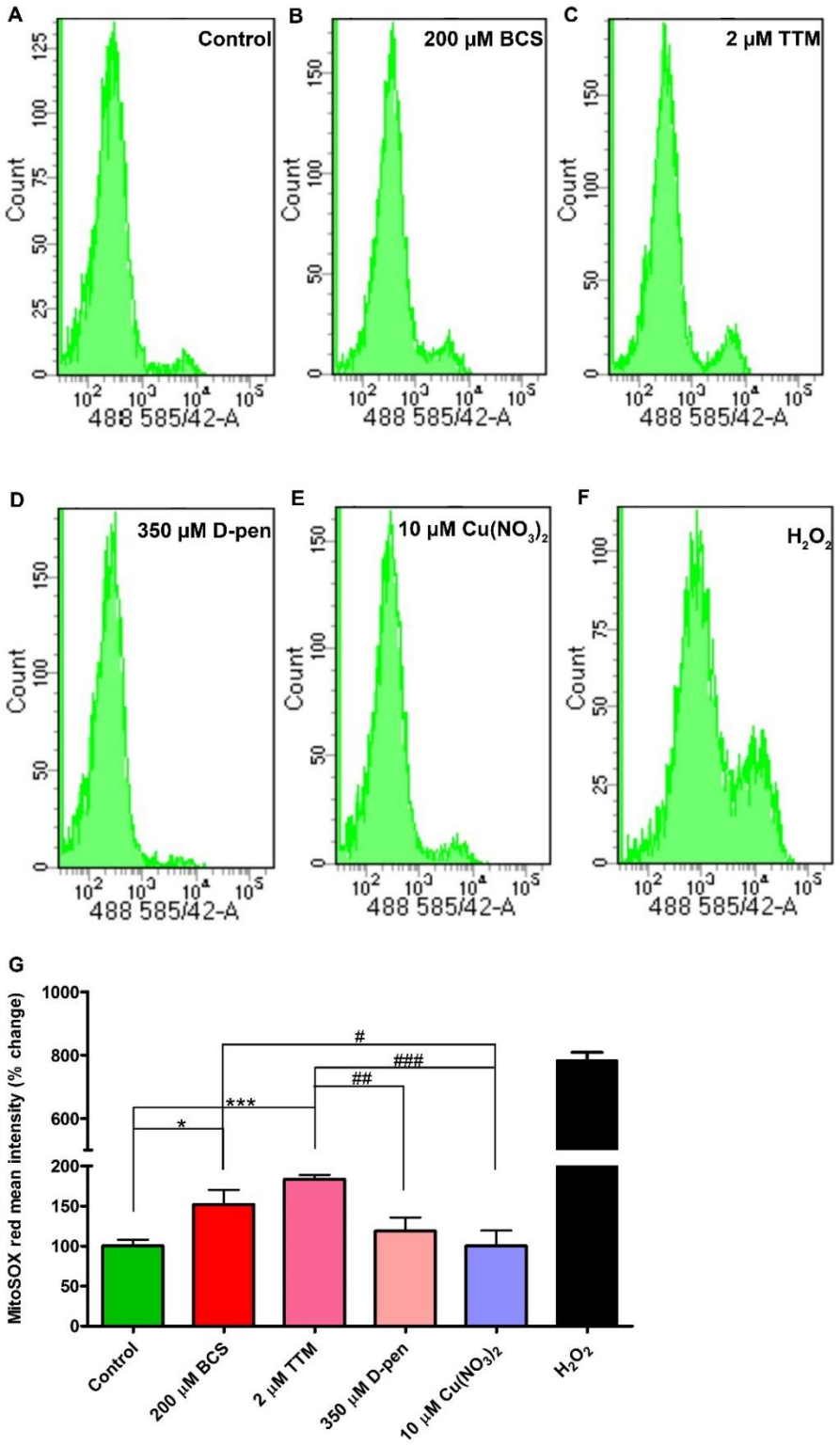

Figure 5.20 Flow Cytometry Analysis of Mitochondrial Superoxide Production in HEK293 cells Treated with Copper or Chelating Agents.

Representative histograms of MitoSOX red emission for **(A)** control cells and cells treated with **(B)** 200 µM BCS, **(C)** 2 µM TTM, **(D)** 350 µM D-pen, **(E)** 10 µM $Cu(NO_3)_2$ and **(F)** H_2O_2. **(G)** Percentage change of the MitoSOX red mean intensity amongst the different treatments. Data were analysed with one-way ANOVA followed by Tukey post-test where H_2O_2 was not taken into consideration. * indicates significant differences between control and treated cells and # amongst different treatments. * or #, $p<0.05$/ ##, $p<0.01$/ *** or ###, $p<0.001$.

5.3.6 Copper supplementation or chelation effects on the copper secretory pathway

From the copper secretory pathways we were only able to determine the protein levels of Atox1 and ATP7a in the HEK293 cells. The cells did not express many of the copper binding enzymes such as PAM or lysisl oxidase. Initially, we measured the protein levels of Atox1 at Day 1 and 3 in cells treated with copper/BCS (Figure 5.21A) or TTM/D-pen (Figure 5.21B). At Day 1 no significant change was observed in the protein levels of Atox1 under any of the conditions compared to controls or amongst different treatments (one-way ANOVA, $p>0.05$) with only a small non-significant decrease in Atox1 protein levels (14-19%) being observed in the BCS and TTM treated cells (one-way ANOVA, $p>0.05$; Figure 5.21C). At Day 3, Atox1 protein levels were significantly decreased by 24% in cells treated with copper (one-way ANOVA, $p<0.01$) and also decreased by 25% following 200 µM BCS treatment (one-way ANOVA, $p<0.01$). Cells treated with 350 µM D-pen showed a significant 43% increase in Atox1 protein levels compared to control (one-way ANOVA, $p<0.05$). At Day 3 Atox1 levels were higher by 32% in the TTM treated cells relative to controls but the change was not significant (one-way ANOVA, $p>0.05$; Figure 5.21D). Next we examined if there were changes amongst the different treatments although there were no significant changes observed at Day 1 (one-way ANOVA, $p>0.05$), at Day 3, cells treated with 50 µM BCS had higher Atox1 protein levels compared to cells treated with 200 µM BCS (one-way ANOVA, $p<0.05$; Figure 5.21C and D).

Finally, ATP7a protein levels were determined at Day 1 and 3 in the copper/BCS (Figure 5.22A) and TTM/D-pen (Figure 5.22B) treated cell where minor changes were only observed at Day 3. No significant change in ATP7a protein levels was observed at Day 1 with the only change being a small non-significant 13% decrease in the copper treated cells (one-way ANOVA, $p>0.05$; Figure 5.22C). At Day 3 ATP7a protein levels were significantly higher by 20% in the copper treated cells compared to controls (one-way ANOVA, $p<0.05$). The remaining of the treatments did not show any significant change except of a small non-significant 12% increase of ATP7a protein levels in the D-pen treated cells (one-way ANOVA, $p>0.05$; Figure 5.22D). The comparison amongst different treatments did not reveal any change at Day 1 but at Day 3 ATP7a protein levels were significantly higher in the copper treated cells relative to the ones treated with 200 µM BCS (one-way ANOVA, $p<0.05$; Figure 5.22C and D).

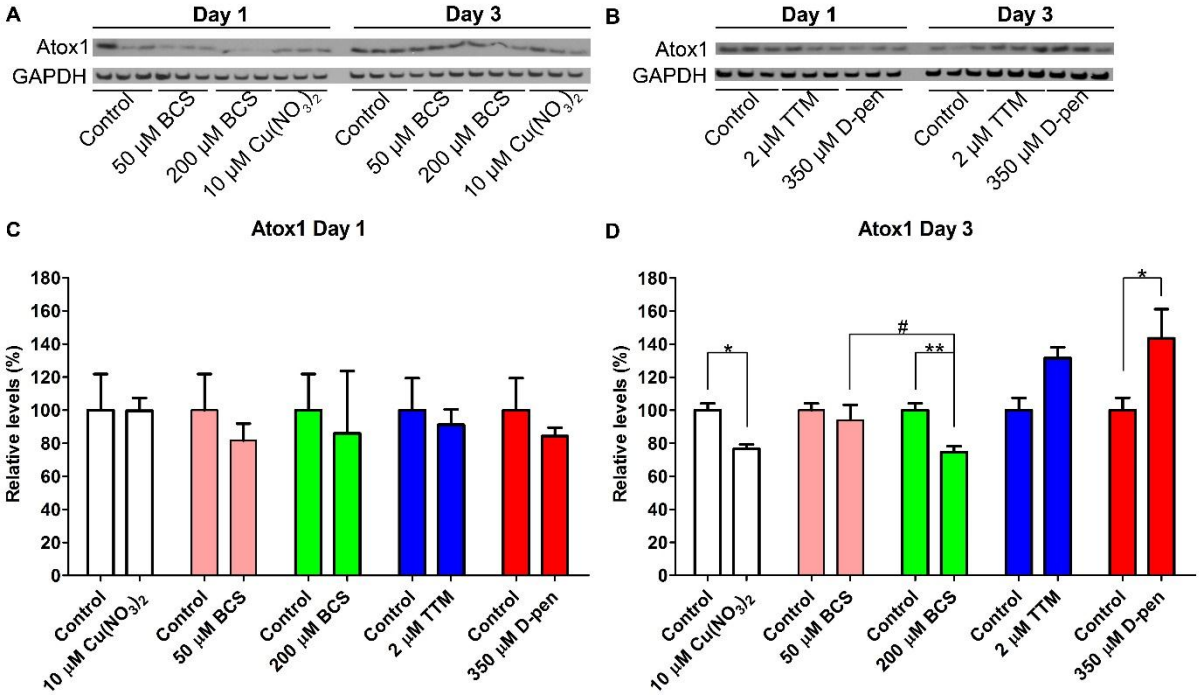

Figure 5.21 Atox1 Protein Levels in HEK293 cell treated with Copper or Chelating Agents.

HEK293 cells were treated with 10 µM $Cu(NO_3)_2$, 50 µM BCS, 200 µM BCS, 2 µM TTM and 350 µM D-pen for 1 or 3 days and proteins extracted. Representative Western blots from cells treated with **(A)** 50, 200 µM BCS or 10 µM $Cu(NO_3)_2$ (n=1) or **(B)** 2 µM TTM or 350 µM D-pen (n=1) at Day 1 and 3. Densitometric analysis of Atox1 normalized with GAPDH at **(C)** Day 1 and **(D)** Day 3. Data were analysed with one-way ANOVA followed by Tukey post-test. * indicates significant differences between control and treated cells and # amongst different treatments. * or #, $p<0.05$; **, $p<0.01$.

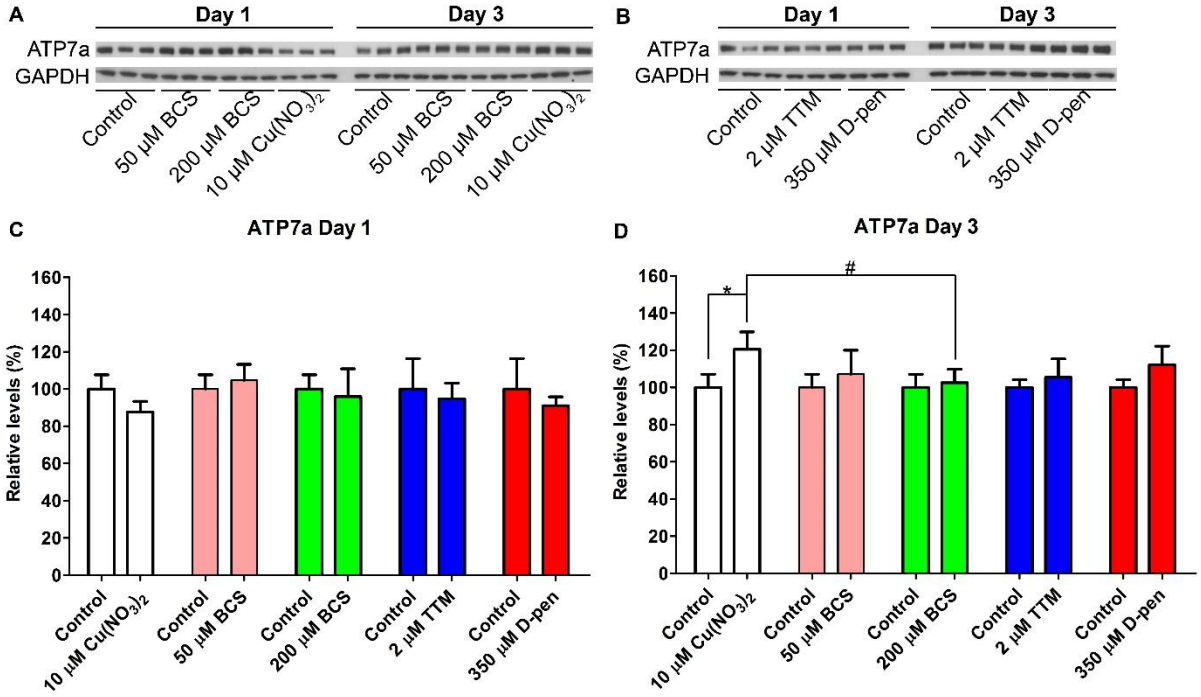

Figure 5.22 ATP7a Protein levels in HEK293 cell treated with Copper or Chelating Agents.

HEK293 cells were treated with 10 µM $Cu(NO_3)_2$, 50 µM BCS, 200 µM BCS, 2 µM TTM and 350 µM D-pen for 1 or 3 days and proteins extracted. Representative Western blots from cells treated with **(A)** 50, 200 µM BCS or 10 µM $Cu(NO_3)_2$ (n=1) and **(B)** 2 µM TTM or 350 µM D-pen (n=1) at Day1 and 3. Densitometric analysis of ATP7a normalized with GAPDH at **(C)** Day 1 and **(D)** Day 3. Data were analysed with one-way ANOVA followed by Tukey post-test. * indicates significant differences between control and treated cells and # amongst different treatments. * or #, $p<0.05$.

5.4 Discussion

Our data analysis from the AD and the ageing brains has shown that the brain faces copper deficiency however the activity of two of the most important copper containing enzymes for the cell survival, SOD and COX, do not seem to be affected. In order to investigate if the effects of copper deficiency in the brain are correlated more with pathology and the brain's energy demands or with cell type requirements we used the model cell line HEK293 to study the effects of both copper deficiency and supplementation. Studies have shown that different mammalian cell lines possess different intracellular copper chelating capacity and that some cells can tolerate higher copper levels[132]. For that reason we initially determined the toxic levels of both copper and specific chelators in the HEK293 cells.

Generally, we observed that HEK293 cells can tolerate up to 40 μM copper in their growth medium which is lower when compared to other cells lines such as MEFs where studies have used more than 150 μM copper or in SH-SY5Y which can tolerate up to 300 μM copper[127, 414]. Since we wanted to avoid cytotoxicity and subsequent effects on protein expression, 10 μM of copper was selected for experimental usage (Figure 5.2A). We also showed that cells can well tolerate BCS since toxicity first started to appear at over 1 mM which is well above what has been used in other studies (Figure 5.3A). Normally, studies with MEFs or K562 cells, have used BCS concentrations from 10 to 30 up to 200 μM, since we wanted also to be able to compare our results with published data, we used 200 μM BCS[127, 415].

Whilst BCS is considered to have the highest chelation affinity for copper[384] it required more than 400 μM in order to see a significant effect on cell viability whereas with TTM, similar effects were observed with only 4 μM TTM which is almost 100 times less than BCS (Figure 5.3A and 5.4A). Other cell lines such as human umbilical vein endothelial cells (HUVEC) or cancer cells (YPEN-1/ ECC-1) show similar toxicity for TTM since they showed decrease viability at concentrations around 5 μM[416, 417]. Taking our results and other published studies into consideration 2 μM TTM was selected experimentally. D-pen did not present any major toxic effect in the HEK293 cells up to the concentrations that we tested (650 μM; Figure 5.5A) similarly studies with MCF-7 or HL-60 cells did not show any effect on viability when cells were treated with up to 400 μM D-pen[396, 397]. In order to select a concentration to continue experimentally with D-pen we also used the MTT assay which is used as an indicator of mitochondrial function, we were able to identify that concentrations around 350 μM can cause small changes in the cell viability or mitochondrial function.

5.4.1 Shift to glycolysis for energy production in cells treated with BCS or TTM

Mammalian cell lines require constant availability of carbon, nitrogen, energy (ATP) and reductant (NADPH) in order to sustain their anabolic function[85, 418]. The main source of energy in the cells is from mitochondrial oxidative phosphorylation which utilizes glucose in order to produce up to 36 moles of ATP however, cells contain a second source of ATP from glycolysis where glucose can be converted to lactate to generate 2 moles of ATP [85]. Under normal condition in cells, 57% of ATP derives from oxidative phosphorylation, 38% from glycolysis and 5% from substrate level phosphorylation within the Krebs cycle[406]. Cells will turn to glycolysis as a main source of energy production if mitochondrial oxidative phosphorylation is inhibited. The shift to glycolysis is associated with an increase in lactate production[419] which can be easily detected visually by changes in the cell medium when it contains phenol red as an observed colour change. Phenol red is turned yellow when the pH in the medium is below 7. Normally during glycolysis, lactate protons are generated which decreases cellular pH[420]. A significant change in medium pH was observed only in cells treated with 200 µM BCS and 2 µM TTM after 3 days (Figure 5.3C and 5.4C). We normally observed a decrease in medium pH in control cells which is considered normal since the cells utilize the glucose in the medium for their growth. However, in the BCS and TTM treated cells that decrease was noticeably higher since they differed by up to 0.6 pH units (Figure 5.3C and 5.4C). The shift toward glycolysis was further established when we measured the ECAR rate in cells treated with BCS and TTM where an increase in the rate was observed even before the addition on oligomycin in the cells which blocks the ATP synthase and shifts the energy production toward glycolysis (Figure 5.13D, E and 5.14D). A study from Cooper *et al.* in feline cardiomyocytes have also shown that ECAR was increased in the presence of potassium cyanide which completely inhibits the COX activity[421].

In order to ensure that the change in pH was a result of shifting to glycolysis for energy production and not an increase in growth rate of the treated cells we also measured the cell number under the same conditions where we found that both TTM and BCS inhibit cell growth. In addition to showing that the pH change from Day 3 in the presence of both chelators, the cells also enter a stationary phase at different time points. The BCS treated cells stopped growing from Day 4 whereas in the TTM treated cells stopped from Day 3 (Figure 5.3B and 5.4B). Furthermore, the BCS treated cells started dying at Day 5 whereas the TTM treated cells continue growing but at a very slow rate. It is worth mentioning that in both treatments the cell number is approximately half of what is observed in the untreated cells.

To the best of our knowledge, no other study has measured the extracellular pH or cell growth of HEK293 cells in the presence of these two copper chelators however there are some studies that have measured the effect of copper chelation on the cell growth of different cell lines. In one of these K562 cells were treated with different concentrations of BCS which showed an inhibition of cell growth from Day 3 when cells were treated with 30 µM BCS[(415)]. TTM was also able to inhibit cell growth and proliferation in both βCT3 and ovarian carcinoma A2780 cell only after 2 days of treatment[(422)].

The inhibition of cell growth can be attributed to either reduced energy/ATP levels or due to inhibition of proteins that regulate the cell cycle. Mitosis is a highly energetically demanding process which is mainly fulfilled by oxidative phosphorylation and secondarily by glycolysis[(423)]. Based on the shift towards glycolysis, which produces enough ATP only to sustain cell survival, cells appear to be placed in cycle arrest since cells are unable to produce sufficient ATP for cell division. It is also worth mentioning that BCS after Day 5 might trigger the apoptotic pathway in the cells since a decrease in cell number is observed. Mitochondrial malfunction and an increase in oxidative stress can trigger programmed cell death and based on our finding BCS treated cells exhibit both of these which could eventually lead to apoptosis after prolonged exposure to BCS.

Furthermore, in the presence of BCS and TTM we measured the cell viability however, since we used different methods for its determination we cannot make direct comparisons. In the BCS treated cells an increase in fluorescence intensity was observed from Day 3 which was further increased by Day 5 (Figure 5.3D). The increased absorbance suggests that in the BCS treated cells more rezasurin is reduced to resorufin which implies that more electrons are available for its reduction. Increased Alamar Blue (rezasurin) reduction probably signifies some form of metabolic impairment coming from mitochondria since Alamar Blue is mainly reduced by molecules that belong to the ETC (NADPH, FADH, cytochromes etc). On the other hand, in the TTM treated cells a decrease in MTT reduction was observed from Day 4 which correlates with either lower cell levels or potentially indicates that the cells have lower reducing power coming from metabolic changes in the mitochondria (Figure 5.4D).

BCS and TTM showed similar effects on the pH and cell number but the BCS treated cells appear to reduce more Alamar Blue whereas the TTM treated less MTT. The only difference between the two dyes is that Alamar Blue can be reduced by cytochromes but MTT is not able to do this. Taking into consideration the decreased COX/CS activity in the BCS or TTM treated cells (Figure 5.7) we can assume that there is more available cytochrome *c* which can

be used to reduce the Alamar Blue and that is why there is an observed higher reduction of Alamar Blue in the BCS treated cells. The current study appears to be the only study which has measured the effects of TTM and BCS for prolonged periods on cell viability.

Our findings about D-pen are of interest in relation to our findings with BCS and TTM. The absence of any major effect in the pH or cell number and the small increase in Alamar Blue fluorescence intensity which may simply reflect a slightly higher cell number at Day 4 and 5 or prolonged growth of the cells (Figure 5.5) differs from TTM and BCS. This may indicate that if D-pen does affect intracellular copper it does so in a different way to BCS and TTM. Copper also did not have any significant effect on cell number or pH and, again, the slight increase in Alamar Blue by Day 5 is probably due to prolonged incubation with copper (Figure 5.2). The results on growth for copper first of all suggest that under basal conditions HEK293 cells have adequate supplies of copper for growth, and furthermore have adequate resource to store copper intracellularly.

5.4.2 The copper chelators BCS and TTM are able to reduce intracellular copper levels

To determine if the copper chelators can sufficiently deplete cellular copper levels we measured the intracellular copper concentration by ICP-MS. The analysis revealed that indeed we were able to manipulate the cellular levels by either adding more copper or depleting it with appropriate copper chelators. Under the experimental conditions we were able to measure copper only after 3 days treatment with the respective compound where we found that copper supplementation can increase intracellular copper levels by about an order of magnitude and copper chelation with BCS and TTM can decrease cellular copper content by more than 80%. The D-pen treated cells instead of measuring reduced intracellular copper levels a small but non-significant increase of 15% was observed (Figure 5.6).

The copper levels were compared in two different ways using copper atoms per cell or by using nmoles copper per mg of protein. That was used in order to be able to see if they were changed at the single cell level since some treatments caused inhibition of the growth rate and also based on the protein concentration in case some of the treatments had an effect on the protein levels. It is worth mentioning that the intracellular levels of copper that we determined for the HEK293 cells are in agreement with a study from Gibon *et al.* who measured copper levels with AAS and define them as 11.9 μg copper/ gr protein or 0.18 nmoles/mg protein which are almost identical with the one that we measured in the control cells (Figure 5.6)[(424)]. Unfortunately, HEK293 cells have not been used in many studies with copper chelators and

so data are unavailable in order to make comparisons with. The data for intracellular copper levels when cells were grown in the presence of different copper chelators showed an unexpected pattern. Initially we observed that both cells treated with the impermeable BCS[385] or the membrane permeable TTM copper chelator[425] reduced the intracellular copper levels. However, the membrane impermeable D-pen[426, 427] increased non-significantly the intracellular copper levels. One assumption is that since TTM is membrane permeable it will cross the cell membrane, remove copper from the copper binding/storage proteins or copper that is imported into the cells by the transporters and accumulate in the cytosol or lysosomes. However, we showed that TTM had a similar effect on intracellular copper levels to the membrane impermeable chelator BCS which chelates copper in the extracellular space and prevents copper from being available to the cells. The increased concentration of copper in the extracellular medium was further confirmed by the increased concentration in the medium of the BCS treated cells. In the TTM treated cells copper was lower in the spent medium which is difficult to explain if TTM is able to cross the cell membrane since no copper was detected either in the extracellular medium or inside the cells. To further investigate this issue we also measured molybdenum levels in the cell digests and spent medium where we showed a 4-fold increase in intracellular molybdenum levels and molybdenum in the spent medium was at 2 µM (data not shown), identical to the applied amount of TTM.

This finding suggests that a small amount of TTM is able to enter the cell but is then secreted back into the medium. The high amounts of molybdenum within the media suggests that the majority of TTM stays outside the cells, and so here it may act in a similar way to BCS in chelating extracellular copper. However, it still does not answer the question of the reduced levels of copper in the medium. One potential answer derives from a study where HUVEK cells were treated for 16 hours with TTM and then intracellular levels of molybdenum measured by ICP-MS[425]. In that study, they identified a positive correlation between the intracellular molybdenum concentration with the concentration of TTM they used to treat the cells[425]. Furthermore, they monitored the levels of molybdenum 24 hours after removing TTM where they showed a gradual decrease in intracellular molybdenum levels over a 24 hour period[425]. Similar observations were also made in animals treated with TTM and copper levels were measured in liver samples at different time points which showed that after 2 days of TTM administration copper levels were higher however after 5 days the liver copper levels dropped significantly[428]. Both studies seem to show that cells are initially importing TTM

where it chelates all the available intracellular copper and then efflux the TTM/copper complex back to the medium.

It still remains to answer why the TTM treatment causes reduced copper in the spent medium. It is suggested that TTM can chelate copper in a 1:3 ratio and it mainly removes copper that is bound to MTs[391]. Ogra *et al.* established in Long-Evans rats the mechanism of copper removal by TTM from MTs where it was suggested that initially TTM interacts with MT and then it forms a TTM/copper complex releasing MT, with the final complex being soluble[391]. The study from Ogra *et al.* also support that the molar ratio of TTM/MT should be around 1 since higher TTM concentrations can cause precipitation of copper together with molybdenum probably by forming insoluble TTM/copper polymers[391]. Under the present experimental conditions we did not determine the intracellular concentration of MT in the HEK293 cells however we know that copper concentration in the growth medium is around 0.35 μM which is 6 times less of the TTM concentration (2 μM) that we used to treat the cells. Based on the above it is possible that TTM/copper complexes formed of insoluble polymers which precipitated in the culture flasks which is why we were unable to detect it in the spent medium. The extensive washes with PBS during sample preparation removed these TTM/copper polymers from the flasks and any cells making the TTM/copper complexes impossible to detect in the cell digests.

D-pen, the most common treatment for Wilson's disease, under our experimental conditions was not able to reduce the intracellular copper but caused a small non-significant increase in copper levels. The mechanism of action of D-pen is not fully understood but according to certain studies, D-pen has poor chelator affinity for copper under normal conditions[429]. Riha *et al.* reported that D-pen was able to chelate only 26% of the Cu^{1+} and 15% of Cu^{2+} at ratio of 400:1 D-pen to copper[429]. Several studies have also shown that D-pen is not able to cross the cell membrane since it is extremely hydrophilic[430] and studies with mouse fibroblasts have shown that D-pen uptake rate was over 100 times lower than L-Den since D-pen cannot utilize the amino acid transport system in order to gain access to the cytosol[426]. The above observation was further supported by a study in HL-60 cells which were treated with 100 μM D-pen for 4 hours and then D-pen concentration in the cell supernatant was determined by high-performance liquid chromatography (HPLC) where no change on its concentration was observed[427]. Taking into consideration the above mentioned studies on D-pen, the increased concentration of copper in the cell digest accompanied by the loss of copper concentration the cell medium cannot be explained by the mechanism of action of D-pen, however, a study from Schumacher and colleagues supports that D-pen can possibly act at the membrane levels

to inhibit lymphocyte stimulation[431]. Based on that study it is possible that the D-pen/copper complex is probably "bound" to a membrane protein(s) and the extensive washes do not remove the complex from the cell surface which results in the increased copper concentrations in the cell digests. That could also explain why there is a 15% difference between the Cu atoms/cell and nmoles Cu/mg protein since the D-pen/copper complexes are accumulating in the cell surface without causing any major effect in the intracellular protein levels.

To the best of our knowledge, non-transfected HEK293 cells have not been used extensively to study the effects of copper chelation or supplementation on copper intracellular pathways, nonetheless, the effects of BCS, TTM and D-pen in other cell lines such as astrocytes or hepatocytes have been tested[432-435]. The only study that used HEK293 cells and determined copper levels in cell treated with 200 μM BCS for 20 hours by using a fluorescence copper sensor and X-ray fluorescence microscopy, found that copper levels were decreased by around 30%[436]. Similar results were also observed in astrocytes where cells incubated with 100 μM BCS and copper levels in both cell digests and medium were determined[435]. In that study they observed a gradual decrease of intracellular copper levels which was accompanied by progressive increase of copper in the medium[435]. The 50% decrease of intracellular copper concentration was accompanied by 50% increase of copper in the spent medium after only 24 hours incubation with BCS[435]. TTM was also able to decrease by 90% the intracellular copper levels of astrocytes treated with 100 μM TTM for 24 hours, a concentration that was also non-toxic to the cells[432].

TTM and D-pen have been most frequently used in studies with mouse hepatocytes since liver is the most affected organ in Wilson's disease patients[433, 434]. Studies with hepatocytes have shown that 25 μM TTM can cause copper deficiency very rapidly since they were able to decrease the intracellular copper levels by 43% after only 18 hours as determined by using AAS[434]. In that study they also measured the copper uptake rate of the cells which was significantly lower in cells treated with TTM[434]. Based on these observations they suggested that TTM acts by increasing the efflux rate, decreasing the rate of uptake and then overtime mobilizing intracellular copper storage[434]. TTM did not seem to have the same effect in all cell types since in the same study they treated human fibroblasts with TTM and found that TTM did not affect either copper uptake or its intracellular levels[434]. Differences amongst these cell lines might simply reflect the requirement of each cell line for copper or the different capacity for intracellular copper chelation which is further supported by our results where we observed that in HEK293 cells TTM or BCS are able to decrease intracellular copper levels by more than 80%. Studies in hepatocytes have shown that D-pen was unable to

decrease intracellular copper levels or the uptake rate of copper even after 40 hours incubation with 100 μM D-pen and in some cases it caused an increase in intracellular copper levels[433]. This chelating function of D-pen was attributed more to its structure since it contains an amino acid with sulphydryl group as well as an α-amino and cardoxylin acid group[433]. These two groups are able to chelate Cu^{2+} ions in a bidentate or tridentate complex[433]. Based on these properties of D-pen they suggested that D-pen binds copper which is capable of rapid exchange and therefore the complex acts as a substrate for the transport system which stabilizes the rate of copper uptake and release[433]. Our results using D-pen in HEK293 cells are in agreement with this possible function of D-pen since we do not see any major change in intracellular copper levels.

5.4.3 The activities of COX/CS and SOD are severely affected in BCS and TTM treated cells

The treatment with BCS and TTM caused significant loss of intracellular copper which consequently affect the activity of two important cellular enzymes, COX and SOD. COX/CS activity in the BCS and TTM treated cells was decreased in a time dependent manner with at Day 3 only half the COX/CS activity remaining relative to Day 1. One copper ion is chelated by two BCS molecules and by titrating the BCS concentration we found that as long as BCS is an excess it can cause a similar effect on COX/CS activity overtime. When BCS was 10-fold higher than that is required to chelate all available copper in the medium (5 μM BCS for 0.35 μM copper in the growth medium) it was able to decrease COX/CS by only 30% at Day 3, approximately half of what 50 and 200 μM BCS can achieve but similar to Day 1 effect (Figure 5.7 and B.4). TTM can chelate up to three copper ions per molecule and our findings shows that TTM can cause slightly greater inhibition of COX/CS activity (Figure 5.7). Also, lower TTM concentrations (0.5 μM) did not change the effect on the final COX/CS activity overtime (Figure B.4A). It is also worth mentioning that both BCS and TTM are able to markedly reduce the protein levels of COX2 overtime however BCS and TTM only caused a minor decrease in COX1 protein levels at Day 3, around 20% (Figure 5.8 and 5.9). For further discussion see section 5.4.3.

BCS also had a similar effect on SOD activity overtime since we initially showed that SOD activity was decreased by 50% at Day 1 and by 70-80% at Day 3 (Figure 5.16). A similar pattern to COX/CS activity was also observed when we titrated BCS and measured SOD activity since the 5 μM BCS only inhibited SOD activity by 35% at Day 3 (Figure B.4B). The effect of TTM on SOD activity was greater than BCS and appeared time and concentration

independent since more than an 80% decrease was measured both at Day 1 and 3 and also when cells were treated with 0.5 or 2 μM TTM (Figure 5.16 and B.4B). Although SOD activity was severely affected by BCS and TTM, the protein levels of SOD1 and SOD2 did not change which indicated that when copper is not available SOD1 remains in the cytosol in apo-SOD1 form until it acquires copper (Figure 5.18 and 5.19).

From the above results it seems that the first enzyme to be affected by copper depletion is SOD and that BCS and TTM have different mechanisms of action. Both copper chelators decreased intracellular copper levels to the same extent but we showed that SOD is affected more severely and earlier in the time course than COX/CS activity which could occur from either due to the different turnover rates of the respective proteins or to their subcellular localization and copper availability within the organelle. In addition, BCS and TTM appear to have different effects on the activity of these two enzymes which potentially correlate with their extracellular and intracellular localization. Given the different results for extracellular copper, BCS and TTM appear to work by slightly different mechanisms of action, even if the final result is similar.

BCS is unable to cross the cellular membrane however it reduces the intracellular copper levels and SOD activity by 80% and COX/CS by 70% at Day 3. The gradual decrease in SOD and COX/CS activities indicates that the cells contain stored copper in dedicated copper ligands. For SOD1 the protein responsible for the delivery/storage of its copper is CCS which is also able to sense the copper availability and adjust CCS protein levels[134]. In our results we also showed that CCS protein levels increase at Day 1 in the BCS treated cells in response to copper limitation however by Day 3 CCS levels returned to normal (Figure 5.17). CCS half-life has been estimated around 17-20 hours whereas SOD1 is around 35-40 hours[134, 321] which indicates that in the first 24 hours CCS protein levels were increased due to copper limitation and then start degrading and that by Day 3 is the intermediate of a degradation and synthesis cycle of the protein. Based on this, it is possible that by Day 1 there is a fraction of CCS that still contained copper and was able to incorporate copper into SOD1 but as time progresses and the existing CCS starts to degrade or lose copper, the newly synthesized protein will not be able to acquire copper, and so will not activate SOD1 in the cytosol.

The ligand that transfers copper to the mitochondria is yet unknown however studies have shown that mitochondria contain their own pool of copper within the mitochondrial matrix[103]. Both mitochondria and theis proteins have around a 100 hour turn over[437, 438] which possibly explains why the remaining COX/CS activity was slightly higher in the

treated cells on both days. That suggests that the already formed complexes remain intact and able to use the incorporated copper to fulfil the cellular energy demands however, newly synthesized proteins are affected by copper availability since COX2 appears to be lost very rapidly. Another possible reason why COX retains greater activity following copper chelation might be correlated with the fact that mitochondria have their own pool of copper which seems to be higher compared to other copper storage locations in the cytosol. Based on study in HUVEC cells, mitochondria contain about 10-times more copper relative to cytosol[103, 439]. Taking this into consideration it is possible that since BCS chelates the extracellular copper, cells are not able to import copper and as they are growing and undergoing cycles of protein degradation and synthesis they have to use their already stored copper which is also going to be eventually "released" in the extracellular space during these processes.

TTM has the property of being able to cross the cell membrane which may allow TTM to remove copper more efficiently from proteins localized in the cytosol and potentially at later stages from the mitochondria. The initial observations on TTM suggests that TTM is able to remove copper efficiently when copper is bound to MTs in the liver of LEC rats and from Cp in the serum, however, more recent studies have shown that TTM can also remove copper from Atox1 and SOD1 in the cytosol[425, 440-442]. Juarez *et al.* reported that TTM is able to inhibit the activity of SOD1 not only in human HUVEC cells but also in a purified SOD1 isolated from bovine heart[425, 440]. In that study they incubated purified bovine SOD1 with increasing concentrations of TTM and found that SOD1 IC_{50} was around 0.33 μM TTM after 24 hours incubation and that the maximal inhibition was achieved after 16 hours of incubation. These results are in agreement with our findings since we also found that 2 μM TTM inhibits SOD activity and that after 24 hours there was more than 85% inhibition without affecting the protein levels of SOD1 and SOD2. Copper atoms in SOD1 dimers are well protected, not easily accessible and also SOD1 binds copper with high affinity[45, 443] which raises the question of how TTM is able to get into the dimer and remove the copper atoms. A possible reason for being able to remove copper from SOD1 might be the small structure of TTM which allows easy access to SOD1 dimer where it removes copper.

An alternative possibility is that TTM removes copper from the cytosolic chaperones Atox1 and CCS. A study by Alvarez *et al.* showed that TTM can form stable complexes with Atox1 in solution by forming a sulfur-bridged copper molybdenum cluster[442]. In this cluster an Atox1 trimer is coordinated with four copper ions and one TTM molecule[442]. CCS D1 is structurally homologous to Atox1[125, 126] and possible interactions amongst the copper ions, TTM and CCS might also occur which is more likely to happen rather than through TTM

directly removing copper from SOD1. Further, experiments should be conducted with human SOD1 and CCS proteins in order to identify from where TTM is efficiently removing copper. The possibility of removing copper from both proteins simultaneously should be also examined. It is worth mentioning that in the TTM treated cells the expected decrease in CCS protein levels under copper depleting conditions was not observed at either Day 1 or Day 3 even if intracellular copper levels were reduced by more than 80% (Figure 5.17). That observation could further support the idea that TTM forms a complex with CCS which might stabilize CCS and prevent or slow the degradation process.

COX/CS activity was also affected in the TTM treated cells in a time dependent manner but at a slightly higher rate than with BCS which might be due to the fact that TTM is possibly removing copper initially from the ligand that delivers copper to the mitochondria which makes mitochondria dependent on the matrix pool of copper for COX activity. Another possibility is that TTM can enter mitochondria at a slower rate and start removing copper from the mitochondrial copper-binding proteins after removing cytosolic copper. COX2 protein levels appear to be rapidly affected by TTM as COX2 was reduced to only 30% of control COX2 within 24 hours.

Copper supplementation or D-pen use had no major effect on COX/CS or SOD activity. Even when the intracellular copper levels were increased by an order of magnitude, no change in COX/CS or SOD activity was observed, possibly due to an efficient copper storage or efflux system of the cells, and use of a copper concentration that was not toxic to cells and did not induce any damage (Figure 5.7 and 5.17). Our results show that D-pen was unable to either effect the cell growth or change the intracellular copper levels however, based on its mechanisms of action, it would be expected to affect SOD activity since D-pen can produce H_2O_2 during chelation of Cu^{2+} to Cu^{1+}[396, 397]. At Day 1, although we observed a significant 8% decrease in SOD activity, changes at these levels, especially in cells, might not be of biological significance (Figure 5.16) and similarly SOD1 protein levels by Day 3 only show a 10% decrease (Figure 5.18). Our conclusion is that D-pen is not able to induce any major change in the intracellular copper pathways in HEK293 cells even if studies in Wistar rats treated with D-pen show a significant decrease of both SOD and COX in different tissues[444, 445], including heart, brain and kidneys which lose more than 50% of COX activity whereas SOD activity was decreased by 20-30% in the liver, kidneys and red cells after D-pen treatment for 20 days[444, 445].

Our results concerning copper chelation are in agreement with studies that have been conducted in cancer cell lines such as ECC-1, IGROV-1 and βTC3 as well as HUVEC and MEFs. Copper chelators have been studied extensively in cancer cell lines due to the pro-angiogenic properties of copper since it acts as a cofactor for several proteins such as VEGF, basic fibroblast growth factor (bFGF) and angiogenin and targeting angiogenesis is considered an effective anti-cancer therapeutic strategy[446, 447]. HEK293 is also an induced tumorogenic cell line and therefore comparison of the effects of copper chelation amongst the different cell lines can be performed.

One study that used TTM to treat HUVEC cells and study the effect on cell proliferation and SOD activity found that TTM can inhibit cell proliferation with an IC_{50} around 1.4 μM, accompanied by a decrease in cellular SOD activity after 48 hours incubation with 7 μM TTM[425]. However, in that study, COX activity did not change even with 100 μM TTM[425]. A study with βTC3 cells showed that TTM was able to reduce COX activity by 50% after treatment with 10 μM for 24 hours where they also observed decrease in $\Delta\Psi_m$ which further indicated diminished activity of the electron transport chain and consequent mitochondrial dysfunction[422]. Similar results were also reported from tumours derived from mice treated with TTM daily for three weeks[422] where both cells and tumours showed higher lactate levels indicating a shift to glycolysis for energy production[422]. Whilst not using CS to normalize COX activity, the effect of TTM on COX activity is similar to the current study despite slightly different TTM concentrations[422].

Further studies on TTM and COX activity showed not only that COX activity is gradually decreased overtime but also the decrease is highly dependent in the cell line[416]. ECC-1, IGROV-1 and 2008 cell lines treated with 30 μM TTM showed after 24 hours that COX was decreased by 80%, 100%, 50%, respectively[416], which may indicate that any effect of TTM is dependent on a cells requirements for copper and energy demands[416]. Once again in that study while CS was not used to normalize COX activity, the large loss of COX especially in the ECC-1 and IGROV-1 cells, are unlikely to change the final results[416].

Other chelators such as TEPA and trientine (which is the second most common treatment for Wilson's disease) have been studied. Studies with TEPA in HL-60 and C_2C_{12} cell lines have shown that TEPA is able to inhibit by over 60-80% the activities of both SOD and COX after 92 hours incubation at 50 μM[448, 449]. In the same study, cells treated with 25 μM copper showed no change in either SOD or COX activity[449]. Trientine has been used to treat SH-SY5Y cells where prolonged (more than 10 days) exposure caused a significant decrease in

both COX and SOD activity with SOD showing a more acute lose (80% after 3 days) whereas COX declined gradually with the activity being eliminated after 9 days of treatment[414]. Both TEPA and trientine are cell membrane permeable and their effects on SOD and COX activity are similar to our studies with TTM[384].

Our findings on SOD and COX activity in HEK293 cells after treatment with BCS and TTM are in agreement with already published studies in other cell lines treated with TTM and also compared to other copper chelators. The general conclusion from our results and published studies indicate that copper deficiency initially inhibits SOD and then mitochondrial function.

5.4.4 Copper chelation with BCS and TTM affects mitochondrial proteins

As noted previously, the protein levels of COX2 but not COX1, were significantly affected in the BCS and TTM treated cells, despite both proteins being part of the catalytic core of COX. COX1 did however, show a 20% decrease in the BCS and TTM treated cells at Day 3 but not at Day 1 (Figure 5.8C and D). Under our experimental conditions the levels of mitochondria (VDAC1) did not show any major change even if the mitochondrial mass assessed by MitoTracker green show a small non-significant change in the BCS and TTM treated cells (Figure and 5.8E, F and 5.15). COX1 protein levels relative to VDAC1 were initially higher at Day 1 and then declined at Day 3 (Figure 5.8G and H) which possibly suggests that the mitochondria detect the lack of COX activity and respond by producing more of the protein that initiates the assembly of COX. In the absence of available copper to create the Cu_B centre, COX1 will begin to degrade by dedicated proteases in the IMS, a process which may take longer compared to COX2[97, 306]. The half-life of the COX subunits has been determined in a hepatoma monolayer culture to be more than 100 hours although studies in fibroblasts have shown that COX half-life was around 48 hours[437, 450]. Possibly the difference in the half-life reflects more the cell type rather than the biogenesis of the complex. In our results we showed that the protein levels of COX1 start to decrease after 72 hours which in between the two cell lines. One assumption is that lack of copper will initiate a faster degradation of COX1, however, it seems that the protein is more stable for a certain period of time which might depend on the incorporation of the heme a/a_3 in the protein during its biogenesis.

Little is known about how copper and heme a/a_3 are inserted into COX1 and the main indications come from studies in yeast and fibroblasts from patients carrying a mutation in one of the assembly factors (COX10, COX15 or SURF-1). Based on these studies after the translation and incorporation of COX1 in the IMS, the hemeylation begins shortly after[451, 452]. COX10 and COX15 play important roles in heme *a* biosynthesis since studies with

fibroblasts missing these proteins have shown that COX1 becomes very unstable and susceptible to degradation[451, 452]. Copper incorporation into COX1 seems to happen at later stage or simultaneously by COX11[106, 116]. In yeast strains lacking COX11 or Sco1 were peroxide sensitive due to the accumulation of COX1-heme a/a_3 intermediate[453]. Also, in COX11 deficient yeast the degradation rate is higher compared to COX1 which further supports that COX2 is prone to degradation when complex biogenesis is inhibited[453]. Similarly, in mammalian cells containing a mutated form of the SURF1 assembly factor, COX1 protein levels accumulated together with COX4 and COX5a suggesting that heme a_3 is present in the subcomplex[117].

In the current study COX11 is unable to insert copper into COX1 due to copper deficiency combined with the lack of COX2 protein which is unable to block the channel within the IMS side of COX1 where heme a/a_3 is inserted[116, 453]. We can assume that the incorporation of heme a/a_3 into COX1 will stabilize the protein for a certain period of time and then the lack of copper will initiate its degradation as we start seeing at Day 3. The lack of a significant effect of copper depletion in COX1 was also present in the brain studies of the healthy controls and AD cases where we observed that the reduced copper levels did not cause any major decrease in COX1 levels which seems to be able to sustain its expression or degradation rate for a longer period. A similar effect was also present in a study that treated mice for 25 days with BCS and which showed only a small decrease in COX1 protein levels[454].

The protein levels of COX2 are severely affected by TTM and BCS chelation. From Day 1 COX2 protein levels were decreased by more than 50% in the BCS treated cells and by 70% in the TTM treated cells (Figure 5.9). Once again the TTM treated cells seems to be affected more than the BCS probably due to TTM intracellular localization which enables it to either remove copper directly from COX2 or the ligand that delivers copper to the mitochondria. As previously discussed, COX2 seems to be more sensitive to copper deficiency where the lack of copper incorporation and assembly into newly synthesized complexes trigger COX2 degradation by dedicated proteases in the IMS[97, 306]. Our results are in agreement with studies in K562 cells which treated with 10 and 20 μM BCS and found that COX2 protein levels were decreased by more than 50% after 3 days[415]. Similar findings with 125 μM trientine in SH-SY5Y cells showed COX2 protein levels also decreased by more than 70% after 3 days treatment[414, 455]. Prolonged exposure with trientine caused the complete elimination of COX2 protein levels[414]. Taking into consideration our results and already published studies we can conclude that copper deficiency mainly affects the protein levels of COX2 rather than COX1 possibly due to its later stage of incorporation in COX biogenesis or

due to the lack of cofactors that can stabilize COX2 for longer or because COX2 contains a more sensitive degradation feedback mechanism which will be activated immediately after failure of copper incorporation. The only exception based in our data is D-pen which was not able to cause any biological significant change in the protein levels of COX or in the mitochondrial mass (Figure 5.8, 5.9 and 5.15).

Copper supplementation did not cause any major effect on mitochondrial levels however it seems that copper supplementation can induce some changes in COX protein levels (Figure 5.8, 5.9 and 5.15). At Day 3 both COX1 and COX2 protein levels were increased in the presence of 10 μM copper although only the 31% increase of COX1 was significant which suggests that prolonged incubation with copper may induce transcriptional activation through metal or oxidative stress mediated mechanisms[456]. Another possible reason may be due to the slightly higher levels (11%) of mitochondria/VDAC1 since the ratio of COX1/VDAC1 did not show any significant change under these conditions. At Day 1 COX2 protein levels were lower by 26% in the copper treated cells but the same time the COX2/VDAC1 ratio did not change which may reflect a small mitochondrial loss.

Recent studies have shown that COX in the mitochondria is associated with Complex I and III in order to form supercomplexes or "respirasome"[400]. The role of supercomplexes is not clear but may involve either substrate channelling or complex stability[400]. Schägger *et al.* has proposed a model of the network in the mammalian respiratory chain complexes which postulates that mitochondria have two copies of the large building block complex comprising Complexes I, III and IV ($I_1III_2IV_4$) and a smaller single building block without Complex I (III_2IV_4)[400]. In order to understand if the effects of COX have any impact in the supercomplex formation and on mitochondrial respiratory function we measured the protein levels of two major subunits of Complex I. Functionally, Complex I is divided into a dehydrogenase module, which oxidises NADH, a hydrogenase module, which transfers the electrons and has been suggested to operate as a redox-driven proton pump, and a transporter module, proposed to act as a conformation-driven proton pump[457]. The dehydrogenase module consists of NDUFV1, NDUFV2 and NDUFS1 subunits, the hydrogenase module of at least the NDUFS2, NDUFS3, NDUFS8, ND1 and ND5 subunits and the transporter module of at least ND2, ND3, ND4, ND4L and ND6 subunits[457]. In the current study we determined the protein levels of the NDUFV1 and NDUFS1 of the behydrogenase module due to the significance of their function in Complex I activity. NDUFV1 contains the first NADH binding site and also binds the FMN, providing the conversion of the 2-electron donor NADH to 1-electron transferring iron-sulfur clusters[458]. Whereas, NDUFS1 contains four out of the

seven iron-sulfur clusters which are essential for the activity of Complex I[459]. Our results showed that the protein levels of NDUFS1 did not seem to be affected by BCS or TTM treatments however, at Day 3 D-pen caused a 20% increase in NDUFS1 protein levels (Figure 5.12). The increased levels of NDUFS1 in the D-pen treated cells possibly correlates with the higher mitochondrial levels (12%) since when normalized with VDAC1 no significant increase in NDUFS1 was observed. Why D-pen causes a small increase in mitochondria levels is unclear given our data and since it is unclear what are its exact mechanisms of action.

Copper supplementation appears to affect the protein levels of both NDUFS1 and NDUFV1 similarly. Initially, at Day 1 both proteins decreased by 22% and 14% respectively, however, by Day 3 their levels returned to normal or even increased. This suggests that initially copper may be toxic to cells but after longer exposure the cells are able to compensate, possibly by producing intracellular copper chelators such as MTs, and can adjust their protein levels based on the environmental copper concentration. It is well established that copper is able to replace the iron within the iron-sulfur clusters and induce toxicity and since both NDUFS1 and NDUFV1 have these clusters we can assume that copper initially is able to affect NDUFS1 and NDUFV1 stability or degradation rates[22]. Similar effects have also been observed in SY-SY5Y cells where the levels of proteins consisting the Complex I were significantly decreased in the presence of 150 or 300 μM copper after 24 hours of treatment[26].

In relation to protein levels of NDUFV1 we observed, especially in the untreated cells, that the levels of NDUFV1 decreased overtime by as much as 50% and secondly that treatment with 200 μM BCS affects NDUFV1 protein levels (Figure 5.10 and 5.11). NDUFV1 assembly into Complex I is suggested to occur by two models, the *de novo* or the "exchange pathway". The *de novo* route supports that assembly takes place in multiple-steps where initially several subunits are first combined into smaller intermediates of the three functional modules and subsequently the holo-enzyme is formed by joining these preassembled modules[460]. The "exchange pathway" is parallel to the *de novo* pathway and suggests that newly imported subunits replace their previously incorporated counterparts in the holo-enzyme[460]. In the "exchange pathway", Dieteren *et al.* measured the live cell dynamics of NDUFV1 together with Complex I proteins and showed that about half of the NDUFV1 protein exists in a mobile fraction whereas NDUFV1 in the dehydrogenase module exists mainly as a membrane bound form[461]. The above suggests that under normal conditions the dehydrogenase module is assembled in a subunit-by-subunit manner on the surface of the mitochondrial inner membrane bound Complex I intermediate, which further supports that this module is highly dynamic and its assembly-disassembly depends on cellular needs[461].

By blocking mitochondrial protein syntheses by adding chloramphenicol they found that Complex I is extensively broken down into intermediates which under normal conditions is avoided by continuous exchange with the bound subunits[461]. Dieteren and colleagues also suggested that increased superoxide production can cause instability of the protein and initiate its degradation[461]. Based on these findings, under our experimental conditions the fact that only NDUFV1 decreases overtime may suggest that the exchange rate between bound and unbound protein is slow with Day 3 being the midpoint of NDUFV1 protein degradation and synthesis. By Day 3 the control cells have reached maximum confluency which possibly places them in the stationary phase and cells consequently reduce mitochondrial respiration and protein synthesis for energy conservation. Also, Dieteran *et al.* suggested that increased superoxide anion production by mitochondria can induce the degradation of NDUFV1 however based on our results with BCS the superoxide anions were higher by almost 60-80% but the protein levels of NDUFV1 were increased by 27% relative to controls and in the TTM treated cells, where superoxide anion production was also increased, NDUFV1 protein levels did not change (Figure 5.10 and 5.20).

Studies in mouse fibroblasts lacking the COX10 assembly factor have shown significant decrease in the assembly and stability of Complex I[451]. The complete lack of COX10 results in faster degradation of Complex I and that low levels of COX activity or assembled complex were able to retain the function of Complex I[451]. This observation is more likely to explain why in the BCS treated cells NDUFV1 protein levels were higher, but also why cells by Day 3 even when COX2 was completely absent they still retained around 10-20% of COX/CS activity since cells can maintain the assembly of the preformed Complex I in the supercomplexes. This is further supported by the fact that the acute presence of BCS (Day 1) caused a small decrease in NDUFV1 protein levels but the longer exposure triggered a mechanism of Complex I survival (Figure 5.10). Further studies will need to be conducted in order to understand the interactions of these two complexes and to determine how Complex I activity is affected.

Taking into consideration all the above mentioned findings we can conclude that NDUFV1 protein levels are possibly decreasing overtime due to adjustment to the cell needs or because even under normal conditions as cell grow they will produce more superoxide anions and this will have an impact to NDUFV1 protein levels[461]. The effects of copper chelation on Complex I proteins may be correlated with undefined mechanisms which attempts to stabilize mitochondrial supercomplexes to maintain maximal respiration.

5.4.5 Does copper chelation affect mitochondrial bioenergetics?

Mitochondria play an essential role in cellular energy metabolism and mitochondrial $\Delta\psi_m$ is a key indicator of cell viability since loss of the $\Delta\psi_m$ is associated with cellular stress and dissipation of $\Delta\psi_m$ may promote apoptosis[462]. The $\Delta\psi_m$ is generated by the accumulation of the proton driven electrochemical gradient across the IMS, as a result of the activity of the protein complexes of the ETC as well as from the integrity of the inner membrane[87]. Electrons are normally generated by the oxidation of the reduced NADH at Complex I and from oxidation of succinate by Complex III, and flow through the ETC with oxygen being the final electron acceptor at COX[463]. Electron transport through ETC is coupled with proton translocation by the inner membrane Complexes I, II and IV[463]. This activity generates the electrochemical proton gradient, which is utilized by the mitochondrial ATP synthase for the production of ATP[464]. The proton pumps of the ETC together with the ATP synthase create proton circuits across the inner membrane, which is central to mitochondrial bioenergetics and cellular homeostasis[87, 462-464].

Identifying changes in the respiratory state of a cell is of major importance and cells have evolved multiple levels of regulation. In the intact cell the major modulator of the respiratory state is the balance of ATP demand with substrate availability. However, other factors such as ROS, cellular/intracellular calcium signalling pools and the redox state of the ETC can influence respiratory activity[465]. Recently, a simple mitochondrial function test has been produced which can be used to examine cellular energetics[402-404]. The assay uses inhibitors of the respiratory chain components and uncoupling agents to examine and quantify ATP-linked oxygen consumption, proton leak, non-mitochondrial oxygen consumption, maximal respiratory capacity, spare capacity as well as coupling efficiency[402-404]. Oligomycin is used to examine the coupling efficiency and allows the calculation of the basal oxygen consumption that is related to ATP demand which can also be ascribed to proton leak[402-404, 466]. Under our experimental conditions we did not observe any significant change in basal respiration in cells treated with TTM, BCS or copper, however, they were some minor changes in cell treated with 50 μM BCS which showed a non-significant increase indicating that under this condition the cells are facing increased ATP demand which forces them to consume more oxygen for ATP production. Under the same conditions ATP production was also higher (Figure 5.13A). The fact that the basal respiration rate was unaffected in the presence of BCS and TTM was surprising since we knew that under these conditions only 10-20% of COX activity remained. That observation could be possibly explained by studies which have shown that superoxide anions, which are produced by Complex I and III, can

directly reduce cytochrome *c*, and the reduced cytochrome *c* can directly pass its electrons into COX, resulting in enhancement of the basal respiration rate[467-469]. Under our experimental conditions we know that in the BCS and TTM treated cell mitochondrial superoxide anions are increased by more than 60% based on the increased fluorescence intensity of MitoSOX red (Figure 5.20). Given that COX is only functioning at a very low rate, cytochrome *c* is available for reduction by other molecules such as superoxide anions, and given that in the BCS and TTM treated cells there is increased production of superoxide anions we can hypothesise that a reduction of cytochrome *c* will occur which makes it able to pass the electrons to COX resulting in mitochondrial respiration.

Studies with the Seahorse mitochondrial stress test have shown decreased basal respiration in the presence of BCS or TTM. K562 cells treated with 10 or 20 μM BCS showed more than 50% decrease in basal respiration and ECC-1 cells grown in the presence of 30 μM TTM showed a similar effect was present[415, 416]. However, both studies failed to normalize the measured OCR (pmoles/min) with the corresponding protein levels or cell number[415, 416]. Our results also showed 30% decrease in basal respiration and 19% in ATP production in cell treated with 2 μM TTM in the absence of a normalization step. Our studies show that by Day 3 in the TTM treated cells the growth rate had been significantly inhibited and the reduced OCR in pmoles/min may simply represent the lower cell number. However, in a study that isolated mitochondria from mouse liver treated with BCS for 25 days, the basal respiration was higher indicating that deficiency of COX is not a limiting factor for total respiration[454].

Coupling efficiently is a bioenergetics parameter that reflects multiple processes underlying oxidative phosphorylation such as ATP turnover and proton leak across the inner membrane which can also be quantified individually by inspecting the oxygen consumption rate[466, 470]. The coupling efficiency represents the proportion of respiratory activity that is used to make ATP and is significantly higher in cells treated with BCS or TTM. Coupling efficiently is around 79% in the HEK293 cells which is similar to other human cell lines such as L6 myoblasts and myotubes (around 80%)[471]. In the presence of BCS an increase by more than 2% and in TTM by 3% of coupling efficiency was observed and these changes further indicate that mitochondria are using the majority of the oxygen to produce ATP (Figure 5.13 C). The changes are so small that erase the question of how biological significant are they. Even if studied in different cell lines have indicated similar changes as significant[471, 472] it is still possible that they might not represent a functional change in the cells. Further study is required in order to understand if that small change reflects a real biological changes in mitochondrial function.

Proton leak can take place at two places: through mitochondrial anion carriers or through the lipid bilayer[473]. In cells treated with 200 μM BCS and 2 μM TTM we observed a small non-significant decrease in proton leak (15% and 16% respectively) which indicated that under the conditions where COX activity is less active there is also less proton leak between the inner membrane and the mitochondrial matrix. COX is one of the complexes that is responsible for the proton leakage and since in the BCS and TTM treated cells COX is impaired and less able to pump protons across the membrane. This decreased proton leak will also affect the ATP synthase function which eventually results in less ATP production by the mitochondria although under the current conditions no change was observed in ATP production. The lack of effect on ATP production from the mitochondria has also been seen in studies with mice fed a copper deficient diet where both COX activity and basal respiration were decreased in copper deficient hearts but there was no change in ATP synthase[474].

The addition of the uncoupler FCCP allowed the determination of the maximal respiration and the spare capacity[466]. FCCP allows protons to cross the mitochondrial inner membrane disrupting the proton gradient and dissociating oxidation in the respiratory chain from phosphorylation, which allows the function of the ETC to be evaluated separately from potential changes in ATP synthase[475]. After the addition of FCCP we showed an increase in the maximal respiratory capacity especially in cells treated with 2 μM TTM. However, the 22% increase was not considered significant (Figure 5.13B). The increase in maximal respiration indicates that in the TTM treated cells protons are flowing faster or that the proton gradient formed in the inner membrane was higher either due to an increased level of protons or due to disruption in the $\Delta\psi_m$ which allows easier transfer of protons.

By subtracting the basal respiration rate from the maximal respiration rate we were able to calculate the spare respiratory capacity an important bioenergetics marker which shows the extra mitochondrial capacity available in a cell to produce energy under conditions of increased work or stress and which is thought to be important for long-term cellular survival and function[407, 476]. We observed that the 2 μM TTM treated cells had 50% more spare capacity (Figure 5.13B). Under these conditions, cells have maximal COX and SOD deficiency however the ETC of the HEK293 cells is still able to move protons from the mitochondrial matrix into the inner membrane in the presence of the uncoupler FCCP. A possible explanation might be due to an increased mitochondrial mass however MitoTracker green studies suggested a 17% non-significant decrease (Figure 5.15). Since the mitochondrial mass is not changing and the remaining COX activity is less than 20% we can assume that the increased respiratory capacity indicates a disruption in the $\Delta\psi_m$. The catalytic activity of COX

is also regulated by the mitochondrial $\Delta\psi_m$[477, 478] and since in the TTM treated cells there is no copper to catalyse the reduction of oxygen to water and transfer protons from the matrix to the inner membrane, this will result in a decrease of the $\Delta\psi_m$. Lastly, the mitochondrial bioenergetics assay allows determination of the non-mitochondrial oxygen consumption which was less than 10% of total oxygen consumption in HEK293 cells[408]. No significant change was observed in the non-mitochondrial oxygen consumption rate with any condition.

Control over oxygen consumption is a combination of different factors including the ability of the respiratory chain to transport electrons, the availability of oxidizable substrate and transport into the mitochondrial membrane, in addition to ATP turnover[465]. Mitochondrial bioenergetics analysis in cells treated with copper chelators (BCS and TTM) showed that mitochondrial function alters since the inhibition of COX causes only minor effects on the ETC. Generally, mitochondria are still able to respire following copper chelation or supplementation since no significant change in the basal and ATP production was observed. This indicated that ATP synthase is still functioning and that electrons are able to reach the synthase possibly via reduction of the available cytochrome *c* by superoxide anions. Furthermore, the increased maximal respiratory capacity in the TTM treated cells indicates that mitochondria are able to respond to changes in conditions where important cofactors are missing, by changing the regulation of certain enzymes. What was surprising is that even if glycolysis was unregulated, as indicated by both increase ECAR and lower pH (Figure 5.3, 5.4 and 5.14) this did not seem to affect oxidative phosphorylation since studies have shown that glycolytic intermediates regulate negatively the oxidative phosphorylation (Crabtree effect)[479]. The above might indicate that copper chelators can cause up-regulation of some of the enzymes in the glycolytic pathway which results in increased production of lactic acid. It is also worth mentioning that only the intracellular copper chelator TTM caused significant changes not only in mitochondrial biogenetics, but also in glycolysis, since at Day 3 the ECAR was slightly higher in the TTM treated compared to BCS treated cells (Figure 5.14D).

Studies in primary cardiomyocytes with complete inhibition of COX with the addition of 2 mM potassium cyanide have shown that the basal OCR is decreased by more than 80% and the ECAR increased by almost 50-fold[480]. These findings suggest that when COX is completely inhibited the ECT is non-functional and that cells have to turn completely to glycolysis to fulfil their energy demands[480]. A possible explanation why copper chelation does not cause the same effect in the mitochondrial bioenergetics and glycolysis might be due to the different mechanism of inhibition between potassium cyanide and chelators. Cyanide inhibits COX activity by binding to the Cu_B and heme a_3 site in COX1 whereas the copper

chelators only remove the copper from COX2 and slowly from COX1[481]. As discussed above, neither TTM or BCS had major effects in COX1 protein levels until later stages of the experiments which further supports the suggestion that if there is not complete inhibition of all the redox centres of COX, the enzyme is still able to function at low levels. On the other hand, cyanide which seems to inhibit two out of the four redox centres causes total inhibition of COX activity.

5.4.6 Protein levels in the copper secretory pathway are not significantly affected by copper chelation

In the secretory pathway we were able to measure only the protein levels of the cytosolic chaperone Atox1 and its target protein ATP7a since we were able to identify other secreted enzymes. Also, we could not use the activity of Cp since the growth medium contained serum which has high amount of bovine derived Cp. For Atox1 protein levels we saw no significant change in any of the tested conditions at Day 1, however, by Day 3 Atox1 protein levels decreased in cells treated with copper or BCS and increased in the TTM and D-pen treated cells. Studies in HeLa cells have shown that Atox1 half-life is around 72 hours and that copper levels did not have any impact on either its levels or degradation rate[482]. The decreased levels of Atox1 by Day 3 in the copper and BCS treated cells may represents the natural degradation process of Atox1 in the cells. However, the fact that in the TTM treated cells Atox1 protein levels increased by Day 3 might be correlated with the ability of TTM to form complexes with Atox1. Since at Day 3 the majority of the copper has been already removed from the cells TTM might have formed stable complexes with Atox1 which inhibits the Atox1degradation process[442].

Why D-pen is able to induce increased expression of Atox1 is unclear since in the D-pen treated cells intracellular copper levels were slightly increased although D-pen is unable to cross the cell membrane and directly interact with Atox1. A possible reason for the increased Atox1 levels in the D-pen treated cells might be correlated with the transcription factor function of Atox1 which is able to regulate not only the protein levels but also the activity of SOD3[55, 56]. SOD3 is an extracellular Cu/Zn SOD which is responsible for the dismutation of superoxide in the extracellular space[55, 56]. Since D-pen is not able to cross the cell membrane and that in the process of copper chelation D-pen generates ROS[396, 397] this may require higher levels of extracellular SOD3. Increased demand for SOD3 might regulate the intracellular protein levels of Atox1 which will further initiate the transcription of SOD3. Unfortunately, under the current experimental conditions we are not able to separate the

activities of the three SOD proteins and were unable to determine SOD3 protein levels in either cells extracts or spent medium.

The protein levels of ATP7a did not change in the majority of the experimental conditions and time points, with the only exception being Day 3 in the copper treated cells where ATP7a protein was significantly increased by 20%. Experiments in different cell lines have shown that copper chelation or supplementation does not affect the expression levels but the localization of ATP7a in the cell[68, 69]. Under normal conditions ATP7a localize to the Golgi membrane but when copper levels are higher it shuttles to the cell membrane in order to export excess copper from the cells[68, 69]. In copper depleting conditions ATP7a is retained in the Golgi membrane without effecting the protein levels[68, 69] which is consistent with our results from treatments with different copper chelators. The 20% increase in ATP7a in copper treated HEK293 cells might be correlated with excess copper concentration with chronic rather than acute exposure inducing a slight increase in ATP7a expression.

From the above mentioned results we can conclude that copper chelation or supplementation does not cause any major effect in the copper secretory pathway and some of the effects in Atox1 might be correlated with its half-life or the mechanism of action of the compound. Finding a way to measure accurately the activity of a secreted copper binding enzyme might give better insight of how copper availability regulates the secretory pathway.

5.5 Conclusions

In the current study we identified the effects of copper chelation on intracellular copper pathways. We showed that the extracellular copper chelator BCS and the intracellular copper chelator TTM affected the activity of two important cell enzymes, SOD and COX. Generally, the two chelators seem to act in a similar way on the activity or the protein levels of these two enzymes, however the ability of TTM to cross the cell membrane leads to rapid inactivation of SOD in the cytosol and induces a slightly higher deficiency of COX activity and greater loss of COX2 protein levels.

An initial finding was that cells shift to glycolysis for ATP production which was identified initially due to decreased pH in the cell medium and further supported by the increased ECAR in the BCS and TTM treated cells. However, the bioenergetics study showed that even if COX activity was significantly reduced, mitochondria are still able to function since no change in basal respiration and ATP production was observed. The only major difference was seen in the spare respiratory capacity which was increased only in cells treated with TTM

which indicates that protons and substrates are more available and implies that the ETC either does not utilize these or that the $\Delta\Psi_m$ is abnormal and allows substrates to circulate through different mitochondrial membrane compartments.

Based on the above, copper deficiency causes a significant loss in COX and SOD activity which contradicts our findings in the healthy ageing and AD brain. In the brain, we showed that even if copper is lower the activities of SOD and COX are not significantly changed, on the contrary, COX and SOD were higher in some cases. The difference between the cell and brain study might be different for two reasons. First, both the AD and healthy ageing brains face only mild copper deficiency (around 45%) but in the cell study copper decreased by more than 80%. Cells may require substantial copper loss before an impact on the activity or protein levels of COX and SOD are seen which further signifies that cells prioritize the available copper towards the function of antioxidant defence and energy production systems which are important for the survival of the cells. Secondly, the brain is a complex system that consists of multiple different cell types and the effects on the activity of SOD and COX may be regulated by multiple signals. The *in vivo* system that we used consists only of one cell type which responds to signals about the availability of necessary nutrients for its survival; on the other hand, in the brain neurons, astrocytes and glia, cells have to collaborate in order to maintain correct brain function. If the brain showed more than an 80% decrease in copper levels the consequences would likely be similar to that observed in the HEK293 cells.

In the present study we were unable to determine the effects of copper chelation on the amyloid pathways. It will be interesting to know if the major effects on mitochondrial function and SOD activity which may have a significant role in the AD pathogenesis, can elevate or decrease amyloid production, and how the two copper binding proteins APP and BACE1 are affected by copper deficient conditions. Even if HEK293 cells are useful for identification of basal changes these may not be an appropriate cell line to correlate with studies on neural cells. The above experiments should also be conducted in neuroblastoma, stem cell derived neurons or even astrocytes in order to be able to draw the appropriate conclusions about the effects of copper chelation in neural function. Furthermore, the effects of copper chelation in the remaining of the respiratory chain complexes and on the glycolitic pathway should be determined in order to obtain a comprehensive view of how copper deficiency and excess affects these two energy production pathways.

6 Effects of copper chelation in HEK293 cells overexpressing the cytosolic copper chaperones

6.1 Introduction

HEK293 cells has been extensively used for transient gene expression studies as a result of the ease of transfection, ability to grow quickly in both adherent and suspension culture, and low cost methodologies for transfection and maintenance[(483)]. HEK293 cells can be used for stable and transient gene expression studies, however, a preference towards transient transfection has grown due to cost-effectiveness and speed compared to establishing stable cell lines[(484)]. The transfection methodology works by introducing a plasmid vector such as those containing the strong Cytomegalovirus (CMV) promoter which very effectively uses the cell's synthetic protein machinery and forces the translation of gene products[(485)]. Plasmids contain sequences from different species and tissue origins can vary in their efficiency of translation and export, and most importantly, type and extent of post-translational modification (glycosylation, folding, acetylation etc.)[(485)]. In order to obtain successful transfection, these factors need to be taken into consideration initially by selecting the correct cell line and the appropriate expression vector.

Very few studies have overexpressed proteins from the copper homeostasis pathway and studied their function in relationship to other copper containing proteins. One study using the derivative HEK293 FLP-In^{TM}T-Rex^{TM} cell line was used to overexpress Ctr1, CCS or Atox1 to identify where copper is delivered after influx into cells by Ctr1[(44)]. This study found that cytosolic Atox1 levels are higher than CCS levels in HEK293[(44)]. Other studies have used HEK293T to overexpress SOD1 and CCS to identify post-translational maturation processes and how these proteins interact in live cells using NMR[(121)]. Also, to overexpress SOD1, CCS, and Copper Metabolism (Murr1) Domain Containing 1 (COMMD1) to determine how protein post-translational modification regulates the final maturation and activation of SOD1[(486)]. However, there is a lack of studies that use overexpression of either CCS or Atox1 to study the effects on intracellular copper pathways.

6.2 Aim

The purpose of this chapter was to transiently overexpress CCS and Atox1 in HEK293 cells and study their effects on the three intracellular copper pathways under normal and copper depleting conditions. In order to accomplish our goals we cloned CCS and Atox1 genes into the mammalian expression vector pCMV6-an-DDK and studied the effects on the activity and protein levels of copper binding proteins under normal conditions and in the presence of BCS and TTM to alter the cytosolic and mitochondria pathways.

6.3 Results

To overexpress CCS or Atox1 in the HEK293 cells we cloned the 825 bp coding sequence of CCS or the 207 bp coding sequence of Atox1 into the mammalian expression vector pCMV6-an-DDK (5929 bp) (Figure 5.1A and B) by following standard procedures. For reasons of simplicity the pCMV6-an-DDK_Atox1 will be referred to as pCMV6_Atox1, the pCMV6-an-DDK_CCS as pCMV6_CCS and the pCMV6-an_DDK as pCMV6.

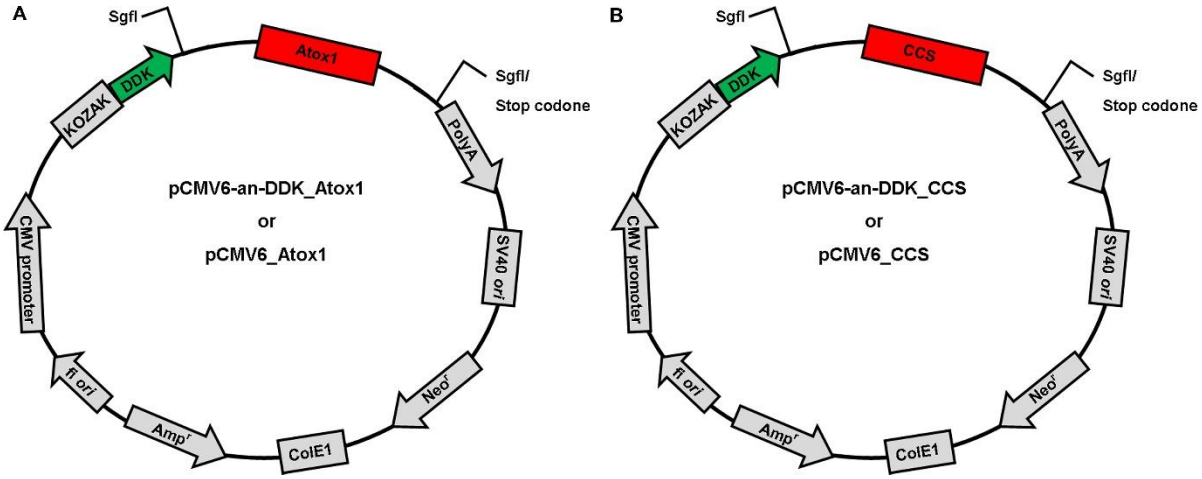

Figure 6.1 Schematic Representation of the Expression Vectors.

The pCMV6-an-DDK vector was used to clone the genes of **(A)** Atox1 (207 bp) and **(B)** CCS (825 bp). The required elements for the expression or replication of the vector in mammalian or *E.coli* cells are presented. SV40 origin of replication for mammalian cells, ColE1 origin of replication for high copies of plasmid in bacteria, fi *ori* for bacterial replication, CMV promoter, neomycin (neo) and ampicillin (amp) resistance genes for selection in mammalian or bacterial cells, respectively.

6.3.1 Transfection of HEK293 with pCMV6_Atox1 and its effects in the copper homeostasis pathways

To determine the appropriate transfection protocol for HEK293 cells and the pCMV6 expression vector, two different protocols were tested: calcium phosphate and PEI. Four-chamber slides were used to determine the transfection efficiency of each method by using a plasmid carrying the green fluorescence protein (pCMV6_GFP) and by adding different amounts of transfection reagent/DNA to each chamber. Twenty four hours after transfection, cell medium was replaced and cells left to grow for 3 additional days (referred to as 3 days post-transfection) and the transfection efficiency determined using fluorescence microscopy.

Transfection of pCMV6_GFP with calcium phosphate (Figure 6.2A) and PEI (Figure 6.2C) showed the highest efficiency, with calcium phosphate transfecting around 7.5% and PEI reagent transfecting approximately 5% of the cells. Since transfection efficiency was low, we

additionally determined transfection efficiency by immunofluorescence in cells transfected with pCMV6_Atox1 by staining the cells for Atox1 3 days post-transfection. This also demonstrated that transfection efficiency was low with calcium phosphate method showing 8% (based on the fluorescence intensity) and with the PEI method approximately 15% (Figure 6.2B and C).

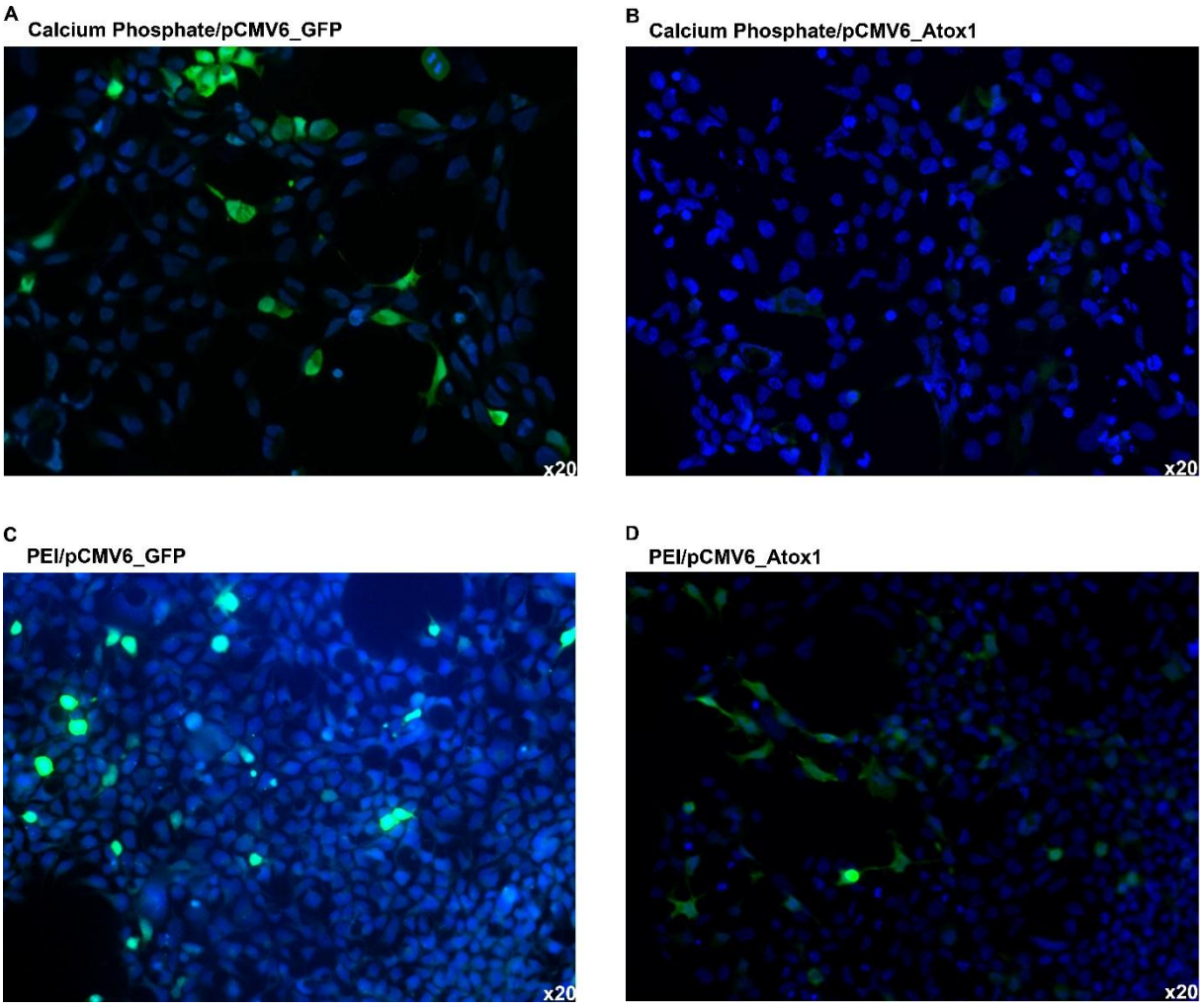

Figure 6.2 Determination of Transfection Efficiency in HEK293 cells.

Cells were transfected with a pCMV6_GFP plasmid expressing the green fluorescent protein or pCMV6_Atox1 (green) with **(A, C)** calcium phosphate or **(B, D)** PEI transfection reagent. Figures were captured under identical exposure times (59 msec) on Zeiss fluorescent microscope using an x20 objective lens. DAPI (blue) was used to stain nuclei.

Parallel to these experiments we also determined the protein levels of Atox1 where when 15% of the cell population was transfected with PEI/pCMV_Atox1 the levels of Atox1 were increased by more than 100-fold (Figure 6.3). Based on this we continued experimentally and treated the cells which overexpress Atox1 with 200 μM BCS and 2 μM TTM.

6.3.1.1 Effects of copper chelation in cells overexpressing Atox1

Experiments with transfected cells were performed into T25cm^2 to determine overexpression levels of Atox1 and consequently the effects on other copper binding proteins. Protein levels of Atox1 in cells transfected with pCMV6 or pCMV6_Atox1 in the presence or absence of 200 μM BCS and 2 μM TTM were determined using Western blot analysis with Atox1 and DDK tag antibodies (Figure 6.3A). In cells transfected with pCMV6_Atox1 the expression of exogenous Atox1 was markedly higher compared to endogenous Atox1 as can been seen from both the Atox1 and DDK bands. The presented film for Atox1 was overexposed to show both endogenous and overexpressed/exogenous protein, although accurate determination of Atox1 expression levels were performed with different films.

To determine differences between treatments in cells transfected with pCMV6 or pCMV6_Atox1 a two-way ANOVA was performed which revealed a significant interaction ($p=0.015$) between the variables and that both treatment ($p<0.0157$) and transfection ($p<0.0001$) had a significant effect on Atox1 protein levels. In untreated cells transfected with pCMV6_Atox1, Atox1 levels were increased by more than 120-fold (two-way ANOVA, $p<0.001$), whereas in cells treated with BCS or TTM and transfected with pCMV6_Atox1, Atox1 protein levels were higher by almost 200-fold (two-way ANOVA, $p<0.001$). Atox1 protein levels in cells transfected with pCMV6_Atox1 were significantly higher in cells transfected with Atox1 and treated with BCS (one-way ANOVA, Tukey post-test $p<0.05$) and TTM (one-way ANOVA, Tukey post-test $p<0.01$; Figure 6.3C).

Under the same experimental conditions we also determined CCS (Figure 6.4A) and SOD1 levels (Figure 6.4C). For CCS, two-way ANOVA analysis revealed the absence of any significant difference following transfection (two-way ANOVA, $p=0.267$) or interaction between variables (two-way ANOVA, $p=0.619$). However a statistically significant effect of treatment was seen (two-way ANOVA, $p=0.0024$) though post-hoc analysis failed to identify any changes (two-way ANOVA, $p>0.05$) between them. No significant differences in CCS protein levels were seen with pCMV6 or pCMV6_Atox1 or with 200 μM BCS or 2 μM TTM (one-way ANOVA, $p>0.05$; Figure 6.4B).

Analysis of SOD1 protein showed an effect of transfection with pCMV6_Atox1 (two-way ANOVA, $p=0.0054$), with an 18% decrease in SOD1 in untreated cells transfected with pCMV6_Atox1 relative to cells transfected with empty vector (two-way ANOVA, $p<0.05$). SOD1 protein levels were decreased by 20% (one-way ANOVA, $p<0.05$) in cells treated with

2 µM TTM and transfected with pCMV6_Atox1 compared to cells treated also with TTM and transfected with an empty vector (Figure 6.4D).

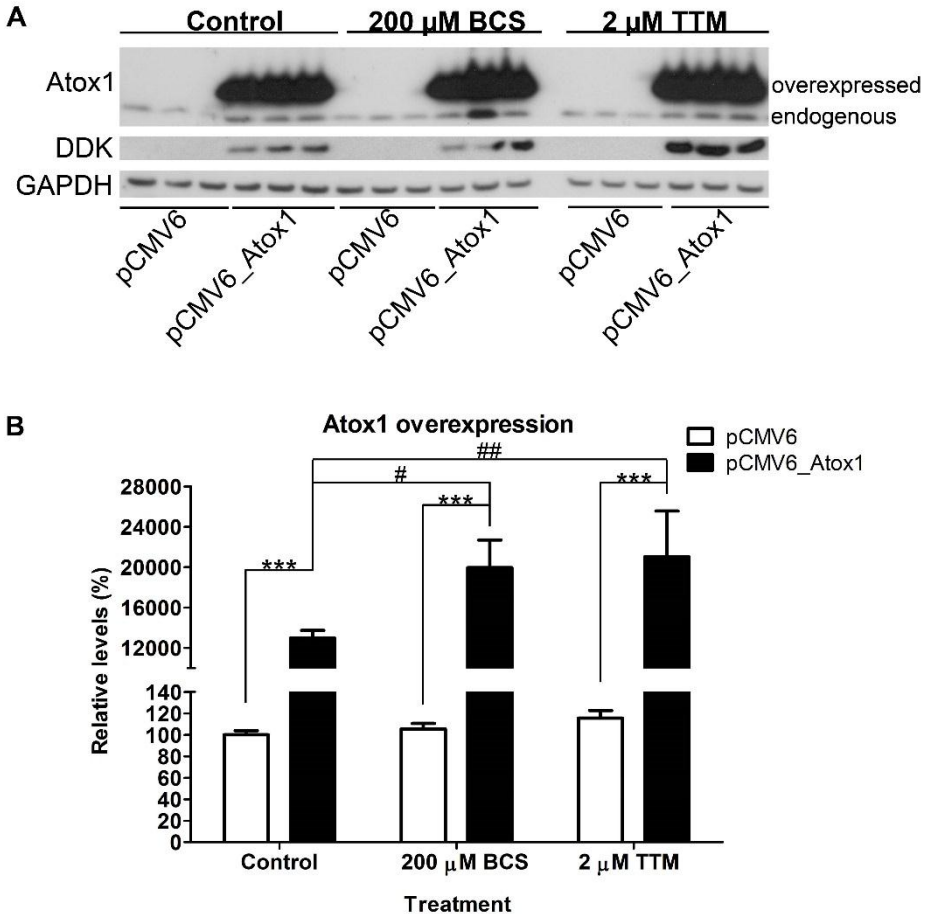

Figure 6.3 Expression Levels of Atox1 in Cells Transfected with pCMV6_Atox1 and Treated with 200 µM BCS and 2 µM TTM.

A) Representative Western blot analysis of cells transfected with pCMV6 or pCMV6_Atox1 and treated 200 µM BCS and 2 µM TTM 3 days post transfection (n=2). The blots were probed with antibodies for Atox1 and DDK which further confirmed the presence of the transfected protein. **B)** Densitometric analysis of the overexpressed Atox1 under the tested conditions. Two-way ANOVA followed by Bonferroni post-test was used to determine differences between treatments and transfection conditions where ***, $p<0.001$. One-way ANOVA followed by Tukey post-test was used to identify changes amongst the different groups where #, $p<0.05$ and ##, $p<0.01$.

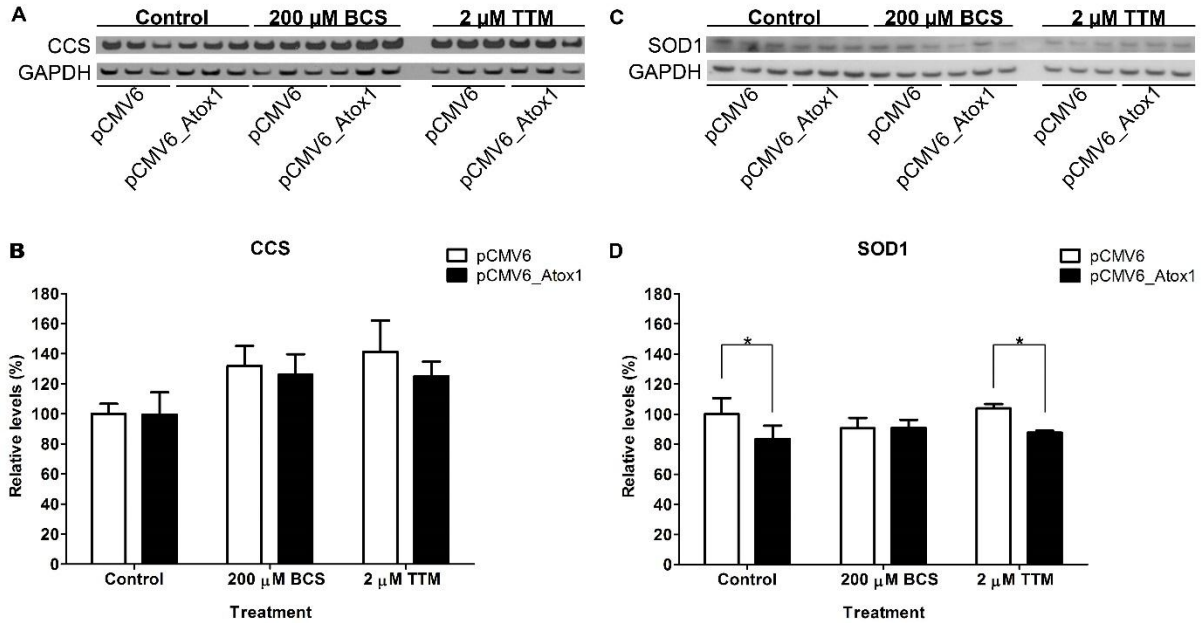

Figure 6.4 Expression Levels of CCS and SOD1 in Atox1 Transfected HEK293 Cells Treated with 200 µM BCS and 2 µM TTM.

Representative Western blot analysis of (**A)** CCS and **(C)** SOD1 in cells transfected with pCMV6 or pCMV6_Atox1 and treated with 200 µM BCS and 2 µM TTM 3 days post transfection (n=2). Densitometric analysis of (**B)** CCS and **(D)** SOD1 proteins under the tested conditions. Two way ANOVA followed by Bonferroni post-test was used to identify differences between treatments and transfection conditions where *, $p<0.05$. One way ANOVA followed by Tukey post-test was used to identify changes amongst the different groups where no significant difference was present.

In the mitochondrial copper pathway, COX2 protein levels were the most severely affected by BCS or TTM treatment and based on this we analysed the effect of Atox1 overexpression. COX2 and VDAC1 protein levels in cells transfected with pCMV6 or pCMV6_Atox1 and treated with 200 µM BCS and 2 µM TTM (Figure 6.5A) showed that pCMV6_Atox1 transfection did not prevent COX2 protein loss following BCS or TTM treatment (two-way ANOVA, $p=0.043$) whereas overexpression of Atox1 caused a significant 18% increase of COX2 protein (two-way ANOVA, $p<0.05$). Furthermore, COX2 protein levels in control cells transfected with pCMV6_Atox1 had higher COX2 levels compared to cells treated with BCS or TTM and transfected with pCMV6_Atox1 (one-way ANOVA, $p<0.001$, Figure 6.5B).

Mitochondrial mass showed significant changes between treatments (two-way ANOVA, $p=0.024$) though post-test analysis did not show any significant change between groups ($p>0.05$) despite a 20% increase in VDAC1 protein in cells transfected with pCMV6_Atox1 and treated with 200 µM BCS compared to cells transfected with an empty vector and treated with BCS (two way ANOVA, $p>0.05$). In HEK293 transfected with pCMV6_Atox1 and treated 200 µM BCS significantly higher VDAC1 levels were observed compared to cells treated with 2 µM TTM and overexpressing Atox1 (one-way ANOVA, $p<0.05$; Figure 6.5C).

The COX2/VDAC1 ratio was examined and treatments had a significant effect (two-way ANOVA, $p<0.0001$) due to COX2 loss in BCS and TTM treated cells. The COX2/VDAC1 ratio was significantly lower by 15% in untreated cells overexpressing Atox1 ($p<0.05$; Figure 6.5D). By comparing the different groups, the COX2/VDAC1 ratio was higher in untreated transfected cells with pCMV6_Atox1 compared to cells treated with BCS or TTM and overexpressing Atox1 (one-way ANOVA, $p<0.001$; Figure 6.5D).

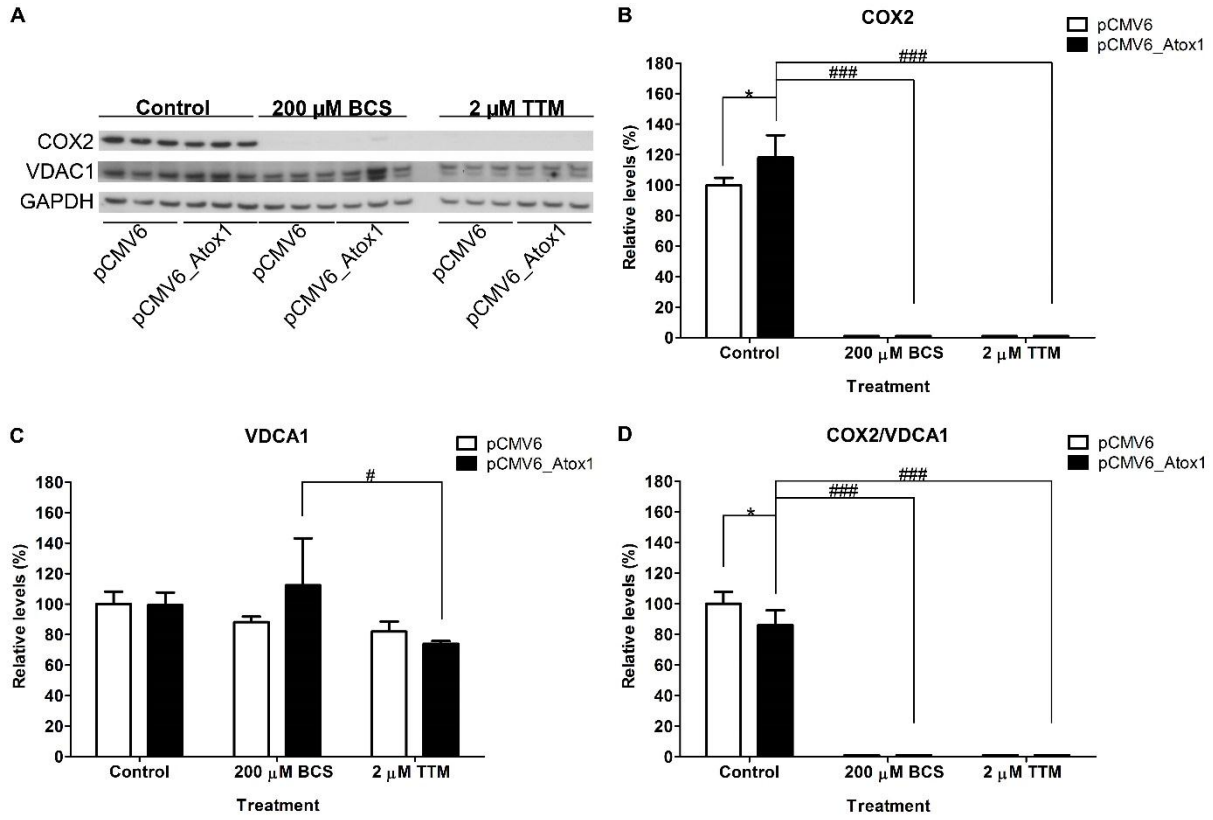

Figure 6.5 Expression Levels of COX2 and VDAC1 in Cells Transfected with pCMV6_Atox1 and Treated with 200 µM BCS and 2 µM TTM.

Representative Western blot analysis of (**A)** COX2 and VDAC1 in cells transfected with pCMV6 or pCMV6_Atox1 and treated with 200 µM BCS and 2 µM TTM 3 days post transfection (n=2). Densitometric analysis of (**B)** COX2 and **(C)** VDAC1 normalized with GAPDH as well as **(D)** COX2 normalized with VDAC1 under the tested conditions. Two-way ANOVA followed by Bonferroni post-test was used to determine differences between treatments and transfection conditions where *, $p<0.05$. One-way ANOVA followed by Tukey post-test was used to identify changes amongst the different groups where #, $p<0.05$ and ###, $p<0.001$.

Since overexpression of Atox1 and treatment with BCS or TTM showed similar results to non-transfected cells (see chapter 5) we determined COX/CS and SOD activity in transfected cells with empty vector or pCMV6_Atox1. COX/CS activity did not change in cells overexpressing Atox1 (t-test, $p=0.7456$) however SOD activity was statistically significant lower by 17% (t-test, $p=0.004$) in cells transfected with pCMV6_Atox1 (Figure 6.6) which was similar to an 18% loss of SOD1 protein under the same conditions.

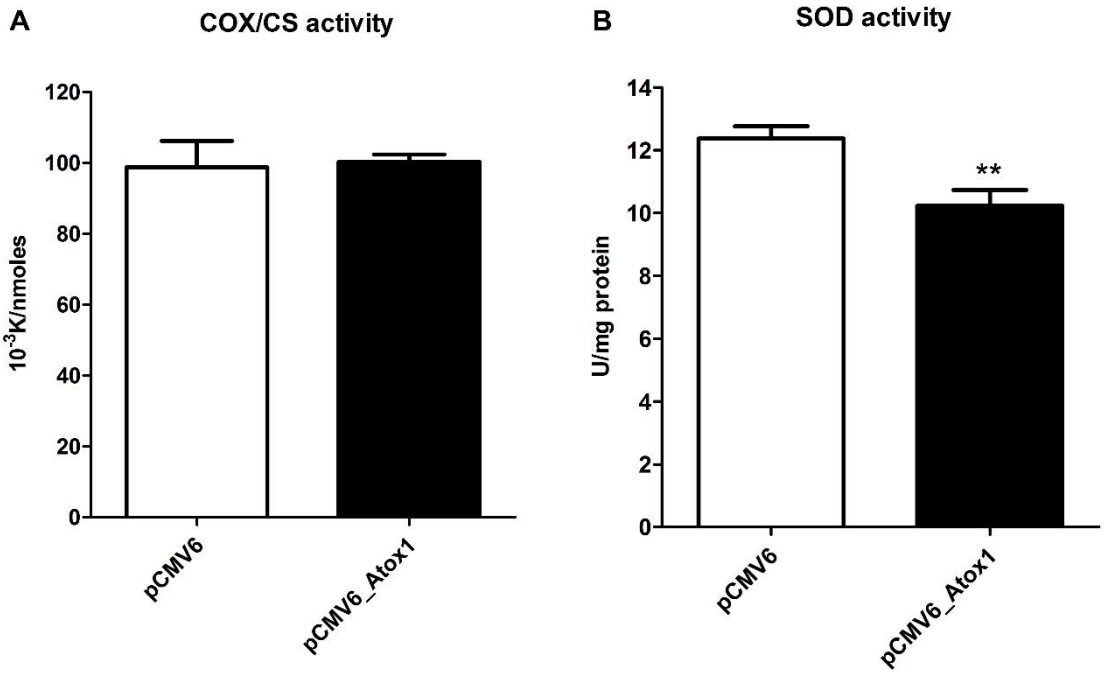

Figure 6.6 Activity Levels of Copper Binding Enzymes in Cells Overexpressing Atox1. Activity of **(A)** COX/CS and **(B)** SOD in cells transfected with pCMV6 or pCMV6_Atox1 as determined 3 days post transfection. Data were analysed with t-test and **, $p<0.01$.

The results indicate that Atox1 overexpression does not cause any major effect on either the activity or levels of copper containing proteins. Furthermore, protein levels of the target protein, ATP7a, did not change following Atox1 overexpression or treatment (data not shown). Combining the absence of any effect in the intracellular copper pathways and the low transfection efficiency of the plasmid we did not continue further experimentally with the HEK293 cells overexpressing Atox1.

6.3.2 Transfection of HEK293 cells with pCMV6_CCS

Transfection of HEK293 cells with the pCMV6_CCS using similar conditions to Atox1 failed to show successful transfection using antibodies for both CCS and the DDK tag (data not shown). Changing the plasmid and again using the standardized conditions we were unable to detect CCS overexpression (data not shown). Using increased plasmid concentrations of 14 µg and different volumes of PEI/DNA in each flask (400-800 µl) showed low level CCS expression at 600 µl and 800 µl PEI/DNA when we used CCS and DDK tag antibodies (Figure 6.7). The 600 µl showed faint CCS bands and a 50% increase of CCS although the DDK antibody did not detect any overexpressed protein (Figure 6.7B). Using 800 µl of PEI/DNA CCS expression increased by 3-fold however the cells appeared unhealthy and the majority started dying or stopped growing (possibly due to PEI toxicity). Under these

conditions, the DDK antibody gave faint CCS bands. Statistical analysis using one-way ANOVA followed by Tukey post-test showed that cells transfected with pCMV6_CCS and 800 µl PEI/DNA had higher total CCS protein levels relative to cells transfected with pCMV6 ($p<0.001$) and against lower PEI/DNA transfection ($p<0.001$; Figure 6.7B). Given the high levels of plasmid required to increase CCS expression and the effects on cell viability/growth after the transfection we did not continue further experimentally.

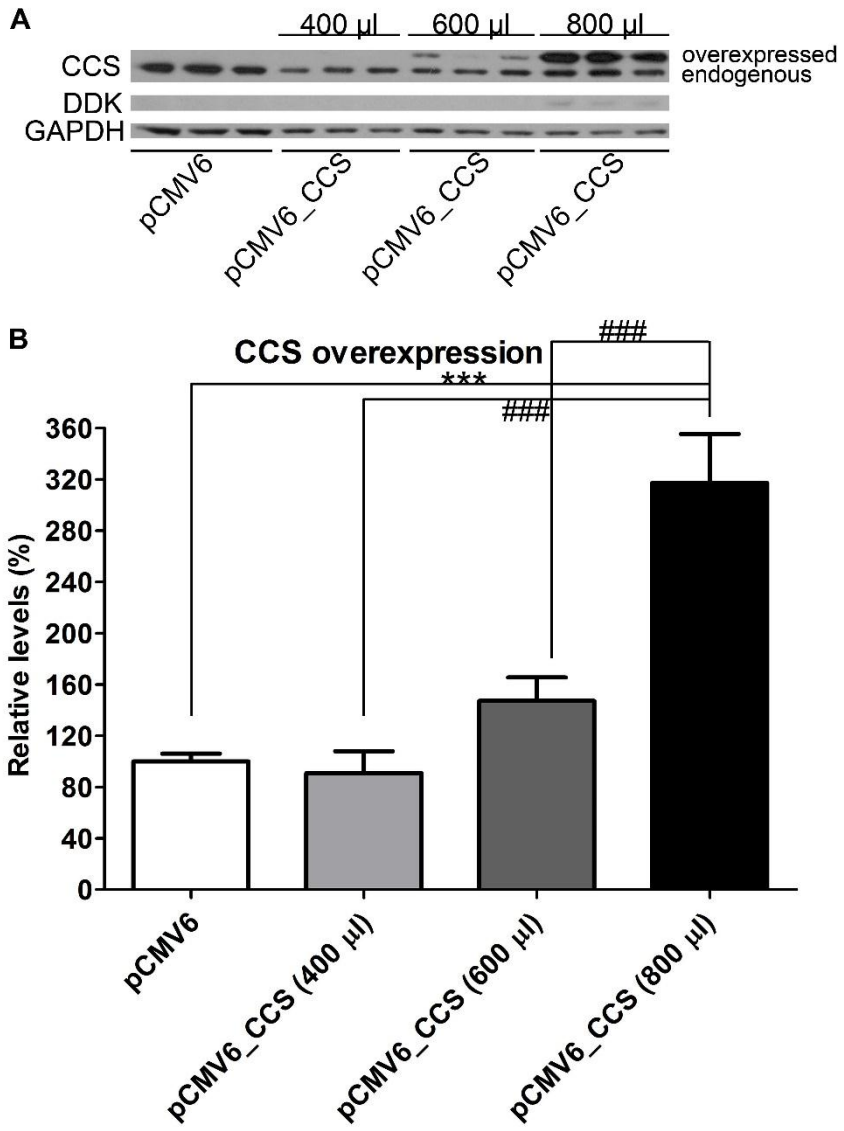

Figure 6.7 Protein Levels of CCS in HEK293 Cells Transfected with pCMV_CCS.

A) Representative Western blot analysis from cells transfected with 14 µg plasmid where different volumes PEI/DNA were used. The protein expression was determined with both a CCS and DDK antibody 3 days post transfection. **B)** Densitometric analysis of CCS protein levels under the tested conditions. Data were analysed with one-way ANOVA followed by Tukey's post-test and *** or ###, $p<0.001$.

6.4 Discussion

HEK293 cells are a common cell line used in transfection experiments especially when determining the function of specific proteins in relation to particular cellular processes/pathways. We utilised HEK293 cells to overexpress the two copper chaperones, CCS and Atox1, to understand their function in relation to the three intracellular copper pathways. To accomplish this we cloned CCS and Atox1 cDNA into the pCMV6 mammalian expression vector which has been successfully used in transfection studies with HEK293 and also other cell lines[487-490]. However, under our experimental conditions the transfection with CCS was unsuccessful and for Atox1 transfection efficiency was low however the protein levels in individual cells were markedly increased.

6.4.1 Transfection with pCMV6_Atox1 had low efficiency but increased protein expression

We were only able to transfect 15% of the cell population with pCMV6_Atox1 (Figure 6.2) when using the PEI method despite Atox1 protein levels being increased by more than 120-fold (Figure 6.3). Both results are unusual since typical transfection efficiencies with HEK293 cells is above 50% and protein levels are normally increased by 40 to 50-fold[491]. In our study (Figure 6.2D) cells transfected with Atox1 showed high fluorescence intensity but in only about 15% of the cell population. This markedly increased protein expression of Atox1 from only 15% of the cells may be detrimental and trigger various intracellular pathways (e.g. proteasomal degradation) or affect other cellular signalling pathways. Given these findings, we wanted to further understand if the transfected cells showed changes in copper containing proteins and if copper chelation could affect this phenomenon. We observed that cells which overexpress Atox1 and treated with 200 µM BCS or 2 µM TTM had significantly higher Atox1 levels compared to non-chelated cells transfected with pCMV6_Atox1, indicating that either the copper chelators TTM and BCS enhance the plasmid uptake by the cells, regulate transcription factors which promote transcription of the epigenetic plasmid, or there is decreased degradation of Atox1. As discussed (Chapter 5), TTM forms complexes with Atox1 which may enhance the stability of the transfected protein in the treated cells leading to higher intracellular protein levels (Figure 6.3)[442].

Overexpression of Atox1 did not affect cytosolic CCS protein levels since no change on its levels were observed under any of the studied conditions. However, Atox1 overexpression appeared to significantly decrease SOD1 protein levels by 18% in both untreated cells and cells treated with 2 µM TTM (Figure 6.4) along with a significant 17% decrease in SOD

activity in untreated cells transfected with pCMV6_Atox1 (Figure 6.6B). These changes (less than 20%), particularly with a 100-fold increase in Atox1, might not be of biological significance. These changes in SOD1 may however be limited to those 15% of the cells transfected with Atox1, potentially suggesting SOD1 is markedly decreased in specific cells. Overexpressing Atox1 by more than 100-fold in the cytosol may trigger degradation or other signalling pathways in the cells which might affect other cytosolic protein levels.

Atox1 overexpression caused only minor effects on COX2 or COX2/VDAC1 expression with less than a 20% increase or decrease (Figure 6.5), or in COX/CS activity (Figure 6.6A) and my reflect changes in intracellular protein synthesis pathways. COX2 is a mitochondrial encoded protein and does not depend on nuclear transcription or cytosolic translation for its synthesis. That, overexpression of a cytosolic chaperone has no effect on mitochondrial encoded proteins can be seen when cells are treated with BCS or TTM since overexpression of Atox1 was unable to prevent the effect on COX2 protein levels (Figure 6.5).

From the above we can conclude that Atox1 overexpression to only 15% of the cells population did not induce any major changes in the protein levels or activity of other copper binding proteins even if Atox1 protein levels were increased by 100-fold. One caveat to this may however be that changes are seen in those cells that are transfected, but these changes are not seen due to dilution of effects in untransfected cells.

6.4.2 HEK293 cells were not able to transfect with the pCMV6_CCS

Our attempts to overexpress CCS in HEK293 cells were unsuccessful, producing either no CCS expression or minimal increases accompanied by toxicity. Both CCS and Atox1 were cloned in the same expression vector and the only difference may be the insert size since Atox1 consists of only 207 bp and encodes a 7 kDa protein whereas CCS is larger with a 825 bp cDNA producing a 28 kDa protein. It is possible that cells are able to take up smaller plasmids and express smaller proteins more efficiently, and indeed increasing insert size significantly decreases promoter activity, an effect which is seen in multiple cell types[492, 493]. Another possible factor which could have contributed to absent CCS expression compared to Atox1 might be the normal cellular regulatory mechanism of these proteins since one study has shown that Atox1 is more abundant compared to CCS in HEK293 cells possibly reflecting the intracellular requirement for these proteins[44].

6.4.3 Future directions

Multiple factors could have contributed to the unsuccessful (CCS) or low transfection efficiency (Atox1) including: DNA structure, size of the vector, stability during intracellular routing, the amount of plasmid that reaches the nucleus, the cell cycle phase during transfection, the passage of the cells and confluence, and cell growth medium.

It is generally believed that the super-coiled form of the plasmid is the physiologically active conformation and that this is the preferable form for transfection of mammalian cells[(494)]. Normally the quality of high yield super-coiled plasmid depends on the strain of *E.coli* that the plasmid was extracted from, in this study we used the common JM101 strain however some studies suggest that Dh5α or XL1-Blue strains can produce higher quality super-coiled plasmid[(495)]. This may have affected the quality of the plasmid since we could only extract 2-4 µg/µl plasmid from 100 ml culture. Poor super-coiled content may also result from sequences within the plasmid such as segments with predominantly purines and AT-rich sequences which can lead to the formation of intramolecular triplexes (H-DNA)[(496)]. These sequences are common in eukaryotic DNA and their presence leads to nicking by endogenous nucleases due to the occurrence of single-stranded DNA along with plasmid DNA[(497)]. This may contribute to the low yield from the larger pCMV6_CCS which was almost half (2.4 µg/µl) to the smaller pCMV6_Atox1 plasmid (3.5 µg/µl). Inverting the orientation of bacterial *ori* relative to the eukaryotic expression cassette or by increasing the distance between the *ori* and these elements can eliminate H-DNA formation[(498)] and since the bacterial fi *ori* is close to the eukaryotic expression cassette in pCMV6 (Figure 6.1) another vector with improved features may be able to produce high-quality super-coiled plasmid.

Plasmid size is able to modulate gene transfer efficiency since transfection efficiency of lipoplexes (liposomes and DNA) containing smaller plasmids is greater than lipoplexes containing the same molarity of larger plasmids[(499)]. The significance of vector size in the expression transfection efficiency in different cell lines has been shown that the addition of 0.65 kb insert on a 5.1 kb vector can cause more than a 30% decrease in promoter/enhancer activity in HEK293 cells and to more than 50% in Jurkat or K562 cells[(492)]. In the current study the vector is more than 5.9 kb and the final size is 6.2 and 6.7 for Atox1 and CCS respectively. These studies are in line with our finding of the larger pCMV6_CCS vector having absent expression and the smaller pCMV6_Atox1 showing only low transfection efficiency. A possible solution to that problem could be a smaller vector, less than 5 kb, or vector with less bacterial elements in the backbone. The pCMV6 contains the neomycin

selection marker for the establishment of stable cell lines however in our hands cells were dying after the addition of G418 due to the low transfection efficiency. Since transient transfection is considered more cost-effective, a vector without a neomycin cassette will significantly reduce the size of the expression vector. Another option could be to replace ampicillin or kanamycin (830 bp or 890 bp) resistance cassettes with the much smaller zeomine (400 bp) bacterial selection marker[500].

PEI is a cost-effective transfection reagent which is an effective cationic compound for *in vitro* delivery of plasmid DNA to mammalian cells. PEI condenses DNA and the formed complexes (polyplexes) are taken up through interactions with heparan sulphate proteoglycans expressed in the cell membrane, followed by endocytosis into acidified endosomal compartments. Once inside the cells the polyplexes have to overcome several major hurdles such as endolysosomal entrapment, cytosolic sequestration, nuclear exclusion of the DNA and metabolic degradation[501]. Nucleases can start degrading the plasmid DNA after delivery to the cells and during trafficking to the nucleus which can be overcome by using circular rather than linear plasmids which are more assessable to nucleases[502]. Also, elements of the vector's sequence can be designed to maximize survival in hostile cell environments[503]. Studies have shown that six homo-purine rich sequences, located inside the polyA signal of the bovine growth hormone (BGH), and an 11-base long inverted repeat in the ColE1 *ori* are more susceptible to nucleases and that results can be improved by replacing the BGHpolyA with the SV40polyA[504]. The pCMV6 vector contains only the ColE1 *ori* on its sequence and the BGHpolyA is replaced with hGHpolyA. If SV40polyA significantly increases the half-life of super-coiled plasmid in the mammalian cytosol, an expression vector with this element might enhance the protein expression of our genes.

Furthermore, several bottlenecks in the process of plasmid DNA delivery to nucleus occur since after PEI transfection both positive and negative HEK293-EBNA1 cells show equal amounts of plasmid DNA however, positive cells show 3-fold higher plasmid content in their nucleus than in negative cells[505]. Apparently, untransfected cells can show significant amounts of plasmid DNA but transcription capability of the plasmid is inefficient and seems to depend on the physiological condition of the cells, indicating that optimal protein production requires the right balance between delivering enough complexes of PEI/DNA to the nucleus without causing adverse effects on the cells[505]. Variable levels of plasmid can be delivered to the nucleus which consequently determines if a cell will produce protein or not. Current research has evolved techniques to isolate cells that only express the desired protein. By using FACS cell sorting or a similar system we could possibly isolate only the cells that

overexpress CCS or Atox1 in order to grow only the positively transfected cells and then conduct further experiments in a cell population where all cells express the exogenous protein.

Another important factor that plays significant role in transfection efficiency and consequent protein expression is the cells condition which includes the cell cycle phase, passage of the cells and confluence during the transfection. A study in CHO cells has shown that when cells were synchronized before transfection by using minosine to inhibit ribonucleotide reductase, it was possible to gain a higher transfection efficiency when cells were in the S-phase[506]. This suggests that a certain period is required during cell cycle progression for the transfection reagent and DNA in endosomes/lysosomes to become distributed within the cells[506]. At mitosis, when the nuclear membrane disintegrates, and before it is reformed the plasmid DNA will have increased chances to be enclosed within the newly formed nucleus if it is in close proximity[506].

It is generally accepted that HEK293 cells can be grown for 20-30 passages (around 4 months if cells are passaged twice a week) after initially reviving cells and throughout this time are considered stable[485]. After obtaining HEK293 cells from ATCC, we made several aliquots of early passage cells and these cells were only grown for 20 passages. For the transfection experiments both early and late passage cells were used without any change to the final results. Another factor which could affect transfection is cell confluence since transfection with PEI requires 40-50% confluence. In the current studies, confluence was around 30-40% as afterwards we wanted to treat the cells for 3 additional days and by that stage the cells would have been over-confluent and possibly forming micro-islands. This may not be considered ideal since the cells will lose the normal monolayer formation and in order to avoid this we decreased the initial seeding density by 10-20%. However, if by increasing the initial seeding density we were able to transfect the HEK293 cells more efficiently, we could possibly treat the cells for 2 instead of 3 days since at this time point cells showed similar changes in copper proteins to cells at 3 days.

Finally, some studies indicate that the presence of FBS in the medium can inhibit transfection efficiency with PEI[507]. The HEK293 cells were grown in the presence of 10% FBS and the PEI/DNA complex was prepared in serum free medium since certain proteins in serum can inhibit formation of the complexes. Four hundred microliters of PEI/DNA were added to the growth medium of the cells which reduced the final FBS concentration to 9%. However, 24 hours post-transfection the medium was replaced with 10% FBS medium therefore if high

serum concentrations contributes to the low transfection efficiency it may be possible to grow cells in lower serum concentrations or even serum free conditions during the transfection procedure, since HEK293 cells can be grown successfully in 0-2% serum conditions[507].

In summary, it may be possible to change the expression vector and then apply small modifications to the transfection protocol in order to accomplish the overexpression of CCS and Atox1. A possible vector is the pCMV-tag epitope tagging vector from Agilent Technologies which is only 4.3 kb and with the addition of CCS or Atox1, the final plasmid it will not exceed the 5.1 kb which may provide maximal expression[492]. Furthermore, the vector contains the strong CMV promoter and the Kozak sequence and the more efficient SV40polyA to significantly increase the half-life of the super-coiled plasmid in the mammalian cytosol. The vector still has the fi *ori* for single strand DNA rescue and the pUC *ori* for high copy number replication in *E.coli*. The vector has the slightly smaller kanamycin resistance gene instead of ampicillin for bacterial selection although it still contains the neomycin resistance cassette for selection in mammalian cells. Moreover, the plasmid carries on its N or C-terminus Flag or myc tags to discriminate endogenous from exogenous protein expression. Finally, by applying small modifications to the transfection protocol including PEI/DNA ratio, serum in growth medium or cell confluence, we may obtain improved transfection results.

6.5 Conclusions

Transfection with the pCMV6_CCS vector was unsuccessful and with the pCMV6_Atox1 we were only able to transfect 15% of the cells but with a 100-times increase in Atox1 protein. Neither of the situations were ideal since they were not representative of the majority of the cell population. Furthermore, since 15% of the cell population expressed Atox1 by more than 100-times, this may have caused further problems to the cells including altered proteasomal degradation, cycle arrest or apoptosis. Using these conditions however, Atox1 overexpression does not seem to cause any major effect in the copper homeostasis pathways or inhibit the effects of copper chelation. Cloning CCS or Atox1 into a smaller vector with less backbone/bacterial elements may improve the transfection efficiency and consequently protein overexpression.

7 Summary

7.1 Introduction

The aim of this thesis was to investigate the link between copper homeostasis and AD pathogenesis and additionally to explore the mechanisms of copper prioritization in mammalian cells. Previous studies have suggested that copper chelation could work as a potential therapeutic strategy for AD. Our study has shown that both in healthy ageing and in AD, the brain shows a significant loss of copper accompanied by changes in the activity and protein levels of important copper binding enzymes/proteins. Furthermore, using an *in vivo* cell model we were able to show that extensive and chronic copper loss could ultimately lead to loss of cellular antioxidant defence and energy production systems.

7.2 Function of copper homeostasis pathway in the ageing and AD brain

One major finding of the brain study is that both ageing and AD brain show major copper loss, essential for the function of two important cell survival enzymes, COX and SOD. However, neither SOD nor COX appears affected by copper availability since for both enzymes their activity or protein levels were increased or unaffected. This suggests that other factors possibly contribute to the regulation of these enzymes in the brain considering the brain's high consumption of energy substrates with 60% of glucose and 20% of body oxygen being utilised[85, 301] along with increased amount of ROS as by-products [308-311]. The combination of neuronal/mitochondrial loss found in the AD brain and, minimally, with ageing together with an increased energy demand for neuronal function may lead to increased COX activity which is accompanied by increased SOD activity to defend against the increasing mitochondrial ROS production. Despite an almost 50% copper loss in the brain, copper binding enzymes were still able to function. Nonetheless, copper deficiency affected the levels of various copper binding proteins including COX2 and CCS.

The general conclusion from the brain study was that the main effects, especially in the AD brain, is that the pathological changes resulting in neuronal loss leads to mitochondrial deficiency and loss of mitochondrial proteins. Increased oxidative stress in the AD brain due to astrocytosis, brain inflammation or amyloid and tau deposition leads to increase SOD activity. The influence of AD pathology on protein, activity, and copper levels can also be seen in the differences between EOAD and LOAD cases where we identified that the most severely affected EOAD cases showed greater changes. Given our results from both the AD and ageing brain, even when copper is reduced, brain neurons are utilizing available copper to maintain mitochondrial function and antioxidant defences.

The theory of treating AD with copper chelators may not be a viable option since our results showed that there is already limited availability of copper. In the brain copper exists in two main oxidation forms the Cu^{1+} which is normally located in the reducing intracellular environment and the Cu^{2+} which is dominant in the more oxidised extracellular environment[508]. The levels of the extracellular Cu^{2+} vary, from 0.5-2.5 μM in the CSF up to 30 μM in the synaptic cleft[508]. The intracellular Cu^{1+} levels within neurons can reach 2 to 3 fold higher concentrations compare to extracellular copper levels[508]. The proposed chelation theory suggests that metal chelators such as CQ will sequester Cu^{2+} from the plaques and then redistributed in neurons[263, 264]. In our study, we measured total brain copper levels (extracellular and intracellular), including the copper within amyloid plaques, and showed a loss. Based on our findings and taking into consideration that the Cu^{2+} is not the most abundant form of copper in the brain; the chelation strategy might need to be reconsidered and possibly changed to a copper supplementation strategy. The supplementation approach is probably more suitable for people before dementia onset and particularly in people with a family history of AD or increased risk factors. Furthermore, our cell study showed the potential effects of copper chelation on cell function, with an almost complete loss of SOD and COX activity. Our studies suggest that people need to increase copper intake, as they get older especially after the age of 70. A diet enriched with copper might be helpful beginning in the fifties, which could be later enhanced by copper containing supplements at later ages.

7.3 Copper chelation inhibits the function of the mitochondrial and cytosolic copper pathways

In the present study, HEK293 cells were used to determine the effects of different copper chelators and supplementation on intracellular copper pathways. From our results we showed that only extracellular BCS and intracellular TTM copper chelators were able to significantly inhibit the activity and/or protein levels of SOD and COX in the cytosol and mitochondria by reducing the intracellular copper levels by more than 80%. The effects of these two copper chelators on COX and SOD function is highly dependent on their mechanism of action since we showed that the cell permeable TTM induced either higher or faster loss of the activity of these proteins.

The inhibition of COX and consequently of the mitochondrial respiratory function led to a shift in glycolysis for energy production as indicated by the low pH measurement and increased ECAR. However, the bioenergetics analysis showed that cells are still able to function under these conditions since no change in basal respiration and ATP production was

observed. The only difference, that of bioenergetics function, was the increased spare respiratory capacity in the TTM treated cells indicating that either the $\Delta\Psi_m$ is disrupted or that ETC is not utilizing the available substrates for its function. It is worth noting that only the intracellular copper chelator was able to induce these changes whereas the extracellular BCS did not affect the mitochondrial bioenergetics even when both chelators were able to reduce COX activity by a similar level. Based on the above we can conclude that the cellular localization of the drug/treatment plays an important role in protein regulation.

The HEK293 results may indicate potential changes during brain copper deficiency. Although HEK293 may not be an exact model for neural cell populations, studies have shown that HEK293 express certain neuronal proteins[509], and the potential outcome of conditions where copper is almost absent can be observed. Copper utilisation for systems other than energy production and oxidative stress defence, is important for the function of other proteins associated with connective tissue, neurotransmitter synthesis and melanin production. Copper loss of over 80% will reduce the activity of COX and SOD, increase oxidative stress, and reduce efficient communication between neurons due to reduced neurotransmitter processing, potentially leading to neuronal death. All these results further signify the importance of copper not only on single cell function but also in a complicated and multiply regulated system such as the brain.

7.4 Study limitations

A major limitation of the present study was the reduced success with CCS and Atox1 transfection where we were not able to overexpress CCS and with Atox1 we could only transfect 15% of the cells. Given time limitations we were unable to clone these genes in another mammalian expression vector to obtain better transfection efficiency and overexpression of the transgene. From the limited results from Atox1 it seems that Atox1 overexpression is not able to induce any major changes in the intracellular copper pathways and therefore focusing only on experiments with cells that overexpress CCS may be more appropriate.

One limitation of the current cell study was that we were unable to determine copper levels from Day 1 and 2. Our aim was to determine both copper levels and activity/protein levels from the same butch of cells however; there were insufficient cells at Day 1 and 2 to conduct all of the assays. A separate set of experiments only determining the copper concentration under the tested conditions will help us understand if intracellular copper decreases gradually or acutely after treatment with BCS and TTM.

An important limitation of the present study was the usage of an epithelia cell line (HEK293) as model for a neurodegenerative disorder. Using neuronal cell lines such as SH-SY5Y cells or neuronal stem cells would be more appropriate in order to draw conclusions about the function of copper homeostasis pathways in AD or the ageing brain and if a copper chelation or supplementation strategy could be helpful for neuronal/brain function. Furthermore, the current study lacked any correlation of the copper homeostasis pathways with the amyloid pathways both in the cell and brain studies. Measuring the activity of BACE1, since it binds copper and interacts with CCS, in our cell and brain samples would provide valuable information about the correlation of these two pathways. Unfortunately, our attempts to measure BACE1 protein levels were unsuccessful since the protein is highly glycosylated and we were unable to measure BACE1 accurately with Western blotting. The assay to measure BACE1 activity is laborious, costly and difficult to establish especially in brain samples and for that reason we were unable to conduct or find collaborators for this work. However, obtaining this information on BACE1 will enlighten our understanding about the connection of these two pathways.

Another limitation of the present study was that in both the brain and cell studies we mainly focused on complex IV (COX) function in the ETC however, there were significant indications that other ETC complexes are also affected under our experimental conditions, particularly complex I. For the brain study it is of major importance to measure the activity and protein levels of complex I and III, the main sources of superoxide anions, and also determine potential changes in other antioxidant deference enzymes. In the cell study, determining the activity of the other ETC complexes will possibly help us understand why the basal OCR does not change and why COX still retains 20% of its activity under conditions of almost complete copper deficiency.

Due to time constraints the levels of copper binding proteins were not determined in cerebellum from the healthy cases or in AD cases. Even though in AD brain we did not show a significant change in copper or activity levels of SOD and COX/CS still it would be interesting to know if the levels of certain proteins where we observed significant changes in frontal and temporal cortex such as COX2, VDAC1 and SOD1 are also affected in AD cerebellum. Similarly, since these proteins change with age, studying cerebellum will provide further information on the ageing process in functionally different brain regions.

7.5 Future Directions

The results of this thesis have opened up various avenues for further investigations in both the brain and the cell studies.

7.5.1 Further brain studies

The study of the ageing healthy brain and AD was conducted only in cerebellum, frontal and temporal cortex including more brain regions such as hippocampus, putamen, occipital and parietal cortex or substantia nigra and locus coeruleus we will able to obtain a more global picture of how copper pathways contribute not only to normal ageing but also the progress of a neurodegenerative disorder such as AD. The above mentioned brain regions were selected in order to get a broader idea of how copper homeostasis pathway is changing in functional different brain areas which also consist from different types of neuronal cells. In addition, the majority of these brain regions (hippocampus, occipital cortex, substantia nigra etc.) are severely affected in neurodegenerative disorders. Substantia nigra and locus are also having the highest copper concentration in the brain since they require copper for the pigmentation of catecholamine neurons[16, 48] and further investigation will provide a better inside of how these regions are affected by ageing or neurodegenerative disorders.

Including additional cases in the study would also be helpful since it will increase the statistical power of the analysis, allowing more robust results especially in instances where changes were only marginally significant (see cerebellum analysis for copper in EOAD). Furthermore, in the present study we only used the grey matter to determine the copper concentration and activity/protein levels of various copper binding proteins. Studying these variables in the white matter, it might give valuable information regarding the role of copper homeostasis pathways in the whole brain tissue. A few studies have shown decrease copper levels in the AD white matter[254] and that copper deficiency can lead to demyelination of the axons and oligodendrocyte damage[510].

Recently studies have shown that transition metals including copper can interact with α-synuclein, which can lead to protein aggregation in the neurons. Also, it seems that α-synuclein is able to reduce Cu^{2+} to Cu^{1+} intracellularly leading to the production of the highly reactive H_2O_2[511]. Two major disorders, Parkinson and Dementia with Lewy Body (DLB) are presenting pathology related to aggregations of α-synuclein. As already mentioned in the introduction section, a few studies have shown change in copper levels in PD substansia nigra however to my best knowledge they are not many studies that have measured the

different components of the copper homeostasis pathway in these two disorders. By including PD and DLB cases a better insight of how copper homeostasis pathway is implicated in other neurodegenerative disorder will be obtained.

In the present study we have indications that ROS production and antioxidant defence mechanisms are increased in both AD and in the healthy ageing brain. Measuring the activity and protein levels of complex I and III, the two major sources of mitochondria-derived ROS, will further support the theory that increased function of the respiratory chain has as a result an increased production of ROS which will require more active SOD. Determining the protein/activity levels of the other enzymes responsible for the antioxidant defence system in the brain, CAT and GPx, we may be able to understand why there is an increased oxidative stress in the brain, even when the first line of antioxidant defence is increased.

Both the AD and ageing brain faces copper deficiency and it is well established that copper levels can change the localization of certain proteins in cells including Ctr1 or ATP7a[41, 68]. In the present study we did not identify any change in Ctr1 or ATP7a protein levels however copper deficiency might alter their distribution and immunohistochemical approaches in tissue sections could identify if there is any difference in their localization. It would also be helpful to correlate the increased or decreased protein levels observed in the AD brain with specific cell populations in the brain since we know there is neuronal loss which could lead to decrease levels of certain proteins, along with increased astrogliosis which could result in higher protein expression.

By measuring the activity and protein levels of BACE1 in the studied cases we will be able to directly correlate if a pathway involving copper homeostasis is implicated with AD pathogenesis. BACE1 not only binds copper on its N-terminus but also interacts with CCS and it will be interesting to know if brain copper deficiency has any effect on BACE1 activity or protein levels and how these correlate with CCS protein levels or SOD1 activity[218].

In the current study we were able to compare AD subtypes (EOAD and LOAD) for copper and activity of COX/CS and SOD, but not for protein levels since the cases were analysed in different gels. It will be interesting to compare these two subtypes for the protein levels also, especially where significant changes occurred such as with SOD1, CCS, COX2 or VDAC1.

7.5.2 Further cell studies

Accomplishing the overexpression of the cytosolic chaperones, CCS and Atox1, in the HEK293 cells will provide further information about copper prioritization in cells. It will be

interesting to see what happens when cells overexpress CCS and treated with copper chelators (BCS and TTM) and if this will reverse or partially inhibit the effects on SOD activity. It will also be interesting to see what happens when copper chaperones are knocked-down by using either siRNA or in MEFs with CCS or Atox1 knockout and how this affects the activity or protein levels of SOD and COX and especially in combination with copper chelators.

The present study demonstrated certain findings concerning mitochondrial function under copper chelating conditions which could not be entirely explained with the present data set. To obtain a better understanding about mitochondrial function it will be necessary to measure the activity of the ETC complexes and especially Complex I. While the remaining ETC complexes may not require copper for activity, it appears that when one ETC complex is down-regulated the remaining complexes appear to compensate for the loss. This could be achieved in part by using Blue-Native PAGE on isolated mitochondria to see how copper chelation affects the holo-complexes and the respirasomes. Also, by measuring the $\Delta\Psi_m$ and ATP turnover in treated cells it may be possible to understand the effects of copper chelation on the ETC and why the decreased COX activity does not affect the OCR. Under copper chelating conditions the protein levels of COX2 are severely affected from Day 1 (more than 70% of the protein is lost) and therefore determining how fast copper chelation affects COX2 levels by collecting cells samples every 2-4 hours up to Day 3 (when there is no COX2 remaining) will provide further information on how COX2 is regulated by copper availability. Experiments involving 2 or 3 days of treatment with BCS or TTM and then placing cells in normal or copper supplemented medium would provide information on reversibility of effects. By collecting cell samples over 24-48 hours, the effects on COX and SOD activity could be determined to see how long it takes to return levels back to normal.

In the present study we showed that the protein levels NDUFV1 of complex I decrease over time. It will be interesting to see if complex I activity is affected in a similar way and if other proteins needed for complex I function, both mitochondrial and nuclear encoded subunits such ND1, NDUFB8 or NDUFS4 or NDUFS6, show similar trends. Furthermore, identifying the time point where NDUFV1 declines and if levels return to normal after Day 3 will be important by undertaking a thorough time course experiment.

One major finding of the present study was the shift to glycolysis for energy production although we did not determine any part of this pathway how it is affected during copper deficiency. One of the most accurate ways of measuring the shift towards glycolysis is by determining lactate levels in the cell medium. Several methods are available to determine

lactate however it is necessary to deproteinate cell medium before use since FBS contains high levels of lactate dehydrogenase which is able to convert lactate to pyruvate. Determining the activity and protein levels of rate limiting glycolytic enzymes such as Hexokinase, Phosphofructokinase, and Pyruvate kinase would provide an understanding of how this pathway is regulated under copper chelating conditions.

Measuring the effects of copper chelation on the amyloid pathway and particularly on BACE1 activity and protein will provide information on how these pathways are linked and which therapeutic strategy, copper chelation or supplementation, might improve not only AD patients, but also healthy people. Measuring Aβ and APP levels since both can bind copper and studies have shown that their function depends on copper concentration would be worthwhile in this context.

HEK293 cells whilst having some neuronal derived genes[509] still cannot be considered an accurate model for normal neurones or neurodegeneration. For that reason the experiments in HEK293 cells should be repeated in neuronal stem cell derived human neurones. Under these experimental conditions the effects of stem cell transfection with BACE1 or APP and the effects of copper chelation on the amyloid pathway under conditions known to produce increased Aβ levels and can lead to AD could be studied. This would provide the necessary information on how copper manipulation affects neuronal function in both health and disease.

7.6 Final conclusions

In conclusion, the main results of this thesis suggest that copper homeostasis pathways are not directly implicated with AD since the majority of our findings are either due to mitochondrial/ neuronal loss or to increased oxidative stress. We showed that both in ageing and in the AD brain copper deficiency is present although that does not seem to affect the activity of COX and SOD. Changes in copper levels have also been observed in PD, another age associated disorder, where significant copper loss was observed in sabstantia nigra the most affected area in the PD brain[16, 17]. Clinical trials with copper chelation or supplementation have been only conducted with AD patients and to my best knowledge not in another age-associated disorder and as already has been discussed in introduction (section 1.6.1) both approaches fail to benefit the AD patients. Through the cell studies, we were able to identify the possible consequences of extensive copper deficiency on two important for the cell survival enzymes, COX and SOD which further support that balancing copper levels properly is important for the function of cells and consequently whole tissues.

A. Appendix A: Decreased copper levels in the ageing cerebellum

In the current investigation we were unable to complete the analysis of the cerebellum samples. However, the acquired data for copper levels and activity of SOD and COX in the ageing cerebellum are in good agreement with those we obtained in frontal and temporal cortex.

A.1 Results: Investigating copper and activity levels in ageing cerebellum

We were only able to obtain cerebellum samples from 22 healthy control cases. Similar to frontal and temporal cortex, Spearman's rank test was used to identify correlations between age of death and copper or activity levels. In cerebellum, a statistically significant negative correlation was observed between age and copper levels (r_s=-0.587, n=22, p=0.0041; Figure A.1A). The result indicates that there is a moderate correlation which shows that in the healthy cerebellum copper levels decrease with age, consistent with the results in frontal and temporal cortex (section 3.3.1). In cerebellum, SOD activity increased with age however the change was not statistically significant (r_s=0.441, n=22, p=0.039; Figure A.1B). The COX/CS activity ratio did not show any change with age in cerebellum (r_s=-0.05, n=22, p=0.816), although in frontal and temporal cortex there was a positive correlation between age and COX/CS activity (Figure A.1C). In cerebellum, no other correlation was identified between copper and activity of SOD or COX/CS (data not shown).

As discussed in chapter 3 each brain regions demonstrates different changes with ageing with cortex being most affected. In order to examine if copper levels and activity of SOD or COX/CS differed amongst brain regions a Kruskal-Wallis test followed by Dunn's Multiple Comparison post-test was performed. The analysis revealed that even if all three brain regions face similar decrease with age, cerebellum had significantly ($p<0.001$) higher copper levels compared to frontal and temporal cortex (Figure A.2A). A similar trend was also observed for SOD activity since cerebellum had significantly higher activity compared to frontal cortex ($p<0.05$) but not compared to temporal cortex ($p>0.05$). COX/CS activity in cerebellum was significantly lower compared to both frontal ($p<0.001$) and temporal cortex ($p<0.001$).

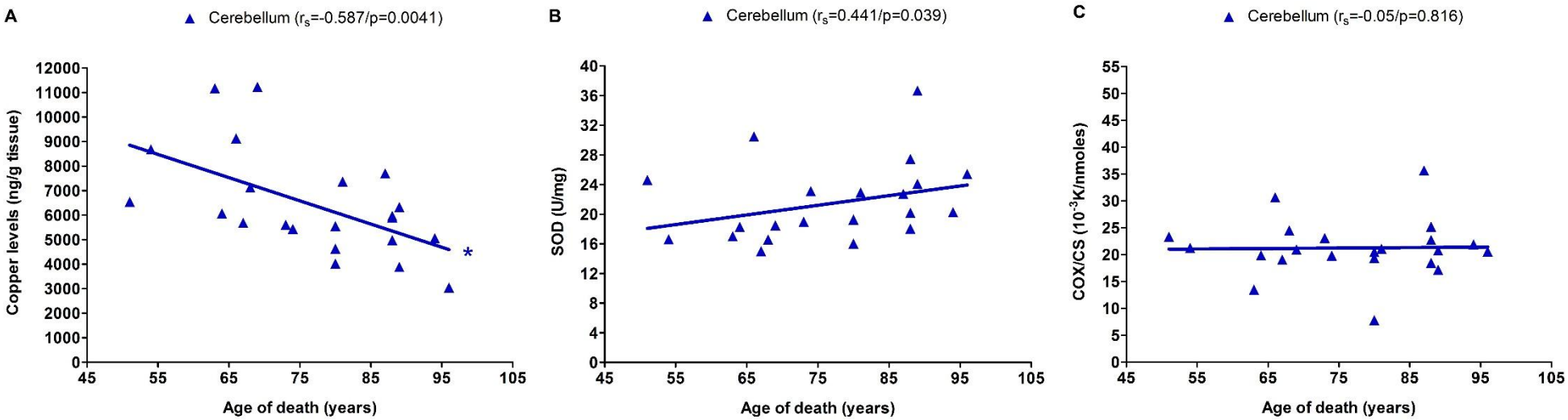

Figure A. 1 Graphical representation of Copper Correlations in Cerebellum.

Age of death of the control samples was correlated with **(A)** copper levels, **(B)** SOD activity and **(C)** COX/CS activity in cerebellum. Spearman r_s correlation for n=22 samples is reported and p values less than 0.01 were considered statistically significant.

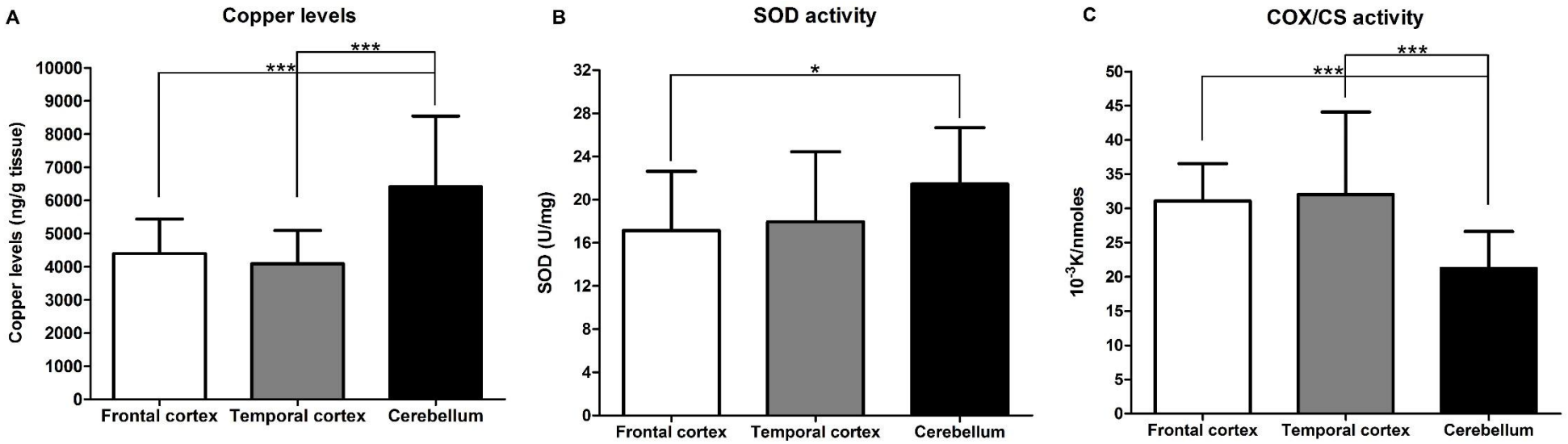

Figure A. 2 Graphical Representation of the Regional Differences in Copper, COX/CS or SOD Activity in the Healthy Brain.

Cerebellar, frontal and temporal cortex were compared for **(A)** copper levels, **(B)** SOD and **(C)** COX/CS activity. Data were analysed with Kruskal-Wallis test followed by Dunn's Multiple Comparison post-test in order to determine if regional differences in levels were apparent and *, $p<0.05$; ***, $p<0.001$.

A.2 Discussion

The above results with cerebellum are in good agreement with those from frontal and temporal cortex. Copper levels in cerebellum decrease with age although it appears that cerebellum contains higher copper levels compared to cortex (Figure A.1A and A.2A). Previously published studies have also reported that copper concentration in cerebellum is higher compared to other brain regions[14, 342] possibly reflecting local demands for higher copper content or due the presence of different cell types in cerebellum compared to cortex. Studies have shown that Purkinje cells in cerebellum show high expression levels of the copper transporters Ctr1 and ATP7a/b which play a fundamental role in copper acquisition and distribution in cells and tissues[48, 73].

Studies have shown that cerebellar grey and white matter volume declines with age but white matter shows a significantly more rapid volume loss compared to grey [512]. Even if cerebellum shows atrophy and volume loss with ageing, this does not appear to affect COX/CS activity, rather activity levels seem to be stable throughout life (Figure A.1B). However, COX/CS activity in the cerebellum appears to be significantly lower compared to cortex (Figure A.2B) reflecting a lower energetic demand, possibly representing the local cell types. Cortex consists of excitatory projection neurons whereas cerebellum contains Purkinje cells and granule cells where potentially these cell types contains fewer mitochondria. To obtain a better understanding of mitochondrial function and COX/CS activity in the cerebellum it would be useful to determine the effects of ageing on mitochondrial VDAC1, COX1 and COX2 proteins.

In the cerebellum, SOD activity also increased with age but the change was not statistically significant however SOD activity seems to be significantly higher in cerebellum relative to frontal and temporal cortex (Figure A.1C and A.2C). Studies have shown that the cerebellum has an elevated antioxidant defence mechanism compared to other brain regions which makes it more resistance to oxidative damage[313, 513]. In our study we did notice that cerebellum had higher antioxidant defence through higher SOD activity which could be attributed to higher SOD2 levels in cerebellum as shown previously[513]. The increased SOD activity in the ageing brain is correlated more with increased ROS production, which might not be produced by the mitochondria since COX/CS activity does not change, but possibly from other sources in cerebellum: cerebellum shows the highest brain copper concentrations which may trigger the production of ROS via the Haber-Weiss reaction. However, in order to get a better understanding of the antioxidant defence system in cerebellum SODs protein levels should be

determined and directly correlated with SOD activity. Our result of a non-significant increase in SOD activity with ageing in cerebellum is in agreement with a previous study which reported a non-significant increase in SOD activity with ageing[313].

From the above results we can conclude that decreased copper levels accompanied by increased activity of SOD or COX/CS is a general feature of the ageing brain since anatomically and structurally different brain regions (cortex and cerebellum) show similar results. Furthermore, we show that healthy and functionally different brain regions have higher or lower requirements for copper and activity of certain enzymes which may depend on regional brain function and possibly the local cellular population.

B. Appendix B: Supplementary Data

B. 1 Supplementary Figures

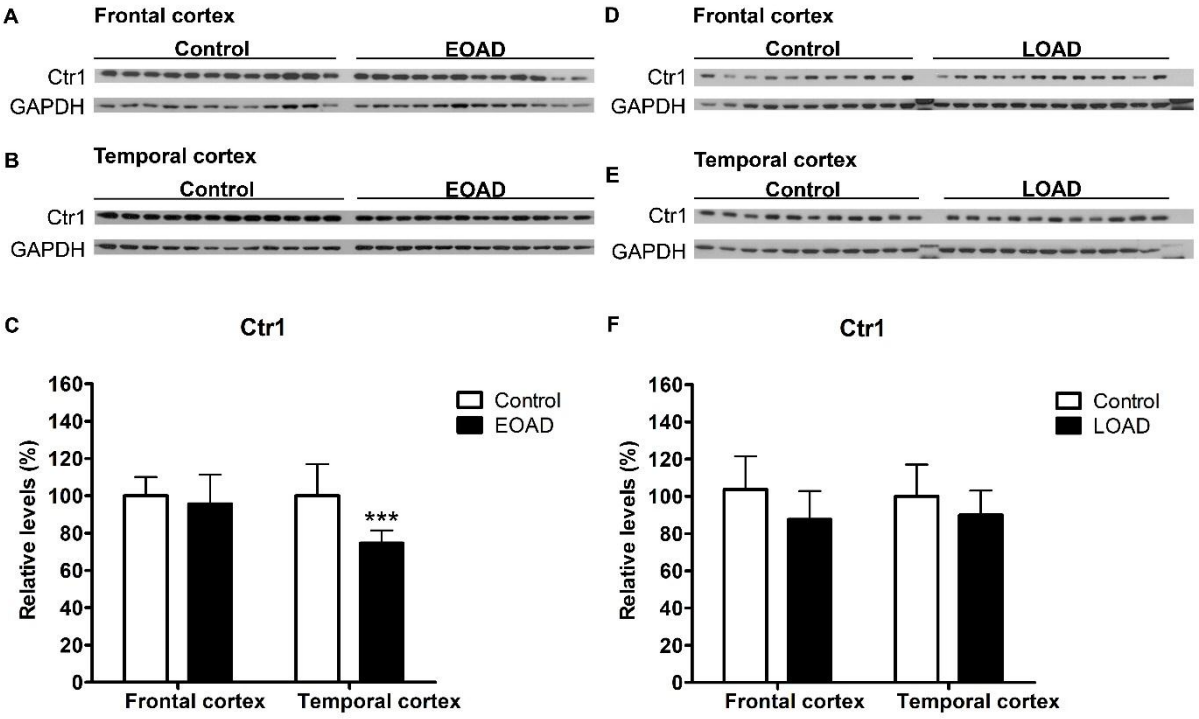

Figure B. 1 Ctr1 Protein Levels in EOAD and LOAD Frontal and Temporal Cortex.

Representative Western blots from EOAD or LOAD and their age matched controls in **(A, D)** frontal and **(B, E)** temporal cortex and their respective **(C, F)** densitometric analysis of Ctr1 normalized with GAPDH. Data were analysed with a nonparametric t-test and ***, $p<0.001$.

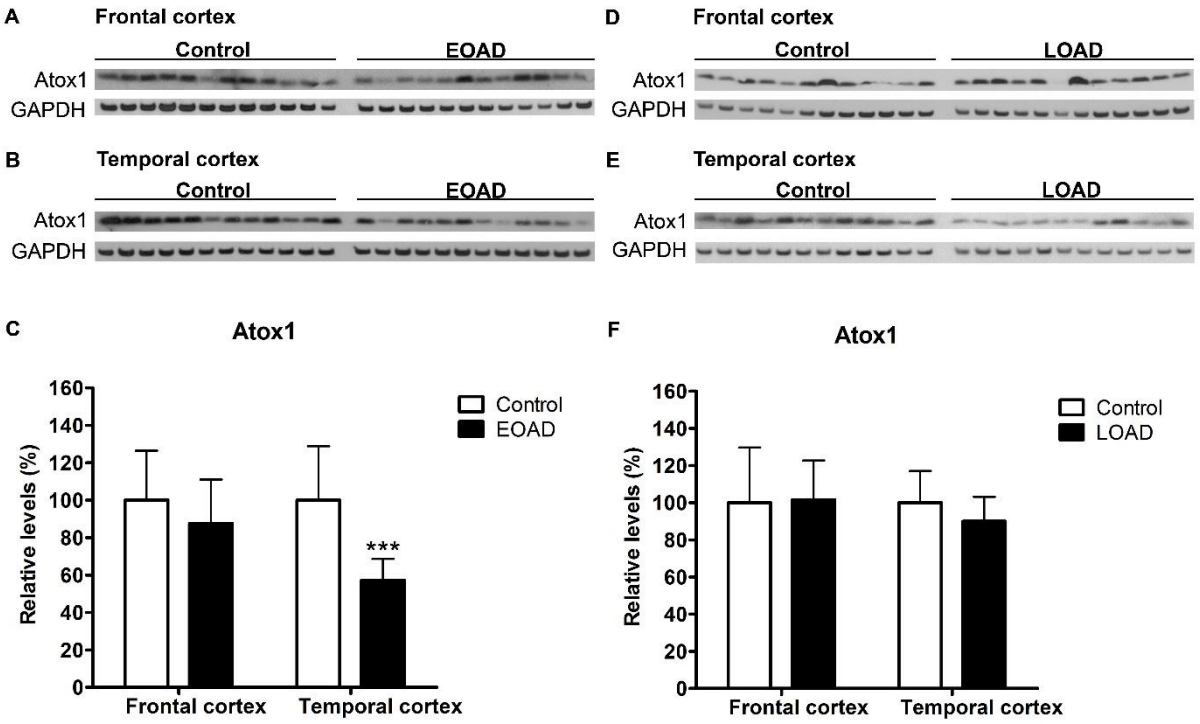

Figure B. 2 Atox1 Protein Levels in EOAD and LOAD Frontal and Temporal Cortex.

Representative Western blots from EOAD or LOAD and their age matched controls in **(A, D)** frontal and **(B, E)** temporal cortex and their respective (**C, F)** densitometric analysis of Atox1 normalized with GAPDH. Data were analysed with a nonparametric t-test and ***, $p<0.001$.

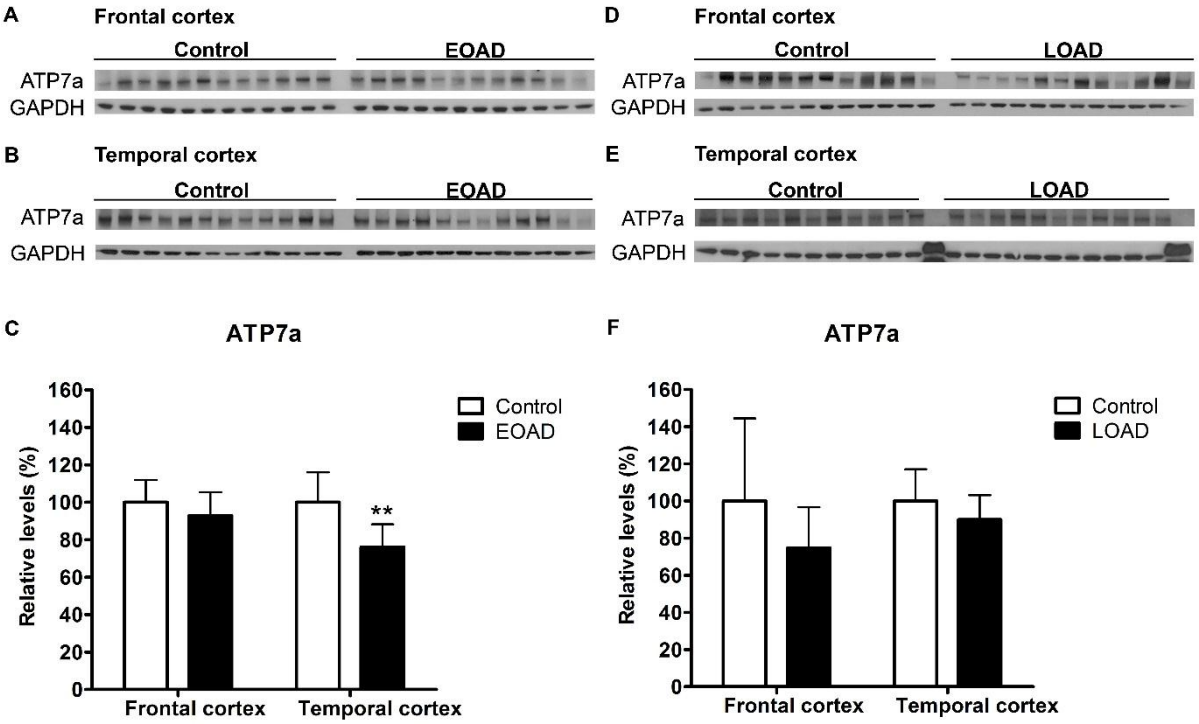

Figure B. 3 ATP7a Protein Levels in EOAD and LOAD Frontal and Temporal Cortex.

Representative Western blots from EOAD or LOAD and their age matched controls in **(A, D)** frontal and **(B, E)** temporal cortex and their respective (**C, F)** densitometric analysis of ATP7a normalized with GAPDH. Data were analysed with a nonparametric t-test and **, $p<0.01$.

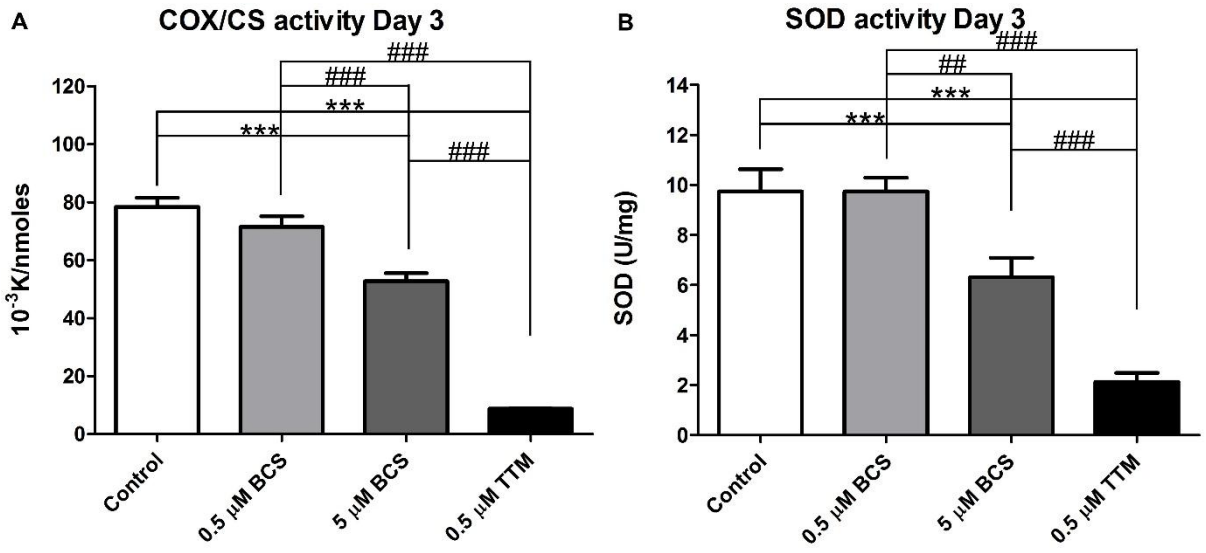

Figure B. 4 Effects of 0.5 μM, 5 μM BCS or 0.5 μM TTM on COX and SOD activity in HEK293 cells.

(A) COX/CS activity was determined after 3 days exposure and activity was negatively correlated with BCS concentration. The 0.5 μM TTM appeared to have similar effects to 2 μM TTM. **(B)** SOD activity was determined after 3 days exposure where SOD activity was negatively correlated with the BCS concentration and 0.5 μM TTM appeared to have a similar effect on SOD activity compared with 2 μM TTM. Data were analysed with one-way ANOVA followed by Tukey post-test. * indicates significant differences between control and treated cells, and # amongst different treatments. ** or ##, $p<0.01$; *** or ###, $p<0.001$.

B. 2 Supplementary Tables

	Frontal cortex (ng/g tissue)				Temporal cortex (ng/g tissue)				Cerebellum (ng/g tissue)			
Metal	**Cu**	**Zn**	**Mn**	**Fe**	**Cu**	**Zn**	**Mn**	**Fe**	**Cu**	**Zn**	**Mn**	**Fe**
Control (n=14)[3]	**5892 ± 923**	13754 ± 1054	233 ± 50	53180 ± 10754	**4503 ± 726**	14456 ± 2051	189 ± 37	**49275 ± 11447**	7915 ± 2102	16138 ± 3855	363 ± 99	55546 ± 14349
EOAD[2] (n=16)	**2913 ± 1249**	13745 ± 3310	206 ± 35	57180 ± 12133	**2623 ± 1036**	14722 ± 2300	203 ± 33	**57586 ± 10366**	5923 ± 1947	15273 ± 2272	361 ± 78	55432 ± 17776
P value	**0.0004**	0.546	0.088	0.603	**<0.0001**	0.917	0.371	**0.026**	0.0507	0.545	1.0	0.859
% Change	**41% decrease**	No change	12% decrease	7% increase	**43% decrease**	No change	8% increase	**17% increase**	25% decrease	5% decrease	No change	No change

Table B. 1 Selected Metal Levels in Frontal, Temporal cortex and Cerebellum EOAD and age matched control brains.
Percentage change compared to controls and p values are also reported.

[3] For cerebellum levels from 9 controls and 12 EOAD cases are presented.

	Frontal cortex (ng/ g tissue)				Temporal cortex (ng/ g tissue)				Cerebellum (ng/ g tissue)			
Metal	**Cu**	**Zn**	**Mn**	**Fe**	**Cu**	**Zn**	**Mn**	**Fe**	**Cu**	**Zn**	**Mn**	**Fe**
Control (n=13)	3860 ± 833	12892 ± 3507	212 ± 37	48058 ± 9243	**3568 ± 969**	13105 ± 2756	187 ± 42	47205 ± 10827	5372 ± 1278	12678 ± 2314	341 ± 64	52074 ± 19816
LOAD (n=13)	3317 ± 880	11564 ± 1788	190 ± 21	45991 ± 8764	**2714 ± 854**	12949 ± 2013	185 ± 32	48049 ± 10402	5247 ± 1205	12446 ± 1797	327 ± 61	46130 ± 11664
P value	0.111	0.608	0.150	0.644	**0.04**	0.681	0.919	0.797	1.0	0.758	0.572	0.356
% Change	14% decrease	10% decrease	11% decrease	4% decrease	**24% decrease**	No change	No change	No change	No change	No change	4% decrease	12% decrease

Table B. 2 Selected Metal Levels in Frontal, Temporal cortex and Cerebellum LOAD and age matched control brains.

Percentage change compared to controls and p values are also reported.

References

1. J. R. Turnlund, W. R. Keyes, G. L. Peiffer, K. C. Scott, *The American journal of clinical nutrition* **67**, 1219 (Jun, 1998).
2. M. C. Linder, *Biochemistry of Copper*. (Springer US, 1991).
3. E. Madsen, J. D. Gitlin, *Curr Opin Gastroenterol* **23**, 187 (Mar, 2007).
4. J. R. Prohaska, A. A. Gybina, *The Journal of nutrition* **134**, 1003 (May, 2004).
5. J. Ma, N. M. Betts, *The Journal of nutrition* **130**, 2838 (Nov, 2000).
6. L. M. Gaetke, C. K. Chow, *Toxicology* **189**, 147 (Jul 15, 2003).
7. J. R. Turnlund *et al.*, *The American journal of clinical nutrition* **65**, 72 (Jan, 1997).
8. M. Linder, K. Weiss, V. Hai, in *Trace Elements in Man and Animals 6*, L. Hurley, C. Keen, B. Lönnerdal, R. Rucker, Eds. (Springer US, 1988), pp. 141-144.
9. N. Liu *et al.*, *The Journal of nutritional biochemistry* **18**, 597 (9//, 2007).
10. I. H. Scheinberg, I. Sternlieb, *The American journal of clinical nutrition* **63**, 842S (May, 1996).
11. J. H. Menkes, M. Alter, G. K. Steigleder, D. R. Weakley, J. H. Sung, *Pediatrics* **29**, 764 (May, 1962).
12. Z. Tumer, L. B. Moller, *Eur J Hum Genet* **18**, 511 (May, 2010).
13. R. Squitti *et al.*, *Neurology* **59**, 1153 (Oct 22, 2002).
14. M. A. Deibel, W. D. Ehmann, W. R. Markesbery, *Journal of the neurological sciences* **143**, 137 (Nov, 1996).
15. G. Forte *et al.*, *J Neural Transm* **111**, 1031 (Aug, 2004).
16. B. F. Popescu *et al.*, *Phys Med Biol* **54**, 651 (Feb 7, 2009).
17. D. T. Dexter *et al.*, *Journal of neurochemistry* **52**, 1830 (Jun, 1989).
18. G. R. Buettner, B. A. Jurkiewicz, *Radiat Res* **145**, 532 (May, 1996).
19. M. J. Burkitt, *Archives of biochemistry and biophysics* **394**, 117 (Oct 1, 2001).
20. M. E. Letelier, S. Sanchez-Jofre, L. Peredo-Silva, J. Cortes-Troncoso, P. Aracena-Parks, *Chem Biol Interact* **188**, 220 (Oct 6, 2010).
21. J. A. Imlay, S. M. Chin, S. Linn, *Science* **240**, 640 (Apr 29, 1988).
22. L. Macomber, J. A. Imlay, *Proceedings of the National Academy of Sciences of the United States of America* **106**, 8344 (May 19, 2009).
23. H. Lauble, M. C. Kennedy, H. Beinert, C. D. Stout, *Biochemistry* **31**, 2735 (Mar 17, 1992).
24. S. Jang, J. A. Imlay, *The Journal of biological chemistry* **282**, 929 (Jan 12, 2007).
25. R. Mehta, D. M. Templeton, J. O'Brien P, *Chem Biol Interact* **163**, 77 (Oct 27, 2006).
26. M. Arciello, G. Rotilio, L. Rossi, *Biochemical and biophysical research communications* **327**, 454 (Feb 11, 2005).

27. J. Pourahmad, A. Mihajlovic, P. J. O'Brien, *Adv Exp Med Biol* **500**, 249 (2001).
28. J. Pourahmad, P. J. O'Brien, *Toxicology* **143**, 263 (Mar 7, 2000).
29. T. Nevitt, H. Ohrvik, D. J. Thiele, *Biochimica et biophysica acta* **1823**, 1580 (Sep, 2012).
30. B. Zhou, J. Gitschier, *Proceedings of the National Academy of Sciences of the United States of America* **94**, 7481 (Jul 8, 1997).
31. M. Arredondo, P. Munoz, C. V. Mura, M. T. Nunez, *Am J Physiol Cell Physiol* **284**, C1525 (Jun, 2003).
32. Y. M. Kuo, B. Zhou, D. Cosco, J. Gitschier, *Proceedings of the National Academy of Sciences of the United States of America* **98**, 6836 (Jun 5, 2001).
33. S. Puig, J. Lee, M. Lau, D. J. Thiele, *The Journal of biological chemistry* **277**, 26021 (Jul 19, 2002).
34. J. F. Eisses, J. H. Kaplan, *The Journal of biological chemistry* **277**, 29162 (Aug 9, 2002).
35. J. Lee, M. J. Petris, D. J. Thiele, *The Journal of biological chemistry* **277**, 40253 (Oct 25, 2002).
36. J. Lee, M. M. Pena, Y. Nose, D. J. Thiele, *The Journal of biological chemistry* **277**, 4380 (Feb 8, 2002).
37. C. J. De Feo, S. G. Aller, G. S. Siluvai, N. J. Blackburn, V. M. Unger, *Proceedings of the National Academy of Sciences of the United States of America* **106**, 4237 (Mar 17, 2009).
38. A. E. Klomp *et al.*, *Biochem J* **370**, 881 (Mar 15, 2003).
39. D. Kahra, M. Kovermann, P. Wittung-Stafshede, *Biophysical Journal* **110**, 95 (1/5/, 2016).
40. M. J. Petris, K. Smith, J. Lee, D. J. Thiele, *The Journal of biological chemistry* **278**, 9639 (Mar 14, 2003).
41. S. A. Molloy, J. H. Kaplan, *The Journal of biological chemistry* **284**, 29704 (Oct 23, 2009).
42. E. B. Maryon, S. A. Molloy, K. Ivy, H. Yu, J. H. Kaplan, *The Journal of biological chemistry* **288**, 18035 (Jun 21, 2013).
43. J. J. A. Cotruvo, A. T. Aron, K. M. Ramos-Torres, C. J. Chang, *Chemical Society Reviews* **44**, 4400 (2015).
44. E. B. Maryon, S. A. Molloy, J. H. Kaplan, *Am J Physiol Cell Physiol* **304**, C768 (Apr 15, 2013).
45. L. Banci *et al.*, *Nature* **465**, 645 (Jun 3, 2010).

46. J. Lee, J. R. Prohaska, D. J. Thiele, *Proceedings of the National Academy of Sciences of the United States of America* **98**, 6842 (Jun 5, 2001).
47. J. Lee, J. R. Prohaska, S. L. Dagenais, T. W. Glover, D. J. Thiele, *Gene* **254**, 87 (Aug 22, 2000).
48. K. M. Davies *et al.*, *Metallomics* **5**, 43 (Jan, 2013).
49. Y. M. Kuo, A. A. Gybina, J. W. Pyatskowit, J. Gitschier, J. R. Prohaska, *The Journal of nutrition* **136**, 21 (Jan, 2006).
50. W. Zheng, A. D. Monnot, *Pharmacol Ther* **133**, 177 (Feb, 2012).
51. L. W. Klomp *et al.*, *The Journal of biological chemistry* **272**, 9221 (Apr 4, 1997).
52. I. H. Hung, R. L. Casareno, G. Labesse, F. S. Mathews, J. D. Gitlin, *The Journal of biological chemistry* **273**, 1749 (Jan 16, 1998).
53. A. Badarau, C. Dennison, *J Am Chem Soc* **133**, 2983 (Mar 9, 2011).
54. S. Itoh *et al.*, *The Journal of biological chemistry* **283**, 9157 (Apr 4, 2008).
55. S. Itoh *et al.*, *Free radical biology & medicine* **46**, 95 (Jan 1, 2009).
56. V. Jeney *et al.*, *Circ Res* **96**, 723 (Apr 15, 2005).
57. I. Hamza *et al.*, *Proceedings of the National Academy of Sciences of the United States of America* **98**, 6848 (Jun 5, 2001).
58. M. M. Pena, J. Lee, D. J. Thiele, *The Journal of nutrition* **129**, 1251 (Jul, 1999).
59. P. C. Bull, G. R. Thomas, J. M. Rommens, J. R. Forbes, D. W. Cox, *Nat Genet* **5**, 327 (Dec, 1993).
60. Y. Yamaguchi, M. E. Heiny, M. Suzuki, J. D. Gitlin, *Proceedings of the National Academy of Sciences of the United States of America* **93**, 14030 (Nov 26, 1996).
61. J. M. Arguello, E. Eren, M. Gonzalez-Guerrero, *Biometals* **20**, 233 (Jun, 2007).
62. Z. Qin, S. Itoh, V. Jeney, M. Ushio-Fukai, T. Fukai, *FASEB J* **20**, 334 (Feb, 2006).
63. M. J. Petris, D. Strausak, J. F. Mercer, *Hum Mol Genet* **9**, 2845 (Nov 22, 2000).
64. R. El Meskini, V. C. Culotta, R. E. Mains, B. A. Eipper, *The Journal of biological chemistry* **278**, 12278 (Apr 4, 2003).
65. M. Schaefer, R. G. Hopkins, M. L. Failla, J. D. Gitlin, *Am J Physiol* **276**, G639 (Mar, 1999).
66. L. Nyasae, R. Bustos, L. Braiterman, B. Eipper, A. Hubbard, *Am J Physiol Gastrointest Liver Physiol* **292**, G1181 (Apr, 2007).
67. D. Larin *et al.*, *The Journal of biological chemistry* **274**, 28497 (Oct 1, 1999).
68. M. J. Petris, J. F. Mercer, *Hum Mol Genet* **8**, 2107 (Oct, 1999).
69. M. J. Petris *et al.*, *The EMBO journal* **15**, 6084 (Nov 15, 1996).

70. J. F. Monty, R. M. Llanos, J. F. Mercer, D. R. Kramer, *The Journal of nutrition* **135**, 2762 (Dec, 2005).
71. M. A. Cater, S. La Fontaine, K. Shield, Y. Deal, J. F. Mercer, *Gastroenterology* **130**, 493 (Feb, 2006).
72. D. Huster, S. Lutsenko, *The Journal of biological chemistry* **278**, 32212 (Aug 22, 2003).
73. N. Barnes, R. Tsivkovskii, N. Tsivkovskaia, S. Lutsenko, *The Journal of biological chemistry* **280**, 9640 (Mar 11, 2005).
74. S. Strand *et al.*, *Nat Med* **4**, 588 (May, 1998).
75. J. Camakaris *et al.*, *Biochem Genet* **18**, 117 (Feb, 1980).
76. B. Weisner, C. Hartard, C. Dieu, *Journal of the neurological sciences* **79**, 229 (Jun, 1987).
77. N. E. Hellman, J. D. Gitlin, *Annu Rev Nutr* **22**, 439 (2002).
78. M. Sato, J. D. Gitlin, *The Journal of biological chemistry* **266**, 5128 (Mar 15, 1991).
79. J. M. Walshe, *Ann Clin Biochem* **40**, 115 (Mar, 2003).
80. A. Zgirski, E. Frieden, *J Inorg Biochem* **39**, 137 (Jun, 1990).
81. J. D. Gitlin, J. J. Schroeder, L. M. Lee-Ambrose, R. J. Cousins, *Biochem J* **282 (Pt 3)**, 835 (Mar 15, 1992).
82. B. N. Patel, S. David, *The Journal of biological chemistry* **272**, 20185 (Aug 8, 1997).
83. B. N. Patel, R. J. Dunn, S. David, *The Journal of biological chemistry* **275**, 4305 (Feb 11, 2000).
84. B. Alberts *et al.*, *Molecular Biology of the Cell, Fourth Edition*. (Garland Science, 2002).
85. J. M. Berg, J. L. Tymoczko, L. Stryer, *Biochemistry, Fifth Edition*. (W.H. Freeman, 2002).
86. Y. Liu, G. Fiskum, D. Schubert, *Journal of neurochemistry* **80**, 780 (Mar, 2002).
87. G. T. Babcock, M. Wikstrom, *Nature* **356**, 301 (Mar 26, 1992).
88. T. Tsukihara *et al.*, *Science* **272**, 1136 (May 24, 1996).
89. R. Lill, F. E. Nargang, W. Neupert, *Curr Opin Cell Biol* **8**, 505 (Aug, 1996).
90. A. Musatov, N. C. Robinson, *Biochemistry* **41**, 4371 (Apr 2, 2002).
91. J. Stanicova, E. Sedlak, A. Musatov, N. C. Robinson, *Biochemistry* **46**, 7146 (Jun 19, 2007).
92. M. Brunori, A. Giuffre, F. Malatesta, P. Sarti, *Journal of bioenergetics and biomembranes* **30**, 41 (Feb, 1998).

93. C. Varotsis, Y. Zhang, E. H. Appelman, G. T. Babcock, *Proceedings of the National Academy of Sciences of the United States of America* **90**, 237 (Jan 1, 1993).
94. T. Tsukihara *et al.*, *Science* **269**, 1069 (Aug 25, 1995).
95. A. Badarau, C. Dennison, *Proceedings of the National Academy of Sciences of the United States of America* **108**, 13007 (Aug 9, 2011).
96. L. Stiburek *et al.*, *Biochem J* **392**, 625 (Dec 15, 2005).
97. D. A. Pearce, F. Sherman, *The Journal of biological chemistry* **270**, 20879 (Sep 8, 1995).
98. D. M. Glerum, A. Shtanko, A. Tzagoloff, *The Journal of biological chemistry* **271**, 14504 (Jun 14, 1996).
99. M. P. Nobrega, S. C. Bandeira, J. Beers, A. Tzagoloff, *The Journal of biological chemistry* **277**, 40206 (Oct 25, 2002).
100. M. H. Barros, A. Johnson, A. Tzagoloff, *The Journal of biological chemistry* **279**, 31943 (Jul 23, 2004).
101. A. B. Maxfield, D. N. Heaton, D. R. Winge, *The Journal of biological chemistry* **279**, 5072 (Feb 13, 2004).
102. K. Rigby, L. Zhang, P. A. Cobine, G. N. George, D. R. Winge, *The Journal of biological chemistry* **282**, 10233 (Apr 6, 2007).
103. P. A. Cobine, L. D. Ojeda, K. M. Rigby, D. R. Winge, *The Journal of biological chemistry* **279**, 14447 (Apr 2, 2004).
104. P. Palumaa, L. Kangur, A. Voronova, R. Sillard, *Biochem J* **382**, 307 (Aug 15, 2004).
105. L. Banci *et al.*, *Proceedings of the National Academy of Sciences of the United States of America* **105**, 6803 (May 13, 2008).
106. L. Hiser, M. Di Valentin, A. G. Hamer, J. P. Hosler, *The Journal of biological chemistry* **275**, 619 (Jan 7, 2000).
107. P. Buchwald, G. Krummeck, G. Rodel, *Mol Gen Genet* **229**, 413 (Oct, 1991).
108. J. C. Williams *et al.*, *The Journal of biological chemistry* **280**, 15202 (Apr 15, 2005).
109. C. Paret, K. Ostermann, U. Krause-Buchholz, A. Rentzsch, G. Rodel, *FEBS letters* **447**, 65 (Mar 19, 1999).
110. L. Banci *et al.*, *Proceedings of the National Academy of Sciences of the United States of America* **104**, 15 (Jan 2, 2007).
111. S. C. Leary, F. Sasarman, T. Nishimura, E. A. Shoubridge, *Hum Mol Genet* **18**, 2230 (Jun 15, 2009).
112. Y. C. Horng *et al.*, *The Journal of biological chemistry* **280**, 34113 (Oct 7, 2005).
113. S. C. Leary *et al.*, *Cell metabolism* **5**, 9 (Jan, 2007).

114. H. S. Carr, A. B. Maxfield, Y. C. Horng, D. R. Winge, *The Journal of biological chemistry* **280**, 22664 (Jun 17, 2005).
115. H. S. Carr, G. N. George, D. R. Winge, *The Journal of biological chemistry* **277**, 31237 (Aug 23, 2002).
116. O. Khalimonchuk, M. Bestwick, B. Meunier, T. C. Watts, D. R. Winge, *Mol Cell Biol* **30**, 1004 (Feb, 2010).
117. D. Smith, J. Gray, L. Mitchell, W. E. Antholine, J. P. Hosler, *The Journal of biological chemistry* **280**, 17652 (May 6, 2005).
118. L. G. Nijtmans, J. W. Taanman, A. O. Muijsers, D. Speijer, C. Van den Bogert, *European journal of biochemistry / FEBS* **254**, 389 (Jun 1, 1998).
119. S. L. Williams, I. Valnot, P. Rustin, J. W. Taanman, *The Journal of biological chemistry* **279**, 7462 (Feb 27, 2004).
120. J. D. Crapo, T. Oury, C. Rabouille, J. W. Slot, L. Y. Chang, *Proceedings of the National Academy of Sciences of the United States of America* **89**, 10405 (Nov 1, 1992).
121. L. Banci *et al.*, *Nat Chem Biol* **9**, 297 (May, 2013).
122. L. A. Sturtz, K. Diekert, L. T. Jensen, R. Lill, V. C. Culotta, *The Journal of biological chemistry* **276**, 38084 (Oct 12, 2001).
123. L. Y. Chang, J. W. Slot, H. J. Geuze, J. D. Crapo, *J Cell Biol* **107**, 2169 (Dec, 1988).
124. V. C. Culotta *et al.*, *The Journal of biological chemistry* **272**, 23469 (Sep 19, 1997).
125. A. L. Lamb *et al.*, *Nat Struct Biol* **6**, 724 (Aug, 1999).
126. P. J. Schmidt *et al.*, *The Journal of biological chemistry* **274**, 23719 (Aug 20, 1999).
127. A. L. Caruano-Yzermans, T. B. Bartnikas, J. D. Gitlin, *The Journal of biological chemistry* **281**, 13581 (May 12, 2006).
128. A. L. Lamb, A. K. Wernimont, R. A. Pufahl, T. V. O'Halloran, A. C. Rosenzweig, *Biochemistry* **39**, 1589 (Feb 22, 2000).
129. T. Endo, T. Fujii, K. Sato, N. Taniguchi, J. Fujii, *Biochemical and biophysical research communications* **276**, 999 (Oct 5, 2000).
130. S. Allen, A. Badarau, C. Dennison, *Biochemistry* **51**, 1439 (Feb 21, 2012).
131. J. D. Rothstein *et al.*, *Journal of neurochemistry* **72**, 422 (Jan, 1999).
132. P. C. Wong *et al.*, *Proceedings of the National Academy of Sciences of the United States of America* **97**, 2886 (Mar 14, 2000).
133. M. C. Carroll *et al.*, *Proceedings of the National Academy of Sciences of the United States of America* **101**, 5964 (Apr 20, 2004).

134. J. Bertinato, M. R. L'Abbe, *The Journal of biological chemistry* **278**, 35071 (Sep 12, 2003).
135. J. R. Prohaska, M. Broderius, B. Brokate, *Archives of biochemistry and biophysics* **417**, 227 (Sep 15, 2003).
136. J. M. McCord, I. Fridovich, *The Journal of biological chemistry* **244**, 6049 (Nov 25, 1969).
137. F. Arnesano *et al.*, *The Journal of biological chemistry* **279**, 47998 (Nov 12, 2004).
138. L. Banci *et al.*, *Proceedings of the National Academy of Sciences of the United States of America* **109**, 13555 (Aug 21, 2012).
139. L. Banci, F. Cantini, T. Kozyreva, J. T. Rubino, *Chembiochem* **14**, 1839 (Sep 23, 2013).
140. Y. Furukawa, A. S. Torres, T. V. O'Halloran, *The EMBO journal* **23**, 2872 (Jul 21, 2004).
141. J. M. Leitch *et al.*, *The Journal of biological chemistry* **284**, 21863 (Aug 14, 2009).
142. S. Elchuri *et al.*, *Oncogene* **24**, 367 (Jan 13, 2005).
143. F. L. Muller *et al.*, *Free radical biology & medicine* **40**, 1993 (Jun 1, 2006).
144. H. X. Deng *et al.*, *Science* **261**, 1047 (Aug 20, 1993).
145. M. Wiedau-Pazos *et al.*, *Science* **271**, 515 (Jan 26, 1996).
146. S. V. Seetharaman *et al.*, *Exp Biol Med (Maywood)* **234**, 1140 (Oct, 2009).
147. C. M. Karch, M. Prudencio, D. D. Winkler, P. J. Hart, D. R. Borchelt, *Proceedings of the National Academy of Sciences of the United States of America* **106**, 7774 (May 12, 2009).
148. H. J. Moller, M. B. Graeber, *Eur Arch Psychiatry Clin Neurosci* **248**, 111 (1998).
149. J. A. Schneider, Z. Arvanitakis, S. E. Leurgans, D. A. Bennett, *Annals of neurology* **66**, 200 (Aug, 2009).
150. K. A. Jellinger, J. Attems, *J Neural Transm*, (Aug 5, 2014).
151. W. W. Barker *et al.*, *Alzheimer Dis Assoc Disord* **16**, 203 (Oct-Dec, 2002).
152. K. Blennow, M. J. de Leon, H. Zetterberg, *Lancet* **368**, 387 (Jul 29, 2006).
153. A. Wimo, B. Winblad, L. Jonsson, *Alzheimers Dement* **6**, 98 (Mar, 2010).
154. M. Prince *et al.*, *Dementia UK: Second Edition - Overview*. (Alzheimer's Society, 2014).
155. T. D. Bird, *Genet Med* **10**, 231 (Apr, 2008).
156. D. Campion *et al.*, *Am J Hum Genet* **65**, 664 (Sep, 1999).
157. A. Joshi, J. M. Ringman, A. S. Lee, K. O. Juarez, M. F. Mendez, *J Neurol* **259**, 2182 (Oct, 2012).

158. J. C. Breitner, M. F. Folstein, *Psychol Med* **14**, 63 (Feb, 1984).
159. E. H. Bigio, L. S. Hynan, E. Sontag, S. Satumtira, C. L. White, *Neuropathol Appl Neurobiol* **28**, 218 (Jun, 2002).
160. D. Ames, A. S. Burns, J. O'Brien, *Dementia*. (Hodder Arnold, 2010).
161. C. M. Wischik *et al.*, *Proceedings of the National Academy of Sciences of the United States of America* **85**, 4884 (Jul, 1988).
162. K. S. Kosik, *Brain Pathol* **3**, 39 (Jan, 1993).
163. H. Braak, E. Braak, *Acta neuropathologica* **82**, 239 (1991).
164. J. A. Hardy, G. A. Higgins, *Science* **256**, 184 (Apr 10, 1992).
165. R. Kayed *et al.*, *Science* **300**, 486 (Apr 18, 2003).
166. D. J. Selkoe, *Neuron* **6**, 487 (Apr, 1991).
167. D. Games *et al.*, *Nature* **373**, 523 (Feb 9, 1995).
168. M. P. Lambert *et al.*, *Proceedings of the National Academy of Sciences of the United States of America* **95**, 6448 (May 26, 1998).
169. I. Kuperstein *et al.*, *The EMBO journal* **29**, 3408 (Oct 6, 2010).
170. J. Hardy, D. Allsop, *Trends Pharmacol Sci* **12**, 383 (Oct, 1991).
171. C. F. Lippa, J. C. Morris, *Neurology* **66**, 1801 (Jun 27, 2006).
172. C. Holmes, *Br J Psychiatry* **180**, 131 (Feb, 2002).
173. M. Hutton *et al.*, *Nature* **393**, 702 (Jun 18, 1998).
174. G. G. Glenner, C. W. Wong, *Biochemical and biophysical research communications* **120**, 885 (May 16, 1984).
175. K. Jacobsen, K. Iverfeldt, *Cell. Mol. Life Sci.* **66**, 2299 (2009/07/01, 2009).
176. S. Tanaka *et al.*, *Biochemical and biophysical research communications* **157**, 472 (Dec 15, 1988).
177. S. Tanaka *et al.*, *Biochemical and biophysical research communications* **165**, 1406 (1989).
178. S. O. Dahms *et al.*, *J Mol Biol* **416**, 438 (Feb 24, 2012).
179. K. J. Barnham *et al.*, *The Journal of biological chemistry* **278**, 17401 (May 9, 2003).
180. Y. Wang, Y. Ha, *Mol Cell* **15**, 343 (Aug 13, 2004).
181. R. E. Tanzi *et al.*, *Nature* **331**, 528 (Feb 11, 1988).
182. P. Soba *et al.*, *The EMBO journal* **24**, 3624 (2005).
183. T. L. Young-Pearse *et al.*, *The Journal of Neuroscience* **27**, 14459 (2007).
184. Y. Joo *et al.*, *PLoS ONE* **5**, e14203 (2010).
185. M. Akaaboune *et al.*, *Molecular and Cellular Neuroscience* **15**, 355 (2000).

186. J. N. Octave, N. Pierrot, S. Ferao Santos, N. N. Nalivaeva, A. J. Turner, *Journal of neurochemistry* **126**, 183 (Jul, 2013).
187. S. A. Bellingham *et al.*, *The Journal of biological chemistry* **279**, 20378 (May 7, 2004).
188. H. Zhang, Q. Ma, Y.-w. Zhang, H. Xu, *Journal of neurochemistry* **120**, 9 (2012).
189. S. S. Sisodia, *Proceedings of the National Academy of Sciences of the United States of America* **89**, 6075 (Jul 1, 1992).
190. S. Lammich *et al.*, *Proceedings of the National Academy of Sciences of the United States of America* **96**, 3922 (Mar 30, 1999).
191. J. Ermolieff, J. A. Loy, G. Koelsch, J. Tang, *Biochemistry* **39**, 12450 (Oct 10, 2000).
192. L. Hesse, D. Beher, C. L. Masters, G. Multhaup, *FEBS letters* **349**, 109 (Jul 25, 1994).
193. G. Multhaup *et al.*, *Science* **271**, 1406 (Mar 8, 1996).
194. K. M. Acevedo *et al.*, *The Journal of biological chemistry* **286**, 8252 (Mar 11, 2011).
195. A. R. White *et al.*, *Brain research* **842**, 439 (Sep 25, 1999).
196. C. Treiber *et al.*, *The Journal of biological chemistry* **279**, 51958 (Dec 10, 2004).
197. M. Suazo *et al.*, *Biochemical and biophysical research communications* **382**, 740 (May 15, 2009).
198. W. F. Cerpa *et al.*, *FASEB J* **18**, 1701 (Nov, 2004).
199. A. Goate *et al.*, *Nature* **349**, 704 (Feb 21, 1991).
200. L. Hendriks *et al.*, *Nat Genet* **1**, 218 (Jun, 1992).
201. X. D. Cai, T. E. Golde, S. G. Younkin, *Science* **259**, 514 (Jan 22, 1993).
202. M. Citron *et al.*, *Nature* **360**, 672 (Dec 17, 1992).
203. T. Jonsson *et al.*, *Nature* **488**, 96 (Aug 2, 2012).
204. I. Hussain *et al.*, *Mol Cell Neurosci* **14**, 419 (Dec, 1999).
205. S. Sinha *et al.*, *Nature* **402**, 537 (Dec 2, 1999).
206. R. Vassar *et al.*, *Science* **286**, 735 (Oct 22, 1999).
207. R. Yan *et al.*, *Nature* **402**, 533 (Dec 2, 1999).
208. X. Lin *et al.*, *Proceedings of the National Academy of Sciences of the United States of America* **97**, 1456 (Feb 15, 2000).
209. J. Zhao *et al.*, *The Journal of biological chemistry* **271**, 31407 (Dec 6, 1996).
210. S. L. Roberds *et al.*, *Hum Mol Genet* **10**, 1317 (Jun 1, 2001).
211. P. C. Kandalepas, R. Vassar, *Journal of neurochemistry* **120 Suppl 1**, 55 (Jan, 2012).
212. C. Costantini, M. H. Ko, M. C. Jonas, L. Puglielli, *Biochem J* **407**, 383 (Nov 1, 2007).
213. B. D. Bennett *et al.*, *The Journal of biological chemistry* **275**, 37712 (Dec 1, 2000).
214. A. Capell *et al.*, *The Journal of biological chemistry* **275**, 30849 (Oct 6, 2000).

215. J. T. Huse, D. S. Pijak, G. J. Leslie, V. M. Lee, R. W. Doms, *The Journal of biological chemistry* **275**, 33729 (Oct 27, 2000).
216. J. Walter *et al.*, *The Journal of biological chemistry* **276**, 14634 (May 4, 2001).
217. I. Levental, D. Lingwood, M. Grzybek, U. Coskun, K. Simons, *Proceedings of the National Academy of Sciences of the United States of America* **107**, 22050 (Dec 21, 2010).
218. B. Angeletti *et al.*, *The Journal of biological chemistry* **280**, 17930 (May 6, 2005).
219. C. Y. Wang *et al.*, *Antioxidants & redox signaling* **19**, 2024 (Dec 10, 2013).
220. L. B. Yang *et al.*, *Nat Med* **9**, 3 (Jan, 2003).
221. R. Li *et al.*, *Proceedings of the National Academy of Sciences of the United States of America* **101**, 3632 (Mar 9, 2004).
222. Y. Luo *et al.*, *Nat Neurosci* **4**, 231 (Mar, 2001).
223. M. S. Brown, J. Ye, R. B. Rawson, J. L. Goldstein, *Cell* **100**, 391 (Feb 18, 2000).
224. B. De Strooper, *Neuron* **38**, 9 (Apr 10, 2003).
225. H. Laudon *et al.*, *The Journal of biological chemistry* **280**, 35352 (Oct 21, 2005).
226. T. Ratovitski *et al.*, *The Journal of biological chemistry* **272**, 24536 (Sep 26, 1997).
227. D. S. Yang *et al.*, *The Journal of biological chemistry* **277**, 28135 (Aug 2, 2002).
228. S. Shah *et al.*, *Cell* **122**, 435 (Aug 12, 2005).
229. A. S. Crystal *et al.*, *The Journal of biological chemistry* **278**, 20117 (May 30, 2003).
230. R. Pardossi-Piquard *et al.*, *The Journal of biological chemistry* **284**, 16298 (Jun 12, 2009).
231. A. C. Chen, L. Y. Guo, B. L. Ostaszewski, D. J. Selkoe, M. J. LaVoie, *The Journal of biological chemistry* **285**, 11378 (Apr 9, 2010).
232. K. S. Vetrivel, Y. W. Zhang, H. Xu, G. Thinakaran, *Molecular neurodegeneration* **1**, 4 (2006).
233. D. G. Flood *et al.*, *Neurobiology of aging* **23**, 335 (May-Jun, 2002).
234. D. Cai *et al.*, *The Journal of biological chemistry* **278**, 3446 (Jan 31, 2003).
235. C. M. Dobson, *Nature* **426**, 884 (Dec 18, 2003).
236. D. K. Klimov, D. Thirumalai, *Structure* **11**, 295 (Mar, 2003).
237. K. M. Lucin, T. Wyss-Coray, *Neuron* **64**, 110 (Oct 15, 2009).
238. C. S. Atwood *et al.*, *Journal of neurochemistry* **75**, 1219 (Sep, 2000).
239. L. M. Miller *et al.*, *J Struct Biol* **155**, 30 (Jul, 2006).
240. X. Huang *et al.*, *The Journal of biological chemistry* **274**, 37111 (Dec 24, 1999).
241. A. S. Pithadia, M. H. Lim, *Curr Opin Chem Biol* **16**, 67 (Apr, 2012).
242. J. Mayes *et al.*, *The Journal of biological chemistry* **289**, 12052 (Apr 25, 2014).

243. B. S. Choi, W. Zheng, *Brain research* **1248**, 14 (Jan 12, 2009).
244. J. Nolte. (Inc, 2002).
245. A. D. Monnot, M. Behl, S. Ho, W. Zheng, *Toxicol Appl Pharmacol* **256**, 249 (Nov 1, 2011).
246. E. Bonilla *et al.*, *Neurochem Res* **9**, 1543 (Nov, 1984).
247. J. Smeyers-Verbeke, E. Defrise-Gussenhoven, G. Ebinger, A. Lowenthal, D. L. Massart, *Clin Chim Acta* **51**, 309 (Mar 26, 1974).
248. Y. Pushkar *et al.*, *Aging Cell* **12**, 823 (Oct, 2013).
249. I. Maurer, S. Zierz, H. J. Moller, *Neurobiology of aging* **21**, 455 (May-Jun, 2000).
250. E. M. Mutisya, A. C. Bowling, M. F. Beal, *Journal of neurochemistry* **63**, 2179 (Dec, 1994).
251. W. D. Parker, Jr., J. Parks, C. M. Filley, B. K. Kleinschmidt-DeMasters, *Neurology* **44**, 1090 (Jun, 1994).
252. L. Chen, J. S. Richardson, J. E. Caldwell, L. C. Ang, *Int J Neurosci* **75**, 83 (Mar, 1994).
253. D. L. Marcus *et al.*, *Experimental neurology* **150**, 40 (Mar, 1998).
254. S. Magaki *et al.*, *Neuroscience letters* **418**, 72 (May 11, 2007).
255. T. A. Bayer, G. Multhaup, *Journal of Alzheimer's disease : JAD* **8**, 201 (Nov, 2005).
256. S. A. James *et al.*, *Free radical biology & medicine* **52**, 298 (Jan 15, 2012).
257. D. J. Hare, E. J. New, M. D. de Jonge, G. McColl, *Chem Soc Rev* **44**, 5941 (Oct 07, 2015).
258. R. McRae, P. Bagchi, S. Sumalekshmy, C. J. Fahrni, *Chem Rev* **109**, 4780 (Oct, 2009).
259. B. R. Roberts, T. M. Ryan, A. I. Bush, C. L. Masters, J. A. Duce, *Journal of neurochemistry* **120 Suppl 1**, 149 (Jan, 2012).
260. J. Birks, *The Cochrane database of systematic reviews*, CD005593 (2006).
261. G. K. Wilcock, *Lancet Neurol* **2**, 503 (Aug, 2003).
262. M. Di Vaira *et al.*, *Inorganic chemistry* **43**, 3795 (Jun 28, 2004).
263. P. A. Adlard *et al.*, *Neuron* **59**, 43 (Jul 10, 2008).
264. Y. B. Nitzan *et al.*, *Journal of molecular medicine (Berlin, Germany)* **81**, 637 (Oct, 2003).
265. C. Grossi *et al.*, *Journal of Alzheimer's disease : JAD* **17**, 423 (2009).
266. C. W. Ritchie *et al.*, *Arch Neurol* **60**, 1685 (Dec, 2003).
267. B. Ibach, E. Haen, J. Marienhagen, G. Hajak, *Pharmacopsychiatry* **38**, 178 (Jul, 2005).
268. A. R. White *et al.*, *The Journal of biological chemistry* **281**, 17670 (Jun 30, 2006).

269. L. Lannfelt *et al.*, *Lancet Neurol* **7**, 779 (Sep, 2008).
270. P. J. Crouch *et al.*, *Journal of neurochemistry* **119**, 220 (Oct, 2011).
271. K. J. Barnham, A. I. Bush, *Chem Soc Rev* **43**, 6727 (Oct 7, 2014).
272. C. J. Maynard *et al.*, *The Journal of biological chemistry* **277**, 44670 (Nov 22, 2002).
273. T. A. Bayer *et al.*, *Proceedings of the National Academy of Sciences of the United States of America* **100**, 14187 (Nov 25, 2003).
274. H. Kessler *et al.*, *J Neural Transm* **115**, 1181 (Aug, 2008).
275. H. Kessler *et al.*, *J Neural Transm* **115**, 1651 (Dec, 2008).
276. P. D. Mehta *et al.*, *Archives of Neurology* **57**, 100 (2000).
277. F. L. Graham, J. Smiley, W. C. Russell, R. Nairn, *J Gen Virol* **36**, 59 (Jul, 1977).
278. G. Liu *et al.*, *Cell Cycle* **13**, 528 (2014).
279. V. M. Kavsan, A. V. Iershov, O. V. Balynska, *BMC Cell Biol* **12**, 23 (2011).
280. G. B. Frisoni *et al.*, *Brain* **130**, 720 (Mar, 2007).
281. J. A. Hardy *et al.*, *J Neural Transm* **61**, 253 (1985).
282. M. M. Bradford, *Anal Biochem* **72**, 248 (May 7, 1976).
283. C. A. Schneider, W. S. Rasband, K. W. Eliceiri, *Nat Methods* **9**, 671 (Jul, 2012).
284. D. M. Kirby, D. R. Thorburn, D. M. Turnbull, R. W. Taylor, *Methods in cell biology* **80**, 93 (2007).
285. Jaykaran, *Indian Journal of Pharmacology* **42**, 329 (2010).
286. D. R. Riddle, *Brain Aging: Models, Methods, and Mechanisms*. (Taylor & Francis Group, LLC, Boca Raton FL, 2007).
287. D. Harman, *Journal of gerontology* **11**, 298 (Jul, 1956).
288. R. Pearl, *The rate of living: being an account of some experimental studies on the biology of life duration*. (1928).
289. D. A. Drachman, *Neurology* **67**, 1340 (Oct 24, 2006).
290. E. R. Sowell *et al.*, *Nat Neurosci* **6**, 309 (Mar, 2003).
291. D. H. Salat *et al.*, *Cerebral cortex (New York, N.Y. : 1991)* **14**, 721 (Jul, 2004).
292. J. St-Pierre, J. A. Buckingham, S. J. Roebuck, M. D. Brand, *The Journal of biological chemistry* **277**, 44784 (Nov 22, 2002).
293. D. G. Nicholls, and Ferguson, S. J, *Biochemistry (Moscow)* **69**, 818 (2004/07/01, 2004).
294. L. O. Thomas, O. B. Boyko, D. C. Anthony, P. C. Burger, *AJNR. American journal of neuroradiology* **14**, 1043 (Sep-Oct, 1993).
295. L. J. Robbins, *Geriatrics* **44**, 31 (1989/04//, 1989).
296. P. Ramos *et al.*, *Biological trace element research* **161**, 190 (Nov, 2014).

297. L. M. Wang *et al.*, *Metallomics* **2**, 348 (May, 2010).
298. R. Palm, G. Wahlstrom, G. Hallmans, *Lab Anim* **24**, 240 (Jul, 1990).
299. S. Bohic *et al.*, *Anal Chem* **80**, 9557 (Dec 15, 2008).
300. S. K. Ludwin, *Lab Invest* **39**, 597 (Dec, 1978).
301. O. Ndubuizu, J. C. LaManna, *Antioxidants & redox signaling* **9**, 1207 (Aug, 2007).
302. Y. Ge *et al.*, *AJNR. American journal of neuroradiology* **23**, 1334 (Sep, 2002).
303. J. M. Cooper, V. M. Mann, A. H. Schapira, *Journal of the neurological sciences* **113**, 91 (Nov, 1992).
304. A. Navarro, A. Boveris, *Am J Physiol Regul Integr Comp Physiol* **287**, R1244 (Nov, 2004).
305. E. H. Sharman, S. C. Bondy, *Neurobiology of aging* **22**, 629 (Jul-Aug, 2001).
306. Z. H. Shah *et al.*, *FEBS letters* **478**, 267 (Aug 4, 2000).
307. E. Gould, B. S. McEwen, *Current opinion in neurobiology* **3**, 676 (Oct, 1993).
308. E. M. Kawamoto *et al.*, *Age (Dordrecht, Netherlands)* **35**, 331 (Apr, 2013).
309. P. Gil, F. Farinas, A. Casado, E. Lopez-Fernandez, *Gerontology* **48**, 209 (Jul-Aug, 2002).
310. R. L. Levine, *Free Radical Biology and Medicine* **32**, 790 (2002).
311. E. R. Stadtman, *Annals of the New York Academy of Sciences* **928**, 22 (Apr, 2001).
312. T. Kaneo, S. Tahara, M. Matsuo, *Mutation Research/DNAging* **316**, 277 (1996).
313. C. Venkateshappa, G. Harish, A. Mahadevan, M. M. Srinivas Bharath, S. K. Shankar, *Neurochem Res* **37**, 1601 (Aug, 2012).
314. C. Venkateshappa *et al.*, *Neurochem Res* **37**, 358 (Feb, 2012).
315. N. Kurobe, T. Inagaki, K. Kato, *Clin Chim Acta* **192**, 171 (Dec 3, 1990).
316. R. S. Sohal, B. H. Sohal, U. T. Brunk, *Mechanisms of ageing and development* **53**, 217 (Apr 30, 1990).
317. H. R. Massie, V. R. Aiello, A. A. Iodice, *Mechanisms of ageing and development* **10**, 93 (Apr, 1979).
318. S. Hussain, W. Slikker, Jr., S. F. Ali, *International journal of developmental neuroscience : the official journal of the International Society for Developmental Neuroscience* **13**, 811 (Dec, 1995).
319. F. Cand, J. Verdetti, *Free radical biology & medicine* **7**, 59 (1989).
320. Y. Mizuno, K. Ohta, *Journal of neurochemistry* **46**, 1344 (May, 1986).
321. T. B. Bartnikas, J. D. Gitlin, *The Journal of biological chemistry* **278**, 33602 (Aug 29, 2003).
322. R. J. Reiter, *FASEB J* **9**, 526 (Apr, 1995).

323. P. D. Coleman, D. G. Flood, *Neurobiology of aging* **8**, 521 (Nov-Dec, 1987).
324. G. Henderson, B. E. Tomlinson, P. H. Gibson, *Journal of the neurological sciences* **46**, 113 (Apr, 1980).
325. B. A. Syed *et al.*, *Protein engineering* **15**, 205 (Mar, 2002).
326. P. Ramos *et al.*, *J Trace Elem Med Biol* **28**, 13 (Jan, 2014).
327. M. F. Folstein, J. C. Breitner, *Johns Hopkins Med J* **149**, 145 (Oct, 1981).
328. H. Braak, I. Alafuzoff, T. Arzberger, H. Kretzschmar, K. Del Tredici, *Acta neuropathologica* **112**, 389 (Oct, 2006).
329. H. Braak, K. Del Trecidi, *Adv Anat Embryol Cell Biol* **215**, 1 (2015).
330. K. Ishii *et al.*, *AJNR. American journal of neuroradiology* **26**, 333 (Feb, 2005).
331. F. Yasuno *et al.*, *Dement Geriatr Cogn Disord* **9**, 63 (Mar-Apr, 1998).
332. D. Nochlin, G. van Belle, T. D. Bird, S. M. Sumi, *Alzheimer Dis Assoc Disord* **7**, 212 (Winter, 1993).
333. C. F. Lippa *et al.*, *Neurology* **46**, 406 (Feb, 1996).
334. G. C. Gregory, V. Macdonald, P. R. Schofield, J. J. Kril, G. M. Halliday, *Neurobiology of aging* **27**, 387 (Mar, 2006).
335. C. E. Shepherd, E. M. Grace, D. M. Mann, G. M. Halliday, *Neuropathol Appl Neurobiol* **33**, 328 (Jun, 2007).
336. Y. Fukutani, N. J. Cairns, M. N. Rossor, P. L. Lantos, *Journal of the neurological sciences* **149**, 177 (Aug, 1997).
337. D. A. Butterfield, A. Castegna, C. M. Lauderback, J. Drake, *Neurobiology of aging* **23**, 655 (Sep-Oct, 2002).
338. U. Keil *et al.*, *Journal of Alzheimer's disease : JAD* **9**, 139 (Jul, 2006).
339. T. D. Rae, P. J. Schmidt, R. A. Pufahl, V. C. Culotta, T. V. O'Halloran, *Science* **284**, 805 (Apr 30, 1999).
340. B. M. Hubbard, J. M. Anderson, *Neuropathol Appl Neurobiol* **11**, 369 (Sep-Oct, 1985).
341. V. F. Shefer, *Neuroscience and behavioral physiology* **6**, 319 (Oct-Dec, 1973).
342. M. T. Rajan *et al.*, *Journal of the neurological sciences* **146**, 153 (Mar 10, 1997).
343. L. O. Plantin, U. Lying-Tunell, K. Kristensson, *Biological trace element research* **13**, 69 (Aug, 1987).
344. D. A. Loeffler *et al.*, *Brain research* **738**, 265 (Nov 4, 1996).
345. A. Rembach *et al.*, *International journal of Alzheimer's disease* **2013**, 623241 (2013).
346. R. Duara *et al.*, *Neurology* **36**, 879 (Jul, 1986).

347. J. W. Pettegrew, K. Panchalingam, W. E. Klunk, R. J. McClure, L. R. Muenz, *Neurobiology of aging* **15**, 117 (Jan-Feb, 1994).
348. I. Maurer, S. Zierz, H. J. Moller, F. Jerusalem, *Neurology* **45**, 1423 (Jul, 1995).
349. M. Wong-Riley *et al.*, *Vision research* **37**, 3593 (Dec, 1997).
350. F. Bosetti *et al.*, *Neurobiology of aging* **23**, 371 (May-Jun, 2002).
351. S. J. Kish *et al.*, *Journal of neurochemistry* **59**, 776 (Aug, 1992).
352. S. J. Kish *et al.*, *Journal of neurochemistry* **72**, 700 (Feb, 1999).
353. J. M. Cooper, C. Wischik, A. H. Schapira, *Lancet* **341**, 969 (Apr 10, 1993).
354. H. Reichmann, S. Florke, G. Hebenstreit, H. Schrubar, P. Riederer, *J Neurol* **240**, 377 (Jun, 1993).
355. L. Cavelier *et al.*, *Genomics* **29**, 217 (Sep 1, 1995).
356. E. K. Perry, R. H. Perry, B. E. Tomlinson, *Neuroscience letters* **29**, 303 (Apr 26, 1982).
357. C. M. Yates, J. Butterworth, M. C. Tennant, A. Gordon, *Journal of neurochemistry* **55**, 1624 (Nov, 1990).
358. S. J. Baloyannis, *Journal of Alzheimer's disease : JAD* **9**, 119 (Jul, 2006).
359. S. J. Baloyannis, V. Costa, D. Michmizos, *Am J Alzheimers Dis Other Demen* **19**, 89 (Mar-Apr, 2004).
360. R. L. Morris, P. J. Hollenbeck, *J Cell Sci* **104 (Pt 3)**, 917 (Mar, 1993).
361. M. Manczak, B. Park, Y. Jung, P. H. Reddy, *Neuromol Med* **5**, 147 (2004/04/01, 2004).
362. G. M. Halliday, K. L. Double, V. Macdonald, J. J. Kril, *Neurobiology of aging* **24**, 797 (Oct, 2003).
363. F. Fontanesi, I. C. Soto, A. Barrientos, *IUBMB life* **60**, 557 (Sep, 2008).
364. L. Frolich, P. Riederer, *Arzneimittelforschung* **45**, 443 (Mar, 1995).
365. E. Karelson *et al.*, *Neurochem Res* **26**, 353 (Apr, 2001).
366. L. Lyras, N. J. Cairns, A. Jenner, P. Jenner, B. Halliwell, *Journal of neurochemistry* **68**, 2061 (May, 1997).
367. P. W. Mantyh *et al.*, *Journal of neurochemistry* **61**, 1171 (Sep, 1993).
368. J. V. Bannister, W. H. Bannister, G. Rotilio, *CRC Crit Rev Biochem* **22**, 111 (1987).
369. L. deToledo-Morrell *et al.*, *Neurobiology of aging* **18**, 463 (1997).
370. C. Ramassamy *et al.*, *Free radical biology & medicine* **27**, 544 (Sep, 1999).
371. K. Schuessel, S. Leutner, N. J. Cairns, W. E. Muller, A. Eckert, *J Neural Transm* **111**, 1167 (Sep, 2004).
372. W. Gsell *et al.*, *Journal of neurochemistry* **64**, 1216 (Mar, 1995).

373. A. Furuta *et al.*, *Am J Pathol* **146**, 357 (Feb, 1995).
374. E. H. Gray, K. J. De Vos, C. Dingwall, M. S. Perkinton, C. C. Miller, *Journal of Alzheimer's disease : JAD* **21**, 1101 (2010).
375. L. Giliberto *et al.*, *The Journal of biological chemistry* **284**, 9027 (Apr 3, 2009).
376. R. Borghi *et al.*, *Neurobiology of aging* **28**, 1009 (Jul, 2007).
377. K. Kato *et al.*, *J Mol Neurosci* **3**, 95 (1991/06/01, 1991).
378. K. Murakami *et al.*, *The Journal of biological chemistry* **286**, 44557 (Dec 30, 2011).
379. H. Funato *et al.*, *Am J Pathol* **152**, 983 (Apr, 1998).
380. L. M. Klevay, *The Journal of nutrition* **130**, 489S (Feb, 2000).
381. G. J. Brewer, *Drug Discov Today* **10**, 1103 (Aug 15, 2005).
382. G. K. Pagenkopf, D. W. Margerum, *J Am Chem Soc* **90**, 6963 (Dec 4, 1968).
383. N. a. list, *British Medical Journal* **2**, 270 (1971).
384. X. Ding, H. Xie, Y. J. Kang, *The Journal of nutritional biochemistry* **22**, 301 (Apr, 2011).
385. R. P. Patel, D. Svistunenko, M. T. Wilson, V. M. Darley-Usmar, *Biochem J* **322 (Pt 2)**, 425 (Mar 1, 1997).
386. B. Z. Zhu, M. Chevion, *Archives of biochemistry and biophysics* **380**, 267 (Aug 15, 2000).
387. H. Zhu *et al.*, *Inorganica Chimica Acta* **256**, 29 (1997).
388. I. Bremner, C. F. Mills, B. W. Young, *J Inorg Biochem* **16**, 109 (Apr, 1982).
389. M. I. CF, T. T. El-Gallad, I. Bremner, G. Weham, *J Inorg Biochem* **14**, 163 (Apr, 1981).
390. Y. Ogra, M. Ohmichi, K. T. Suzuki, *J Trace Elem Med Biol* **9**, 165 (Oct, 1995).
391. Y. Ogra, M. Ohmichi, K. T. Suzuki, *Toxicology* **106**, 75 (Jan 8, 1996).
392. Y. Ogra, H. Chikusa, K. T. Suzuki, *J Inorg Biochem* **78**, 123 (Jan 30, 2000).
393. P. J. Birker, H. C. Freeman, *J Am Chem Soc* **99**, 6890 (Oct 12, 1977).
394. B. Sarkar, A. Sass-Kortsak, R. Clarke, S. H. Laurie, P. Wei, *Proc R Soc Med* **70 Suppl 3**, 13 (1977).
395. J. Peisach, W. E. Blumberg, *Mol Pharmacol* **5**, 200 (Mar, 1969).
396. A. Gupte, R. J. Mumper, *Free radical biology & medicine* **43**, 1271 (Nov 1, 2007).
397. A. Gupte, R. J. Mumper, *J Inorg Biochem* **101**, 594 (Apr, 2007).
398. B. Page, M. Page, C. Noel, *International journal of oncology* **3**, 473 (Sep, 1993).
399. F. Denizot, R. Lang, *J Immunol Methods* **89**, 271 (May 22, 1986).
400. H. Schagger, K. Pfeiffer, *The EMBO journal* **19**, 1777 (Apr 17, 2000).

401. R. J. Janssen, L. G. Nijtmans, L. P. van den Heuvel, J. A. Smeitink, *J Inherit Metab Dis* **29**, 499 (Aug, 2006).
402. B. G. Hill, B. P. Dranka, L. Zou, J. C. Chatham, V. M. Darley-Usmar, *Biochem J* **424**, 99 (Nov 15, 2009).
403. B. G. Hill, A. N. Higdon, B. P. Dranka, V. M. Darley-Usmar, *Biochimica et biophysica acta* **1797**, 285 (Feb, 2010).
404. J. Perez, B. G. Hill, G. A. Benavides, B. P. Dranka, V. M. Darley-Usmar, *Biochem J* **428**, 255 (Jun 1, 2010).
405. Y. Abe, T. Sakairi, C. Beeson, J. B. Kopp, *Am J Physiol Renal Physiol* **305**, F1477 (Nov 15, 2013).
406. E. K. Ainscow, M. D. Brand, *European journal of biochemistry / FEBS* **263**, 671 (Aug, 1999).
407. N. Yadava, D. G. Nicholls, *J Neurosci* **27**, 7310 (Jul 4, 2007).
408. M. Wu *et al.*, *Am J Physiol Cell Physiol* **292**, C125 (Jan, 2007).
409. M. B. Jekabsons, D. G. Nicholls, *The Journal of biological chemistry* **279**, 32989 (Jul 30, 2004).
410. C. Affourtit, M. D. Brand, *Biochem J* **409**, 199 (Jan 1, 2008).
411. C. Vizler, T. Nagy, E. Kusz, H. Glavinas, E. Duda, *Cytometry* **47**, 158 (Mar 1, 2002).
412. W. Pendergrass, N. Wolf, M. Poot, *Cytometry A* **61**, 162 (Oct, 2004).
413. K. M. Robinson *et al.*, *Proceedings of the National Academy of Sciences of the United States of America* **103**, 15038 (Oct 10, 2006).
414. M. F. Lombardo, M. R. Ciriolo, G. Rotilio, L. Rossi, *Cell Mol Life Sci* **60**, 1733 (Aug, 2003).
415. R. I. Bustos *et al.*, *Biochemical and biophysical research communications* **437**, 426 (Aug 2, 2013).
416. K. Kwang Kim *et al.*, *Sci Rep* **5**, 14296 (2015).
417. A. Carpenter *et al.*, *Inflamm Res* **56**, 515 (Dec, 2007).
418. M. G. Vander Heiden, L. C. Cantley, C. B. Thompson, *Science* **324**, 1029 (May 22, 2009).
419. B. C. Mulukutla, M. Gramer, W. S. Hu, *Metab Eng* **14**, 138 (Mar, 2012).
420. G. Kemp, *Am J Physiol Regul Integr Comp Physiol* **289**, R895 (Sep, 2005).
421. G. t. Cooper *et al.*, *Circ Res* **58**, 692 (May, 1986).
422. S. Ishida, P. Andreux, C. Poitry-Yamate, J. Auwerx, D. Hanahan, *Proceedings of the National Academy of Sciences of the United States of America* **110**, 19507 (Nov 26, 2013).

423. S. Sweet, G. Singh, *Cancer Res* **55**, 5164 (Nov 15, 1995).
424. J. Gibon *et al.*, *Biochimica et biophysica acta* **1808**, 2807 (Dec, 2011).
425. J. C. Juarez *et al.*, *Clin Cancer Res* **12**, 4974 (Aug 15, 2006).
426. E. Lodemann, *Biochemical and biophysical research communications* **102**, 775 (Sep 30, 1981).
427. A. Gupte, S. Wadhwa, R. J. Mumper, *Bioconjug Chem* **19**, 1382 (Jul, 2008).
428. A. Crowe, C. Jackaman, K. M. Beddoes, B. Ricciardo, D. J. Nelson, *PLoS ONE* **8**, e73684 (2013).
429. M. Riha *et al.*, *J Inorg Biochem* **123**, 80 (Jun, 2013).
430. M. Chvapil, F. Kielar, F. Liska, A. Silhankova, K. Brendel, *Connect Tissue Res* **46**, 242 (2005).
431. K. Schumacher, G. Maerker-Alzer, R. Preuss, *Arzneimittelforschung* **25**, 603 (Apr, 1975).
432. F. Bulcke, R. Dringen, *Neurochem Res* **40**, 15 (Jan, 2015).
433. H. J. McArdle, S. M. Gross, I. Creaser, A. M. Sargeson, D. M. Danks, *Am J Physiol* **256**, G667 (Apr, 1989).
434. H. J. McArdle, S. M. Gross, H. M. Vogel, M. L. Ackland, D. M. Danks, *Biological trace element research* **22**, 179 (Nov, 1989).
435. I. F. Scheiber, M. M. Schmidt, R. Dringen, *Neurochem Int* **60**, 292 (Feb, 2012).
436. S. C. Dodani *et al.*, *Proceedings of the National Academy of Sciences of the United States of America* **108**, 5980 (Apr 12, 2011).
437. J. F. Hare, R. Hodges, *The Journal of biological chemistry* **257**, 12950 (Nov 10, 1982).
438. B. Aschenbrenner, R. Druyan, R. Albin, M. Rabinowitz, *Biochem J* **119**, 157 (Sep, 1970).
439. B. Wang, D. Dong, Y. J. Kang, *Exp Biol Med (Maywood)* **238**, 1017 (Sep, 2013).
440. J. C. Juarez *et al.*, *Proceedings of the National Academy of Sciences of the United States of America* **105**, 7147 (May 20, 2008).
441. M. V. Chidambaram, G. Barnes, E. Frieden, *J Inorg Biochem* **22**, 231 (Dec, 1984).
442. H. M. Alvarez *et al.*, *Science* **327**, 331 (Jan 15, 2010).
443. R. W. Strange *et al.*, *J Mol Biol* **328**, 877 (May 9, 2003).
444. V. Albergoni, A. Cassini, N. Favero, G. P. Rocco, *Biochem Pharmacol* **24**, 1131 (May 15, 1975).
445. V. Albergoni, N. Favero, F. Ghiretti, *Experientia* **33**, 17 (Jan 15, 1977).
446. F. Mamou *et al.*, *Anticancer Res* **26**, 1753 (May-Jun, 2006).

447. Q. Pan *et al.*, *Cancer Res* **62**, 4854 (Sep 1, 2002).
448. X. Chen, D. M. Medeiros, D. Jennings, *Biological trace element research* **106**, 51 (Jul, 2005).
449. S. S. Percival, B. Bae, M. Patrice, *Proc Soc Exp Biol Med* **203**, 78 (May, 1993).
450. R. Adman, D. A. Pious, *Science* **168**, 370 (Apr 17, 1970).
451. F. Diaz, H. Fukui, S. Garcia, C. T. Moraes, *Mol Cell Biol* **26**, 4872 (Jul, 2006).
452. H. Antonicka *et al.*, *Am J Hum Genet* **72**, 101 (Jan, 2003).
453. O. Khalimonchuk, A. Bird, D. R. Winge, *The Journal of biological chemistry* **282**, 17442 (Jun 15, 2007).
454. L. M. Ruiz *et al.*, *J Cell Physiol* **229**, 607 (May, 2014).
455. L. Rossi, E. Marchese, M. F. Lombardo, G. Rotilio, M. R. Ciriolo, *Free radical biology & medicine* **30**, 1177 (May 15, 2001).
456. M. D. Mattie, J. H. Freedman, *Am J Physiol Cell Physiol* **286**, C293 (Feb, 2004).
457. T. Friedrich, *Journal of bioenergetics and biomembranes* **33**, 169 (Jun, 2001).
458. U. Brandt, S. Kerscher, S. Drose, K. Zwicker, V. Zickermann, *FEBS letters* **545**, 9 (Jun 12, 2003).
459. P. Hinchliffe, L. A. Sazanov, *Science* **309**, 771 (Jul 29, 2005).
460. M. Lazarou, M. McKenzie, A. Ohtake, D. R. Thorburn, M. T. Ryan, *Mol Cell Biol* **27**, 4228 (Jun, 2007).
461. C. E. Dieteren *et al.*, *Biochimica et biophysica acta* **1807**, 1624 (Dec, 2011).
462. G. Kroemer, B. Dallaporta, M. Resche-Rigon, *Annu Rev Physiol* **60**, 619 (1998).
463. Y. Hatefi, *Annu Rev Biochem* **54**, 1015 (1985).
464. H. Itoh *et al.*, *Nature* **427**, 465 (Jan 29, 2004).
465. B. E. Sansbury, S. P. Jones, D. W. Riggs, V. M. Darley-Usmar, B. G. Hill, *Chem Biol Interact* **191**, 288 (May 30, 2011).
466. M. D. Brand, D. G. Nicholls, *Biochem J* **435**, 297 (Apr 15, 2011).
467. K. Mailer, *Biochemical and biophysical research communications* **170**, 59 (Jul 16, 1990).
468. J. Butler, G. G. Jayson, A. J. Swallow, *Biochimica et biophysica acta* **408**, 215 (Dec 11, 1975).
469. Y. Zhao, Z. B. Wang, J. X. Xu, *The Journal of biological chemistry* **278**, 2356 (Jan 24, 2003).
470. C. Affourtit, M. D. Brand, *Methods Enzymol* **457**, 405 (2009).
471. R. B. Nisr, C. Affourtit, *Biochimica et biophysica acta* **1837**, 270 (Feb, 2014).
472. K. Richardson *et al.*, *PLoS ONE* **8**, e68256 (2013).

473. M. Jastroch, A. S. Divakaruni, S. Mookerjee, J. R. Treberg, M. D. Brand, *Essays Biochem* **47**, 53 (2010).
474. J. C. Chao, D. M. Medeiros, R. A. Altschuld, C. M. Hohl, *Comp Biochem Physiol Comp Physiol* **104**, 163 (Jan, 1993).
475. X. Chen, D. B. Jennings, D. M. Medeiros, *Journal of bioenergetics and biomembranes* **34**, 397 (Oct, 2002).
476. D. G. Nicholls, *Biochem Soc Trans* **37**, 1385 (Dec, 2009).
477. C. Piccoli, R. Scrima, D. Boffoli, N. Capitanio, *Biochem J* **396**, 573 (Jun 15, 2006).
478. M. E. Dalmonte *et al.*, *The Journal of biological chemistry* **284**, 32331 (Nov 20, 2009).
479. R. Diaz-Ruiz *et al.*, *The Journal of biological chemistry* **283**, 26948 (Oct 3, 2008).
480. D. A. Ferrick, A. Neilson, C. Beeson, *Drug Discov Today* **13**, 268 (Mar, 2008).
481. R. Boelens, H. Rademaker, R. Wever, B. F. Van Gelder, *Biochimica et biophysica acta* **765**, 196 (May 29, 1984).
482. I. Hamza, M. Schaefer, L. W. Klomp, J. D. Gitlin, *Proceedings of the National Academy of Sciences of the United States of America* **96**, 13363 (Nov 9, 1999).
483. P. Meissner *et al.*, *Biotechnol Bioeng* **75**, 197 (Oct 20, 2001).
484. F. Wurm, A. Bernard, *Curr Opin Biotechnol* **10**, 156 (Apr, 1999).
485. P. Thomas, T. G. Smart, *J Pharmacol Toxicol Methods* **51**, 187 (May-Jun, 2005).
486. W. I. Vonk, C. Wijmenga, R. Berger, B. van de Sluis, L. W. Klomp, *The Journal of biological chemistry* **285**, 28991 (Sep 10, 2010).
487. E. Greco *et al.*, *Arthritis Res Ther* **17**, 93 (2015).
488. W. Liu *et al.*, *Cell Biosci* **4**, 14 (2014).
489. B. Chen, X. Wang, W. Zhao, J. Wu, *J Exp Clin Cancer Res* **29**, 99 (2010).
490. T. Itakura, D. M. Peters, M. E. Fini, *Mol Vis* **21**, 1071 (2015).
491. K. Swiech *et al.*, *BMC Biotechnol* **11**, 114 (2011).
492. W. Yin, P. Xiang, Q. Li, *Anal Biochem* **346**, 289 (Nov 15, 2005).
493. J. Mairhofer, R. Grabherr, *Mol Biotechnol* **39**, 97 (Jun, 2008).
494. J. Y. Cherng *et al.*, *J Control Release* **60**, 343 (Aug 5, 1999).
495. R. G. Taylor, D. C. Walker, R. R. McInnes, *Nucleic Acids Res* **21**, 1677 (Apr 11, 1993).
496. J. R. Cooke, E. A. McKie, J. M. Ward, E. Keshavarz-Moore, *J Biotechnol* **114**, 239 (Nov 9, 2004).
497. D. Ussery *et al.*, *Comput Chem* **26**, 531 (Jul, 2002).
498. J. A. Williams, J. Luke, L. Johnson, C. Hodgson, *Vaccine* **24**, 4671 (May 22, 2006).

499. P. Kreiss *et al.*, *Nucleic Acids Res* **27**, 3792 (Oct 1, 1999).
500. V. Jäger, K. Büssow, T. Schirrmann, in *Animal Cell Culture*. (Springer, 2015), pp. 27-64.
501. D. Lechardeur, A. S. Verkman, G. L. Lukacs, *Adv Drug Deliv Rev* **57**, 755 (Apr 5, 2005).
502. J. Glasspool-Malone *et al.*, *J Gene Med* **4**, 323 (May-Jun, 2002).
503. A. R. Azzoni, S. C. Ribeiro, G. A. Monteiro, D. M. Prazeres, *J Gene Med* **9**, 392 (May, 2007).
504. S. C. Ribeiro, G. A. Monteiro, D. M. Prazeres, *J Gene Med* **6**, 565 (May, 2004).
505. E. Carpentier, S. Paris, A. A. Kamen, Y. Durocher, *J Biotechnol* **128**, 268 (Feb 1, 2007).
506. F. Grosjean, P. Batard, M. Jordan, F. M. Wurm, *Cytotechnology* **38**, 57 (Jan, 2002).
507. A. R. Aricescu, W. Lu, E. Y. Jones, *Acta Crystallogr D Biol Crystallogr* **62**, 1243 (Oct, 2006).
508. E. L. Que, D. W. Domaille, C. J. Chang, *Chemical Reviews* **108**, 1517 (2008/05/01, 2008).
509. G. Shaw, S. Morse, M. Ararat, F. L. Graham, *FASEB J* **16**, 869 (Jun, 2002).
510. G. Bartzokis, *Neurobiology of aging* **25**, 5 (Jan, 2004).
511. M. C. Miotto *et al.*, *Inorganic chemistry* **53**, 4350 (May 05, 2014).
512. T. L. Jernigan *et al.*, *Neurobiology of aging* **22**, 581 (2001).
513. C. Colombrita *et al.*, *Exp Biol Med (Maywood)* **228**, 517 (May, 2003).